Fire dynamics and carbon cycling in miombo woodlands

Samuel Jonathan Bowers

Thesis submitted for the degree of Doctor of Philosophy

School of Geosciences

The University of Edinburgh

2017

Abstract

Savannah ecosystems play a prominent role in the global carbon (C) cycle, yet fluxes are poorly quantified, and the key processes regulating vegetation dynamics are uncertain. Insight is particularly deficient in southern Africa's miombo woodlands, a woody savannah that is home to over 100 million people. This biome is heavily disturbed, with widespread deforestation and degradation associated with agriculture, charcoal and timber extraction, and frequent fires from anthropogenic sources. In this thesis I combine plot inventory data with remote sensing and modelling techniques to improve our understanding of the miombo woodland C cycle.

Using a network of forest inventory plots, I characterise floristic and functional diversity in a savannah-forest mosaic in southeastern Tanzania. Divergent vegetation structures are associated with variation in fire frequency, water supply, and soil chemo-physical properties. Corresponding differences are noted in fire resilience, water-use, and nutrient acquisition plant functional traits, suggesting that multiple interrelated environmental filters act to assemble heterogeneous tree communities. Re-inventory of forest plots was used to quantify key aspects of the woody C cycle. Tree growth rates are slow, calling for careful management of woodland resources, and significantly reduced where stems were damaged. Stem mortality is rare, though elevated in the smallest trees and where damage was recorded.

Contemporary strategies to incentivise the conservation of miombo woodland ecosystems, such as the REDD+ programme of the United Nations, advocate payments for sustaining ecosystem services such as C sequestration. I report on a pilot REDD+ project aiming to reduce woodland degradation from frequent high intensity fires in southeastern Tanzania. Model simulations suggest that woody biomass is being gradually lost from the region, and that setting early season fires has the potential to reverse this trend. Realising substantial changes in C storage requires a demanding reduction to late fire frequency, and uncertainty in model predictions remains high.

I quantify the C cycle of southern African woodlands by combining observational data with a diagnostic C cycle model under a model-data fusion framework. Model outputs show substantial variation in primary production, C allocation patterns, and foliar and canopy traits, which are associated with differences in woody cover, fire, and precipitation properties. C cycle dynamics correspond poorly to conventional land cover maps, indicating they may be unsuited to upscaling measurements and models of the terrestrial C cycle.

Lay Summary

With the emergence of climate change as a global threat, developing a predictive understanding of the global carbon (C) cycle is of paramount importance. Uncertainties in emissions of CO_2 to the atmosphere, the major driver of global warming, are particularly large in savannah ecosystems such as the miombo woodlands of southern Africa. Miombo woodlands are important as a result of their extent, their biological diversity, and as a home to over 100 million people. Miombo woodland ecosystems are threatened by deforestation and degradation, and are vulnerable to future climate change. In this thesis I use forest plots, satellite observations, and computational models to better understand the miombo woodland C cycle.

Using a network of forest plots in Tanzania, I identify the main tree species communities in a diverse landscape of savannahs, woodland and forests. Vegetation types are associated with differences in fire frequency, water supply, and soil properties. Tree species show a variety of adaptations to these conditions, suggesting these factors are key determinants of vegetation diversity. Reliable estimates of tree growth and mortality rates are important for developing effective models of savannah ecosystem dynamics. Using re-measurement of forest plots, I estimate rates of tree growth, mortality, and regeneration, and identify differences in tree demography relating to stem damage, competitive stress, and tree size.

Fires are an innate part of savannah ecology, though frequent high intensity fires have the potential to degrade miombo woodlands. I report on a conservation project aiming to reduce the impact of high intensity fires through burning early in the year. These fires tend to burn slowly and patchily, and result in limited tree mortality. Model simulations suggest that early burning has the potential to reverse woodland degradation resulting from fire, though benefits will require a large reduction to late season fire frequency, and model outputs are very uncertain.

Reliable data from ecological surveys in miombo woodlands are rare, posing a challenge to evaluation of the C cycle. Over the past two decades a large quantity of data has been accumulated from Earth observation satellites, which when combined with computational models can be used to generate estimates of the C cycle in miombo woodlands. The model predicts large differences in ecosystem properties across southern Africa, associated with variation in tree cover, fire, and rainfall properties.

Author's Declaration

I declare that this thesis has been composed solely by myself and that it has not been submitted, either in whole or in part, in any previous application for a degree. Except where otherwise acknowledged, the work presented is entirely my own.

Samuel Bowers

2017

Project funded by the Natural Environment Research Council in partnership with the Mpingo Conservation & Development Initiative, with fieldwork support from Derek and Maureen Moss.

Acknowledgements

I would like to express my appreciation and thanks to my supervisor Mathew Williams. Mat is an excellent advisor, and his observations and thoughtful guidance were indispensable in shaping this thesis. I also thank my second supervisor, Casey Ryan, who was a great source of inspiration. His perceptiveness and experience in working with miombo woodlands was invaluable. I have also received academic assistance from a number of other sources throughout my PhD; my thanks are due in particular to Steve Ball, Jean-François Exbrayat, Jose Gómez-Dans, and Iain McNicol.

The staff of the Mpingo Conservation & Development Initiative (MCDI) in Tanzania were extremely obliging in hosting my fieldwork. Jasper Makala and Steve Ball went out of their way to assist with planning and logistics. I was lucky to have the support of MCDI's team of field assistants, whose expertise and good humour made my time in Tanzania productive and enjoyable. My thanks go to Andrew, Iddy, Issa, Mnyama, Mohamed, Ndossi, Peter, Walter, and Yusuph, without whom a large part of this thesis would have been impossible. I was also the recipient of help in the field from the residents of Kiwawa, Likawage, Migeregere, Nainokwe, Nanjirinji, and Ngea villages in Kilwa District, who I thank for being tolerant and engaging, and for being excellent scientists.

Fieldwork for this project was funded in part by Derek and Maureen Moss, whose kind contribution allowed me to take a reconnaissance trip to Tanzania. Without this reality-check, my data collection would have been ill-fated.

My time in Edinburgh was made enjoyable in large part due to the friends and colleagues I have had the pleasure of getting to know. The inhabitants of the Crew Attic, too numerous to mention individually, were by turns amusing, thought-provoking, and inspiring. I have learnt as much through them as I have from my work for this PhD. I have had the pleasure of living with a series of excellent housemates; Andy, Freddie, John, Julie-Anne, Neil, Phil, and Sam together kept me well-entertained and well-nourished. Special thanks also go to Paula, whose wisdom and positivity has been very much appreciated.

Lastly, I'd like to thank my family for all their support and encouragement over the years. This thesis is dedicated to Eleanor, Len, Jessica, and George.

Sam Bowers
August 2016

Contents

List of Figures

List of Tables

List of Abbreviations

ACM	Aggregated Canopy Model
AGB	Aboveground (woody) biomass
ALOS	Advanced Land Observation Satellite
C	Carbon
CARDAMOM	CARbon DAta MOdel fraMework
CO_2e	Carbon dioxide equivalent
CWM	Community-weighted mean
DALEC	Data Assimilation Linked Ecosystem Carbon model
DBH	Diameter at breast height
ECMWF	European Centre for Medium-Range Weather Forecasts
EDC	Ecological and dynamic constraint
ETM+	Landsat Enhanced Thematic Mapper
FLI	Byram's fireline intensity
FSC	Forest Stewardship Council
GFED	Global Fire Emissions Database
GPP	Gross primary production
HWSD	Harmonized World Soil Database
LAI	Leaf area index
LSP	Large sample plot
MCDI	Mpingo Conservation & Development Initiative
MDF	Model-data fusion
MHMCMC	Metropolis-Hastings Monte Carlo Markov Chain
MODIS	Moderate-resolution imaging spectroradiometer
N	Nitrogen
NBP	Net biome production
NEP	Net ecosystem production
NPP	Net primary production
P	Phosphorus
PALSAR	Phased Array type L-band Synthetic Aperture Radar
PAR	Photosynthetically active radiation
PC	Principal component
PCA	Principal component analysis
PSP	Permanent sample plot
REDD+	Reducing emissions from deforestation and forest degradation
SPA	Soil-Plant-Atmosphere model
TM	Landsat Thematic Mapper
TRMM	Tropical Rainfall Monitoring Mission
UNFCCC	United Nations Framework Convention on Climate Change
VCS	Verified Carbon Standard
VLFR	Village Land Forest Reserve
WALFA	West Arnhem Land Fire Abatement Project

CHAPTER 1

Introduction

1.1 Uncertainty in the global carbon cycle

The global carbon cycle is the biogeochemical cycle by which carbon (C) is circulated between storage pools in the atmosphere, hydrosphere, pedosphere, geosphere, biosphere, and anthroposphere of the Earth system. Along with water and nutrient cycles, the C cycle is integral to the support of life on Earth. The global C cycle is inordinately complex; movement (or flux) of C between storage pools is continuous, resulting from a large set of interacting physical, chemical, geological, and biological processes. Together these processes determine the global C balance, which fluctuates over daily to geological timescales (Keeling et al., 1976; Sundquist, 1986; Lüthi et al., 2008).

Efforts to understand the C cycle have risen in urgency as the result of rapid anthropogenic emission of carbon dioxide (CO_2) into the atmosphere (Fig. 1.1). CO_2 is one of a number of atmospheric gases that has a greenhouse warming effect on the Earth system, and is the dominant driver of ongoing climate change (IPCC, 2013). Net C flux to the atmosphere is presently dominated by emissions from fossil fuel combustion (87 % of CO_2 emissions in 2011), with further substantial emissions from land use change (9 %) and industrial processes such as cement production (4 %) (Le Quéré et al., 2013). The concentration of CO_2 in the atmosphere has recently surpassed the symbolic milestone of 400 ppm (Conway and Tans, 2016), an increase of *ca.* 120 ppm on the pre-industrial era (Gerber et al., 2003). Global temperatures continue to climb, with 2016 presently 1.03 °C warmer than the global mean temperature of the 20th century, and on-track to be by far the warmest year on record (NOAA, 2016). In the rapidly changing climate of the 'Anthropocene' (Steffen et al., 2007), developing an understanding of the C cycle is required to form reliable forecasts of future climate. Such predictions are important both at a global and local scale in allowing societies to mitigate against the environmental changes and adapt to probable impacts.

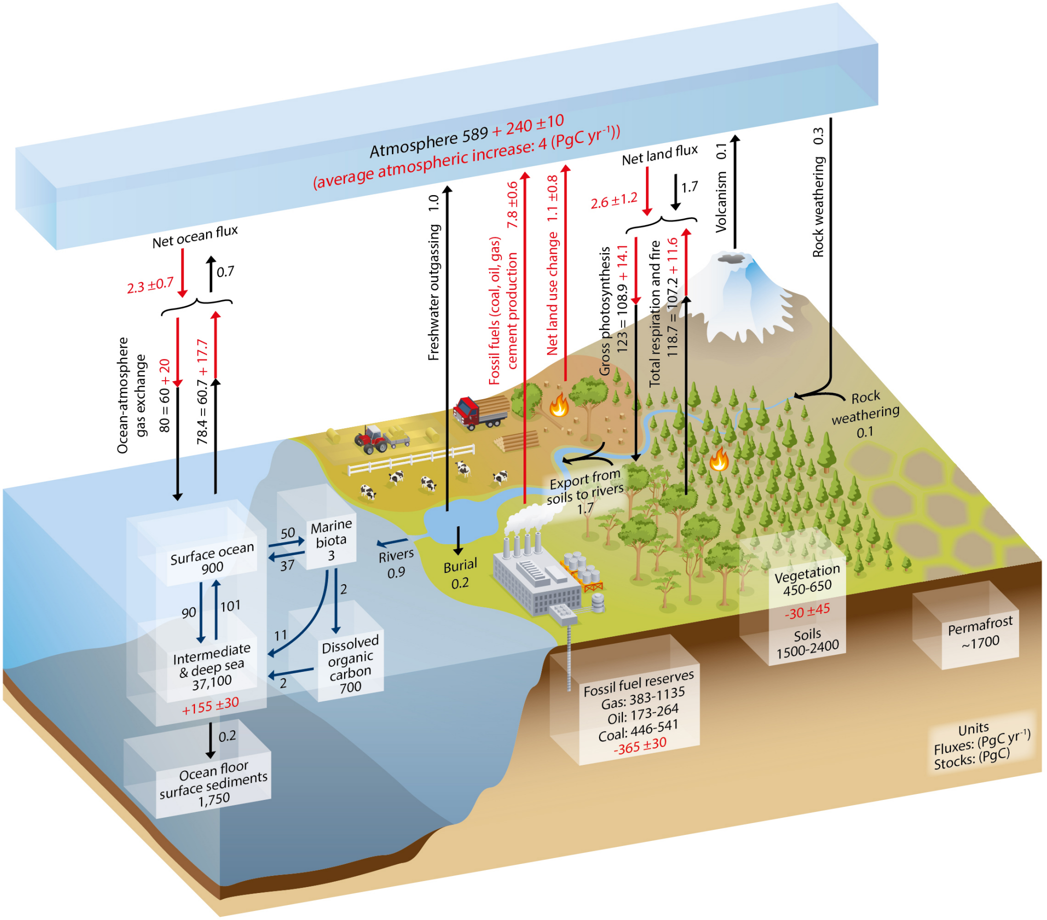

Figure 1.1: Schematic representation of the global carbon cycle. Carbon stocks are enumerated for major pools (PgC), and for the main fluxes connecting them (PgC/yr). Elements in black are estimates for the pre-Industrial era, and elements in red denote cumulative anthropogenic changes to the present day. Uncertainties are particularly large in vegetation carbon stocks and flux to the atmosphere from land use change. Diagram reproduced from IPCC (2013).

The terrestrial C cycle is by far the most poorly constrained aspect of the global C cycle (Le Quéré et al., 2013), with uncertainty stemming from a poor knowledge of the magnitude, distribution, and dynamics of the major terrestrial C pools. Accurate estimation of the state and fluxes of the terrestrial C cycle is very difficult; vegetation structure and soil properties are spatially variable (Fischer et al., 2008; Saatchi et al., 2011; Baccini et al., 2012), and ecosystems in different regions have profoundly divergent characteristics. For example, deforestation and degradation are thought to

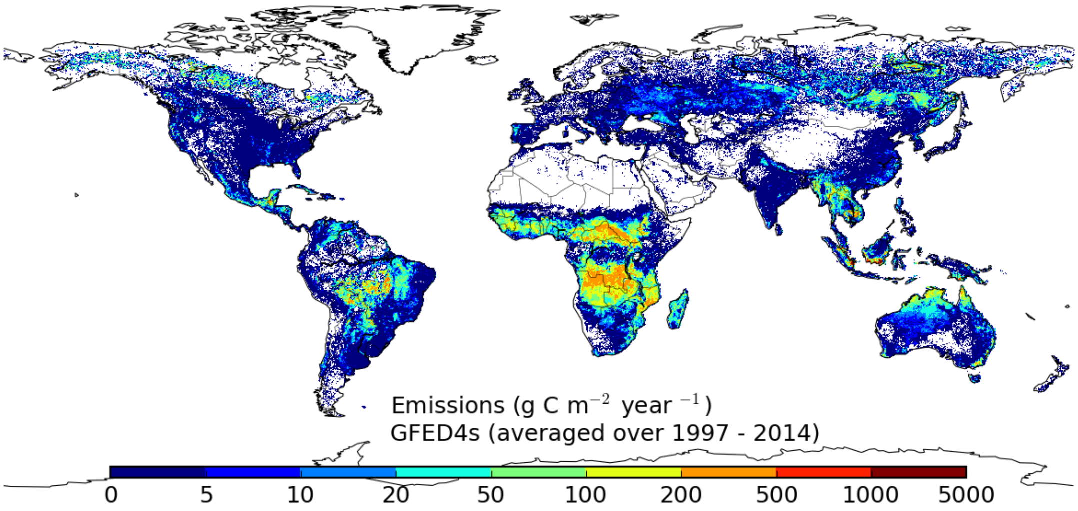

Figure 1.2: Fires are a large source of CO_2 emissions to the atmosphere. The Global Fire Emissions Database (GFED) shows how these emissions are distributed across the planet (van der Werf et al., 2010). Emissions of carbon from fire are concentrated in tropical regions where savannahs are prevalent, and are particularly large on the African continent. Diagram from `http://www.globalfiredata.org/`.

account for 6 - 17 % of anthropogenic CO_2 emissions, with most of this uncertainty resulting from inadequate estimates of C pools in terrestrial ecosystems (Houghton, 2005; Houghton et al., 2012; van der Werf et al., 2009; Mertz et al., 2012). Although a large source of greenhouse gas emissions, terrestrial ecosystems act as a net sink of C, slowing the accumulation of CO_2 in the atmosphere by capturing 2.6 ± 0.8 PgC/yr over the decade 2002 - 2011 (Pan et al., 2011; Le Quéré et al., 2013). The terrestrial biosphere also contributes significantly to inter-annual variability in net CO_2 emission, varying from a 4.1 PgC/yr sink to a 0.4 PgC/yr source (Le Quéré et al., 2013). The exact nature of the terrestrial C sink and the root causes of its variability remain obscure, contributing significant uncertainty to projections of future climate change.

Of the land surface processes that globally impact biosphere to atmosphere C fluxes, fire is one of the least understood and potentially most influential (Bond et al., 2005; Bowman et al., 2009; Hantson et al., 2016). Each year around 4 % of vegetated land burns. This results in global CO_2 emissions of *ca.* 2.5 PgC/yr, equivalent to around a quarter of annual CO_2 emissions from fossil fuels (van der Werf et al., 2010; Randerson et al., 2012; Giglio et al., 2013) (Fig. 1.2). Fire is a major ecosystem disturbance, with influences on species distributions, ecosystem function, and C storage. Of particular significance is the role of fire in maintaining the separation between fire-prone savannah and fire-resistant forest ecosystems in the tropics (Bond et al., 2005), which has important implications for ecosystem dynamics and C cycling.

The African continent plays a prominent role in the global C cycle, accounting for one fifth of total land area, around 20 % of net primary production (Ciais et al., 2011), and more than half of global C emissions from fire (van der Werf et al., 2010). Notwithstanding its importance, the African continent is one of the weakest links in our knowledge of the C cycle, and contributes a large uncertainty to the global C budget (Williams et al., 2007; Ciais et al., 2011). Unusually, fossil fuel use accounts for only a small fraction of total CO_2 emissions, equivalent to just 3 % of the global total (Boden et al., 2011). However, emissions from land use change are significant, with African deforestation accounting for around half of losses of global woodland and forest area over the period 2000 - 2005 (FAO, 2007). Uncertainty in the African C cycle is exacerbated by a very limited observational network; sources of scientific funding are distant, long-term experiments are rare, and the establishment and maintenance of tools such as flux towers is prohibitively difficult (Scholes, 2009). The result is that we have little understanding of the spatial patterns of C exchange, very limited knowledge of land-use change emissions, and we do not know whether Africa is a net source or sink of C.

1.2 The importance of savannah ecosystems

Savannah ecosystems occupy around one fifth of the Earth's land surface area, forming the dominant land cover of the tropics (Scholes and Walker, 1993) (Fig

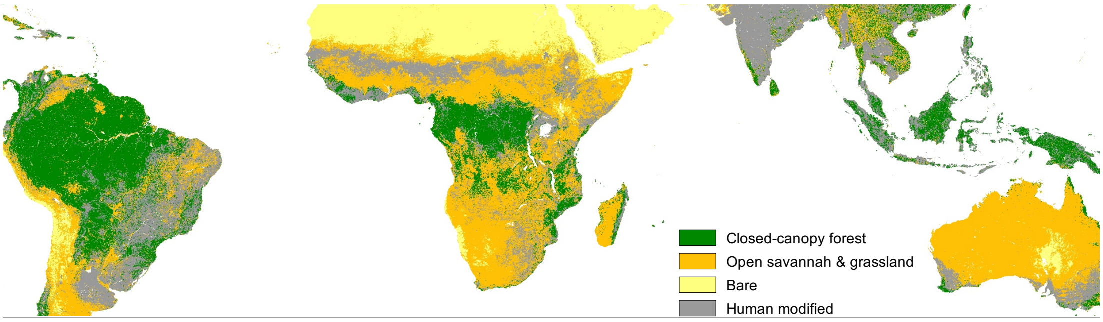

Figure 1.3: Savannahs and grasslands are the most extensive land cover type of the tropics, covering a greater area than the more intensely studied tropical forest biome. Data from ESA GlobCover 2009 land cover map.

1.3). Classifications of savannah vegetation differ, but all are characterised by the co-dominance of C_3 trees and C_4 grasses (Ratnam et al., 2011). Savannah ecosystems are distinct from grasslands or deserts, which support little woody biomass, and from forests, which are characterised by a closed canopy that excludes shade-intolerant C_4 grasses (Sage, 2004). Within this definition savannahs are extremely variable, ranging from areas of sparse tree cover through to dense woodlands. The grassy nature of savannahs often supports large populations of grazing animals, and is the main source of fuel for pervasive fires.

Conventionally, ecosystem distributions have been considered to be rigidly determined by climate (e.g. Schimper, 1898; Holdridge, 1947), though it is now apparent that savannahs may dominate in areas that are climatically and nutritionally able to support forests (Sankaran et al., 2005; Bond, 2010; Lehmann et al., 2011; Staver et al., 2011; Murphy and Bowman, 2012). This is particularly noticeable at regional spatial-scales, where the existence of mosaics of savannahs and forests are evidence of the decoupling of vegetation structure from climate. The persistence of grasses with trees, and savannahs with forests, is not fully understood. Explanations have invoked functional differentiation through root (Walter et al., 1971) and phenological (Archibald and Scholes, 2007) niche separation, and the local to continental scale influences of water availability (Sankaran et al., 2005; Rossatto et al., 2012), nutrient limitation (Cole, 1986; Ruggiero et al., 2002), and disturbance from herbivory (McNaughton, 1992; van Langevelde et al., 2003) and fire (Bond et al., 2005). As many of these processes interact, it is likely that no single explanation can account for the global distribution of the savannah biome (Bond, 2008).

Of all the processes structuring savannah ecosystems, it is the impacts of fire that are the most clearly apparent over human timescales. Fire modifies savannah vegetation mainly through the 'top-kill' of juvenile tree stems, forcing rootstocks to resprout in order to survive (Hoffmann et al., 2003; Hoffmann et al., 2009). The high frequency of fires results in a demographic bottleneck in savannahs, with the consequence that tree demographic transitions have a large impact on vegetation dynamics (Bond, 2008; Ryan and Williams, 2011). Savannahs are understood to exist in a state of dynamic equilibrium, where feedbacks between canopy cover, grass growth and fire amplify differences between fire-prone open savannahs and fire-resistant closed-canopy forests (Hoffmann et al., 2012). Understanding the mechanisms by which disturbance modifies vegetation structure, and vegetation structure begets disturbance, is a continuing challenge for savannah science.

Savannahs are of critical importance to the global C cycle, accounting for *ca.* 30 % of global net primary production (Grace et al., 2006), over 70 % of global burned area (Giglio et al., 2013), and *ca.* 44 % of all C emissions from fire (van der Werf et al., 2010). The savannah C cycle is not well understood; we do not have good data on the sizes of C pools, fluxes and residence times, and there is a poor understanding of how these vary spatially and temporally. A representative C cycle is presented in Figure 1.4, in which the major C pools and fluxes of savannah ecosystems are defined.

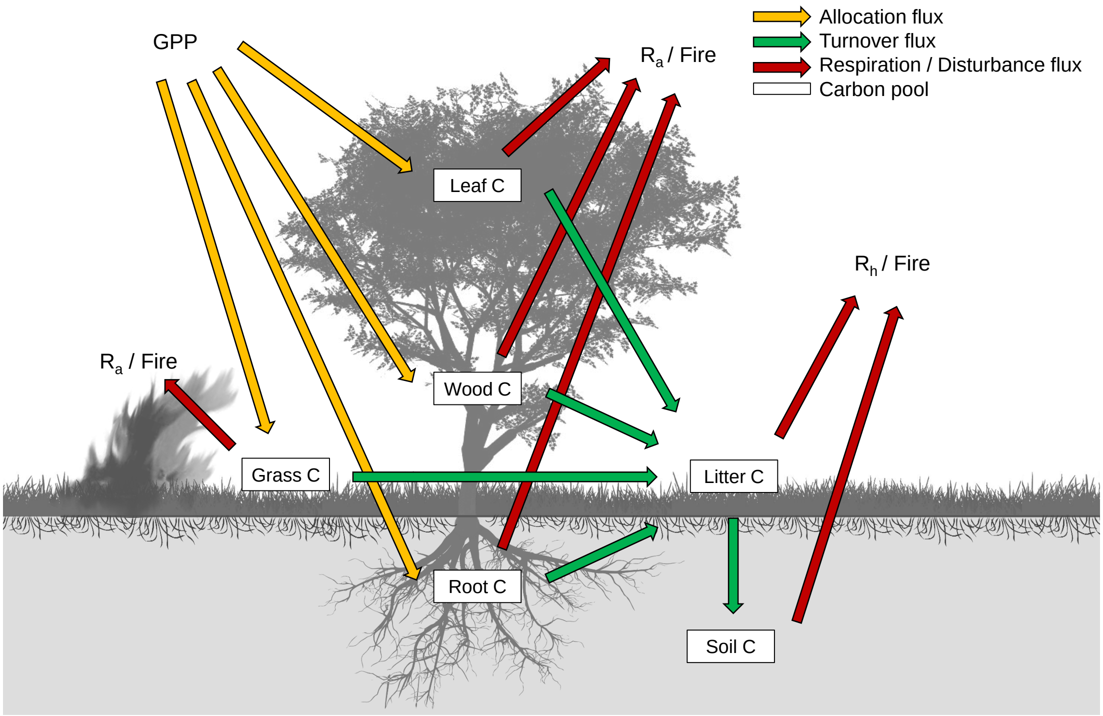

Figure 1.4: Representation of the main carbon pools and fluxes in a savannah ecosystem. Gross primary production (GPP) is allocated to carbon pools in living biomass, which turnover to carbon pools in litter and soil. Carbon is lost to the atmosphere by autotrophic respiration (R_a), heterotrophic respiration (R_h), and disturbance from fire. The size of carbon pools and fluxes, and the mechanisms that regulate them, are not well understood in savannah ecosystems.

1.3 The miombo woodlands of southern Africa

In this thesis I focus on miombo woodlands, a woody savannah ecosystem unique to the African continent. Miombo woodlands are the most extensive type of vegetation south of the equator in Africa, covering approximately 2.7 million km^2 (Frost, 1996). Miombo woodlands span sub-Saharan Africa from Tanzania and DR Congo in the north, through Angola, Zambia, and Malawi, to Mozambique and Zimbabwe in the south (Fig. 1.5). Despite their widespread nature, miombo woodlands are poorly studied (Mistry, 2014), a situation particularly apparent when compared to Africa's high-profile forest ecosystems (e.g. Lewis et al., 2009; Malhi, 2010). As an ecosystem under threat from rapid land clearance and future climate change, research into Africa's savannah ecosystems is an important and urgent requirement (Bond and Parr, 2010).

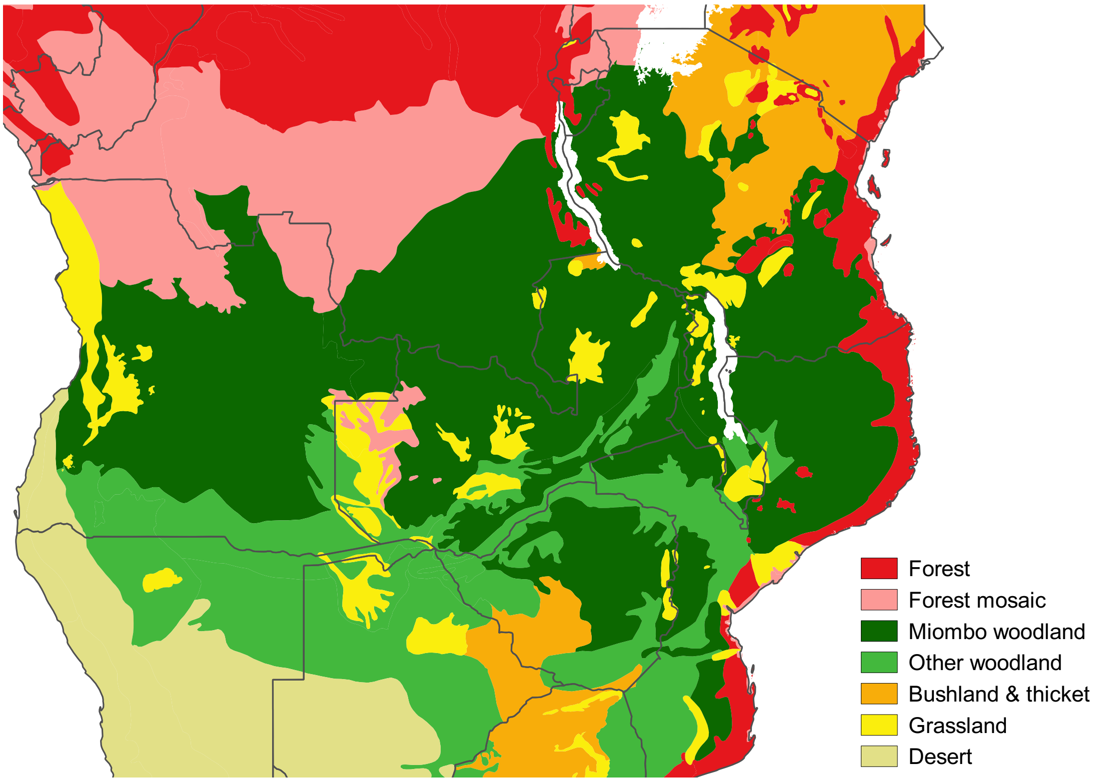

Figure 1.5: The distribution of characteristic vegetation structures across southern Africa. Adapted from White (1983) and Olson et al. (2001).

Miombo woodlands are the source of high levels of biodiversity and endemicity, supporting an estimated 8500 vascular plant species, including over 300 tree species (Frost, 1996). Miombo woodlands are typified by trees of the genera *Brachystegia*, *Julbernardia* and *Isoberlinia*, all belonging to the subfamily *Caesalpinioideae*. In common with other savannahs, miombo woodlands are characterised by the co-existence of trees and C_4 grasses, though as they exist at the woodier end of the savannah spectrum they are frequently referred to as a variety of forest. The structure of miombo woodlands is highly variable at regional to continental spatial-scales, ranging from open grasslands to dense woodlands. The mechanisms that drive this variation are not well understood.

Mean annual rainfall in miombo woodlands averages 540 - 1700 mm/yr (Frost, 1996), with a protracted dry season in which grasses dry out and most deciduous trees shed their leaves (Chidumayo, 2001). Miombo woodlands are by convention divided into 'dry' (< 1000 mm/yr) and 'wet' (> 1000 mm/yr) classes, with aboveground biomass positively correlated with rainfall (Frost, 1996). Unlike the more frequently studied arid and semi-arid savannahs of South Africa where dynamics are thought to be largely 'climatically determined', the dynamics of mesic savannahs such as miombo woodlands are 'disturbance-driven' (Sankaran et al., 2005). This means that top-down mechanisms such as fire are likely necessary to prevent the establishment of forests.

Miombo woodlands are typically found on soils that are acidic and nutrient-poor, with a low organic content. Specialised adaptations for nutrient acquisition such as N-fixation and ectomychorrizae are common, traits that aid the persistence of these species on infertile soils (Högberg, 1986; Högberg and Piearce, 1986). Soils supporting miombo woodlands are usually sandy and well-drained, though poorly drained soils subject to seasonal inundation are locally common. These areas, known as 'dambos', support very limited woody biomass (von der Heyden, 2004; Woollen et al., 2012). A number of miombo woodland tree species have been observed to invest in long taproots (Timberlake et al., 1993), an adaptation for obtaining water from deep sources.

Miombo woodlands have a mean fire return interval of 1.6 - 3 years (Frost, 1996), a figure that varies widely between regions (Archibald et al., 2010). The vast majority of fires in miombo woodlands are ignited by humans (Chidumayo and Gumbo, 2012), often originating accidentally from burning during land preparation or making charcoal, but also set deliberately whilst hunting, clearing land to reduce wildlife hazards or to stimulate grass growth for livestock (Frost, 1996). Fires are mostly fuelled by the C_4 grass understory, which grows up to 2 metres in height during the rainy season and dries out to form a highly flammable and well aerated fuel. Woody material also burns and may continue to smoulder long after the fire front has passed,

Figure 1.6: Results of a 50 year fire experiment in miombo woodlands in Marondera, Zimbabwe (Furley et al., 2008). Clockwise from top left, images show the outcome of annual burns, triennial burns, quadrennial burns and exclusion of fire. *Images by Casey Ryan*.

though this is a much less significant source of fuel than grasses (Chidumayo and Gumbo, 2012). Fire is an important determinant of C stocks in miombo woodlands (Trapnell, 1959; Furley et al., 2008; Ryan and Williams, 2011), and has a profound impact on vegetation structure (Fig. 1.6). A high frequency of severe fires can shift woodlands to an open state where grasses dominate, wheres reductions in fire regime severity can lead to canopy-closure and the exclusion of C_4 grasses (Trapnell, 1959). The capacity of fire to alter woodland structure has made modification of fire regimes a central goal of many miombo woodland management plans.

Miombo woodlands sustain a population of over 100 million people (Syampungani et al., 2009), most of whom are poor and heavily reliant on the resources that woodlands provide. African woodlands provide a range of environmental goods

Figure 1.7: Miombo woodlands are threatened by deforestation and degradation resulting from a range of human uses. Clockwise from top left, images show examples of smallholder agriculture, timber extraction, fire, and charcoal production in Kilwa District, Tanzania.

and services, including charcoal and fuelwood (Jones et al., 2016; Woollen et al., 2016), construction materials (Kalaba et al., 2013), traditional medicine (Stangeland et al., 2008), and food (Carpaneto and Fusari, 2000; Akinnifesi et al., 2006). Miombo woodlands are in a state of rapid change. Large and growing populations have placed pressure on African woodlands, with ecosystems under pressure from agricultural expansion (Ryan et al., 2012), timber and charcoal extraction (Ahrends et al., 2010), and, reportedly, fire (Fig. 1.7). Rates of deforestation in miombo woodlands are high (Hansen et al., 2013), largely driven by expansion of smallholder agriculture (Fisher, 2010), though its magnitude may be equalled by less readily-detected woodland degradation (Ryan et al., 2012). The future of miombo woodlands is in the balance; over half of global population growth before 2050 is projected to occur in Africa, with

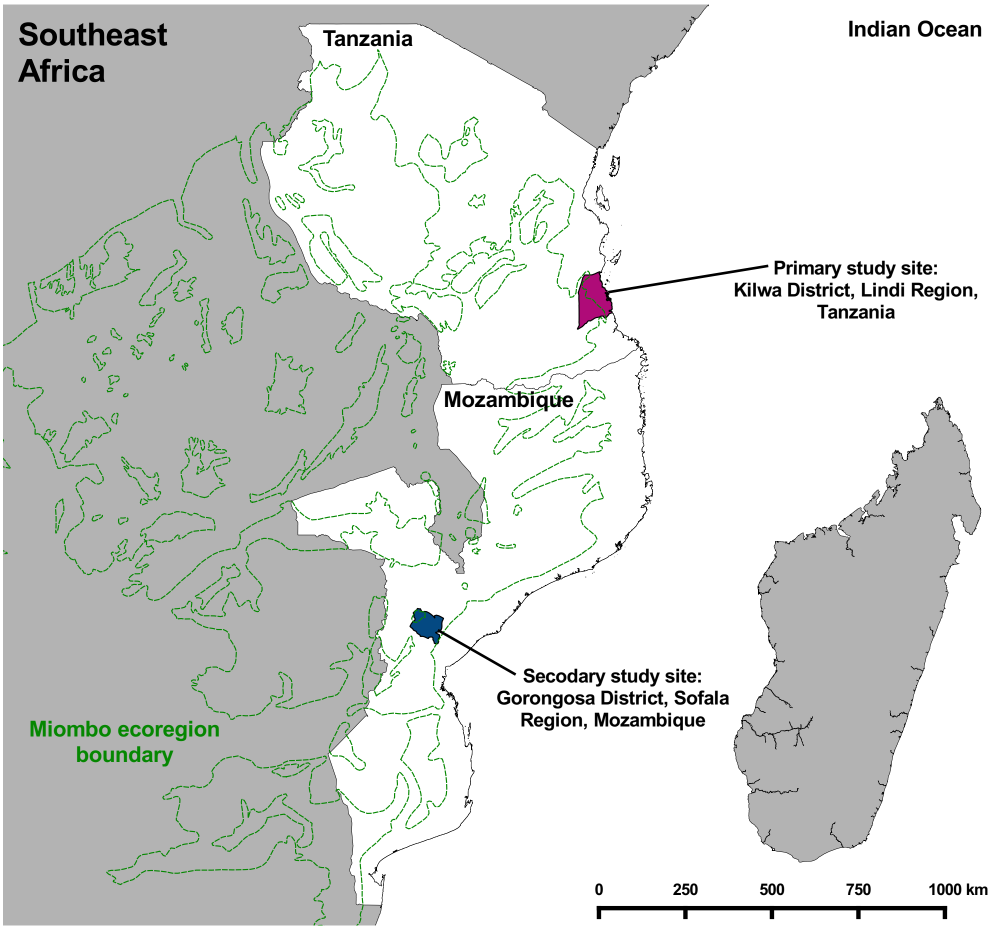

Figure 1.8: Location of Kilwa District and Gorongosa District study sites in southeast Africa, overlaid with the Eastern miombo ecoregion boundary (Olson et al., 2001).

the population of the least developed countries such as Tanzania projected to quintuple by 2100 (United Nations, 2015). Future expansion of smallholder and commercial agriculture will likely result in further largescale deforestation (Laurance et al., 2014; Searchinger et al., 2015), whilst future climate change threatens the long-term stability of African woodlands.

1.4 Overview of the study areas

1.4.1 Kilwa District

This thesis makes particular reference to Kilwa District of Tanzania, a low lying region of 13,920 km^2 located in southeastern Tanzania between the Indian Ocean and the Selous Game Reserve (Fig. 1.8). Kilwa District is location of the 'Kilwa lowland forest mosaic', a dynamic patchwork of miombo woodland and coastal forest variants. As a result of its relative isolation, Kilwa District has some of the least modified vegetation of Tanzania (Milledge et al., 2007), including several patches of internationally important East African coastal forest (Myers et al., 2000; Prins and Clarke, 2007).

Annual rainfall in Kilwa District averages 900 - 1100 mm/yr (McNicol, 2014), placing vegetation between the 'dry' and 'wet' categories of miombo woodland. Precipitation shows considerable inter-annual variation and is highly seasonal; typically there will be a short period of rains from November to January, followed by a relatively dry February, then a heavier rainy season from March to May. A dry season follows, during which the majority of fire activity is observed. Like much of the region, soils in Kilwa District are mostly sandy in texture and nutrient-poor. Miombo woodlands in Kilwa District have been observed to burn frequently, largely in the late dry season.

Kilwa District has a small population of around 175,000, equivalent to 12.6 people/km^2. The majority of Kilwa's inhabitants are subsistence farmers practising shifting cultivation, with other important sources of income including timber extraction, charcoal production, fishing, and hunting. Most of the population of Kilwa District is very poor; they live in houses constructed of mud and grass, get water from an unprotected well, and light their houses using a kerosine wick lamp (Tanzania

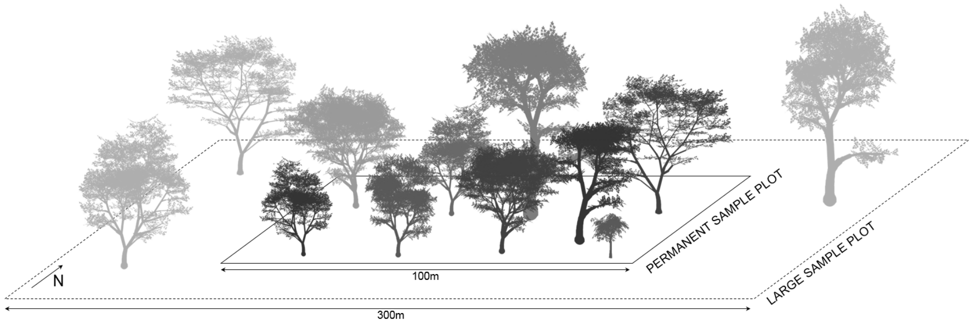

Figure 1.9: Layout of the 25 Permanent Sample Plots (PSPs) established in Kilwa District in 2010/11.

National Bureau of Statistics, 2002). The miombo woodlands of Kilwa District are under pressure from shifting cultivation (McNicol et al., 2015) and timber extraction (Ahrends et al., 2010), though the extent of woodland utilisation and its long-term impacts are unclear.

Kilwa District is location of 25 recently established Permanent Sample Plots (PSPs), which aim to characterise woody biomass, species composition, and environmental variation of a miombo woodland landscape. PSPs are 1 hectare in size (100 x 100 m), in which all tree stems greater than 5 cm diameter at breast height (DBH) were identified and measured with diameter tape once in 2010/11, and re-measured in 2012/13. To ensure effective measurement of relatively rare large tree stems, an additional Large Sample Plot (LSP) was established at each location covering 300 x 300 m in which all stems > 40 cm DBH were measured (Fig. 1.9). Kilwa District has ahosted a chronosequence study that measures woodland regrowth rate following clearance events (McNicol et al., 2015), providing an estimate of woody productivity. Kilwa District is also the focus of two novel medium resolution remote sensing datasets measuring aboveground woody biomass and fire frequency, allowing for a landscape view of the distribution of vegetation structures and fire activity.

The Mpingo Conservation & Development Initiative (MCDI) are an organisation based in Kilwa District, and partners in the funding of this PhD project. Established in 1995, MCDI promotes the environmentally sustainable and socially equitable exploitation of valuable 'mpingo' trees (East African blackwood, *Dalbergia melanoxylon*). The work of MCDI has enabled local communities to sell Forest Stewardship Council (FSC) certified mpingo to markets that seek demonstrably legal and sustainably produced timber, helping it attain a premium price that incentivises its sustainable management (MCDI, 2011). In 2009 MCDI were awarded a grant of USD $1.95 million from the Royal Norwegian Embassy in Tanzania to develop a project to allow villages to benefit from the carbon value of the woodlands under community management (MCDI, 2012; VCS, 2015). The project aims to reduce miombo woodland degradation resulting from severe late dry season fires. It is predicted that ignition of fires early in the year will prevent the build up of highly flammable dry fuel, and reduce the loss of biomass from high intensity fires in the late dry season. The University of Edinburgh worked with MCDI to characterise Kilwa District's historical fire regime, and model the impacts of an early burning regime on miombo woodland C storage.

1.4.2 Gorongosa District

Gorongosa District is located in Sofala Province of central Mozambique (Fig. 1.8), and data gathered in this region are used extensively in this thesis. Vegetation in Gorongosa District is similar to that of Kilwa District, largely consisting of miombo woodlands. Rainfall in Gorongosa District is similar to Kilwa District, with annual precipitation averaging 850 mm/yr, with a similar seasonality to that of Kilwa District (Ryan, 2009). Miombo woodlands in this region have hosted a series of experimental fires where fire intensity and tree top-kill rates were quantified (Ryan and Williams, 2011). Data from this site produced a series of allometric equations used for estimation of aboveground biomass (AGB) (Ryan et al., 2011). Gorongosa District is also location of a further chronosequence study used to estimate woodland regrowth rate (Williams et al., 2008).

1.5 Thesis objectives and overview

The objective of this thesis is to improve our understanding of the miombo woodland C cycle. Using PSP data from Kilwa District I investigate the state and variability of miombo woodlands, and aim to identify the primary drivers of landscape heterogeneity. PSP re-inventory data are used to investigate the woody C cycle, and to test how tree demographic rates in miombo woodlands respond to resource availability and disturbance. I use a process-based model and remote sensing observations to predict the impact of fire management on miombo woodland biomass. Finally, I retrieve spatially-explicit estimates of C cycle state and process variables across southern Africa by combining remote sensing observations with a mass balance model of the C cycle. I use these studies to address the following important and presently unresolved research questions:

1. What are the causes and consequences of structural heterogeneity in miombo woodlands?
2. What is the role of fire in miombo woodlands?
3. How can we most effectively resolve the carbon cycle of miombo woodlands?

This thesis is structured as four stand-alone research chapters, each of which is intended for publication. Below I summarise the objectives of each research chapter, and state their key research questions and hypotheses. In the final chapter I summarise the results of this thesis, discuss its implications for the quantification of the African C cycle, and identify important areas for further research.

1.5.1 Paper 1: Floristic and functional divergence in an East African savannah-forest mosaic

Some of the largest uncertainties in the terrestrial C balance stem from a poor knowledge of the size of vegetation C pools, and how they vary spatially (Houghton, 2005). Miombo woodland landscapes are extremely heterogeneous, with a range of vegetation structures persisting within landscapes, which support a diversity of species communities (Backéus et al., 2006; Ribeiro et al., 2008; McNicol, 2014; Jew et al., 2016). Vegetation can take the form of open savannahs dominated by grasses, woodlands where grasses and trees are co-dominant, and closed-canopy forests where C_4 grasses are excluded. The factors maintaining heterogeneous vegetation structures in climatically homogeneous landscapes are not well understood. Prominent hypotheses suggest that vegetation structure may be an expression of bottom-up regulation from differences in soil fertility and water supply, top-down regulation from fire and herbivory, or random alternate stable-states. Determination of which processes affect vegetation dynamics is of importance for modelling of the C cycle, and projecting how future changes to management and climate will modify their distributions in the future.

In addition to differences in floristic composition and vegetation structure, plant communities display a range of adaptations to environmental conditions. For instance, areas with a high frequency of fire may be associated with thick bark, nutrient deficiency with N-fixing strategies or ectomycorrhizae, and water limitation with physiological adaptations for water-use efficiency and drought tolerance. These strategies can be identified through measurement of plant functional traits, which are morphological, anatomical, physiological, biochemical and phenological characteristics that reflect how plants are adapted to their environment (Kattge et al., 2011). By diagnosing the functional traits present in plant communities we can interpret which processes are acting to promote or exclude certain growth forms, and identify the main drivers of vegetation heterogeneity.

The objective of this paper is to explore variation of tree species communities, environmental properties, and plant functional traits associated with divergent vegetation structures in Kilwa District. I present tree species composition data from the Kilwa District PSP network. I measure a range of biotic and abiotic environmental characteristics at each PSP, which describe vegetation structure, fire susceptibility, soil properties, and water supply. I also construct a database of 11 commonly measured plant functional traits for 30 species, which together describe the adaptations of species to competition, disturbance, water stress, and nutrient limitation.

In this paper I address the following hypotheses:

1. Heterogeneous vegetation structures in miombo woodland landscapes are composed of divergent tree communities which are associated with differing disturbance regimes, hydrology, and soil properties.

2. Functional traits vary between tree species and communities, reflecting evolutionary trade-offs and environmental filtering into assemblages.

3. Tree community assembly is driven by a combination of disturbance, water supply, nutrient limitation, and competition for light.

1.5.2 Paper 2: What drives variation in woody productivity and tree mortality in miombo woodlands?

Woody C stocks are the largest living biomass pool in miombo woodlands (Ryan et al., 2011). Despite their importance, there exist few robust estimates of the size of this C pool, with a particular deficiency in repeat-measurements of *in situ* plots to estimate woody C fluxes. Key parameters such as woody productivity and C residence times are not well constrained in miombo woodlands, contributing to large uncertainties in the African C cycle (Friend et al., 2014). Moreover, we do not have a clear idea how these vary with landscape heterogeneity.

The magnitude of C fluxes in savannahs is closely related to tree population dynamics, where demographic transitions exert a large influence on vegetation structure. For example, stem growth rates relate to the probability of juvenile stems escaping from fire, and rates of stem top-kill are associated with canopy openness and exposure to fire (Hoffmann et al., 2012). Reliable estimates of stem growth, mortality and recruitment are therefore important for building accurate predictive models of miombo woodland C cycling. Demographic rates in savannah ecosystems may be mediated by a number of processes, including fire, nutrient availability, hydrology, and canopy cover (Bond, 2008), though the size of these effects and their relative importance is not clear.

In this paper I use re-measurement data from 12,201 tree stems in the Kilwa District PSP network to quantify rates of tree growth, mortality and recruitment. Allometric equations are used to generate estimates of woody productivity, C residence times, as well as first estimates of net woody biomass change. I assess the impact of a range of environmental (vegetation structure, fire, soil properties) and stem-specific (damage, size, competitive stress) measurements on stem growth and mortality to identify which are the key processes regulating savannah demographic rates.

I addresses the following research questions:

1. What are rates of woody carbon cycling in miombo woodlands, and how do they vary?
2. What are rates of growth, mortality and recruitment in miombo woodlands, and how do they vary?

3. What biotic and abiotic processes regulate demographic rates in miombo woodlands?

1.5.3 Paper 3: Early burning in miombo woodlands for climate change mitigation

There is an urgent requirement for viable strategies to combat widespread and rapid loss of miombo woodlands. Recent efforts to reduce deforestation and degradation have focussed on valuing woodland resources effectively and paying for the ecosystem services they provide. One such mechanism, the Reducing Emissions from Deforestation and forest Degradation (REDD+) programme of the United Nations, aims to reduce net emissions of C through payments for improved forest management (UNFCCC, 2014). Monitoring for degradation of miombo woodlands is particularly challenging. For instance, it is difficult to determine whether fire is increasing and resulting in degradation of miombo woodlands over landscapes. Though the effects of fire on miombo woodland structure are significant (Trapnell, 1959; Furley et al., 2008; Ryan and Williams, 2011), we possess few practical methods to predict its impacts on woody biomass.

In this chapter I report MCDI's pilot REDD+ project, which aims to introduce early burning to miombo woodlands as a management tool. The method uses burn scar measurements from a 10 year time-series of Landsat imagery to determine a baseline frequency of early and late season fires. A process-based model is used to predict the change in biomass resulting from a continuation of the baseline fire regime and a range of scenarios under an early burning project. I assess the reliability of the model, and discuss strategies to generate useful estimates of woody biomass change given limitations in model driving data and parameterisation.

I address the following key research questions:

1. What is the likely magnitude of emissions reductions achieved from early burning in miombo woodlands?

2. What are the key uncertainties in the method, and how can uncertainty be mitigated in an operational fire-management project?

1.5.4 Paper 4: Retrieval of a data-consistent carbon cycle for southern Africa

Uncertainty in the terrestrial C cycle is substantial (Le Quéré et al., 2013), with obstacles to constraining the terrestrial C budget particularly great in tropical ecosystems such as miombo woodlands, where the size of C pools, C allocation patterns and C residence times are highly uncertain. Though *in situ* ecological measurements are limited, an abundance of remote sensing data is now available over southern Africa, providing information on canopy properties, woody biomass and fire emissions. One approach to using this data to constrain the miombo woodland C cycle exists in model-data fusion (MDF) techniques, where observational data are merged with a vegetation models to generate data-consistent estimates of the C cycle and quantify parametric uncertainty.

In this study I use the CARbon DAta MOdel fraMework (CARDAMOM) to generate estimates of the magnitudes of C pools and fluxes across southern Africa (Bloom et al., 2016). Retrieved C cycle parameters are used to quantify the C cycle of the miombo ecoregion, and calculate whether miombo woodlands are a net sink or source of C to the atmosphere. Spatial differences in C cycle dynamics are indicative of variation in ecosystem functional properties, and so can be used to investigate the nature of savannah heterogeneity over continental spatial-scales. I compare ecosystem functional properties to a range of environmental characteristics relating to vegetation structure, precipitation, soil properties, disturbance, and anthropogenic management to identify the major drivers of miombo woodland heterogeneity over large scales.

I aim to answer the following key research questions:

1. What is the magnitude of carbon fluxes and residence times in the miombo ecoregion?
2. Is vegetation in the miombo ecoregion a net source or sink of carbon?
3. How do ecosystem functional properties vary across the miombo woodland ecoregion, and what are its main environmental drivers?

1.6 References

Ahrends, A., Burgess, N.D., Milledge, S.A.H., Bulling, M.T., Fisher, B., Smart, J.C.R., Clarke, G.P., Mhoro, B.E., and Lewis, S.L. (2010), 'Predictable waves of sequential forest degradation and biodiversity loss spreading from an African city', *Proceedings of the National Academy of Sciences*, **107**, pp. 14556–14561.

Akinnifesi, F.K., Kwesiga, F., Mhango, J., Chilanga, T., Mkonda, A., Kadu, C.A.C., Kadzere, I., Mithofer, D., Saka, J.D.K., Sileshi, G., Ramadhani, T., and Dhilwayo, P. (2006), 'Towards the development of miombo fruit trees as commercial tree crops in southern Africa', *Forests, Trees and Livelihoods*, **16**, pp. 103–121.

Archibald, S. and Scholes, R.J. (2007), 'Leaf green-up in a semi-arid African savanna-separating tree and grass responses to environmental cues', *Journal of Vegetation Science*, **18**, pp. 583–594.

Archibald, S., Scholes, R.J., Roy, D.P., Roberts, G., and Boschetti, L. (2010), 'Southern African fire regimes as revealed by remote sensing', *International Journal of Wildland Fire*, **19**, pp. 861–878.

Baccini, A., Goetz, S.J., Walker, W.S., Laporte, N.T., Sun, M., Sulla-Menashe, D., Hackler, J., Beck, P.S.A., Dubayah, R., Friedl, M.A., Samanta, S., and Houghton, R.A. (2012), 'Estimated carbon dioxide emissions from tropical deforestation improved by carbon-density maps', *Nature Climate Change*, **2**, pp. 182–185.

Backéus, I., Pettersson, B., Strömquist, L., and Ruffo, C. (2006), 'Tree communities and structural dynamics in miombo (Brachystegia–Julbernardia) woodland, Tanzania', *Forest Ecology and Management*, **230**, pp. 171–178.

Bloom, A.A., Exbrayat, J.-F., van der Velde, I.R., Feng, L., and Williams, M. (2016), 'The decadal state of the terrestrial carbon cycle: Global retrievals of terrestrial carbon allocation, pools, and residence times', *Proceedings of the National Academy of Sciences*, **113**, pp. 1285–1290.

Boden, T.A., Marland, G., and Andres, R.J. (2011), *Global, regional, and national fossil fuel CO_2 emissions*, Carbon Dioxide Information Analysis Center, Oak Ridge National Laboratory, U.S. Department of Energy, Tennessee, U.S.A.

Bond, W.J. (2008), 'What Limits Trees in C_4 Grasslands and Savannas?', *Annual Review of Ecology, Evolution, and Systematics*, **39**, pp. 641–659.

Bond, W.J. (2010), 'Do nutrient-poor soils inhibit development of forests? A nutrient stock analysis', *Plant and Soil*, **334**, pp. 47–60.

Bond, W.J. and Parr, C.L. (2010), 'Beyond the forest edge: ecology, diversity and conservation of the grassy biomes', *Biological Conservation*, **143**, pp. 2395–2404.

Bond, W.J., Woodward, F.I., and Midgley, G.F. (2005), 'The global distribution of ecosystems in a world without fire', *New Phytologist*, **165**, pp. 525–538.

Bowman, D.M.J.S., Balch, J.K., Artaxo, P., Bond, W.J., Carlson, J.M., Cochrane, M.A., D'Antonio, C.M., DeFries, R.S., Doyle, J.C., Harrison, S.P., Johnston, F.H., Keeley, J.E., Krawchuk, M.A., Christian, A.K., Marston, J.B., Moritz, M.A., Prentice, I.C., Roos, C.I., Scott, A.C., Swetnam, T.W., van der Werf, G.R., and Pyne, S.J. (2009), 'Fire in the Earth system', *Science*, **324**, pp. 481–484.

Carpaneto, G.M. and Fusari, A. (2000), 'Subsistence hunting and bushmeat exploitation in central-western Tanzania', *Biodiversity & Conservation*, **9**, pp. 1571–1585.

Chidumayo, E.N. (2001), 'Climate and phenology of savanna vegetation in southern Africa', *Journal of Vegetation Science*, **12**, pp. 347–354.

Chidumayo, E.N. and Gumbo, D.J. (2012), *The Dry Forests and Woodlands of Africa: Managing for Products and Services*, London, UK: Earthscan.

Ciais, P., Bombelli, A., Williams, M., Piao, S.L., Chave, J., Ryan, C.M., Henry, M., Brender, P., and Valentini, R. (2011), 'The carbon balance of Africa: synthesis of recent research studies', *Philosophical Transactions of the Royal Society of London A: Mathematical, Physical and Engineering Sciences*, **369**, pp. 2038–2057.

Cole, M.M. (1986), *The savannas: Biogeography and Geobotany*, Academic Press.

Conway, T.J. and Tans, P.P. (2016), *Trends in atmospheric carbon dioxide*, url: `http://www.esrl.noaa.gov/gmd/ccgg/trends/` (visited on 06/22/2016).

FAO (2007), *State of the World's Forests 2007*, Food & Agriculture Organisation.

Fischer, G., Nachtergaele, F., Prieler, S., Velthuizen, H.T. van, Verelst, L., and Wiberg, D. (2008), *Global Agro-ecological Zones Assessment for Agriculture (GAEZ 2008)*, IIASA, Laxenburg, Austria and FAO, Rome, Italy.

Fisher, B. (2010), 'African exception to drivers of deforestation', *Nature Geoscience*, **3**, pp. 375–376.

Friend, A.D., Lucht, W., Rademacher, T.T., Keribin, R., Betts, R., Cadule, P., Ciais, P., Clark, D.B., Dankers, R., Falloon, P.D., Ito, A., Kahana, R., Kleidon, A., Lomas, M.R., Nishina, K., Ostberg, S., Pavlick, R., Peylin, P., Chaphoff, S., Vuichard, N., Warszawski, L., Wiltshire, A., and Woodward, F.I. (2014), 'Carbon residence time dominates uncertainty in terrestrial vegetation responses to future climate and atmospheric CO_2', *Proceedings of the National Academy of Sciences*, **111**, pp. 3280–3285.

Frost, P. (1996), 'The ecology of miombo woodlands', *The miombo in transition: Woodlands and welfare in Africa*, ed. by B. Campbell, CIFOR, Bogor, Indonesia.

Furley, P.A., Rees, R.M., Ryan, C.M., and Saiz, G. (2008), 'Savanna burning and the assessment of long-term fire experiments with particular reference to Zimbabwe', *Progress in Physical Geography*, **32**, pp. 611–634.

Gerber, S., Joos, F., Brügger, P., Stocker, T., Mann, M., Sitch, S., and Scholze, M. (2003), 'Constraining temperature variations over the last millennium by comparing simulated and observed atmospheric CO_2', *Climate Dynamics*, **20**, pp. 281–299.

Giglio, L., Randerson, J.T., and Werf, G.R. (2013), ‘Analysis of daily, monthly, and annual burned area using the fourth-generation global fire emissions database (GFED4)’, *Biogeosciences*, **118**, pp. 317–328.

Grace, J., José, J.S., Meir, P., Miranda, H.S., and Montes, R.A. (2006), ‘Productivity and carbon fluxes of tropical savannas’, *Journal of Biogeography*, **33**, pp. 387–400.

Hansen, M.C., Potapov, P.V., Moore, R., Hancher, M., Turubanova, S.A., Tyukavina, A., Thau, D., Stehman, S.V., Goetz, S.J., Loveland, T.R., Kommareddy, A., Egorov, A., Chini, L., O, J.C., and Townshend, J.R.G. (2013), ‘High-resolution global maps of 21st-century forest cover change’, *Science*, **342**, pp. 850–853.

Hantson, S., Arneth, A., Harrison, S.P., Kelley, D.I., Prentice, I.C., Rabin, S.S., Archibald, S., Mouillot, F., Arnold, S.R., Artaxo, P., Bachelet, D., Ciais, P., Forrest, M., Friedlingstein, P., Hickler, T., Kaplan, J.O., Kloser, S., Knorr, W., Lasslop, G., Li, F., Mangeon, S., Melton, J.R., Meyn, A., Sitch, S., Spessa, A., van der Werf, G.R., Voulgarakis, A., and Yue, C. (2016), ‘The status and challenge of global fire modelling’, *Biogeosciences*, **13**, pp. 3359–3375.

Hoffmann, W.A., Adasme, R., Haridasan, M., de Carvalho, M.T., Geiger, E.L., Pereira, M.A.B., Gotsch, S.G., and Franco, A.C. (2009), ‘Tree topkill, not mortality, governs the dynamics of savanna-forest boundaries under frequent fire in central Brazil’, *Ecology*, **90**, pp. 1326–1337.

Hoffmann, W.A., Geiger, E.L., Gotsch, S.G., Rossatto, D.R., Silva, L.C.R., Lau, O.L., Haridasan, M., and Franco, A.C. (2012), ‘Ecological thresholds at the savanna-forest boundary: how plant traits, resources and fire govern the distribution of tropical biomes’, *Ecology Letters*, **15**, pp. 759–768.

Hoffmann, W.A., Orthen, B., and Nascimento, P.K.V.d. (2003), ‘Comparative fire ecology of tropical savanna and forest trees’, *Functional Ecology*, **17**, pp. 720–726.

Högberg, P. and Piearce, G.D. (1986), ‘Mycorrhizas in Zambian trees in relation to host taxonomy, vegetation type and successional patterns’, *Journal of Ecology*, **74**, pp. 775–785.

Högberg, P. (1986), ‘Nitrogen-fixation and nutrient relations in savanna woodland trees (Tanzania)’, *Journal of Applied Ecology*, **23**, pp. 675–688.

Holdridge, L.R. (1947), ‘Determination of World Plant Formations From Simple Climatic Data’, *Science*, **105**, pp. 367–368.

Houghton, R.A. (2005), ‘Aboveground forest biomass and the global carbon balance’, *Global Change Biology*, **11**, pp. 945–958.

Houghton, R.A., House, J.I., Pongratz, J., van der Werf, G.R., DeFries, R.S., Hansen, M.C., Le Quéré, C., and Ramankutty, N. (2012), ‘Carbon emissions from land use and land-cover change’, *Journal of Geophysical Research: Biogeosciences*, **9**, pp. 5125–5142.

IPCC (2013), *Summary for Policymakers*, ed. by T.F. Stocker, D. Qin, G.-K. Plattner, M. Tignor, S.K. Allen, J. Boschung, A. Nauels, Y. Xia, V. Bex, and P.M. Midgley, Cambridge, U.K and New York, NY, U.S.A: Cambridge University Press, url: `http://www.climatechange2013.org`.

Jew, E.K.K., Dougill, A.J., Sallu, S.M., O'Connell, J., and Benton, T.G. (2016), 'Miombo woodland under threat: Consequences for tree diversity and carbon storage', *Forest Ecology and Management*, **361**, pp. 144–153.

Jones, D., Ryan, C.M., and Fisher, J. (2016), 'Charcoal as a diversification strategy: The flexible role of charcoal production in the livelihoods of smallholders in central Mozambique', *Energy for Sustainable Development*, **32**, pp. 14–21.

Kalaba, F.K., Quinn, C.H., and Dougill, A.J. (2013), 'Contribution of forest provisioning ecosystem services to rural livelihoods in the Miombo woodlands of Zambia', *Population and Environment*, **35**, pp. 159–182.

Kattge, J., Diaz, S., Lavorel, S., Prentice, C., Leadley, P., Boenisch, G., Garnier, E., Westoby, M., Reich, P.B., Wright, I.J., Cornelissen, J.H.C., Violle, C., Harrison, S.P., van, B.P.M., Reichstein, M., Enquist, B.J., Soudzilovskaia, N.A., Ackerly, D.D., Anand, M., Atkin, O., Bahn, M., Baker, T.R., Baldocchi, D., Bekker, R., Blanco, C.C., Blonder, B., Bond, W.J., Bradstock, R., Bunker, D.E., Casanoves, F., Cavender-Bares, J., Chambers, J.Q., Chapin, F.S., Chave, J., Coomes, D., Cornwell, W.K., Craine, J.M., Dobrin, B.H., Duarte, L., Durka, W., Elser, J., Esser, G., Estiarte, M., Fagan, W.F., Fang, J., Fernandez-Mendez, F., Fidelis, A., Finegan, B., Flores, O., Ford, H., Frank, D., Freschet, G.T., Fyllas, N.M., Gallagher, R.V., Green, W.A., Gutierrez, A.G., Hickler, T., Higgins, S.I., Hodgson, J.G., Jalili, A., Jansen, S., Joly, C.A., Kerkhoff, A.J., Kirkup, D., Kitajima, K., Kleyer, M., Klotz, S., Knops, J.M.H., Kramer, K., Kühn, I.., Kurokawa, H., Laughlin, D., Lee, T.D., Leishman, M., Lens, F., Lenz, T., Lewis, S.L., Lloyd, J., Llusià, J., Louault, F., Ma, S., Mahecha, M.D., Manning, P., Massad, T., Medlyn, B.E., Messier, J., Moles, A.T., Müller, S.C., Nadrowski, K., Naeem, S., Niinemets, Ü., Nöllert, S., Nüske, A., Ogaya, R., Oleksyn, J., Onipchenko, V.G., Onoda, Y., Ordoñez, J., Overbeck, G., Ozinga, W.A., Patiño, S., Paula, S., Pausas, J.G., Peñuelas, J., Phillips, O.L., Pillar, V., Poorter, H., Poorter, L., Poschlod, P., Prinzing, A., Proulx, R., Rammig, A., Reinsch, S., Reu, B., Sack, L., Salgado-negret, B., Sardans, J., Shiodera, S., Shipley, B., Siefert, A., Sosinski, E., Soussana, J.-f., Swaine, E., Swenson, N., Thompson, K., Thornton, P., Waldram, M., Weiher, E., White, M., White, S., Wright, S.J., Yguel, B., Zaehle, S., Zanne, A.E., and Wirth, C. (2011), 'TRY–a global database of plant traits', *Global Change Biology*, **17**, pp. 2905–2935.

Keeling, C.D., Bacastow, R.B., Bainbridge, A.E., Ekdahl, C.A., Guenther, P.R., Waterman, L.S., and Chin, J.F.S. (1976), 'Atmospheric carbon dioxide variations at Mauna Loa observatory, Hawaii', *Tellus*, **28**, pp. 538–551.

Laurance, W.F., Sayer, J., and Cassman, K.G. (2014), 'Agricultural expansion and its impacts on tropical nature', *Trends in ecology & evolution*, **29**, pp. 107–116.

Le Quéré, C., Andres, R.J., Boden, T., Conway, T., Houghton, R.A., House, J.I., Marland, G., Peters, G.P., van der Werf, G.R., Ahlström, A., Andrew, R.M., Bopp, L., Canadell, J.G., Ciais, P., Doney, S.C., Enright, C., Friedlingstein, P., Huntingford, C., Jain, A.K., Jourdain, C., Kato, E., Keeling, R.F., Klein Goldewijk, K., Levis, S., Levy, P., Lomas, M., Poulter, B., Raupach, M.R., Schwinger, J., Sitch, S., Stocker, B.D., Viovy, N., Zaehle, S., and Zeng, N. (2013), 'The global carbon budget 1959–2011', *Earth System Science Data*, **5**, pp. 165–185.

Lehmann, C.E., Archibald, S.A., Hoffmann, W.A., and Bond, W.J. (2011), ‘Deciphering the distribution of the savanna biome’, *New Phytologist*, **191**, pp. 197–209.

Lewis, S.L., Lopez-Gonzalez, G., Sonke, B., Affum-Baffoe, K., Baker, T.R., Ojo, L.O., Phillips, O.L., Reitsma, J.M., White, L., Comiskey, J.A., Djuikouo, M.-N., Ewango, C.E.N., Feldpausch, T.R., Hamilton, A.C., Gloor, M., Hart, T., Hladik, A., Lloyd, J., Lovett, J.C., Makana, J.-R., Malhi, Y., Mbago, F.M., Ndangalasi, H.J., Peacock, J., Peh, K.S.H., Sheil, D., Sunderland, T., Swaine, M.D., Taplin, J., Taylor, D., Thomas, S.C., Votere, R., and Woll, H. (2009), ‘Increasing carbon storage in intact African tropical forests’, *Nature*, **457**, pp. 1003–1006.

Lüthi, D., Le Floch, M., Bereiter, B., Blunier, T., Barnola, J.-M., Siegenthaler, U., Raynaud, D., Jouzel, J., Fischer, H., Kawamura, K., and Stocker, T.F. (2008), ‘High-resolution carbon dioxide concentration record 650,000–800,000 years before present’, *Nature*, **453**, pp. 379–382.

Malhi, Y. (2010), ‘The carbon balance of tropical forest regions, 1990–2005’, *Current Opinion in Environmental Sustainability*, **2**, pp. 237–244.

MCDI (2011), *MCDI Tanzania Community-Managed Forests FSC Group: ED01 Group Administration Manual*, ED01 v3.0, Mpingo Conservation & Development Initiative, Kilwa Masoko, Tanzania.

MCDI (2012), *Combining REDD, PFM and FSC Certification in SE Tanzania: Project Revision 2012*, Mpingo Conservation & Development Initiative, Kilwa Masoko, Tanzania.

McNaughton, S.J. (1992), ‘The propagation of disturbance in savannas through food webs’, *Journal of Vegetation Science*, **3**, pp. 301–314.

McNicol, I.M. (2014), ‘Deforestation, Forest Degradation and the Carbon Cycle of African Miombo Woodlands’, PhD thesis, University of Edinburgh.

McNicol, I.M., Ryan, C.M., and Williams, M. (2015), ‘How resilient are African woodlands to disturbance from shifting cultivation?’, *Ecological Applications*, **25**, pp. 2320–2336.

Mertz, O., Müller, D., Sikor, T., Hett, C., Heinimann, A., Castella, J.-C., Lestrelin, G., Ryan, C.M., Reay, D.S., Schmidt-Vogt, D., Danielsen, F., Theilade, I., van Noordwijk, M., Verchot, L.V., Burgess, N.D., Berry, N.J., Pham, T.T., Messerli, P., Xu, J., Fensholt, R., Hostert, P., Pflugmacher, D., Bruun, T.B., de Neergaard, A., Dons, K., Dewi, S., Rutishauser, E., and Sun, Z. (2012), ‘The forgotten D: challenges of addressing forest degradation in complex mosaic landscapes under REDD+’, *Geografisk Tidsskrift-Danish Journal of Geography*, **112**, pp. 63–76.

Milledge, S.A.H., Gelvas, I.K., and Ahrends, A. (2007), *Forestry, governance and national development: Lessons learned from a logging boom in southern Tanzania*, Traffic East/Southern Africa.

Mistry, J. (2014), *World savannas: ecology and human use*, 2nd ed., Routledge.

Murphy, B.P. and Bowman, D.M.J.S. (2012), ‘What controls the distribution of tropical forest and savanna?’, *Ecology Letters*, **15**, pp. 748–758.

Myers, N., Mittermeier, R.A., Mittermeier, C.G., Da Fonseca, G.A.B., and Kent, J. (2000), 'Biodiversity hotspots for conservation priorities', *Nature*, **403**, pp. 853–858.

NOAA (2016), *National Centers for Environmental Information, State of the Climate: Global Analysis for May 2016*, url: `http://www.ncdc.noaa.gov/sotc/global/201607/` (visited on 08/29/2016).

Olson, D.M., Dinerstein, E., Wikramanayake, E.D., Burgess, N.D., Powell, G.V.N., Underwood, E.C., D'amico, J.A., Itoua, I., Strand, H.E., Morrison, J.C., Loucks, C.J., Allnutt, T.F., Ricketts, T.H., Kura, Y., Lamoreux, J.F., Wettengel, W.W., Hedao, P., and Kassem, K.R. (2001), 'Terrestrial Ecoregions of the World: A New Map of Life on Earth A new global map of terrestrial ecoregions provides an innovative tool for conserving biodiversity', *BioScience*, **51**, pp. 933–938.

Pan, Y., Birdsey, R.A., Fang, J., Houghton, R., Kauppi, P.E., Kurz, W.A., Phillips, O.L., Shvidenko, A., Lewis, S.L., Canadell, J.G., Ciais, P., Jackson, R.B., Pacala, S.W., McGuire, A.D., Piao, S., Rautiainen, A., Sitch, S., and Hayes, D. (2011), 'A large and persistent carbon sink in the world's forests', *Science*, **333**, pp. 988–993.

Prins, E. and Clarke, G.P. (2007), 'Discovery and enumeration of Swahilian Coastal Forests in Lindi region, Tanzania, using Landsat TM data analysis', *Biodiversity and Conservation*, **16**, pp. 1551–1565.

Randerson, J.T., Chen, Y., van der Werf, G.R., Rogers, B.M., and Morton, D.C. (2012), 'Global burned area and biomass burning emissions from small fires', *Journal of Geophysical Research: Biogeosciences*, **117**, G04012.

Ratnam, J., Bond, W.J., Fensham, R.J., Hoffmann, W.A., Archibald, S., Lehmann, C.E.R., Anderson, M.T., Higgins, S.I., and Sankaran, M. (2011), 'When is a 'forest' a savanna, and why does it matter?', *Global Ecology and Biogeography*, **20**, pp. 653–660.

Ribeiro, N.S., Shugart, H.H., and Washington-Allen, R. (2008), 'The effects of fire and elephants on species composition and structure of the Niassa Reserve, northern Mozambique', *Forest Ecology and Management*, **255**, pp. 1626–1636.

Rossatto, D.R., Silva, L.d.C.R., Villalobos-Vega, R., Sternberg, L.d.L., and Franco, A.C. (2012), 'Depth of water uptake in woody plants relates to groundwater level and vegetation structure along a topographic gradient in a neotropical savanna', *Environmental and Experimental Botany*, **77**, pp. 259–266.

Ruggiero, P.G.C., Batalha, M.A., Pivello, V.R., and Meirelles, S.T. (2002), 'Soil-vegetation relationships in cerrado (Brazilian savanna) and semideciduous forest, Southeastern Brazil', *Plant Ecology*, **160**, pp. 1–16.

Ryan, C.M., Hill, T., Woollen, E., Ghee, C., Mitchard, E., Cassells, G., Grace, J., Woodhouse, I.H., and Williams, M. (2012), 'Quantifying small-scale deforestation and forest degradation in African woodlands using radar imagery', *Global Change Biology*, **18**, pp. 243–257.

Ryan, C.M. and Williams, M. (2011), ‘How does fire intensity and frequency affect miombo woodland tree populations and biomass?’, *Ecological Applications*, **21**, pp. 48–60.

Ryan, C.M., Williams, M., and Grace, J. (2011), ‘Above-and Belowground Carbon Stocks in a Miombo Woodland Landscape of Mozambique’, *Biotropica*, **43**, pp. 423–432.

Ryan, C.M. (2009), ‘Carbon cycling, fire and phenology in a tropical savanna woodland in Nhambita, Mozambique’, PhD thesis, The University of Edinburgh.

Saatchi, S.S., Harris, N.L., Brown, S., Lefsky, M., Mitchard, E.T.A., Salas, W., Zutta, B.R., Buermann, W., Lewis, S.L., Hagen, S., Petrova, S., White, L., Silman, M., and Morel, A. (2011), ‘Benchmark map of forest carbon stocks in tropical regions across three continents’, *Proceedings of the National Academy of Sciences*, **108**, pp. 9899–9904.

Sage, R.F. (2004), ‘The evolution of C_4 photosynthesis’, *New phytologist*, **161**, pp. 341–370.

Sankaran, M., Hanan, N.P., Scholes, R.J., Ratnam, J., Augustine, D.J., Cade, B.S., Gignoux, J., Higgins, S.I., Le Roux, X., Ludwig, F., Ardo, J., Banyikwa, F., Bronn, A., Bucini, G., Caylor, K.K., Coughenour, M.B., Diouf, A., Ekaya, W., Feral, C.J., February, E.C., Frost, P.G.H., Hiernaux, P., Hrabar, H., Metzger, K.L., Prins, H.H.T., Ringrose, S., Sea, W., Tews, J., Worden, J., and Zambatis, N. (2005), ‘Determinants of woody cover in African savannas’, *Nature*, **438**, pp. 846–849.

Schimper, A.F.W. (1898), *Pflanzen-geographie auf physiologischer Grundlage*, Jena: Verlag von Gustav Fischer.

Scholes, B. (2009), ‘Why is it so hard to sustain a flux network in Africa’, *The Newsletter of FLUXNET*, **2**, pp. 4–5.

Scholes, R.J. and Walker, B.H. (1993), *Nylsvley: the study of an African savanna*, Cambridge University Press, Cambridge, UK.

Searchinger, T.D., Estes, L., Thornton, P.K., Beringer, T., Notenbaert, A., Rubenstein, D., Heimlich, R., Licker, R., and Herrero, M. (2015), ‘High carbon and biodiversity costs from converting Africa/’s wet savannahs to cropland’, *Nature Climate Change*, **5**, pp. 481–486.

Stangeland, T., Dhillion, S.S., and Reksten, H. (2008), ‘Recognition and development of traditional medicine in Tanzania’, *Journal of ethnopharmacology*, **117**, pp. 290–299.

Staver, A.C., Archibald, S., and Levin, S.A. (2011), ‘The global extent and determinants of savanna and forest as alternative biome states’, *Science*, **334**, pp. 230–232.

Steffen, W., Crutzen, P.J., and McNeill, J.R. (2007), ‘The Anthropocene: are humans now overwhelming the great forces of nature’, *AMBIO: A Journal of the Human Environment*, **36**, pp. 614–621.

Sundquist, E.T. (1986), ‘Geologic analogs: Their value and limitations in carbon dioxide research’, *The changing carbon cycle*, Springer, pp. 371–402.

Syampungani, S., Chirwa, P.W., Akinnifesi, F.K., Sileshi, G., and Ajayi, O.C. (2009), 'The miombo woodlands at the cross roads: Potential threats, sustainable livelihoods, policy gaps and challenges', *Natural Resources Forum*, **33**, pp. 150–159.

Tanzania National Bureau of Statistics (2002), *Tanzania Population and Housing Census*, Ministry of Planning, Economy and Empowerment, Dodoma, Tanzania.

Timberlake, J.R., Calvert, G.M., and Morris, J.A. (1993), 'Preliminary root atlas for Zimbabwe and Zambia', **96**.

Trapnell, C. (1959), 'Ecological results of woodland and burning experiments in Northern Rhodesia', *The Journal of Ecology*, **41**, pp. 129–168.

UNFCCC (2014), *Report of the Conference of the Parties on its nineteenth session, held in Warsaw from 11 to 23 November 2013*, FCCC/CP/2013/10, United Nations Framework Convention on Climate Change, url: `http://unfccc.int/meetings/warsaw_nov_2013/meeting/7649/php/view/reports.php` (visited on 07/21/2016).

United Nations (2015), *World Population Prospects: The 2015 Revision, Key Findings and Advance Tables*, VESA/P/WP.241, United Nations Department of Economic and Social Affairs, url: `http://esa.un.org/unpd/wpp/Publications/`.

van der Werf, G.R., Morton, D.C., DeFries, R.S., Olivier, J.G.J., Kasibhatla, P.S., Jackson, R.B., Collatz, G.J., and Randerson, J.T. (2009), 'CO_2 emissions from forest loss', *Nature geoscience*, **2**, pp. 737–738.

van der Werf, G.R., Randerson, J.T., Giglio, L., Collatz, G.J., Mu, M., Kasibhatla, P.S., Morton, D.C., DeFries, R.S., van Jin, Y., and van Leeuwen, T.T. (2010), 'Global fire emissions and the contribution of deforestation, savanna, forest, agricultural, and peat fires (1997–2009)', *Atmospheric Chemistry and Physics*, **10**, pp. 11707–11735.

van Langevelde, F., van De Vijver, C.A., Kumar, L., van De Koppel, J., De Ridder, N., Van Andel, J., Skidmore, A.K., Hearne, J.W., Stroosnijder, L., Bond, W.J., Prins, H.H.T., and Rietkere, M. (2003), 'Effects of fire and herbivory on the stability of savanna ecosystems', *Ecology*, **84**, pp. 337–350.

VCS (2015), *Methodology for Avoided Forest Degradation through Fire Management.* VM0029, Verified Carbon Standard, url: `http://www.v-c-s.org/methodologies/avoiding-degradation-through-fire-management/`.

von der Heyden, C.J. (2004), 'The hydrology and hydrogeology of dambos: a review', *Progress in Physical Geography*, **28**, pp. 544–564.

Walter, H., Burnett, J.H., and Mueller-Dombois, D. (1971), *Ecology of tropical and subtropical vegetation*, Oliver and Boyd, Edinburgh.

White, F. (1983), *The vegetation of Africa: a descriptive memoir to accompany the Unesco/AETFAT/UNSO vegetation map of Africa*, UNESCO, Paris, France.

Williams, C.A., Hanan, N.P., Neff, J.C., Scholes, R.J., Berry, J.A., Denning, S.A., and Baker, D.F. (2007), ‘Africa and the global carbon cycle’, *Carbon balance and management*, **2**, pp. 1–13.

Williams, M., Ryan, C.M., Rees, R.M., Sambane, E., Fernando, J., and Grace, J. (2008), ‘Carbon sequestration and biodiversity of re-growing miombo woodlands in Mozambique’, *Forest Ecology and management*, **254**, pp. 145–155.

Woollen, E., Ryan, C.M., Baumert, S., Vollmer, F., Grundy, I., Fisher, J., Fernando, J., Luz, A., Ribeiro, N., and Lisboa, S.N. (2016), ‘Charcoal production in the Mopane woodlands of Mozambique: what are the trade-offs with other ecosystem services?’, *Philosophical Transactions of the Royal Society B*, **371**, p. 20150315.

Woollen, E., Ryan, C.M., and Williams, M. (2012), ‘Carbon stocks in an African woodland landscape: spatial distributions and scales of variation’, *Ecosystems*, **15**, pp. 804–818.

CHAPTER 2

Floristic and functional divergence in an African woodland landscape

ABSTRACT

Background and aims: Vegetation structure in southern Africa's miombo woodlands is highly variable, with a dynamic mosaic of open savannahs, woodlands, and closed-canopy forests persisting within landscapes. We aimed to measure vegetation heterogeneity, assess plant functional traits, and determine the key ecological processes operating to assemble divergent tree communities.

Methods: Hectare-scale permanent sample plots (PSPs) were established across a savannah-forest mosaic in southeastern Tanzania and measured for tree species composition. A range of properties related to the biotic (basal area, LAI, grass biomass) and abiotic (soil chemical and physical properties, fire frequency, elevation) environment were quantified at each PSP. We assembled a database of plant functional traits (bark thickness, leaf area:sapwood area, and foliar nitrogen, phosphorus, and stable isotopes of carbon and nitrogen) for 30 common species to assess variation in ecological strategy.

Results: We identify three prominent tree communities, which were associated with a single dominant axis of variation related to canopy cover, grass biomass, fire, and soil chemical properties. Plant functional traits were variable, with a range of fire defence, resource acquisition and use, and water regulation strategies identified. Functional types are linked to vegetation structure, notably being associated with a continuum of leaf structure, macronutrient content and stable isotope ratios.

Conclusions: Analysis of community assemblages suggests that areas of sparse tree cover dominated by species with resource conservation strategies and areas of dense tree cover are dominated by species with resource acquisition strategies, coinciding with a gradient of environmental habitability. We note evidence that fire, hydrology, nutrient cycling, and competition all relate to differences in vegetation structure.

2.1 Introduction

The miombo woodlands of south-central Africa are an extensive savannah formation, spanning the continent from Tanzania and DR Congo in the north to Mozambique and Zimbabwe in the south (White, 1983). Miombo woodlands derive importance from their biodiversity, supporting an estimated 8500 vascular plant species including over 300 tree species (Frost, 1996), and the ecosystem services they provide, with a population of over 100 million people heavily reliant on woodlands for food, fuel and timber resources (Campbell et al., 2007; Syampungani et al., 2009). As the result of their size, susceptibility to fire, and inter-annual variation in productivity, miombo woodlands play an important role in the African carbon (C) balance (Bombelli et al., 2009), and contribute a large uncertainty to efforts to quantify the global C cycle (Ciais et al., 2011).

Developing a predictive understanding of miombo woodland landscapes is complicated by their heterogeneity. Neighbouring and otherwise similar locations support markedly dissimilar growth forms, ranging from open savannah where C_4 grasses dominate over sparse trees and shrubs, through open canopy woodland where C_4 grasses and trees are co-dominant, to closed-canopy forest where a C_4 grass understory is excluded by low light penetration to the forest floor (Fig. 2.1). Divergent vegetation structures are associated with a diversity of species assemblages (Backéus et al., 2006; Ribeiro et al., 2008; Jew et al., 2016), which have a range of vegetation and soil carbon stocks and associated ecological properties (Williams et al., 2008; Rossi et al., 2009; Ryan et al., 2011; Woollen et al., 2012). Heterogeneity of miombo woodlands is particularly poorly understood at regional spatial-scales, where a spectrum of land cover varieties will persist under a single climate regime.

Studies have identified a number of biotic and abiotic mechanisms that govern ecosystem structure and function in savannahs. Fires are frequent in southern Africa's savannahs (Archibald et al., 2010), fuelled by the senescence C_4 grasses in the dry season. Fires do not occur uniformly across the landscape, being dependent upon sources of ignition, topographic barriers, and fuel conditions, and largely limited under closed forest canopy where C_4 grasses are excluded (Hoffmann et al., 2012). Fires alter vegetation structure by interrupting tree regeneration and reducing standing biomass (Trapnell, 1959; Furley et al., 2008; Ryan and Williams, 2011; Saito et al., 2014), reinforcing the separation between open and closed-canopy vegetation. Other work has emphasised the importance of water in limiting the growth of trees, noting correlations between woody biomass and annual rainfall (Frost, 1996), the preference of miombo woodland species for well-drained soils (Chidumayo, 1997; Woollen et al., 2012), and investment in deep taproots in many species (Timberlake et al., 1993). Water supply is closely related to topography, with seasonally waterlogged low-lying ‘dambos’ supporting only sparse tree populations (von der Heyden, 2004; Woollen et al., 2012), the possible result of inhibited wet-season growth rates (Tinley, 1982) or the intolerance of deep-rooting species to inundation (Rossatto et al., 2012). Miombo woodlands are typically found on highly-weathered and nutrient-poor soils (Frost, 1996), raising questions about the extent to which soil properties inhibit the vegetation growth. Studies across a range of savannah ecosystems have noted a correlation between woody cover and soil nutrient availability (Cole, 1986; Bowman, 2000; Lloyd et al., 2008), including in miombo woodlands (Högberg, 1986). Although soil nutrient stocks are unlikely to be limiting in the formation of forests (Bond, 2010), soil properties may structure savannah vegetation by impeding rates of succession (Bond, 2008). Studies have also noted that the coastal forests of east Africa are associated with particular soil formations (Timberlake et al., 2011), implying a nutrient or soil textural determinant of distributions of dry forest.

In addition to conspicuous differences in vegetation structure and floristic composition, tree communities in savannahs exhibit an array of adaptations to prevailing environmental conditions. These strategies can be characterised through the assessment of plant functional traits (Violle et al., 2007). For example, resilience to fire is associated with thick insulating bark (Hoffmann et al., 2012; Simon and Pennington, 2012), water-stress with a reduced leaf area (Gutschick, 1999; Niinemets, 2001) and conservative opening of stomata (Farquhar et al., 1989), and nutrient-poor soils with strategies for nutrient-use efficiency (Bloom et al., 1985) and mechanisms for nutrient acquisition from N-fixation and ectomychorrizae (Högberg, 1986). As the range of viable strategies in a plant community is constrained by environmental conditions (Weiher and Keddy, 2001), trait-based approaches offer a means to identify the dominant drivers of tree community assembly.

Where access to resources is limited and contested, and threats from disturbance are varied, plants must perform trade-offs to optimally allocate resources towards objectives of growth and persistence. At one extreme lies the conservative resource-use of plants in a marginal habitat, where a slow-return on energy and nutrient investment leads to a reduced risk of mortality. The opposite strategy is reliant upon resource acquisition and rapid growth in a benign environment, where competition with other plants limits reproductive success. This trade-off, previously expressed as the continuum between ‘stress tolerators’ and ‘competitors’ (Grime, 2006) and the resource-ratio hypothesis (Tilman, 1982), can be characterised through assessment of plant functional traits (Violle et al., 2007). For example, in the ‘leaf economics spectrum’, resource conservation strategies are identified from thick or dense leaves with low nutrient content, and competitive strategies by less investment in leaf structure and high nutrient content (Wright et al., 2004).

In this paper our objective is to identify the key biotic and abiotic factors associated with the distribution of vegetation across a gradient of land cover ranging from open savannah to closed-canopy forest in southeastern Tanzania, and understand how dominant trees are adapted to these conditions. We hypothesise that this gradient of vegetation structure is associated with a general trend from frequently-inundated, nutrient-poor and highly disturbed sites to well-drained, nutrient-rich and fire-resistant sites. We further measure a series of functional traits associated with resource-acquisition, resource-use and resilience to disturbance, hypothesising that a range of strategies exist amongst tree species, and that these strategies are filtered into species assemblages by environmental variation in miombo woodland landscapes. Whilst the impacts of fire, water availability and soil fertility on vegetation dynamics have all been described in savannah ecosystems, it is unclear which are the dominant processes acting to promote structural heterogeneity in miombo woodland ecosystems. We expect the most limiting environmental factor to be driving trait expression in each vegetation form, hypothesising that disturbance, water supply, nutrient limitation, and competition for light all act to limit vegetation growth across the vegetation gradient.

We address the following specific hypotheses:

H1: Heterogeneous vegetation structures in miombo woodland landscapes are composed of divergent tree communities which are associated with differing disturbance regimes, hydrology, and soil properties.

H2: Functional traits vary between tree species and communities, reflecting evolutionary trade-offs and environmental filtering into assemblages.

H3: Tree community assembly is driven by a combination of disturbance, water supply, nutrient limitation, and competition for light.

Figure 2.1: Vegetation structure in Kilwa District, Tanzania is highly heterogeneous, forming a mosaic of grassland savannah (top), through woodlands (middle), to closed-canopy forests (bottom).

2.2 Methods

2.2.1 Study area

Kilwa District (8°15’ - 10°00’ S, 38°40’ - 39°40’ E) in the Lindi region of coastal southern Tanzania is location of the ‘Kilwa Lowland Forest Mosaic’, a dynamic patchwork of miombo woodland and coastal forest variants. For the purposes of this study we refer to three land cover classes identified on the basis of differing growth form: ‘savannahs’, ‘woodlands’ and ‘forests’. Savannahs are grass-dominated with discontinuous tree cover, and are found extensively to the west of Kilwa District and in low-lying dambos. Woodlands consist of a mixture of tall trees with a continuous C_4 grass layer, and are the dominant land cover of Kilwa District. Forests, with tall-stature, continuous tree cover and a closed-canopy, predominate in riparian areas and on higher ground. Rainfall in Kilwa District averages 900 - 1100 mm/yr, which is concentrated in the months December - April, and has a weak precipitation gradient from a relatively moist coast to more arid inland areas (McNicol, 2014). Kilwa District has a low population density (*ca.* 12.6 people /km^2), and retains a high level of tree cover relative to other parts of Tanzania.

2.2.2 Plot inventory

A network of 25 permanent sample plots (PSPs) were established across Kilwa District in 2010/11. PSPs were semi-randomly located, ensuring accessibility and representation of a range of land cover types (Fig. 2.2). Each PSP measures 100 x 100 m, in which every tree stem above 5 cm diameter at breast height (DBH) was measured with a diameter tape at 1.3 m above ground level, and identified using local vernacular species names. Accurate species identification is subject to the limits of local knowledge, and our ability to translate to binomial nomenclature. PSPs were

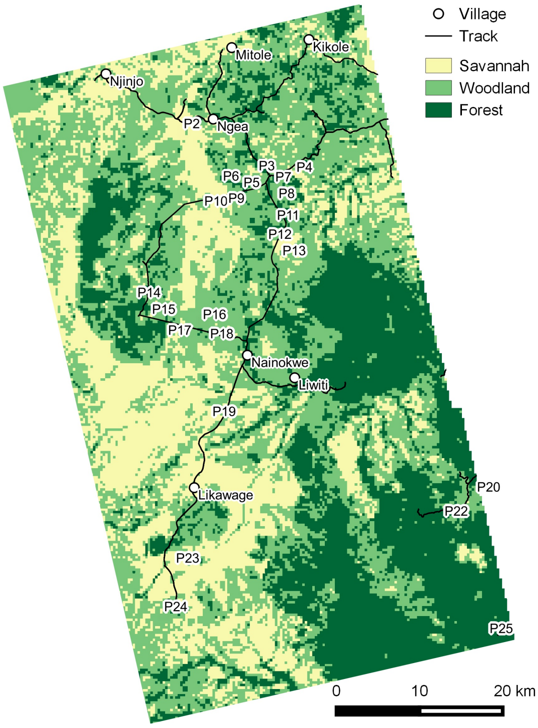

Figure 2.2: Approximate distribution of vegetation types in Kilwa District study site, overlaid with permanent sample plot locations and population centres.

re-inventoried in 2012/13; we use data from the second inventory in this study, which is corrected for gross errors in stem diameter increments using the methods of Phillips et al. (2009).

2.2.3 Ecological properties

A series of properties relating to vegetation structure, soil chemo-physical characteristics, topographic position, and disturbance were measured for each PSP (Table 2.1); for brevity these biotic and abiotic properties are all termed ‘ecological properties’.

Woody cover was estimated from PSP inventory data expressed as tree basal area, and from measurements of leaf area index (LAI). LAI was measured using hemispherical photographs from a camera mounted on a level 1.3 m tall tripod prior to leaf fall in 2014 (Coolpix 4500 fitted with Fisheye Converter FC-E8 0.21x, Nikon, Tokyo, Japan). Images were processed using Gap Light Analyzer v2.0 (Frazer et al., 1999), integrated over zenith angles 0° - 60°. Grass biomass was measured using a disc pasture meter (Bransby and Tainton, 1977), calibrated locally by measuring, air-drying and weighing grass samples, and fitting with a linear model against disc height ($R^2 = 0.3$). Samples of topsoil (5 cm depth core) and subsoil (30 cm depth core) were collected, air-dried, and passed through a 2 mm sieve to remove the coarse fraction. Soil bulk density was calculated using the dry soil mass and the volume of the subsoil core, correcting where core depth was limited by rocks or hardpan. Soil moisture was calculated as the volumetric water content of subsoil cores based on dry and wet soil mass measurements. Estimates of LAI, grass biomass and soil physical properties were replicated at 9 equispaced locations at each PSP.

Soil cores were aggregated column-wise into 3 topsoil and 3 subsoil samples for further analysis at Sokoine University of Agriculture. Each sample was measured for organic carbon content (C) using the Walkey-Black wet combustion method (Walkley and Black, 1934; Nelson and Sommers, 1996), total nitrogen content (N) using the Kjedahl method (Kjeldahl, 1883; Klute, 1986), and extractable phosphorus content (P) using the Bray-1 test (Bray and Kurtz, 1945; Klute, 1986). Nutrient stocks in topsoil and subsoil are expressed on an areal basis using bulk density and core cross-sectional area, subtracting the nutrient content contained in topsoil from estimates of subsoil nutrient content. One plot (P23) had substantially outlying estimates for subsoil N, and this measurement is excluded as a probable error. An additional sample from each PSP was formed through a combination of sub-samples from all 9 subsoil cores and measured for pH in water, and for soil texture using the Bouyoucos hydrometer method (Bouyoucos, 1962; Klute, 1986). All sub-sampling was conducted with a riffle-splitter to ensure representative and homogenised soil samples.

Remote sensing data products were used to quantify PSP topographic position

Table 2.1: Summary of ecological properties and plant functional traits measured in Kilwa District.

Parameter	Description	Units
Ecological properties		
Basal area	Tree basal area at 1.3 m	m^2/ha
LAI	Leaf area index	m^2/m^2
Grass biomass	Estimate from disc pasture meter	t/ha
Soil bulk density	Soil mass per unit volume	kg/m^3
Soil moisture	Soil volumetric water content	%
Soil texture	Soil particle size distribution	%
Soil pH	Soil pH in water	pH
Soil C	Organic carbon content (topsoil & subsoil)	kg/ha
Soil N	Total nitrogen content (topsoil & subsoil)	kg/ha
Soil P	Extractable phosphorus content (topsoil & subsoil)	kg/ha
Fire frequency	Estimate from classified Landsat data	/yr
Elevation	Height above sea level from SRTM	m
Plant functional traits		
B_T	Bark thickness	mm
L_a:S_a	Leaf area to branch cross-sectional area ratio	m^2/cm^2
LMA	Leaf mass (dry) per unit area (fresh)	g/m^2
N_m	Nitrogen content per unit mass	%
N_a	Nitrogen content per unit area	g/m^2
C:N	Mass ratio of carbon to nitrogen	g/g
P_m	Phosphorus content per unit mass	%
P_a	Phosphorus content per unit area	g/m^2
N:P	Mass ratio nitrogen to phosphorus	g/g
$\delta^{13}C$	Stable isotope ratio ^{13}C : ^{12}C	‰
$\delta^{15}N$	Stable isotope ratio ^{15}N : ^{14}N	‰

and disturbance history. PSP elevation was extracted from 1 arc-second data from the Shuttle Radar Topography Mission (USGS, 2006). Fire frequency was estimated using a ten year burn scar time-series from Kilwa District (see Chapter 4). All available Landsat Thematic Mapper and Enhanced Thematic Mapper data acquisitions between 2001 - 2010 underwent cloud masking, atmospheric correction, and conversion to surface reflectance using the LEDAPS algorithm (Masek et al., 2008). A series of vegetation indices were calculated using the multispectral imagery (Bastarrika et al., 2011), and classified using a regularised logistic regression function trained using operator-identified burned and unburned pixels. Resultant burn probability maps were summed for each year at each PSP to generate an estimate of fire frequency.

2.2.4 Functional trait measurement

A database of plant functional traits was compiled for common tree species in Kilwa District. Dominant species were identified from vernacular names in PSP data, yielding a list of 30 unique species that accounting for 76 % of total basal area (Table 2.2). One PSP (P01) uniquely positioned over a recently abandoned field was excluded from further analysis as it contained a tree species community poorly represented by the trait database. Individuals from each species (n = 8 - 10) were sampled from trees in the PSPs in May - July 2014. Only mature trees (> 10 cm DBH) showing no sign of disease or damage were considered, with a preference for sampling from locations where a species showed a high relative dominance. Each species was measured at a minimum of three locations, except where a species' distribution was limited to fewer PSPs. For each tree we measured eleven functional traits representing resource-use, fire-defence, nutrient acquisition and water-use strategies (Table 2.1). Where applicable, measurement protocols were based on the recommendations of Pérez-Harguindeguy et al. (2013).

Bark thickness (B_T), a predictor of resilience to fire (Hoffmann et al., 2009), was measured at three points on each sampled tree with a bark depth gauge (Barktax, Haglöf, Långsele, Sweden). Three sun-exposed branches off approximately 1 cm diameter were collected from the upper-canopy of each tree using a pole pruner. The ratio of leaf area to sapwood area (L_a:S_a) is associated with drought resilience, and the structural costs required to support a given leaf area (Waring et al., 1982). L_a:S_a was determined from the basal area of each branch, measured with vernier callipers, and its total leaf area, calculated from total dry leaf mass and leaf mass per unit area (LMA).

LMA describes the trade-off associated with thicker or denser leaves with a high construction cost in return for greater resilience, longer leaf lifespan and increased nutrient use efficiency (Niinemets, 2001; Westoby and Wright, 2006). LMA is an anchor trait of the ‘leaf economics spectrum’, separating resource-acquisition from resource-conservation plant strategies (Wright et al., 2004). A single healthy and fully-expanded leaf was selected from each branch sample, scanned at 600 DPI (CanoScan LiDE 210, Canon, Tokyo, Japan), and the resulting image masked to calculate one-sided leaf area using ImageJ (Schneider et al., 2012). Leaves were oven dried at 60 °C for a minimum of 72 hours, weighed to a precision of 0.001 g, and LMA calculated as dry mass divided by projected leaf area. Compound leaves were measured at the leaflet scale, including the petiole/petiolule.

Foliar macronutrients nitrogen (N) and phosphorus (P) are closely related to photosynthetic capacity and nutrient use efficiency (Tuohy et al., 1991; Reich et al., 1992; Wright et al., 2004). The ratio of carbon (C) to N relates to physiological adjustments to nutrient supply and palatability to browsers (Poorter et al., 2004), and ratio of N:P can indicate N or P limitation in biomass production (Güsewell, 2004). Leaf samples underwent elemental analysis at The University of Edinburgh. Dried leaves from each sampled tree were combined and powdered in a ball mill (MM200, Retsch, Haan, Germany). Foliar C and N content were measured using an elemental analyser (NA2500, Carlo Erba Instruments, Milan, Italy). Foliar P content was measured on half of the available leaf samples using the molybdenum blue method (Grimshaw et al., 1989) with a continuous flow analyser (Auto Analyser III, Bran+Luebbe, Norderstedt, Germany). Foliar nutrient contents were expressed on both a mass basis (N_m/P_m, % by mass), and on an area basis (N_a/P_a, g/cm^2) using LMA estimates. Foliar nutrient stoichiometry was assessed using mass-based ratios of C:N and N:P.

Folar stable isotope ratio ^{15}N:^{14}N (δ^{15}N) is an integrated measure of nutrient-acquisition, relating to N source and the influence of mycorrhizal interactions (Högberg, 1997; Robinson, 2001). In miombo woodlands, low δ^{15}N values are associated with N_2-fixing trees and trees with ectomycorrhizae (Högberg, 1986;

Högberg, 1990; Schmidt and Stewart, 2003). The ratio of ^{13}C:^{12}C (δ^{13}C) is a measure of intrinsic water-use efficiency, where high δ^{13}C is associated with conservative opening of stomata (Farquhar et al., 1989). Stable isotopes ratios δ^{15}N and δ^{13}C were measured using a mass spectrometer (Thermo Electron Delta+ Advantage, Thermo Scientific, Waltham, Massachusetts, USA), set up in series with the continuous flow analyser.

2.2.5 Data analysis

Statistical analysis of species composition, ecological properties, and functional trait variation was performed in R (R Core Team, 2015) with the vegan package (Oksanen et al., 2013). We use principal component analysis (PCA) to identify the main assemblages of woody species at the PSPs. Ordination was based on species abundance by basal area transformed by the Hellinger transformation (Legendre and Gallagher, 2001). We further restrict the ordination to species noted a minimum of 20 times in order to concentrate on distributions of species noted at multiple sites and to counter the effect of rare synonyms and misspellings. Species communities were identified using k-means clustering, specifying 3 groups in the first two principal components. Correlations between floristic composition and ecological properties were assessed with multiple regression, where ecological variables were fitted to ordination scores using the ‘envfit’ functional of the vegan package.

Variation in plant functional traits was assessed for both species and plant communities. Community traits were expressed as a community weighted mean (CWM), where mean trait values for each species were weighted by the relative abundance by basal area of species present at each PSP (Garnier et al., 2004; Violle et al., 2007). CWM traits represent strategies of the dominant species in a plant community, and therefore reflect the environmental filters that are main determinants

Table 2.2: Summary table of measured species, the proportion of total basal area they represent, and their representation in 24 PSPs. Vernacular names largely derive from Swahili and Makonde languages, and here represent the most common synonym.

Species	**Family**	**Vernacular Name**	**Abundance by total basal area (%)**	**Number of PSPs with species**	**Tree sample size**
Acacia nigrescens Oliv.	Fabaceae	msenjele	0.8	6	8
Acacia nilotica (L.) Delile	Fabaceae	mnyenye	0.7	8	8
Afzelia quanzensis Welw.	Fabaceae	mkongo	1.0	6	8
Bauhinia petersiana Bolle.	Fabaceae	msekese	0.3	2	9
Brachystegia spiciformis Benth.	Fabaceae	mtondoo	3.4	6	10
Bridelia scleroneura Müll.-Arg.	Euphorbiaceae	mcherenje	2.0	7	8
Burkea africana Hook.	Fabaceae	mkarati	4.2	15	8
Combretum apiculatum Sond.	Combretaceae	kingonogo	7.0	21	10
Combretum zeyheri Sond.	Combretaceae	nakapweo	1.7	15	9
Dalbergia melanoxylon Guill. & Perr.	Fabaceae	mpingo	4.0	11	10
Diospyros mespiliformis Hochst. ex A. DC.	Ebenaceae	mtachi	1.5	4	8
Diospyros quiloensis (Hiern) F. White	Ebenaceae	mdomolomo	1.4	6	10
Diplorhynchus condylocarpon (Müll. Arg.) Pichon	Apocynaceae	mtomoni	6.4	14	10
Flueggea virosa (Roxb.ex Willd.) Voigt	Euphorbiaceae	msakala	0.1	2	8
Grewia microcarpa K. Schum.	Tiliaceae	mlamakoa	0.7	4	8
Hymenaea verrucosa Gaertn.	Fabaceae	mnangu	2.8	2	10
Hymenocardia ulmoides Oliv.	Phyllanthaceae	mtete	5.7	7	10
Julbernardia globiflora (Benth.) Troupin	Fabaceae	mchenga	8.9	11	10
Manilkara discolour Sond.	Sapotaceae	mkwichimbi	1.6	1	8
Markhamia obtusifolia (Baker) Sprague	Bignoniaceae	mpugupugu	1.5	5	8
Millettia stuhlmannii Taub.	Fabaceae	mpangapanga	2.5	10	8
Pseudolachnostylis maprouneifolia Pax	Phyllanthaceae	msolo	5.6	17	10
Pteleopsis myrtifolia (M.A. Lawson) Engl. & Diels	Combretaceae	mnepa	3.6	16	8
Pterocarpus angolensis DC.	Fabaceae	mninga	1.5	11	10
Rytigynia sp.	Rubiaceae	mmbutuka	1.2	1	8
Sclerocarya birrea (A. Rich.) Hochst.	Anacardiaceae	mgongo	0.9	5	10
Strychnos cocculuoides Baker.	Loganiaceae	mngulunguya	2.1	12	10
Strychnos spinosa Lam.	Loganiaceae	mchungwapori	0.8	2	9
Suregada zanzibariensis Baill.	Euphorbiaceae	mdimupori	1.3	4	8
Xeroderris stuhlmannii (Taub.) Mendonça & E.P. Sousa	Fabaceae	mlondondo	1.7	12	8

of community assembly (Grime, 1998; Cingolani et al., 2007; Domínguez et al., 2012). PCA was used to test for collinearity between individual species and CWM traits, and identify trade-offs between plant strategies. Variation of CWM functional traits with ecological properties was assessed by plotting CWM traits against PSP basal area, a correlate of the major differences in ecological properties at PSPs. AICc scores (Burnham and Anderson, 2002) were generated for three models (linear, logarithmic and quadratic), selecting the most parsimonious model where $p < 0.05$. Where appropriate a separate model was fitted that excluded data from forest plots, acknowledging the presence of a potential threshold in species traits and ecological properties between savannah (with C_4 grasses) and forest ecosystems.

2.3 Results

2.3.1 Ecosystem properties

A total of 11,851 living stems were surveyed across 24 PSPs in 2012/13. Vegetation structure is diverse; stocking density ranges between 70 – 1456 stems/ha, basal area between 0.9 - 18.7 m^2/ha, and LAI between 0.94 and 3.5 m^2/m^2. Ordination of species abundances shows three principal tree communities, corresponding to *a priori* observations of savannah, woodland and forest vegetation structures (Fig. 2.3). K-means clustering results in a classification of 11 plots as savannahs, 10 plots as woodlands, and 3 plots as forests. Floristic dissimilarity is high in forest plots, whereas savannah and woodland plots appear to form a compositional gradient with a number of shared species.

Tree community composition is strongly correlated with basal area ($p < 0.0001$, $R^2 = 0.84$), with savannahs possessing low woody cover, forests high woody cover, and woodlands falling in-between. Fires are on average more frequent in low basal area

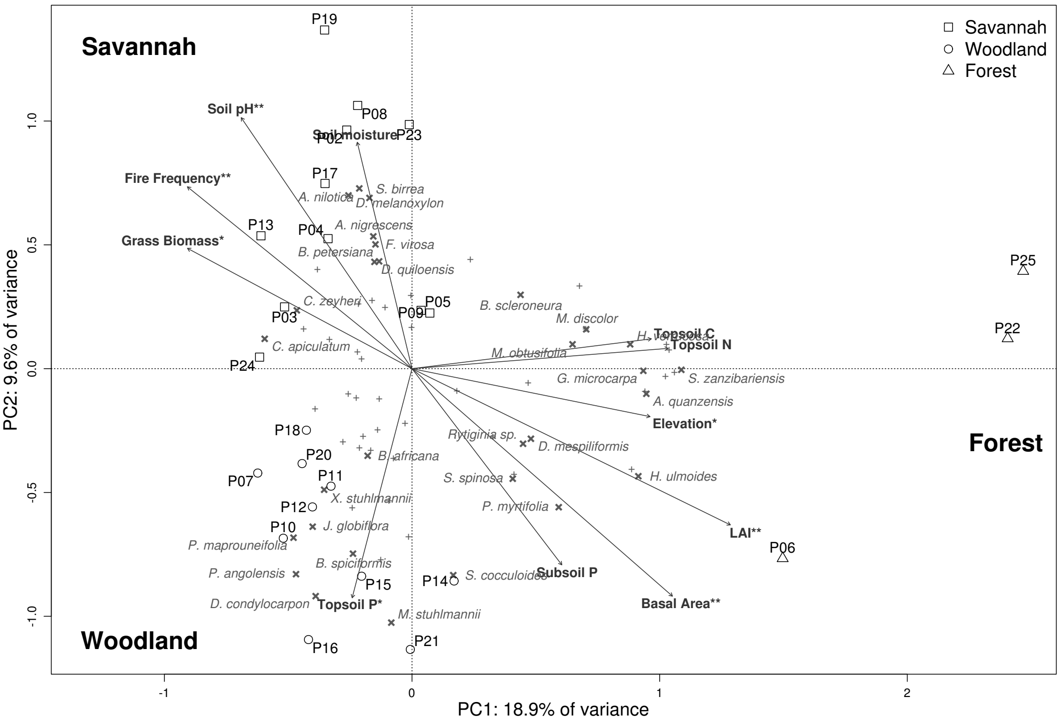

Figure 2.3: PCA ordination of PSP tree species assemblages, where species abundance is measured as the total basal area of each species adjusted by the 'Hellinger transformation' (Legendre and Gallagher, 2001). Species loadings are indicated by + where identified > 20 times across all PSPs, and **x** and named where measured in this study. K-means clustering identifies species communities corresponding to observations of savannah (square markers), woodland (circular markers) and forest (triangular markers) vegetation types. Where correlated with floristic composition, environmental vectors are displayed as arrows (where $p < 0.05$, * where $p < 0.01$, and ** where $p < 0.001$). Arrow lengths are proportional to R^2.

PSPs ($p < 0.001$, $R^2 = 0.58$), associated with a high grass biomass ($p < 0.001$, $R^2 = 0.54$) and low LAI ($p < 0.001$, $R^2 = 0.87$). No fires were observed in the three forest PSPs, coinciding with a closed forest canopy and near-absence of a grassy understory. Tree density increases with elevation ($p = 0.006$, $R^2 = 0.41$), a pattern particularly notable in forest plots P22 and P25. Soil moisture was elevated in many, though not all, savannah locations ($p = 0.010$, $R^2 = 0.37$), consistent with observations of seasonal inundation in dambo areas. Although there is broad variation in soil properties between PSPs, only soil pH was strongly coupled to vegetation composition ($p < 0.001$, $R^2 = 0.64$), ranging from neutral in savannahs to acidic in forests. Whilst subsoil P increases in line with basal area ($p = 0.004$, $R^2 = 0.42$), there was limited evidence of subsoil N relating to tree species composition ($p = 0.077$, $R^2 = 0.21$). Topsoil nutrient status is biome-specific; topsoil P is greater in woodlands ($p = 0.005$, $R^2 = 0.39$), and topsoil C ($p = 0.006$, $R^2 = 0.40$) and N ($p = 0.003$, $R^2 = 0.46$) elevated in forests. The data show no evidence that vegetation type was associated with soil bulk density, soil texture, or subsoil C. For clarity, plots of ecological variation against tree basal area are presented in Fig. S2.1.

2.3.2 Plant functional traits

Plant functional trait measurements suggest substantial differences in ecological strategies between studied species and communities, with most traits displaying between two and four-fold variation (Tables S2.1 and S2.2). The divergences we observe in species and CWM traits are associated with multiple significantly correlated traits (Table S2.3).

Over half of variance in species traits is described by two principal components of variation (Fig. 2.4a). The first principal component (describing 38.4 % of variance) relates to foliar structure and nutrient content, correlating positively with N_m and

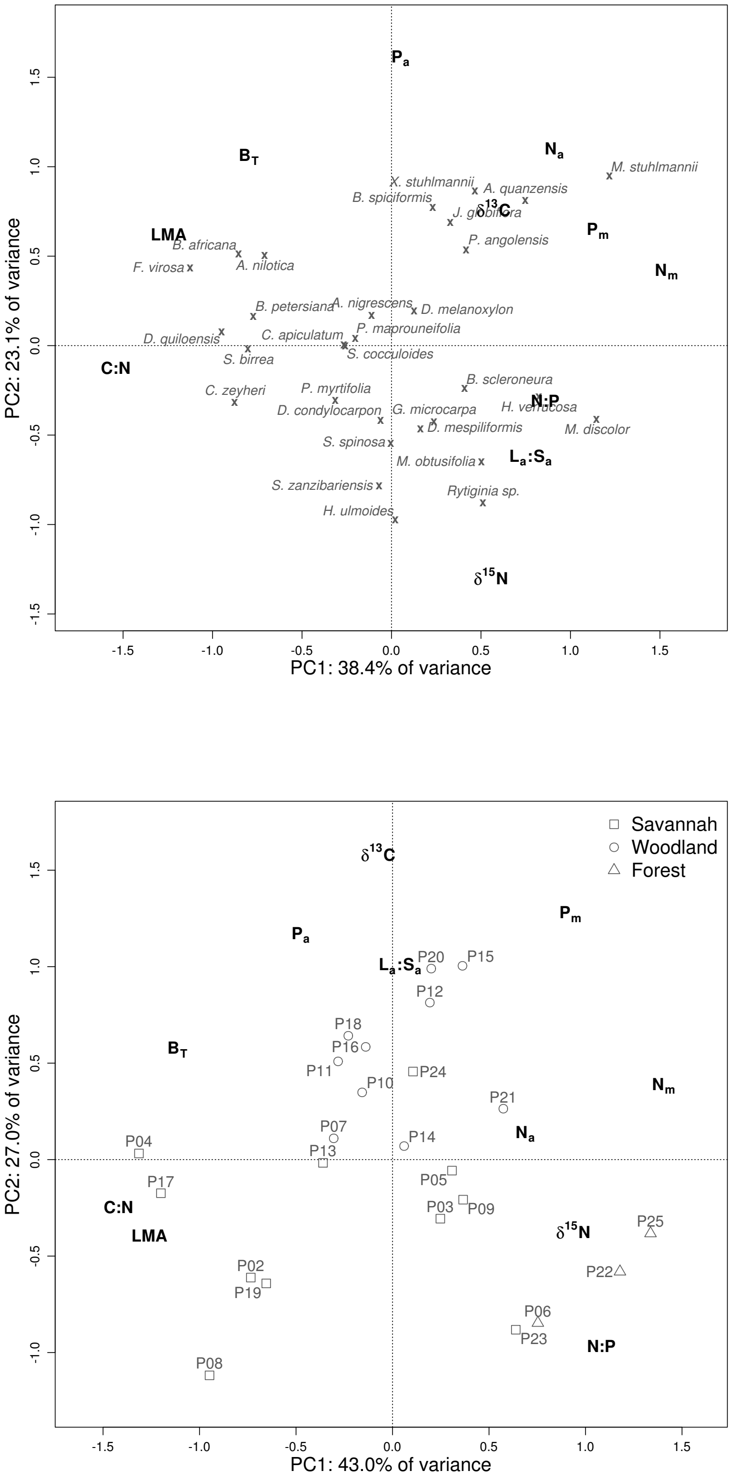

Figure 2.4: PCA biplot of woody plant functional traits for **(a)** species and **(b)** community weighted mean traits. Species are described in Table 2.2, and trait abbreviations are described in Table 2.1.

P_m, and negatively with LMA and C:N. The second principal component (23.1 % of variance) is negatively correlated with $\delta^{15}N$, and positively correlated with P_a, separating species by nutrient acquisition strategy and phosphorus use. PCA of CWM traits depicts strengthened coordination between trait values (Fig. 2.4b). The first principal component (43.0 % of variance) again relates to foliar investment, but with a stronger negative correlation with B_T. The second principal component (27.0 % of variance) is positively correlated with $\delta^{13}C$ and L_a:S_a, and is less strongly correlated with $\delta^{15}N$ and P_a. PCA of CWM traits broadly sorts PSPs into land cover types, with savannah, woodland and forest plots having low, intermediate and high scores in the first principal component, and woodland plots further delineated from savannah and forest plots by high scores in the second principal component. Of the three land cover types, CWM traits in savannah plots appear most variable, either relating to a greater range of community characteristics, or low tree densities leading to a less stable mean.

2.3.3 Ecological properties and plant functional traits

CWM plant functional traits were closely related to variation in ecological properties, represented by basal area (Fig. 2.5). There is strong evidence of a negative relationship between LMA and basal area ($p < 0.001$, $R^2 = 0.71$), and likewise C:N and basal area ($p < 0.001$, $R^2 = 0.63$), where thick nutrient-efficient leaves are particularly apparent in savannah plots. Foliar N_m increases with basal area ($p < 0.001$, $R^2 = 0.64$) as does P_m ($p < 0.001$, $R^2 = 0.68$), though a quadratic relationship also indicates a peak in P_m in woodland PSPs. For both N_m and P_m, nutrient use appears most conservative where basal area is very low. Bark thickness is notably lower in forest PSPs ($p < 0.001$, $R^2 = 0.54$), coinciding with the split between flammable and non-flammable locations. Foliar $\delta^{15}N$ shows a similar threshold ($p < 0.001$, $R^2 = 0.77$), with much higher values in the three forest PSPs. There is some evidence that L_a:S_a is reduced in low basal

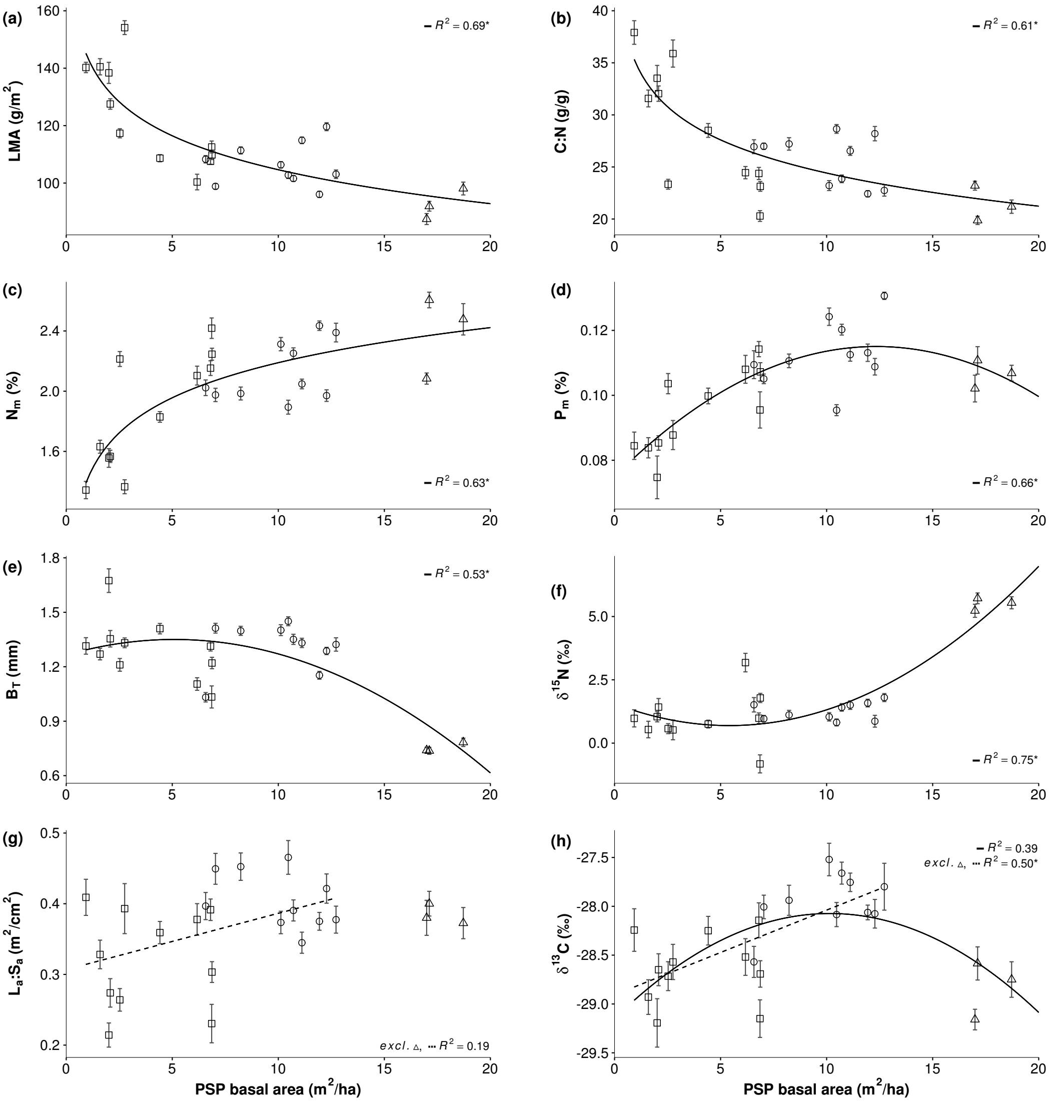

Figure 2.5: Community weighted mean plant traits along PSP basal area gradient. Graphs are only displayed for plant traits that showed significant ($p < 0.05$) differences with basal area. Lines of best fit are drawn using the lowest AICc value from linear, quadratic or logarithmic functions where significant ($p < 0.05$, * where $p < 0.01$). Dashed lines exclude forest PSPs (P06, P22 and P25), a more honest fit where a discontinuity separating forest plots from savannahs and woodlands is apparent. Error bars show ± 1 standard error of the mean.

area PSPs, though this is only apparent when forest plots are excluded ($p = 0.047$, $R^2 = 0.19$). Foliar $\delta^{13}C$ is elevated in woodland plots relative to savannahs and forests ($p = 0.006$, $R^2 = 0.38$), with strong evidence of a continuous linear increase in $\delta^{13}C$ across the savannah-woodland gradient ($p < 0.001$, $R^2 = 0.51$). Little evidence was found of directional differences to N_a, P_a, or N:P, with basal area.

2.4 Discussion

In this study we investigated floristic and functional variation of dominant species in a structurally heterogeneous miombo woodland landscape. We hypothesised that vegetation structural differences were associated with a range of biotic and abiotic properties, supporting a diversity of species with divergent functional traits, which are filtered into species assemblages by fire, water supply, nutrient availability, and competition. Our analysis indicates the presence of three dominant tree communities corresponding to *a priori* observations of savannahs, woodlands and forest vegetation structures. We identified a number of ecological differences between plots, with a single axis correlated with basal area, LAI, grass biomass, fire frequency, elevation, soil pH, subsoil P, and soil moisture describing the bulk of environmental variability. Functional trait differences were observed between tree-species, with clear differences in fire resilience, water regulation, and nutrient acquisition and use strategies. CWM traits reflect environmental variation, with a trend from stress-tolerance to competition centred traits coinciding with a sequence from open, frequently disturbed and poorly drained sites to densely vegetated, fire resistant and well-drained sites.

2.4.1 H1: Heterogeneous vegetation structures in miombo woodland landscapes are composed of divergent tree communities which are associated with differing disturbance regimes, hydrology, and soil properties

Our study supports a non-random distribution of species in Kilwa District, with distinct tree communities associated with open savannahs, miombo woodlands and forests. Open savannahs are not sparse woodlands, nor forests dense woodlands. The most apparent species assemblage exists in forested areas, where dominant species *H. verrucosa*, *H. ulmoides* and *P. myrtifolia* are rare or absent in savannahs and woodlands. The separation between savannahs, dominated by *D. melanoxylon*, *A. nilotica* and *S. birrea*, and woodlands, dominated by characteristic miombo species *B. spiciformis*, *J. globiflora* and *P. angolensis*, is less distinct. A number of species are shared between savannah and woodland areas (e.g. *C. apiculatum*), and species composition is more diffuse, implying savannahs and woodlands represent a gradient of land cover rather than distinct classes. There are indications of further land cover classes existing; for instance forest plot P06, characterised by *H. ulmoides* and *S. spinosa*, had a species assemblage isolated from other plots and may represent a ‘thicket’ land cover type (Parr et al., 2012; Charles-Dominique et al., 2015). Whilst the savannah/woodland/forest classification is a useful framework for conceptualising miombo woodland heterogeneity, we acknowledge the limitations of a small-scale study in being able to identify only the largest tree communities.

Running from sparse in savannahs to dense in forests, tree cover is the most conspicuous ecological difference between land cover types. Sparse woody cover is associated with a discontinuous tree canopy with low LAI, transmitting sufficient light to support a C_4 grassy understory. As a defining characteristic that separates savannah from forest ecosystems (Ratnam et al., 2011), savannah and woodland land cover classes with extensive grassy understories will likely have very different dynamics to the three forest PSPs. The strong association we note between the presence of grass and fire highlights the importance of fire-exclusion in maintenance of a distinct forest ecosystem, a pattern noted in other savannah landscapes (Hoffmann et al., 2012; Charles-Dominique et al., 2015). The canopy-grass-fire relationship we observe was not without exception: heavily grazed plot P06 had little grass biomass and few indications of fire, whereas fire was near-absent from woodland plot P09 which may be isolated from fire by surrounding topography.

Ecological differences between savannah and woodland areas is apparent in the prevalence of water inundation, with the seven PSPs with greatest volumetric water content all classified as savannahs. This is consistent with observations of dambos limiting woody biomass in miombo woodlands (Woollen et al., 2012). The importance of drainage is also reflected in elevation data, with savannahs predominating over woodlands at the lowest elevations. There were two conspicuous exceptions amongst the savannah plots (P03 and P24), where soils were amongst the driest measured yet tree communities resembled those of the dambo plots. Both locations were notable for shallow soils with a high coarse fraction, suggesting that the savannah tree community can arise from a range of conditions resulting in a marginal habitat. The importance of hydrology in separating woodlands from forests is less clear, with no apparent differences in soil moisture data outside of savannahs. However, two of the three forest plots (P22 & P25) are located on the highest ground in the study area, which may relate to good drainage and a favourable position for the receipt of orographic precipitation.

Evidence that soil properties were a major determinant of vegetation structure was limited. Of all measured soil properties, only soil pH was strongly associated with species composition, ranging from near neutral in savannahs to strongly acidic in forests. Acidic soils are a feature typical of miombo woodland landscapes that generally reduces soil fertility (Frost, 1996). Similar observations have previously been related to frequent fires resulting in cation enrichment (Trapnell et al., 1976), with the implication that fire plays an important role in the nutrient cycle. Evidence that subsoil nutrient content controls vegetation structure was weak; of the subsoil chemical properties measured, only extractable P is clearly associated with tree species composition. Biome-specific variation in topsoil properties suggests that soil nutrient content may follow from vegetation structure, with inputs from litterfall and volitalisation by fire modifying underlying soil nutrient stocks.

2.4.2 H2: Functional traits vary between tree species and communities, reflecting evolutionary trade-offs and environmental filtering into assemblages

The functional traits of miombo woodland tree species are widely variable. The most apparent divergence occurs between foliar traits, with species separated by a trade-off between high structural investment (LMA/C:N) and leaf macronutrient concentration (N_m/P_m). This same pattern is described in the 'leaf economics spectrum', where it is ascribed to a trade-off from slow to fast return on investment of C and macronutrients to leaves (Wright et al., 2004). The differences we observe suggest there exist niches for both persistent and productive tree species in miombo woodland landscapes.

Divisions in fire defence, nutrient acquisition strategies, and water-use are also apparent between tree species. B_T, indicative of fire-resilience, was in particular associated with species at the 'slow' reaches of the leaf economics spectrum. Many trees had low δ^{15}N, a result consistent with the dominance of ectomycorrhizal trees in miombo woodlands (Högberg, 1982; Högberg, 1986; Högberg and Piearce, 1986), though the presence of high δ^{15}N in some species suggests that there are enough nutrients in at least some areas to support trees without costly adaptations for nutrient-acquisition. Water-use, measured by δ^{13}C and L_a:S_a, was broadly variable between species, with traits indicative of niches for both both water-conservation and rapid transpiration. Coordination between fire-defence, nutrient-acquisition and water-use strategies was weak.

Relationships between traits are largely consistent between tree species and plant communities. Convergence of species with similar traits implies that environmental filters are acting to sort species into communities with similar adaptations. It is notable that trait inter-relationships are strengthened when considered as a CWM relative to between species, a phenomenon that has been observed in other ecosystems (e.g. Ackerly et al., 2002; Domínguez et al., 2012). This may relate to competitive dominance by the best adapted species in tree communities, or parallel shifts between traits that are unrelated within species in response to environmental variation.

2.4.3 H3: Tree community assembly is driven by a combination of disturbance, water supply, nutrient limitation, and competition for light

The pervasiveness of fire in savannahs and woodlands is reflected in the thick bark of their tree communities, with a clear threshold in both fire frequency and B_T found across the woodland-forest transition. This observation indicates the importance of fire in maintaining distinct species communities, with fire acting to prevent the spread of forest adapted species into woodland and savannahs. This is a result consistent with the mechanisms reported in other savannah-forest mosaics (Hoffmann et al., 2003; Dantas et al., 2013). Though woody biomass is closely associated with the severity of fire regimes in miombo woodlands (Trapnell, 1959; Ryan and Williams, 2011), we note little evidence of differences in fire frequency or bark thickness between savannah and woodland PSPs. This suggests that factors other than fire may be the limiting determinants of woody cover differences outside of forests.

Water-use traits show distinct patterns in savannah, woodland and forest tree communities. Savannahs are characterised by a relatively low L_a:S_a, a conservative allocation pattern associated with drought tolerance, coupled with a low δ^{13}C, suggesting a low water-use efficiency. Contrastingly, woodland species issue a greater leaf area with a greater water-use efficiency. This is interpretable as a trade-off between a high leaf area allowing for rapid growth in favourable conditions against the necessity for judicious opening of stomata in water-limited conditions. The high leaf area and low water-use efficiency of forest communities suggests these trees are not water-stressed, possibly linked to the closed-canopy sustaining a humid environment or to greater rainfall. Uniquely amongst our measurements, water availability can be related to landscape morphology, and therefore points toward some resilience in vegetation patterns across the landscape.

Though there is little evidence of pronounced nutrient scarcity at any single location, a number of traits relating to nutrient acquisition and use differed between tree communities. Savannahs are associated with high LMA and C:N and low N_m and P_m, traits which suggest the efficient use of available nutrients. Further evidence of nutrient scarcity is present in the prevalence of species from the family *Fabaceae* and low δ^{15}N in savannah and woodland tree communities. Similar observations by Högberg (1982) are attributed to large losses of N following fires, compensated for by N fixation by leguminous species. Observations may also relate to the use of ectomycorrhize for direct uptake of P from soils (Högberg, 1986). The hypothesis that P availability governs vegetation structure is supported by high foliar N:P values, with 18 species averaging > 20 g/g, generally indicative of P limitation, and no species recording < 10 g/g, generally indicative of N limitation (Güsewell, 2004). The forest species assemblage has few species from the family *Fabaceae* and high values of δ^{15}N, suggesting that nutrients are not a strong limitation in forests. As forests were not associated with a greatly increased soil nutrient pool, the greater nutrient accessibility in these communities is probably related to a closed nutrient cycle rather the underlying differences in soil properties.

The open canopy of savannah and woodland vegetation structures suggests that competition for light is less important in structuring these tree communities. The lower LMA, C:N and greater N_m and P_m in the woodland species assemblage relative to savannahs are consistent with greater photosynthetic capacity (Wright et al., 2004), suggesting greater productivity in these locations. Forest plots show foliar characteristics associated with rapid growth and competitive life strategies, which along with a closed-canopy suggest that woody production is limited by light availability in these locations.

2.5 Conclusions

In this study we investigated the nature of vegetation heterogeneity in a miombo woodland landscape consisting of structurally distinct savannah, woodland, and forest vegetation forms. Divergent vegetation structures are floristically distinct, and associated with a range of environmental conditions that run from harsh in savannahs to relatively benign in forests. Variation in functional traits suggests a trade-off between resource-conservation to resource-acquisition strategies, with further notable differences in fire-defence, nutrient cycling and water-use. We note evidence that environmental variability acts to assemble divergent tree communities, though it seems unlikely that any one mechanism can alone account for the heterogeneity of miombo woodland landscapes.

2.6 Acknowledgements

PSPs in Kilwa District were established by the staff of the Mpingo Conservation and Development Initiative (MCDI) in collaboration with the University of Edinburgh. Fieldwork was hosted by MCDI, with additional support from Derek and Maureen Moss. Functional trait measurements were performed with the help of the indefatigable Mohamed Mkubugwa, Hamisi Ulega, and Yusuph Kassim, with able assistance from the residents of Kiwawa, Likawage, Migeregere, Nainokwe, and Ngea villages.

2.7 References

Ackerly, D., Knight, C., Weiss, S., Barton, K., and Starmer, K. (2002), ‘Leaf size, specific leaf area and microhabitat distribution of chaparral woody plants: contrasting patterns in species level and community level analyses’, *Oecologia*, **130**, pp. 449–457.

Archibald, S., Scholes, R.J., Roy, D.P., Roberts, G., and Boschetti, L. (2010), ‘Southern African fire regimes as revealed by remote sensing’, *International Journal of Wildland Fire*, **19**, pp. 861–878.

Backéus, I., Pettersson, B., Strömquist, L., and Ruffo, C. (2006), ‘Tree communities and structural dynamics in miombo (Brachystegia–Julbernardia) woodland, Tanzania’, *Forest Ecology and Management*, **230**, pp. 171–178.

Bastarrika, A., Chuvieco, E., and Martín, M.P. (2011), ‘Mapping burned areas from Landsat TM/ETM+ data with a two-phase algorithm: Balancing omission and commission errors’, *Remote Sensing of Environment*, **115**, pp. 1003–1012.

Bloom, A.J., Chapin, F.S., and Mooney, H.A. (1985), ‘Resource limitation in plants–an economic analogy’, *Annual review of Ecology and Systematics*, **16**, pp. 363–392.

Bombelli, A., Henry, M., Castaldi, S., Adu-Bredu, S., Arneth, A., de Grandcourt, A., Grieco, E., Kutsch, W.L., Lehsten, V., Rasile, G.A., Reichstein, M., Tansey, K., Weber, U., and Valentini, R. (2009), ‘The Sub-Saharan Africa carbon balance, an overview’, *Journal of Geophysical Research: Biogeosciences*, **6**, pp. 2085–2123.

Bond, W.J. (2008), ‘What Limits Trees in C_4 Grasslands and Savannas?’, *Annual Review of Ecology, Evolution, and Systematics*, **39**, pp. 641–659.

Bond, W.J. (2010), ‘Do nutrient-poor soils inhibit development of forests? A nutrient stock analysis’, *Plant and Soil*, **334**, pp. 47–60.

Bouyoucos, G.J. (1962), ‘Hydrometer method improved for making particle size analyses of soils’, *Agronomy Journal*, **54**, pp. 464–465.

Bowman, D.M.J.S. (2000), *Australian rainforests: islands of green in a land of fire*, Cambridge University Press.

Bransby, D.I. and Tainton, N.M. (1977), ‘The disc pasture meter: possible applications in grazing management’, *Proceedings of the Annual Congresses of the Grassland Society of Southern Africa*, **12**, pp. 115–118.

Bray, R.H. and Kurtz, L.T. (1945), ‘Determination of total, organic, and available forms of phosphorus in soils.’, *Soil science*, **59**, pp. 39–46.

Burnham, K.P. and Anderson, D.R. (2002), *Model selection and multimodel inference: a practical information-theoretic approach*, Springer-Verlag, New York, USA.

Campbell, B.M., Angelsen, A., Cunningham, A., Katerere, Y., Sitoe, A., and Wunder, S. (2007), *Miombo woodlands–opportunities and barriers to sustainable forest management*, CIFOR, Bogor, Indonesia.

Charles-Dominique, T., Staver, A.C., Midgley, G.F., and Bond, W.J. (2015), 'Functional differentiation of biomes in an African savanna/forest mosaic', *South African Journal of Botany*, **101**, pp. 82–90.

Chidumayo, E.N. (1997), *Miombo ecology and management: an introduction*, Intermediate Technology Publications Ltd (ITP).

Ciais, P., Bombelli, A., Williams, M., Piao, S.L., Chave, J., Ryan, C.M., Henry, M., Brender, P., and Valentini, R. (2011), 'The carbon balance of Africa: synthesis of recent research studies', *Philosophical Transactions of the Royal Society of London A: Mathematical, Physical and Engineering Sciences*, **369**, pp. 2038–2057.

Cingolani, A.M., Cabido, M., Gurvich, D.E., Renison, D., and Díaz, S. (2007), 'Filtering processes in the assembly of plant communities: Are species presence and abundance driven by the same traits?', *Journal of Vegetation Science*, **18**, pp. 911–920.

Cole, M.M. (1986), *The savannas: Biogeography and Geobotany*, Academic Press.

Dantas, V., Batalha, M.A., and Pausas, J.G. (2013), 'Fire drives functional thresholds on the savanna–forest transition', *Ecology*, **94**, pp. 2454–2463.

Domínguez, M.T., Aponte, C., Pérez-Ramos Ignacio, M., García, L.V., Villar, R., and Marañón, T. (2012), 'Relationships between leaf morphological traits, nutrient concentrations and isotopic signatures for Mediterranean woody plant species and communities', *Plant and Soil*, **357**, pp. 407–424.

Farquhar, G.D., Ehleringer, J.R., and Hubick, K.T. (1989), 'Carbon isotope discrimination and photosynthesis', *Annual review of plant biology*, **40**, pp. 503–537.

Frazer, G.W., Canham, C.D., and Lertzman, K.P. (1999), *Gap Light Analyzer (GLA), Version 2.0: Imaging software to extract canopy structure and gap light transmission indices from true-colour fisheye photographs*, version 2.0, Simon Fraser University, Burnaby, British Columbia, Canada, and the Institute of Ecosystem Studies, Millbrook, New York, USA.

Frost, P. (1996), 'The ecology of miombo woodlands', *The miombo in transition: Woodlands and welfare in Africa*, ed. by B. Campbell, CIFOR, Bogor, Indonesia.

Furley, P.A., Rees, R.M., Ryan, C.M., and Saiz, G. (2008), 'Savanna burning and the assessment of long-term fire experiments with particular reference to Zimbabwe', *Progress in Physical Geography*, **32**, pp. 611–634.

Garnier, E., Cortez, J., Billès, G., Navas, M.-L., Roumet, C., Debussche, M., Laurent, G., Blanchard, A., Aubry, D., Bellmann, A., Neill, C., and Toussaint, J.-P. (2004), 'Plant functional markers capture ecosystem properties during secondary succession', *Ecology*, **85**, pp. 2630–2637.

Grime, J.P. (1998), ‘Benefits of plant diversity to ecosystems: immediate, filter and founder effects’, *Journal of Ecology*, **86**, pp. 902–910.

Grime, J.P. (2006), *Plant strategies, vegetation processes, and ecosystem properties*, John Wiley & Sons.

Grimshaw, H.M., Allen, S.E., and A., P.J. (1989), ‘Chemical analysis of ecological materials’, *Chemical Analysis of Ecological Materials*, ed. by S. Allen, Blackwell Scientific Publications, pp. 81–159.

Güsewell, S. (2004), ‘N:P ratios in terrestrial plants: variation and functional significance’, *New phytologist*, **164**, pp. 243–266.

Gutschick, V.P. (1999), ‘Biotic and abiotic consequences of differences in leaf structure’, *New phytologist*, **143**, pp. 3–18.

Hoffmann, W.A., Adasme, R., Haridasan, M., de Carvalho, M.T., Geiger, E.L., Pereira, M.A.B., Gotsch, S.G., and Franco, A.C. (2009), ‘Tree topkill, not mortality, governs the dynamics of savanna-forest boundaries under frequent fire in central Brazil’, *Ecology*, **90**, pp. 1326–1337.

Hoffmann, W.A., Geiger, E.L., Gotsch, S.G., Rossatto, D.R., Silva, L.C.R., Lau, O.L., Haridasan, M., and Franco, A.C. (2012), ‘Ecological thresholds at the savanna-forest boundary: how plant traits, resources and fire govern the distribution of tropical biomes’, *Ecology Letters*, **15**, pp. 759–768.

Hoffmann, W.A., Orthen, B., and Nascimento, P.K.V.d. (2003), ‘Comparative fire ecology of tropical savanna and forest trees’, *Functional Ecology*, **17**, pp. 720–726.

Högberg, P. and Piearce, G.D. (1986), ‘Mycorrhizas in Zambian trees in relation to host taxonomy, vegetation type and successional patterns’, *Journal of Ecology*, **74**, pp. 775–785.

Högberg, P. (1982), ‘Mycorrhizal associations in some woodland and forest trees and shrubs in Tanzania’, *New Phytologist*, **92**, pp. 407–415.

Högberg, P. (1986), ‘Nitrogen-fixation and nutrient relations in savanna woodland trees (Tanzania)’, *Journal of Applied Ecology*, **23**, pp. 675–688.

Högberg, P. (1986), ‘Soil nutrient availability, root symbioses and tree species composition in tropical Africa: a review’, *Journal of Tropical Ecology*, **2**, pp. 359–372.

Högberg, P. (1990), ‘^{15}N natural abundance as a possible marker of the ectomycorrhizal habit of trees in mixed African woodlands’, *New Phytologist*, **115**, pp. 483–486.

Högberg, P. (1997), ‘Tansley Review No. 95: ^{15}N natural abundance in soil-plant systems’, *New Phytologist*, **137**, pp. 179–203.

Jew, E.K.K., Dougill, A.J., Sallu, S.M., O’Connell, J., and Benton, T.G. (2016), ‘Miombo woodland under threat: Consequences for tree diversity and carbon storage’, *Forest Ecology and Management*, **361**, pp. 144–153.

Kjeldahl, J. (1883), ‘Neue Methode zur Bestimmung des Stickstoffs in organischen Körpern’, *Zeitschrift für analytische Chemie*, **22**, pp. 366–382.

Klute, A. (1986), *Methods of soil analysis. Physical and mineralogical methods*, 2nd ed., American Society of Agronomy.

Legendre, P. and Gallagher, E.D. (2001), 'Ecologically meaningful transformations for ordination of species data', *Oecologia*, **129**, pp. 271–280.

Lloyd, J., Bird, M.I., Vellen, L., Miranda, A.C., Veenendaal, E.M., Djagbletey, G., Miranda, H.S., Cook, G., and Farquhar, G.D. (2008), 'Contributions of woody and herbaceous vegetation to tropical savanna ecosystem productivity: a quasi-global estimate', *Tree physiology*, **28**, pp. 451–468.

Masek, J.G., Huang, C., Wolfe, R., Cohen, W., Hall, F., Kutler, J., and Nelson, P. (2008), 'North American forest disturbance mapped from a decadal Landsat record', *Remote Sensing of Environment*, **112**, pp. 2914–2926.

McNicol, I.M. (2014), 'Deforestation, Forest Degradation and the Carbon Cycle of African Miombo Woodlands', PhD thesis, University of Edinburgh.

Nelson, D.W. and Sommers, L.E. (1996), 'Total carbon, organic carbon, and organic matter', *Methods of Soil Analysis, Part 3, Chemical Methods*, ed. by D.L. Sparks, pp. 961–1010.

Niinemets, Ü. (2001), 'Global-scale climatic controls of leaf dry mass per area, density, and thickness in trees and shrubs', *Ecology*, **82**, pp. 453–469.

Oksanen, J., Blanchet, F.G., Kindt, R., Legendre, P., Minchin, P.R., O'Hara, R.B., Simpson, G.L., Solymos, P., Stevens, M.H.H., and Wagner, H. (2013), *vegan: Community Ecology Package*, R package version 2.0-10, url: `http://CRAN.R-project.org/package=vegan`.

Parr, C.L., Gray, E.F., and Bond, W.J. (2012), 'Cascading biodiversity and functional consequences of a global change–induced biome switch', *Diversity and Distributions*, **18**, pp. 493–503.

Pérez-Harguindeguy, N., Díaz, S., Garnier, E., Lavorel, S., Poorter, H., Jaureguiberry, P., Bret-Harte, M.S., Cornwell, W.K., Craine, J.M., Gurvich, D.E., Urcelay, C., Veneklaas, E.J., Reich, P.B., Poorter, L., Wright I. J.and Ray, P., Enrico, L., Pausas, J.G., de Vos, A.C., Buchmann, N., Funes, G., Quétier, F., Hodgson, J.G., Thompson, K., Morgan, H.D., ter Steege, H., van der Heijden, M.G.A., Sack, L., Blonder, B., Poschlod, P., Vaieretti, M.V., Conti, G., Staver, A.C., Aquino, S., and Cornelissen, J.H.C. (2013), 'New handbook for standardised measurement of plant functional traits worldwide', *Australian Journal of Botany*, **61**, pp. 167–234.

Phillips, O.L., Aragão, L.E.O.C., Lewis, S.L., Fisher, J.B., Lloyd, J., López-González, G., Malhi, Y., Monteagudo, A., Peacock, J., Quesada, C.A., Heijden, G. van der, Almeida, S., Amaral, I., Arroyo, L., Aymard, G., Baker, T.R., Bánki, O., Blanc, L., Bonal, D., Brando, P., Chave, J., Oliveira, Á.C.A. de, Cardozo, N.D., Czimczik, C.I., Feldpausch, T.R., Freitas, M.A., Gloor, E., Higuchi, N., Jiménez, E., Lloyd, G., Meir, P., Mendoza, C., Morel, A., Neill, D.A., Nepstad, D., Patiño, S., Peñuela, M.C., Prieto, A., Ramírez, F., Schwarz, M., Silva, J., Silveira, M., Thomas, A.S., Steege, H.t., Stropp, J., Vásquez, R., Zelazowski, P., Dávila, E.A., Andelman, S., Andrade, A., Chao, K.-J., Erwin, T., Di Fiore, A., C., E.H., Keeling, H., Killeen, T.J., Laurance, W.F., Cruz, A.P., Pitman, N.C.A., Vargas, P.N., Ramírez-Angulo, H., Rudas, A., Salamão, R., Silva, N., Terborgh, J., and Torres-Lezama, A. (2009), 'Drought sensitivity of the Amazon rainforest', *Science*, **323**, pp. 1344–1347.

Poorter, L., van de Plassche, M., Willems, S., and Boot, R.G.A. (2004), 'Leaf traits and herbivory rates of tropical tree species differing in successional status', *Plant Biology*, **6**, pp. 746–754.

R Core Team (2015), *R: A Language and Environment for Statistical Computing*, R Foundation for Statistical Computing, Vienna, Austria, url: `http://www.R-project.org/`.

Ratnam, J., Bond, W.J., Fensham, R.J., Hoffmann, W.A., Archibald, S., Lehmann, C.E.R., Anderson, M.T., Higgins, S.I., and Sankaran, M. (2011), 'When is a 'forest' a savanna, and why does it matter?', *Global Ecology and Biogeography*, **20**, pp. 653–660.

Reich, P.B., Walters, M.B., and Ellsworth, D. (1992), 'Leaf life-span in relation to leaf, plant, and stand characteristics among diverse ecosystems', *Ecological monographs*, **62**, pp. 365–392.

Ribeiro, N.S., Shugart, H.H., and Washington-Allen, R. (2008), 'The effects of fire and elephants on species composition and structure of the Niassa Reserve, northern Mozambique', *Forest Ecology and Management*, **255**, pp. 1626–1636.

Robinson, D. (2001), '$\delta 15$ N as an integrator of the nitrogen cycle', *Trends in Ecology & Evolution*, **16**, pp. 153–162.

Rossatto, D.R., Silva, L.d.C.R., Villalobos-Vega, R., Sternberg, L.d.L., and Franco, A.C. (2012), 'Depth of water uptake in woody plants relates to groundwater level and vegetation structure along a topographic gradient in a neotropical savanna', *Environmental and Experimental Botany*, **77**, pp. 259–266.

Rossi, J., Govaerts, A., De Vos, B., Verbist, B., Vervoort, A., Poesen, J., Muys, B., and Deckers, J. (2009), 'Spatial structures of soil organic carbon in tropical forests—a case study of Southeastern Tanzania', *Catena*, **77**, pp. 19–27.

Ryan, C.M. and Williams, M. (2011), 'How does fire intensity and frequency affect miombo woodland tree populations and biomass?', *Ecological Applications*, **21**, pp. 48–60.

Ryan, C.M., Williams, M., and Grace, J. (2011), 'Above-and Belowground Carbon Stocks in a Miombo Woodland Landscape of Mozambique', *Biotropica*, **43**, pp. 423–432.

Saito, M., Luyssaert, S., Poulter, B., Williams, M., Ciais, P., Bellassen, V., Ryan, C.M., Yue, C., Cadule, P., and Peylin, P. (2014), 'Fire regimes and variability in aboveground woody biomass in miombo woodland', *Biogeosciences*, **119**, pp. 1014–1029.

Schmidt, S. and Stewart, G.R. (2003), 'δ^{15}N values of tropical savanna and monsoon forest species reflect root specialisations and soil nitrogen status', *Oecologia*, **134**, pp. 569–577.

Schneider, C.A., Rasband, W.S., and Eliceiri, K.W. (2012), 'NIH Image to ImageJ: 25 years of image analysis', *Nature methods*, **9**, pp. 671–675.

Simon, M.F. and Pennington, T. (2012), ‘Evidence for adaptation to fire regimes in the tropical savannas of the Brazilian Cerrado’, *International Journal of Plant Sciences*, **173**, pp. 711–723.

Syampungani, S., Chirwa, P.W., Akinnifesi, F.K., Sileshi, G., and Ajayi, O.C. (2009), ‘The miombo woodlands at the cross roads: Potential threats, sustainable livelihoods, policy gaps and challenges’, *Natural Resources Forum*, **33**, pp. 150–159.

Tilman, D. (1982), *Resource Competition and Community Structure*, Princeton University Press Princeton, New Jersey, USA.

Timberlake, J.R., Calvert, G.M., and Morris, J.A. (1993), ‘Preliminary root atlas for Zimbabwe and Zambia’, **96**.

Timberlake, J., Goyder, D., Crawford, F., Burrows, J., Clarke, G.P., Luke, Q., Matimele, H., Müller, T., Pascal, O., Sousa, C. de, et al. (2011), ‘Coastal dry forests in northern Mozambique’, *Plant Ecology and Evolution*, **144**, pp. 126–137.

Tinley, K.L. (1982), ‘The influence of soil moisture balance on ecosystem patterns in southern Africa’, *Ecology of tropical savannas*, ed. by B.J. Huntley and B.H. Walker, Springer, pp. 175–192.

Trapnell, C., Friend, M., Chamberlain, G., and Birch, H. (1976), ‘The effects of fire and termites on a Zambian woodland soil’, *The Journal of Ecology*, **64**, pp. 577–588.

Trapnell, C. (1959), ‘Ecological results of woodland and burning experiments in Northern Rhodesia’, *The Journal of Ecology*, **41**, pp. 129–168.

Tuohy, J.M., Prior, J.A.B., and Stewart, G.R. (1991), ‘Photosynthesis in relation to leaf nitrogen and phosphorus content in Zimbabwean trees’, *Oecologia*, **88**, pp. 378–382.

USGS (2006), *Shuttle Radar Topography Mission, 1 Arc Second, Unfilled Finished-B 2.0.*

Violle, C., Navas, M.-L., Vile, D., Kazakou, E., Fortunel, C., Hummel, I., and Garnier, E. (2007), ‘Let the concept of trait be functional!’, *Oikos*, **116**, pp. 882–892.

von der Heyden, C.J. (2004), ‘The hydrology and hydrogeology of dambos: a review’, *Progress in Physical Geography*, **28**, pp. 544–564.

Walkley, A. and Black, I.A. (1934), ‘An examination of the Degtjareff method for determining soil organic matter, and a proposed modification of the chromic acid titration method.’, *Soil science*, **37**, pp. 29–38.

Waring, R.H., Schroeder, P.E., and Oren, R. (1982), ‘Application of the pipe model theory to predict canopy leaf area’, *Canadian Journal of Forest Research*, **12**, pp. 556–560.

Weiher, E. and Keddy, P. (2001), *Ecological assembly rules: perspectives, advances, retreats*, Cambridge University Press.

Westoby, M. and Wright, I.J. (2006), ‘Land-plant ecology on the basis of functional traits’, *Trends in Ecology & Evolution*, **21**, pp. 261–268.

White, F. (1983), *The vegetation of Africa: a descriptive memoir to accompany the Unesco/AETFAT/UNSO vegetation map of Africa*, UNESCO, Paris, France.

Williams, M., Ryan, C.M., Rees, R.M., Sambane, E., Fernando, J., and Grace, J. (2008), 'Carbon sequestration and biodiversity of re-growing miombo woodlands in Mozambique', *Forest Ecology and management*, **254**, pp. 145–155.

Woollen, E., Ryan, C.M., and Williams, M. (2012), 'Carbon stocks in an African woodland landscape: spatial distributions and scales of variation', *Ecosystems*, **15**, pp. 804–818.

Wright, I.J., Reich, P.B., Westoby, M., Ackerly, D.D., Baruch, Z., Bongers, F., Cavender-Bares, J., Chapin, T., Cornelissen, J.H., Diemer, M., Flexas, J., Garnier, E., Groom, P., Gulias, J., Hikosaka, K., Lamont, B.B., Lee, T., Lee, W., Lusk, C., Midgley, J.J., Navas, M.L., Niinemets, Ü., Oleksyn, J., Osada, N., Poorter, H., Poot, P., Prior, L., Pyankov, V.I., Roumet, C., Thomas, S.C., Tjoelker, M.G., Veneklaas, E.J., and Villar, R. (2004), 'The worldwide leaf economics spectrum', *Nature*, **428**, pp. 821–827.

2.8 Supplementary materials

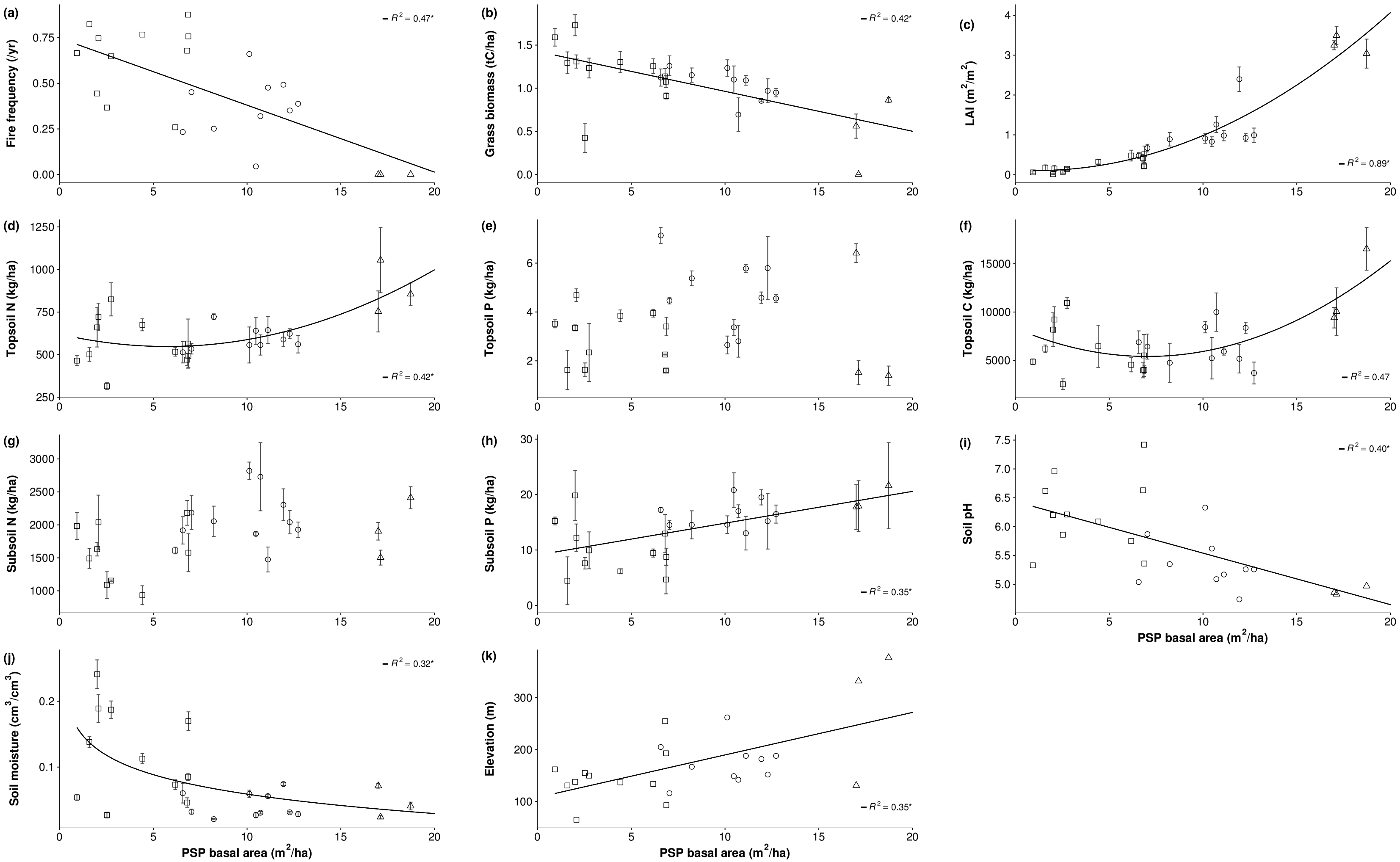

Figure S2.1: Ecological and environmental characteristics measured along PSP basal area gradient. Lines show the best fitting of linear, quadratic, or logarithmic functions where $p < 0.05$.

Table S2.1: Table showing mean foliar traits (± 1 SEM) by species.

Species	**LMA (g/m^2)**	**B$_T$ (mm)**	**L$_a$:S$_a$ (m^2/cm^2)**	**N$_m$ (%)**	**N$_a$ (g/m^2)**	**C:N (g/g)**	**P$_m$ (g/m^2)**	**P$_a$ (g/m^2)**	**N:P (g/g)**	**δ^{13}C (‰)**	**δ^{15}N (‰)**
A. nigrescens	109.6 ± 3.9	1.49 ± 0.10	0.23 ± 0.04	2.25 ± 0.11	2.38 ± 0.06	20.7 ± 1.0	0.096 ± 0.003	0.105 ± 0.005	23.1 ± 0.9	-29.3 ± 0.5	-0.466 ± 0.406
A. nilotica	185.3 ± 12.4	1.59 ± 0.09	0.20 ± 0.04	1.64 ± 0.04	3.18 ± 0.2	30.4 ± 0.6	0.064 ± 0.005	0.132 ± 0.011	25.5 ± 2.3	-30.6 ± 0.5	-0.600 ± 0.513
A. quanzensis	101.2 ± 4.0	0.95 ± 0.07	0.42 ± 0.05	2.96 ± 0.15	2.94 ± 0.12	16.4 ± 0.7	0.192 ± 0.027	0.172 ± 0.011	16.0 ± 0.7	-27.7 ± 0.2	3.246 ± 1.001
B. africana	168.4 ± 4.2	1.44 ± 0.05	0.36 ± 0.06	1.22 ± 0.05	2.06 ± 0.11	38.4 ± 2.0	0.083 ± 0.008	0.150 ± 0.019	14.5 ± 2.0	-28.2 ± 0.2	-0.052 ± 0.617
B. petersiana	146.6 ± 3.6	1.34 ± 0.06	0.25 ± 0.03	1.41 ± 0.13	2.12 ± 0.14	35.4 ± 3.1	0.089 ± 0.006	0.134 ± 0.006	14.5 ± 1.2	-29.9 ± 0.3	1.851 ± 0.606
B. scleroneura	106.0 ± 9.2	1.14 ± 0.10	0.44 ± 0.06	2.71 ± 0.20	2.82 ± 0.38	18.1 ± 1.4	0.091 ± 0.014	0.104 ± 0.013	29.4 ± 3.0	-29.3 ± 0.5	4.917 ± 1.145
B. spiciformis	103.7 ± 2.1	1.46 ± 0.09	0.23 ± 0.03	2.46 ± 0.08	2.55 ± 0.09	20.8 ± 0.7	0.135 ± 0.007	0.148 ± 0.007	17.7 ± 1.0	-26.5 ± 0.2	2.279 ± 0.482
C. apiculatum	129.2 ± 3.5	1.09 ± 0.06	0.58 ± 0.05	1.61 ± 0.13	2.09 ± 0.19	31.3 ± 2.2	0.097 ± 0.008	0.122 ± 0.008	18.1 ± 1.5	-28.3 ± 0.5	0.780 ± 0.714
C. zeyheri	139.1 ± 2.7	1.16 ± 0.05	0.38 ± 0.04	1.10 ± 0.03	1.53 ± 0.05	44.2 ± 1.3	0.071 ± 0.004	0.095 ± 0.006	16.5 ± 1.5	-28.3 ± 0.1	1.847 ± 0.553
D. condylocarpon	83.7 ± 2.3	1.55 ± 0.06	0.64 ± 0.06	1.93 ± 0.10	1.61 ± 0.09	26.9 ± 0.6	0.088 ± 0.002	0.076 ± 0.004	20.3 ± 0.6	-27.8 ± 0.2	1.012 ± 0.208
D. melanoxylon	111.5 ± 2.6	0.94 ± 0.07	0.21 ± 0.04	2.51 ± 0.09	2.77 ± 0.10	19.1 ± 0.7	0.097 ± 0.007	0.106 ± 0.006	26.5 ± 2.1	-29.2 ± 0.2	-1.796 ± 0.485
D. mespiliformis	94.1 ± 3.7	0.68 ± 0.04	0.36 ± 0.05	2.13 ± 0.07	2.03 ± 0.16	22.1 ± 0.9	0.092 ± 0.006	0.092 ± 0.010	22.4 ± 1.9	-28.1 ± 0.3	4.218 ± 0.749
D. quiloensis	145.2 ± 6.2	2.07 ± 0.11	0.18 ± 0.03	1.32 ± 0.10	1.89 ± 0.16	37.0 ± 2.2	0.065 ± 0.010	0.100 ± 0.013	20.3 ± 0.8	-29.1 ± 0.4	1.734 ± 0.278
F. virosa	163.3 ± 3.3	1.86 ± 0.12	0.16 ± 0.02	1.13 ± 0.03	1.86 ± 0.08	43.0 ± 1.0	0.076 ± 0.008	0.124 ± 0.014	15.5 ± 1.6	-28.1 ± 0.2	0.364 ± 0.124
G. microcarpa	86.2 ± 3.8	1.02 ± 0.06	0.35 ± 0.03	2.41 ± 0.18	2.09 ± 0.12	19.9 ± 1.6	0.112 ± 0.011	0.091 ± 0.009	22.7 ± 1.4	-29.3 ± 0.7	4.502 ± 0.602
H. ulmoides	73.5 ± 3.9	0.59 ± 0.03	0.26 ± 0.02	2.04 ± 0.07	1.47 ± 0.07	22.6 ± 1.0	0.091 ± 0.010	0.067 ± 0.006	22.3 ± 1.0	-29.8 ± 0.1	4.798 ± 0.586
H. verrucosa	94.2 ± 4.5	0.69 ± 0.05	0.43 ± 0.04	3.10 ± 0.23	2.87 ± 0.24	16.0 ± 1.3	0.121 ± 0.002	0.108 ± 0.011	29.0 ± 4.0	-28.3 ± 0.4	7.732 ± 0.423
J. globiflora	98.1 ± 2.7	1.46 ± 0.07	0.36 ± 0.04	2.57 ± 0.11	2.52 ± 0.16	19.7 ± 1.0	0.150 ± 0.001	0.157 ± 0.008	16.8 ± 0.4	-27.6 ± 0.4	2.501 ± 0.251
M. discolor	83.1 ± 3.7	0.64 ± 0.06	0.49 ± 0.05	3.60 ± 0.16	3.00 ± 0.28	12.8 ± 0.6	0.112 ± 0.005	0.089 ± 0.012	31.9 ± 3.4	-27.1 ± 0.5	8.744 ± 0.316
M. obtusifolia	80.6 ± 5.6	0.55 ± 0.04	0.52 ± 0.06	2.56 ± 0.16	1.98 ± 0.11	19.1 ± 1.3	0.118 ± 0.011	0.100 ± 0.008	21.2 ± 0.7	-28.9 ± 0.4	6.849 ± 0.288
M. stuhlmannii	93.9 ± 4.7	0.80 ± 0.06	0.39 ± 0.04	4.26 ± 0.08	3.99 ± 0.18	11.0 ± 0.3	0.150 ± 0.009	0.149 ± 0.010	28.6 ± 2.3	-27.6 ± 0.2	-1.162 ± 0.136
P. angolensis	81.8 ± 2.1	1.91 ± 0.07	0.39 ± 0.03	3.07 ± 0.09	2.52 ± 0.13	15.9 ± 0.4	0.129 ± 0.013	0.111 ± 0.008	24.4 ± 1.9	-28.1 ± 0.3	-1.85 ± 0.253
P. maprouneifolia	87.6 ± 2.3	1.27 ± 0.06	0.27 ± 0.02	1.77 ± 0.05	1.55 ± 0.07	26.9 ± 0.7	0.122 ± 0.004	0.111 ± 0.005	14.4 ± 0.5	-27.8 ± 0.3	1.269 ± 0.287
P. myrtifolia	105.6 ± 3.3	1.03 ± 0.05	0.37 ± 0.04	1.63 ± 0.08	1.71 ± 0.09	29.4 ± 1.3	0.104 ± 0.010	0.108 ± 0.014	16.2 ± 1.3	-29.4 ± 0.3	2.768 ± 0.776
Rytiginia sp.	59.2 ± 3.0	0.93 ± 0.04	0.75 ± 0.15	2.41 ± 0.09	1.43 ± 0.16	19.8 ± 0.8	0.164 ± 0.007	0.092 ± 0.008	14.2 ± 0.7	-30.1 ± 0.4	7.449 ± 0.356
S. birrea	134.4 ± 3.1	1.44 ± 0.08	0.14 ± 0.01	1.28 ± 0.04	1.72 ± 0.10	35.8 ± 1.1	0.077 ± 0.004	0.108 ± 0.005	16.9 ± 1.0	-28.5 ± 0.2	2.675 ± 0.622
S. cocculoides	133.3 ± 6.4	0.69 ± 0.02	0.17 ± 0.02	1.83 ± 0.10	2.34 ± 0.13	26.6 ± 1.7	0.094 ± 0.004	0.126 ± 0.012	20.5 ± 1.2	-29.3 ± 0.3	2.737 ± 0.633
S. spinosa	133.7 ± 3.7	0.70 ± 0.04	0.32 ± 0.04	1.83 ± 0.10	2.43 ± 0.15	27.1 ± 1.9	0.070 ± 0.003	0.096 ± 0.006	25.9 ± 2.5	-27.8 ± 0.2	9.249 ± 0.259
S. zanzibariensis	111.3 ± 7.2	0.49 ± 0.02	0.24 ± 0.04	1.83 ± 0.17	2.01 ± 0.16	27.4 ± 2.9	0.064 ± 0.013	0.077 ± 0.009	30.2 ± 2.9	-28.8 ± 0.7	5.256 ± 0.314
X. stuhlmannii	98.9 ± 2.1	1.63 ± 0.06	0.26 ± 0.03	3.06 ± 0.05	3.03 ± 0.12	15.9 ± 0.2	0.132 ± 0.010	0.128 ± 0.012	23.1 ± 1.8	-26.9 ± 0.4	-1.030 ± 0.160

Table S2.2: Table showing mean foliar traits as a community weighted mean (± 1 SEM) by permanent sample plot.

PSP	**LMA (g/m^2)**	**B$_T$ (mm)**	**L$_a$:S$_a$ (m^2/cm^2)**	**N$_m$ (%)**	**N$_a$ (g/m^2)**	**C:N (g/g)**	**P$_m$ (g/m^2)**	**P$_a$ (g/m^2)**	**N:P**	δ^{13}**C (‰)**	δ^{15}**N (‰)**
P02	127.5 ± 1.7	1.35 ± 0.05	0.27 ± 0.02	1.57 ± 0.04	1.94 ± 0.07	32.0 ± 0.6	0.085 ± 0.002	0.108 ± 0.003	18.6 ± 0.7	-28.6 ± 0.2	1.424 ± 0.309
P03	117.3 ± 1.6	1.21 ± 0.04	0.26 ± 0.02	2.21 ± 0.04	2.51 ± 0.06	23.3 ± 0.5	0.104 ± 0.003	0.120 ± 0.004	22.2 ± 0.8	-28.7 ± 0.1	0.572 ± 0.215
P04	154.1 ± 2.7	1.33 ± 0.03	0.39 ± 0.04	1.37 ± 0.05	2.09 ± 0.07	35.9 ± 1.3	0.088 ± 0.005	0.139 ± 0.010	15.6 ± 1.0	-28.6 ± 0.2	0.523 ± 0.373
P05	100.4 ± 2.7	1.10 ± 0.04	0.38 ± 0.02	2.10 ± 0.06	2.03 ± 0.09	24.5 ± 0.6	0.108 ± 0.005	0.111 ± 0.004	19.7 ± 0.9	-28.5 ± 0.2	3.181 ± 0.314
P06	87.5 ± 1.8	0.74 ± 0.02	0.38 ± 0.03	2.08 ± 0.03	1.78 ± 0.05	23.2 ± 0.5	0.102 ± 0.005	0.085 ± 0.004	21.2 ± 0.7	-29.2 ± 0.1	5.228 ± 0.277
P07	102.8 ± 1.3	1.45 ± 0.03	0.47 ± 0.03	1.89 ± 0.04	1.85 ± 0.05	28.7 ± 0.4	0.095 ± 0.002	0.098 ± 0.003	19.3 ± 0.4	-28.1 ± 0.1	0.817 ± 0.118
P08	138.4 ± 3.5	1.67 ± 0.06	0.21 ± 0.02	1.56 ± 0.06	2.09 ± 0.10	33.5 ± 1.3	0.075 ± 0.006	0.105 ± 0.007	20.8 ± 0.6	-29.2 ± 0.2	1.043 ± 0.203
P09	109.8 ± 1.8	1.22 ± 0.03	0.30 ± 0.01	2.25 ± 0.04	2.38 ± 0.06	23.1 ± 0.5	0.107 ± 0.003	0.117 ± 0.003	21.9 ± 0.6	-28.7 ± 0.1	1.785 ± 0.195
P10	98.8 ± 1.0	1.41 ± 0.03	0.45 ± 0.02	1.98 ± 0.04	1.88 ± 0.05	27.0 ± 0.4	0.105 ± 0.002	0.105 ± 0.003	18.6 ± 0.3	-28.0 ± 0.1	0.963 ± 0.113
P11	119.6 ± 1.4	1.29 ± 0.02	0.42 ± 0.02	1.97 ± 0.04	2.19 ± 0.05	28.2 ± 0.7	0.109 ± 0.002	0.129 ± 0.004	17.9 ± 0.6	-28.1 ± 0.1	0.865 ± 0.196
P12	101.6 ± 0.9	1.35 ± 0.03	0.39 ± 0.02	2.25 ± 0.04	2.24 ± 0.05	23.9 ± 0.4	0.120 ± 0.002	0.126 ± 0.002	18.5 ± 0.3	-27.7 ± 0.1	1.412 ± 0.149
P13	108.7 ± 1.6	1.41 ± 0.03	0.36 ± 0.01	1.83 ± 0.04	1.92 ± 0.05	28.5 ± 0.6	0.100 ± 0.003	0.106 ± 0.003	18.7 ± 0.4	-28.2 ± 0.2	0.753 ± 0.171
P14	108.3 ± 1.6	1.03 ± 0.03	0.40 ± 0.02	2.02 ± 0.05	2.11 ± 0.06	26.9 ± 0.7	0.109 ± 0.004	0.117 ± 0.006	18.5 ± 0.7	-28.6 ± 0.1	1.515 ± 0.287
P15	103.1 ± 1.5	1.32 ± 0.04	0.38 ± 0.02	2.39 ± 0.06	2.40 ± 0.08	22.7 ± 0.5	0.131 ± 0.001	0.138 ± 0.004	18.2 ± 0.3	-27.8 ± 0.2	1.800 ± 0.160
P16	114.9 ± 1.0	1.33 ± 0.02	0.34 ± 0.01	2.05 ± 0.03	2.22 ± 0.04	26.5 ± 0.5	0.113 ± 0.002	0.130 ± 0.004	18.0 ± 0.5	-27.8 ± 0.1	1.502 ± 0.166
P17	140.3 ± 1.9	1.31 ± 0.04	0.41 ± 0.03	1.34 ± 0.05	1.86 ± 0.09	37.9 ± 1.1	0.084 ± 0.004	0.115 ± 0.005	16.9 ± 0.9	-28.2 ± 0.2	0.978 ± 0.328
P18	111.4 ± 1.2	1.40 ± 0.03	0.45 ± 0.02	1.98 ± 0.04	2.10 ± 0.06	27.2 ± 0.6	0.111 ± 0.002	0.123 ± 0.004	17.9 ± 0.5	-27.9 ± 0.1	1.114 ± 0.181
P19	140.5 ± 2.6	1.27 ± 0.03	0.33 ± 0.02	1.63 ± 0.05	2.28 ± 0.08	31.6 ± 0.8	0.084 ± 0.003	0.116 ± 0.004	20.4 ± 0.8	-28.9 ± 0.2	0.537 ± 0.287
P20	106.4 ± 1.1	1.40 ± 0.03	0.37 ± 0.02	2.31 ± 0.04	2.39 ± 0.07	23.2 ± 0.5	0.124 ± 0.003	0.133 ± 0.004	18.6 ± 0.5	-27.5 ± 0.2	1.039 ± 0.176
P21	96.1 ± 1.1	1.15 ± 0.02	0.38 ± 0.01	2.43 ± 0.03	2.29 ± 0.04	22.4 ± 0.3	0.113 ± 0.002	0.112 ± 0.003	21.2 ± 0.5	-28.1 ± 0.1	1.582 ± 0.143
P22	98.1 ± 2.5	0.78 ± 0.02	0.37 ± 0.02	2.48 ± 0.11	2.34 ± 0.10	21.2 ± 0.6	0.107 ± 0.003	0.101 ± 0.005	25.1 ± 1.8	-28.7 ± 0.2	5.542 ± 0.203
P23	112.6 ± 2.3	1.03 ± 0.05	0.23 ± 0.03	2.42 ± 0.07	2.67 ± 0.08	20.3 ± 0.5	0.095 ± 0.005	0.106 ± 0.005	25.7 ± 1.7	-29.2 ± 0.2	-0.820 ± 0.372
P24	107.6 ± 1.4	1.31 ± 0.03	0.39 ± 0.02	2.15 ± 0.05	2.26 ± 0.06	24.4 ± 0.6	0.114 ± 0.002	0.123 ± 0.003	19.3 ± 0.4	-28.1 ± 0.2	0.984 ± 0.211
P25	91.9 ± 1.7	0.74 ± 0.02	0.40 ± 0.02	2.61 ± 0.06	2.32 ± 0.07	19.9 ± 0.4	0.111 ± 0.004	0.100 ± 0.004	24.4 ± 0.9	-28.6 ± 0.2	5.718 ± 0.219

Table S2.3: Species and community weighted mean trait Pearson correlation coefficients. Correlations are labelled bold where $p < 0.05$, * where $p < 0.01$, and ** where $p < 0.001$. The lower left portion of the table show species correlations, whilst the upper right portion of the table shows community weighted mean traits.

	LMA	**B$_T$**	**L$_a$:S$_a$**	**N$_m$**	**N$_a$**	**C:N**	**P$_m$**	**P$_a$**	**N:P**	**δ^{13}C**	**δ^{15}N**
LMA	-	__0.50__	-0.33	__-0.81**__	-0.06	__0.84**__	__-0.69**__	0.39	-0.40	-0.24	__-0.54*__
B$_T$	__0.40__	-	-0.06	__-0.54*__	-0.20	__0.57*__	-0.21	__0.43__	__-0.63*__	0.40	__-0.74**__
L$_a$:S$_a$	__-0.54*__	-0.27	-	0.03	__-0.45__	0.03	0.40	0.09	__-0.45__	__0.60*__	0.21
N$_m$	__-0.64**__	-0.30	0.32	-	__0.62__	__-0.98**__	__0.76**__	-0.08	__0.63*__	0.17	__0.41__
N$_a$	0.04	-0.06	-0.10	__0.72**__	-	__-0.57__	0.37	0.38	__0.53*__	-0.03	-0.13
C:N	__0.75**__	__0.38__	-0.33	__-0.93**__	__-0.59**__	-	__-0.72**__	0.15	__-0.65**__	-0.07	__-0.42__
P$_m$	__-0.62**__	-0.12	__0.43__	__0.69**__	0.34	__-0.68**__	-	0.39	-0.02	__0.66**__	0.23
P$_a$	0.34	0.31	-0.18	0.16	__0.51*__	-0.04	__0.48*__	-	__-0.57*__	__0.57*__	__-0.47__
N:P	-0.20	__-0.38__	-0.02	__0.57**__	__0.60**__	__-0.55*__	-0.15	-0.34	-	__-0.57*__	__0.41__
δ^{13}C	-0.20	0.09	0.08	__0.37__	0.28	-0.24	0.35	0.32	0.03	-	-0.20
δ^{15}N	-0.35	__-0.65**__	__0.37__	0.12	-0.17	-0.21	0.04	__-0.42__	0.24	-0.04	-

CHAPTER 3

What drives variation in woody productivity and tree mortality in miombo woodlands?

ABSTRACT

Background and aims: Savannah ecosystems are complex and dynamic, with vegetation structural changes occurring continuously as a result of the altering balance between the growth, mortality, and recruitment of individual tree stems. Developing a predictive understanding of the savannah carbon cycle requires quantification of stem demographic rates, and identification of the key processes that regulate stem growth and mortality.

Methods: This study measured tree growth, mortality and recruitment in 24 Permanent Sample Plots (PSPs) in the structurally diverse miombo woodland landscape of Kilwa District, southeastern Tanzania. Tree demographic rates are calculated from changes in PSP inventory data over 2 years, and rates of woody carbon cycling estimated using tree allometry. We use hierarchical models and multi-model inference to relate tree growth and mortality rates to stem size, damage, competitive stress, vegetation structure, fire frequency and soil properties.

Results: Growth rates in miombo woodlands are slow (1.55 ± 0.57 mm/yr), and top-kill (4.0 %/yr) and recruitment (2.9 %/yr) are rare. Carbon fluxes from woody production and loss are widely variable, and closely associated with standing woody biomass. Stem growth and mortality did not occur at random, though models suggest a limited deterministic component to individual stem development. Growth rates were slowed by damage, and mortality was observed to be elevated in the smallest stems, and in cases where prior damage had been observed.

Conclusions: Stem demographic rates and woody carbon cycling are widely variable in miombo woodlands, though differences were for the most part not predictable. We note some evidence that environmental influences are altering tree population dynamics, which may translate into heterogeneity of vegetation structure.

3.1 Introduction

Savannah ecosystems play a prominent role in the global carbon (C) cycle, accounting for approximately 20 % of the land surface and 30 % of global net primary production (Grace et al., 2006). As the result of few dedicated observational networks, the C cycle of savannahs is very poorly resolved (Williams et al., 2007), and the key processes regulating vegetation dynamics are uncertain. This problem is particularly acute in miombo woodlands, a woody savannah ecosystem characterised by tree species of the genera *Brachystegia*, *Julbernardia* and *Isoberlinia* which forms the dominant land cover of southern Africa (White, 1983). Unlike the forests of central Africa (e.g. Lewis et al., 2009; Willcock et al., 2014), the C cycle of miombo woodlands has received relatively little attention, having been only infrequently measured for C stocks, and rarely re-censused for estimates of C stock changes.

C cycling in savannah ecosystems is closely related to tree population dynamics, where demographic transitions exert a large influence on ecosystem structure and function (Bond, 2008; Hoffmann et al., 2012). Understanding the processes that regulate savannah demography, and as a result the C cycle, is fundamental to building accurate predictive models of savannah ecosystems. For example, the rate at which a tree stem grows relates to its capacity to withstand fires by attaining sufficient height (Bond and Midgley, 2000) or bark thickness (Hoffmann et al., 2009). Stem top-kill is similarly pivotal to the dynamics of savannah ecosystems, with processes such as fire resulting in a wide array of vegetation structures (Furley et al., 2008; Ryan and Williams, 2011). Reliable estimates of tree growth, mortality, and recruitment are also important for sustainable forest management, where demographic rates are required to calculate supportable rates of harvesting for timber and fuelwood.

Studies have identified a range of factors that mediate demographic rates in savannah ecosystems, though the magnitude and relative importance of these mechanisms in miombo woodlands is uncertain. Savannah landscapes are often extremely heterogeneous, with divergent vegetation structures related to the supply of light, competition with other trees and grasses, and exposure to fire (see Chapter 2). Fires in particular may have a large impact on woodland structure, increasing top-kill and impeding recruitment of woody plants (Ryan and Williams, 2011), but also resulting in reductions in stem growth (Murphy et al., 2010). Soils in miombo woodlands generally have a low nutrient status, leading to questions about the extent to which woody production is limited by nutrient availability. Variation in soil fertility may drive divergence of savannah structure (Dantas et al., 2015), an effect we may detect in more rapid growth rates and a reduced risk of top-kill in fertile soils.

As well as aggregate tree community drivers, there exist a range of stem-scale drivers that modify stem growth and mortality. As savannah trees mature they gain greater resilience to fire and herbivory (Midgley et al., 2010; Ryan and Williams, 2011), as well as gaining localised access to resources such as water and nutrients. Savannahs are often heavily disturbed, with trees showing accumulated damage from fires, elephants, and termites (Ribeiro et al., 2008). Frequent top-kill and crown-distortion can reduce growth by diminishing a tree's photosynthetic capacity (Holdo, 2006), and may be a precursor to mortality by leaving trees vulnerable to fire ingress (Holdo, 2005). Tree growth and survival may also be strongly reduced by contested access to limited soil nutrients, water and light, which are patchily distributed in savannah ecosystems (Woollen et al., 2012). Alternately, high disturbance frequency may lead to competition playing a relatively small role in tree communities that are prevented from reaching their maximum potential woody biomass.

In this paper we report on data from the Kilwa Permanent Sample Plot (PSP) network, established in 2010/11 in southeastern Tanzania. PSP re-inventory data from 2012/13 is used to generate estimates of productivity and turnover of woody biomass in miombo woodlands, and estimate rates of rates of growth, mortality, and recruitment

Table 3.1: Summary of hypothesised predictors of stem growth and mortality. The global model contains all candidate model terms used in the complete subsets regression.

Analysis	**Global Model**
Growth Annualised stem DBH increment in relation to stem diameter (DBH), aboveground woody biomass (AGB), indications of damage, inter-tree competition, fire occurrence between inventories (F_{OBS}), historical fire frequency (F_{FREQ}), soil properties (soil), and interactions between DBH and fire/damage.	DBH increment ~ DBH + AGB + damage + competition + F_{OBS} + F_{FREQ} + soil properties + DBH:damage + DBH:F_{OBS} + DBH:F_{FREQ}, random = species, plot
Mortality Probability of stem mortality between inventories in relation to stem diameter (DBH), aboveground woody biomass (AGB), indications of damage, inter-tree competition, fire occurrence between inventories (F_{OBS}), historical fire frequency (F_{FREQ}), soil properties (soil), and interactions between DBH and fire/damage	Stem mortality ~ log(DBH) + AGB + damage + competition + F_{OBS} + F_{FREQ} + soil + DBH:damage + DBH:F_{OBS} + DBH:F_{FREQ}, random = species, plot, link = logit

of individual stems. Our aim was to relate estimates of stem growth and mortality to the influence of stem size, damage, competition, fire, soil fertility, and vegetation structure (Table 3.1).

Our research questions were:

1. What are rates of woody carbon cycling in miombo woodlands, and how do they vary?
2. What are rates of growth, mortality and recruitment in miombo woodlands, and how do they vary?
3. What biotic and abiotic processes regulate demographic rates in miombo woodlands?

3.2 Methods

3.2.1 Plot inventory

PSPs (n = 25) measuring 100 x 100 m (1 ha) were established across Kilwa District, Tanzania in 2010/11. PSPs were were spread across a range of structurally-defined vegetation types, here referred to as savannahs (dominated by grasses with sparse tree cover), woodlands (with co-dominance of grasses and trees), and forests (closed-canopy, excluding a grassy understory) (see Chapter 2). One PSP (P01) was excluded from further analysis *post hoc* after it was established to represent regrowth of recently abandoned field. The diameter at breast height (DBH) and species of all stems > 5 cm DBH was recorded, and each tree tagged with a unique code for re-identification. DBH was measured at 1.3 m above ground level, and the point of measurement marked with spray paint to aid comparable re-measurement. Where trees were split below the point of measurement, stems was measured separately and the tree base was assigned a unique tag. The status (live / dead), condition (any evidence of bark loss, stem damage or leaning), and coordinate location of each tree was recorded. As large trees are relatively rare and mortality in these stems is infrequent, an additional Large Sample Plot (LSP) was established at each location covering 300 x 300 m (9 ha), in which the status of all large stems (> 40 cm DBH) was measured to ensure a sufficient sample size for reliable estimation of large stem mortality rates.

PSPs were re-inventoried following 2 years of growth, at the same time of year to minimise any impact of variation in water availability on DBH. Trees were relocated, remeasured, and an assessment made as to whether each stem was alive or dead. Where a stem was marked as dead, field teams recorded the mode of death (snapped, standing, uprooted, or vanished), type of death (totally killed, top-killed with resprouting, or top-killed with no sign of resprouting), and assessed the probable cause of mortality (elephants, fire, human activity, impact of a neighbouring tree, termites, or wind) for all stems where readily ascertainable.

3.2.2 Estimation of carbon fluxes

A range of parameters relating to the aboveground woody C cycle were calculated for each PSP (Fig. 3.1). Plot aboveground living woody biomass (AGB) was estimated using a miombo-specific allometric equation relating the DBH of each stem to its biomass (Ryan et al., 2011). C increases through growth and recruitment (woody

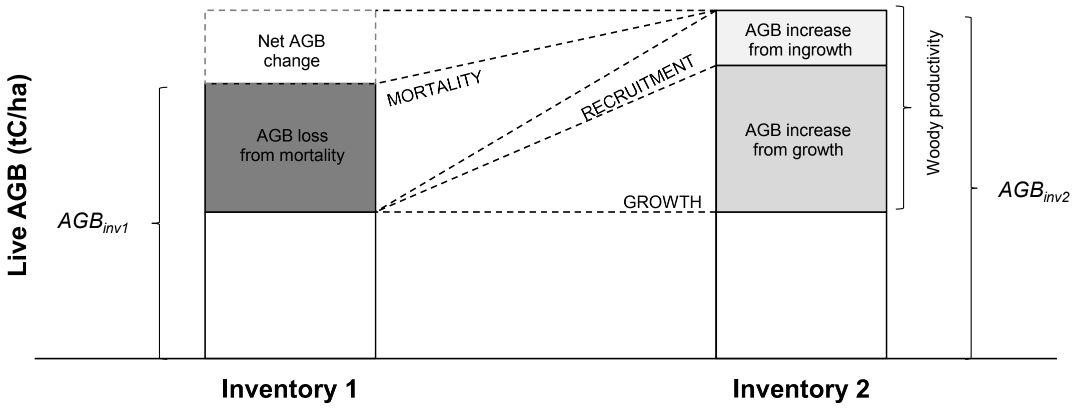

Figure 3.1: Important parameters relating to the woody carbon cycle of miombo woodlands were estimated using repeat forest inventory data from permanent sample plots. The translation from measurements of stem diameter increment, mortality and recruitment, to aboveground biomass (AGB) changes are illustrated in this schematic diagram.

productivity), and C loss through mortality were calculated from changes in AGB between inventories. Net AGB change was determined from the difference between woody productivity and woody loss from mortality. Woody productivity divided by AGB measured in the first inventory provides an estimate of woody residence time, a crucial yet highly uncertain parameter in terrestrial C cycle models (Galbraith et al., 2013; Friend et al., 2014). This calculation assumes that PSPs are near-equilibrium, and are not recovering from disturbance (Malhi, 2012); the extent to which this applies to miombo woodlands cannot be verified. To mitigate gross errors in DBH measurements, any stem that exhibited an unrealistically high (> 40 mm/yr) or low (< -5 mm/yr) DBH increment was estimated using the median stem diameter increment each PSP, assuming the second DBH measurement is the more reliable assessment. This is a conservative correction with respect to woody productivity (Phillips et al., 2009), and affected a total of 200 (1.5 %) of all stems.

3.2.3 Quantification of demographic rates

Growth rates were estimated for each stem, expressed as the annual DBH increment for trees that were recorded as living in both plot inventories. DBH increment was selected as a measure of stem growth as it is largely self-scaling, whereby the generally greater growth rate of large trees is offset against the reduction in diameter increment for each additional unit of woody biomass accumulated (Prior et al., 2004). Where gross errors were detected in growth rates and in cases where it was necessary to change the point of measurement between inventories, stem diameter increment estimates were omitted.

Stem mortality was noted where a tree that was recorded as alive in the first inventory was recorded as dead in the second inventory. Tree mortality took the form of both stem top-kill and whole-tree mortality; here both are referred to as mortality. Mortality was recorded separately for all stems of each tree. Where stems were recorded as living in the second inventory but not the first, stems were treated as not dead. It should be noted that our estimates may represent an upper bound on stem mortality rates as it can be difficult to distinguish a stem that is dead from one that remains alive but dormant. Recruitment was recorded as a count of stems that were only documented the second inventory. Mortality and recruitment are expressed as counts and as a rate corrected for the stems that are recruited and die within the re-inventory period (Sheil and May, 1996). The mean of stem mortality and recruitment rates is reported as the turnover, describing the the rate at which woodland stems are replaced.

Demographic rates and C fluxes are presented as PSP mean averages, and by land cover classes representing savannahs, woodlands and forests (± 1 standard deviation) (see Chapter 2). Systematic variation in vegetation dynamics was evaluated with ANOVA to test for differences between land cover classes, and linear regression to test for changes with AGB.

3.2.4 Regulation of stem growth and mortality

We hypothesised that the growth and mortality of individual stems is influenced by stem size, damage, competition, fire, soil fertility and vegetation structure (Table 3.1). These variables have all previously been shown to relate to vegetation dynamics in other studies of savannah ecosystems, justifying their inclusion in the candidate model set. Model variables considered are:

Stem size Stem size is represented by the DBH measurement of each stem at the first PSP inventory. Stem size is included as a linear term in growth models (DBH) and a logarithmic term in mortality models (log(DBH)) in recognition of observations of considerably greater mortality in the smallest of stems (Williams et al., 1999; Prior et al., 2009; Ryan and Williams, 2011)

Stem damage A binary predictor of tree health is used (0 where undamaged, 1 where damaged), with any observation of leaning, broken stems or loss of bark in the first inventory marked as tree damage.

Vegetation structure Vegetation structure in miomvo woodlands is associated with a range of biotic and abiotic environmental differences (see Chapter 2). Vegetation structure was expressed as AGB, calculated as the sum of living stem biomass in each PSP in the first inventory.

Competition Stem competitive stress was assessed using a simple index of the DBH of nearest neighbouring stems and their distance (Hegyi, 1974). Where a tree is multi-stemmed, the effective DBH of all stems was considered as a single tree. As only stems > 40 cm DBH were measured in LSPs these stems were assigned the median competition value for each PSP.

Fire activity Fire was included in two model terms: a descriptor of whether a plot was observed to have burned between inventories (F_{OBS}), and the historical frequency of burn scars at each plot (F_{FREQ}). These predictors aim to respectively encode the impact of an individual fire, and the long-term impacts of fire-prone environments on stem demography. F_{OBS} was determined using a combination of ground observations at the time of PSP measurement, aerial photography (October 2010), and manually identified burn scars in Landsat data. F_{FREQ} was estimated computationally from a series of probabilistically classified Landsat scenes dating back to 10 years prior to the first stem inventory (see Chapter 4). F_{FREQ} was calculated by summing the probability of the plot having burned over each year.

Soil properties A range of soil properties (organic C, nitrogen, phosphorus, pH, and texture) were measured at PSPs in 2014 (see Chapter 2), which are reduced to a single soil fertility measure using principal component analysis (PCA) (Fig. S3.1). Positive values of the resulting index (describing 35.2 % of variance in soil properties) are associated with increased nutrient availability, lower pH, and sandy texture.

Interactions Interactions were included between DBH and key model terms competition, F_{FREQ} and F_{OBS}, all of which are expected to vary with stem size.

Data were analysed using hierarchical models, an approach allowing for the investigation of predictors measured at both individual stem and plot-scales without losing data through aggregation or committing pseudoreplication by treating spatially-clustered individuals as independent samples (Gelman and Hill, 2007). We employ linear mixed models for analysis of growth data, and generalised linear mixed models with a logit link for analysis of binary mortality data. Plot and species were specified as random effects, correcting for within-plot correlations and inter-specific differences in stem responses by varying the intercept term.

Models of growth and mortality were evaluated using full-subsets regression, in which all additive combinations of parameters are represented in the candidate model set. We acknowledge that many interactions between predictor variables probably exist, though as their inclusion rapidly increases model complexity we limit this study to those likely to be associated with stem size. Models were ranked using the Bayesian Information Criterion (BIC), a measure of the relative quality of statistical models that strongly penalises the addition of parameters with poor explanatory power (Burnham and Anderson, 2002). Models were compared by their probability of a particular model offering the best fit to the data (w_i) (Hurvich and Tsai, 1989). The sum of w_i for all models in which a predictor appears is reported as the weight of evidence ($w+$), a measure of the probability that a parameter is present in the top ranked model. Model averaged parameters and standard deviations were calculated from models weighted by their w_i, a procedure reducing the uncertainty of selecting a single 'best' model (Burnham and Anderson, 2002). Model fit was assessed using the pseudo-R^2 measure of Nakagawa and Schielzeth (2013), which approximates the variance explained by both fixed and random effects ($R^2_{conditional}$), and fixed effects alone ($R^2_{marginal}$).

All data analysis was performed in R (R Core Team, 2015), using lme4 (Bates et al., 2014), MuMIn (Bartoń, 2015), siplab (Garcia, 2014), and spatstat (Baddeley et al., 2015) packages.

3.3 Results

3.3.1 Vegetation properties

Across the 24 investigated PSPs, 12,201 living stems were measured in the first inventory, of which 11,266 were still living by the second inventory. A total of 585 recruited stems were recorded in the inventory period (Table 3.2). Plot AGB varied

Table 3.2: Vegetation properties in Kilwa District permanent sample plots. Where presented errors are ± 1 standard deviation, describing variation by land cover type. Dominant species are the top three species by basal area.

	Plot	**Live stems (/ha)**	**Basal area (m^2/ha)**	**AGB (tC/ha)**	**Stem damage**	**Dominant species**
Savannah:	P17	75	0.9	1.9	9 (12.0 %)	*Combretum apiculatum*, *Combretum zeyheri*, *Flueggea virosa*
	P19	204	1.5	2.4	11 (5.4 %)	*C. apiculatum*, *Sclerocarya birrea*, *Acacia nilotica*
	P04	527	2.7	3.5	96 (18.2 %)	*Burkea africana*, *C. apiculatum*, *Bauhinia petersiana*
	P02	160	1.9	4.7	23 (14.4 %)	*S. birrea*, *Acacia nigrescens*, *C. apiculatum*
	P03	255	2.8	5.1	34 (13.3 %)	*Dalbergia melanoxylon*, *Diospyros fischeri*, *Julbernardia globiflora*
	P08	72	2	6.9	19 (26.4 %)	*Diospyros quiloensis*, *D. melanoxylon*, *B. petersiana*
	P13	206	4.4	12.1	39 (18.9 %)	*Brachystegia boehmii*, *Pseudolachnostylis maprouneifolia*, *C. apiculatum*
	P24	358	6.6	15.2	53 (14.8 %)	*C. apiculatum*, *J. globiflora*, *Acacia reficiens*
	P05	311	6.5	15.4	34 (10.9 %)	*Pseudolachnostylis maprouneifolia*, *Bridelia scleroneura*, *Brachystegia tamarindoides*
	P23	275	6.5	16.1	77 (28.0 %)	*D. melanoxylon*, *Acacia nigrescens*, *B. scleroneura*
	P09	374	6.9	16.8	52 (13.9 %)	*Julbernardia globiflora*, *D. melanoxylon*, *D. quiloensis*
	Mean	256 ± 135	3.9 ± 2.3	9.1 ± 6.0	41 (16.0 %)	*D. melanoxylon*, *C. apiculatum*, *S. birrea*
Woodland:	P10	572	6.9	15.8	108 (18.9 %)	*Diplorhynchus condylocarpon*, *P. maprouneifolia*, *B. boehmii*
	P14	426	6.9	16.2	59 (13.8 %)	*Pteleopsis myrtifolia*, *C. apiculatum*, *P. maprouneifolia*
	P18	328	8.1	22.7	78 (23.8 %)	*B. boehmii*, *J. globiflora*, *D. condylocarpon*
	P21	862	11.6	24.9	92 (10.7 %)	*Brachystegia spiciformis*, *Hymenocardia ulmoides*, *Millettia stuhlmannii*
	P12	632	11	27.3	88 (13.9 %)	*J. globiflora*, *B. spiciformis*, *D. condylocarpon*
	P16	608	11.6	29	72 (11.8 %)	*B. spiciformis*, *Combretum binderianum*, *B. africana*
	P07	464	10.6	29.7	47 (10.1 %)	*B. boehmii*, *D. condylocarpon*, *Julbernardia paniculata*)
	P20	258	10.1	30.7	52 (20.2 %)	*J. globiflora*, *C. apiculatum*, *Xeroderris stuhlmannii*)
	P15	686	13	33	60 (8.7 %)	*J. globiflora*, *C. apiculatum*, *M. stuhlmannii*
	P11	441	12.3	33.2	118 (26.8 %)	*C. apiculatum*, *B. africana*, *J. globiflora*
	Mean	528 ± 180	10.2 ± 2.2	26.3 ± 6.3	77 (15.9 %)	*J. globiflora*, *C. apiculatum*, *D. condylocarpon*
Forest:	P06	1481	17.1	36.6	231 (15.6 %)	*H. ulmoides*, *Diospyros mespiliformis*, *Rytigynia sp.*
	P25	1145	17.5	41.5	245 (21.4 %)	*Manilkara discolour*, *H. ulmoides*, *Markhamia obtusifolia*
	P22	1481	19.1	43.6	435 (29.4 %)	*Hymenaea verrucosa*, *H. ulmoides*, *Suregada zanzibariensis*
	Mean	1369 ± 194	17.9 ± 1.1	40.6 ± 3.6	304 (22.1 %)	*H. verrucosa*, *H. ulmoides*, *P. myrtifolia*
All:	*Mean*	508 ± 389	8.3 ± 5.2	20.2 ± 12.7	89 (16.7 %)	*J. globiflora*, *C. apiculatum*, *D. condylocarpon*

Table 3.3: Demographic rates and woody carbon cycling in Kilwa District permanent sample plots. Where presented errors are ± 1 standard deviation, describing variation by land cover type.

	Plot	**DBH increment (mm/yr)**	**Stem mortality (stems/ha/yr)**	**Recruitment (stems/ha/yr)**	**Turnover (%)**	**Growth (tC/ha/yr)**	**Recruitment (tC/ha/yr)**	**Productivity (tC/ha/yr)**	**Mortality (tC/ha/yr)**	**Net change (tC/ha/yr)**	**Residence time (yr)**
Savannah:	P17	0.9 ± 1.4	4 (2.9 %)	6 (4.2 %)	3.6	0.01	0.01	0.02	-0.01	0.01	85
	P19	2.2 ± 2.0	13 (3.3 %)	41 (9.7 %)	6.5	0.11	0.04	0.15	-0.05	0.10	16
	P04	1.5 ± 1.6	45 (4.6 %)	11 (1.1 %)	2.8	0.16	0.01	0.17	-0.09	0.08	21
	P02	2.5 ± 2.7	6 (1.9 %)	11 (3.4 %)	2.7	0.17	0.01	0.18	-0.01	0.17	26
	P03	1.4 ± 1.7	26 (5.8 %)	16 (3.3 %)	4.6	0.09	0.02	0.11	-0.39	-0.28	46
	P08	2.1 ± 2.3	2 (1.4 %)	0 (0.0 %)	0.7	0.09	0.00	0.09	-0.02	0.07	80
	P13	0.6 ± 1.3	16 (4.1 %)	14 (3.4 %)	3.7	0.03	0.02	0.05	-0.08	-0.03	269
	P24	1.9 ± 2.9	24 (4.0 %)	32 (5.0 %)	4.5	0.44	0.04	0.48	-0.12	0.36	31
	P05	1.6 ± 2.0	39 (6.9 %)	9 (1.5 %)	4.2	0.30	0.01	0.31	-0.58	-0.27	49
	P23	2.3 ± 2.8	10 (2.4 %)	29 (6.6 %)	4.5	0.51	0.04	0.55	-0.08	0.47	29
	P09	1.3 ± 2.1	28 (4.1 %)	17 (2.4 %)	3.2	0.25	0.02	0.27	-0.20	0.07	61
	Mean	1.66 ± 0.6	19 (3.8 %)	17 (3.7 %)	3.7 ± 1.5	0.2 ± 0.16	0.02 ± 0.01	0.22 ± 0.17	-0.15 ± 0.18	0.07 ± 0.23	65 ± 72
Woodland:	P10	1.5 ± 2.1	39 (3.6 %)	18 (1.6 %)	2.6	0.36	0.02	0.38	-0.17	0.21	41
	P14	1.4 ± 1.5	49 (6.3 %)	22 (2.6 %)	4.5	0.24	0.03	0.27	-0.64	-0.37	61
	P18	1.5 ± 2.2	15 (2.4 %)	5 (0.8 %)	1.6	0.37	0.01	0.38	-0.11	0.27	61
	P21	2.5 ± 1.8	62 (3.7 %)	63 (3.6 %)	3.7	0.85	0.07	0.92	-0.48	0.44	27
	P12	0.4 ± 1.7	31 (2.5 %)	36 (2.8 %)	2.7	0.27	0.04	0.31	-0.72	-0.41	86
	P16	1.3 ± 2.5	98 (9.3 %)	15 (1.3 %)	5.3	0.42	0.02	0.44	-0.95	-0.51	67
	P07	1.6 ± 2.6	31 (3.6 %)	88 (9.5 %)	6.6	0.33	0.10	0.43	-0.84	-0.41	69
	P20	2.2 ± 3.9	8 (1.6 %)	0 (0.0 %)	0.8	0.74	0.00	0.74	-0.64	0.10	41
	P15	1.5 ± 2.8	83 (6.5 %)	26 (1.9 %)	4.2	0.58	0.03	0.61	-0.76	-0.15	54
	P11	0.7 ± 1.5	26 (3.2 %)	1 (0.1 %)	1.7	0.28	0.00	0.28	-0.19	0.09	118
	Mean	1.46 ± 0.61	44 (4.3 %)	27 (2.4 %)	3.4 ± 1.8	0.44 ± 0.21	0.03 ± 0.03	0.48 ± 0.21	-0.55 ± 0.3	-0.07 ± 0.34	63 ± 26
Forest:	P06	1.8 ± 1.4	88 (3.2 %)	63 (2.2 %)	2.7	0.91	0.08	0.99	-1.14	-0.15	37
	P25	1.3 ± 1.5	92 (4.2 %)	39 (1.7 %)	3.0	0.68	0.04	0.72	-0.99	-0.27	58
	P22	1.2 ± 1.6	100 (3.7 %)	23 (0.8 %)	2.3	0.73	0.03	0.76	-1.17	-0.41	57
	Mean	1.43 ± 0.32	93 (3.7 %)	42 (1.6 %)	2.6 ± 0.4	0.77 ± 0.12	0.05 ± 0.03	0.82 ± 0.15	-1.1 ± 0.1	-0.28 ± 0.13	51 ± 12
All:	*Mean*	1.55 ± 0.57	39 (4.0 %)	24 (2.9 %)	3.4 ± 1.5	0.37 ± 0.26	0.03 ± 0.03	0.40 ± 0.27	-0.43 ± 0.39	-0.03 ± 0.29	62 ± 50

widely, falling between 1.9 and 43.6 tC/ha, reflecting a wide range of vegetation structures. A large number of living trees showed some form of damage, amounting to 2,132 stems (17.5 %) in the first inventory. All recorded forms of stem damage were fairly common, with 2.9 % of stems showing lost bark, 12.1 % leaning, and 4.2 % with broken stems. There was no evidence that the proportion of stems showing damage systematically differed between land cover types ($p = 0.321$) or with AGB ($p = 0.203$).

3.3.2 Carbon cycling

Woody productivity averaged 0.40 ± 0.27 tC/ha/yr across all PSPs, and showed appreciable variability across the landscape (Table 3.3). Woody productivity is strongly associated with AGB ($p < 0.001$, $R^2 = 0.59$), though not when considered as a proportional increase of AGB ($p = 0.067$). Woody loss to mortality averaged 0.43 ± 0.39 tC/ha/yr, and is again a strong correlate of AGB ($p < 0.001$, $R^2 = 0.65$). The increase in woody productivity with AGB was balanced by increases in woody biomass loss through stem mortality, giving a mean net biomass change of -0.03 ± 0.29 tC/ha/yr. Mean AGB change was not significantly different from a change of 0 tC/ha/yr ($p = 0.577$), giving no evidence of directional changes to AGB in Kilwa District (Fig. 3.2). Woody C residence time averaged 63 ± 50 years, and though variable between PSPs, was unrelated to land cover type ($p = 0.917$) or AGB ($p = 0.915$). We found no evidence that plots that burned between PSP inventories showed any differences in woody productivity ($p = 0.121$), or experienced a net loss of AGB ($p = 0.129$). There is some evidence that PSPs that burned were associated with less AGB lost to stem mortality ($p = 0.0235$, $R^2 = 0.18$), a result which is also apparent when mortality is considered as a proportion of initial AGB ($p = 0.0382$, $R^2 = 0.14$).

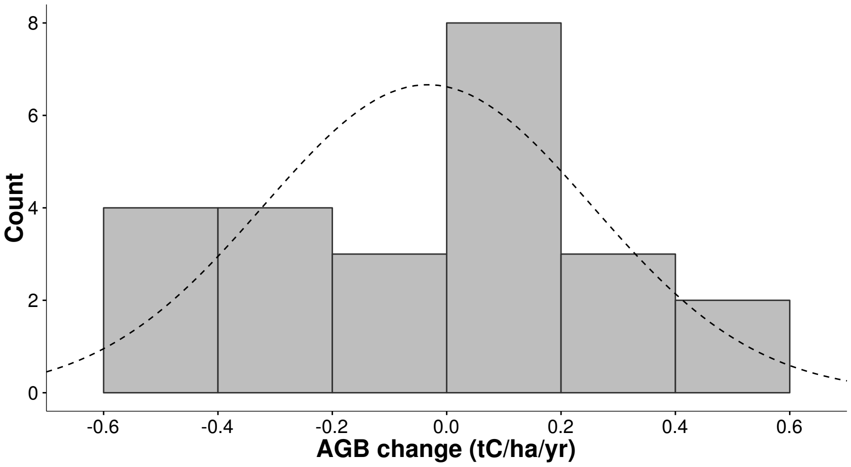

Figure 3.2: Net AGB change in Kilwa permanent sample plots between stem inventories in 2010/11 and 2012/3. AGB change averages -0.03 tC/ha/yr, with no evidence that this differs from no net AGB change (p = 0.577).

3.3.3 Demographic rates

PSP re-inventory data show broad variation in tree population dynamics (Table 3.3). Growth increment averaged 1.55 ± 0.57 mm/yr across all PSPs, and though apparently variable between locations and between species (Table S3.1), did not systematically vary with land cover (p = 0.710) or AGB (p = 0.366). Rates of stem mortality and recruitment were similar, with mortality rates averaging 4.0 %/yr and recruitment averaging 2.9 %/yr, an average stem turnover rate of 3.5 %/yr. Counts of stem mortality increased with AGB ($p < 0.001$, $R^2 = 0.46$) and were different between land cover types ($p < 0.001$, $R^2 = 0.54$), likely related to the greater stocking density of densely vegetated PSPs. There was no equivalent trend in recruitment counts with AGB (p = 0.103) or land cover (p = 0.196), suggesting that recruitment events are stochastic, or are simply difficult to measure. As a proportion of measured stems, there was no evidence that mortality or recruitment differed between land cover types (p = 0.799/0.638) or with AGB (p = 0.641/0.166).

Table 3.4: Growth and mortality models selected from complete subsets regression. Detailed are the three top-ranked models, and a null model with random effects only. Models are ranked by ΔBIC_c (relative to the best model) and the weight of evidence (w_i). Model fit is assessed with pseudo-R^2 measures approximating variance explained fixed (marginal) and both fixed and random (conditional) effects

Response variable	Model	df	ΔBIC_c	w_i	$R^2_{marginal}$	$R^2_{conditional}$
Growth						
	Damage	5	0.00	0.71	0.006	0.153
	Damage + Competition	6	3.00	0.16	0.007	0.149
	Damage + F_{FREQ}	6	5.28	0.05	0.017	0.152
	Null	4	54.69	0.00	0.000	0.151
Mortality						
	Damage + log(DBH)	5	0.00	0.94	0.085	0.253
	Damage + log(DBH) + AGB	6	8.11	0.02	0.089	0.257
	Damage + log(DBH) + F_{FREQ}	6	8.62	0.01	0.088	0.255
	Null	3	176.28	0.00	0.000	0.233

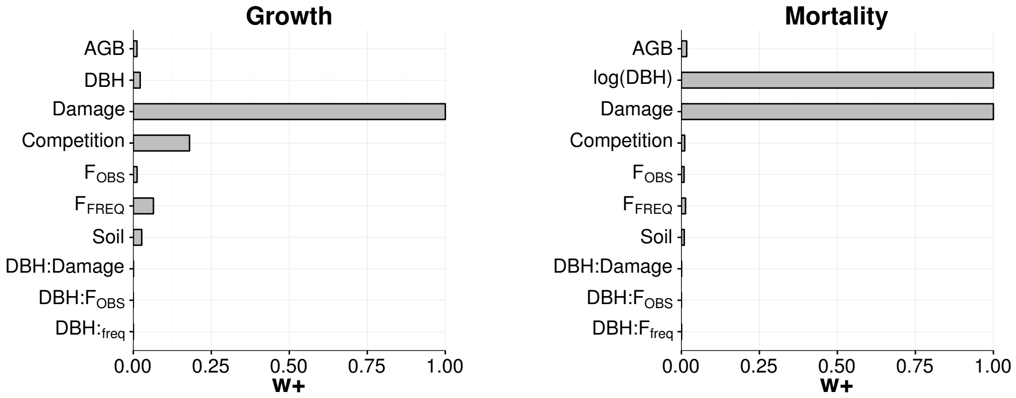

Figure 3.3: Weight of evidence (w+) for growth and mortality model parameters, equivalent to the probability that the parameter is present in the best model. Most parameters have w+ values close to zero, implying that lowest ranked parameters add no predictive power to the model.

3.3.4 Predictors of stem growth

The top ranked models of stem growth included predictors of damage, competition and F_{FREQ} (Table 3.4, Fig. 3.3). Stem damage was a strong predictor of growth rate, coinciding with a 0.45 ± 0.06 mm/yr reduction in diameter increment. Competition between stems predicted a reduction in growth rate, though with a much smaller effect size than stem damage and a much greater uncertainty. Increases in F_{FREQ} were associated with an increased growth rate, where stems in a plot with annual fires have a predicted diameter growth 0.98 ± 0.49 mm/yr greater than in a fire-free stand. A low w_i and large error term associated with this model term indicates a large uncertainty

Table 3.5: Model averaged parameter values for growth and mortality models (± 1 standard error of the mean). Model parameters relate to a reference condition of no damage and no fire, and are presented as the weighted average of all models containing the parameter (conditional average).

Variable	Units	Growth (mm/yr)	Mortality (/yr)
Intercept	-	1.68 (0.16)	-0.715 (0.108)
AGB	tC/ha	-0.0058 (0.0102)	0.00431 (0.00382)
Competition	-	-0.0158 (0.0063)	0.00402 (0.00573)
Damage	binary	-0.451 (0.056)	0.468 (0.042)
DBH, log(DBH)	cm, log(cm)	0.00332 (0.00263)	-0.309 (0.036)
F_{FREQ}	fires/year	0.975 (0.485)	-0.173 (0.188)
F_{OBS}	binary	0.197 (0.302)	-0.017 (0.112)
Soil	-	-0.233 (0.159)	0.0219 (0.0652)
DBH:Damage	-	-0.00890 (0.00783)	0.00370 (0.00686)
DBH:F_{FREQ}	-	0.0221 (0.0101)	0.00479 (0.00839)
DBH:F_{OBS}	-	-0.00619 (0.00550)	0.00463 (0.00506)

associated with this prediction. There was no evidence that DBH, AGB, F_{OBS}, soil properties, or interaction terms were predictors of stem growth. $R^2_{marginal}$ was very low at ~2 % for the top models, whereas $R^2_{conditional}$ was ~15 %, suggesting there exist large inter-specific or localised differences in stem growth that were not captured by this study. Model-averaged parameter values are detailed in Table 3.5.

3.3.5 Predictors of stem mortality

The top ranked models of stem mortality included terms DBH and damage (Table 3.4, Figs. 3.3 and 3.4). DBH is a strong predictor of stem mortality, with low DBH stems observed to have a much higher likelihood of mortality between PSP inventories. Observations of stem damage were associated with a significantly higher probability of mortality. There was no evidence of AGB, competition, F_{OBS}, F_{FREQ}, soil properties, or interaction terms having any influence on rates of stem mortality. $R^2_{marginal}$ in the best models was low (< 8.8 %) as was $R^2_{conditional}$ (~25 %), with both measures indicating that stem mortality was more readily predicted than for equivalent models of stem growth.

Qualitative reports of the causes of stem mortality revealed a range of processes leading to stem death (Fig. 3.5). The majority of stems (55.6 %) were left standing,

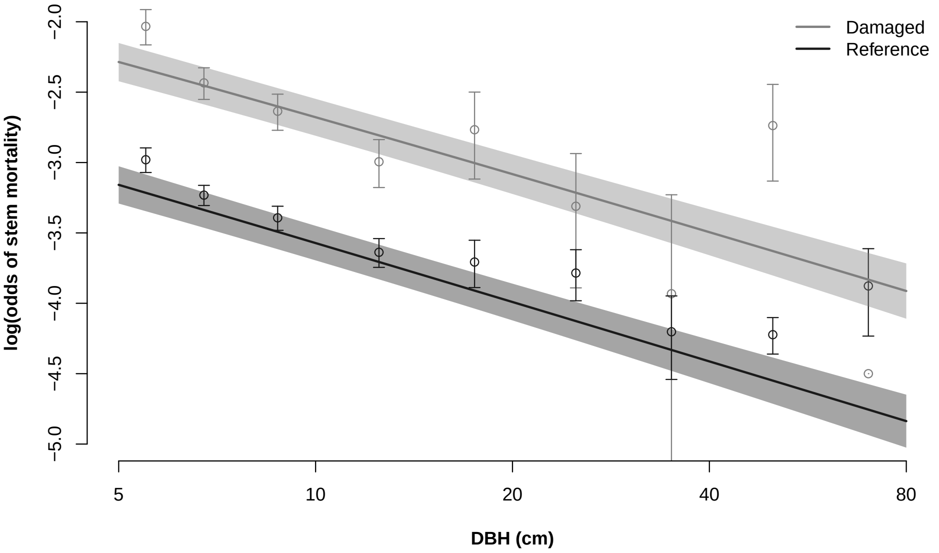

Figure 3.4: Model representation of stem mortality rates, showing effect of stem damage relative to a reference stem with no damage. Mean mortality rates from all measured stems are plotted as an illustrative histogram.

though large numbers of stems were also reported as snapped (17.0 %) and vanished (8.5 %). Most stems were reported as totally killed (90.2 %), with few observations of resprouting (8.9 %) and almost no indication of top-kill without resprouting (0.7 %). Dominant processes reported as leading to stem mortality were elephants (10.5 %), termites (3.5 %) , humans (3.1 %), and fire (2.2 %). In the majority of cases (79.0 %) it was not possible to determine the likely cause of stem mortality.

3.4 Discussion

In this study we generated estimates woody C cycling, quantified tree demographic rates, and assessed the importance of a range of biotic and abiotic conditions on stem growth and mortality in a structurally heterogeneous miombo woodland landscape. C fluxes from woody productivity and woody loss varied widely, though differences

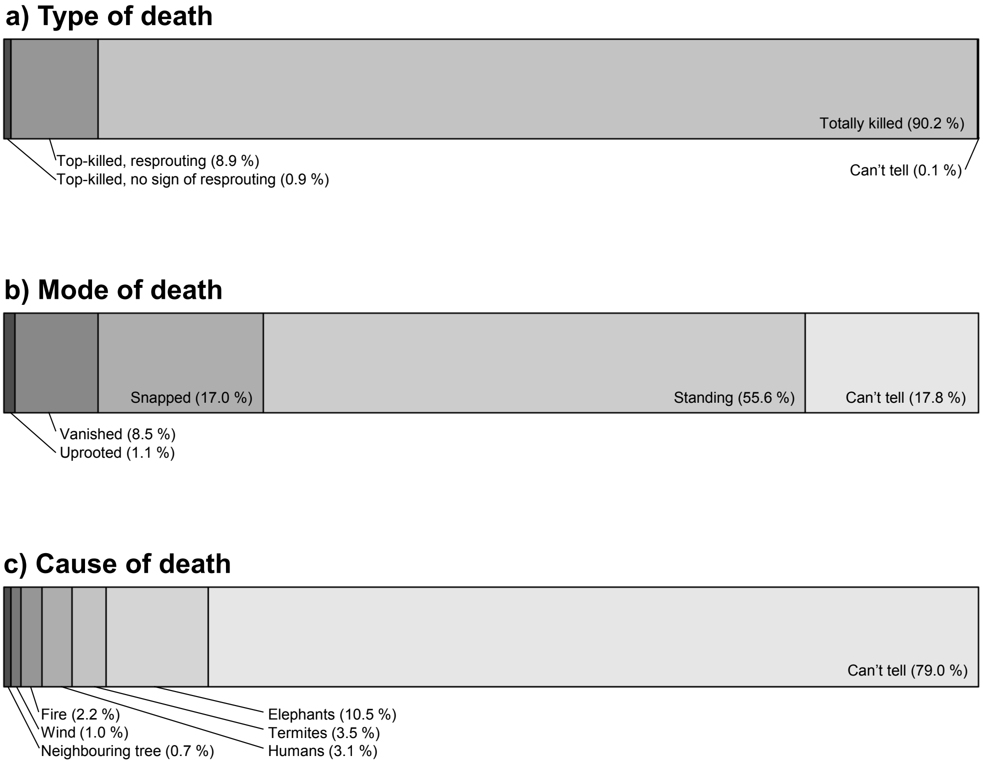

Figure 3.5: Type, mode, and cause of stem mortality of all stems recorded in Kilwa District Permanent Sample Plots.

were only strongly associated with AGB. Woody biomass increments from recruitment were much smaller than growth, and were not correlated with AGB. Rates of stem growth, mortality, and recruitment were diverse, though few patterns were apparent in demographic rates at the plot-scale. Stem diameter increments were observed to be reduced by stem damage, and mortality rates were elevated in the smallest stems and in cases where prior damage had been observed. Plot AGB, competition, fire, and soil properties all showed little bearing on stem demographic rates.

3.4.1 RQ1: What are rates of woody carbon cycling in miombo woodlands, and how do they vary?

Woody productivity in Kilwa District varies by a factor of 50, with plot-scale productivity estimates ranging between 0.02 - 0.99 tC/ha/yr. This variation is tightly coupled to AGB yet is unrelated to woody residence time, implying a degree of stability to the distribution of vegetation structures across the landscape. The mean woody productivity we observe in this study is low, though broadly similar to other studies in 'dry' (< 1000 mm/yr precipitation) miombo woodlands (0.6 - 1.0 tC/ha/yr, Chidumayo, 1991; Chidumayo, 1993), and somewhat lower than that recorded in 'wet' (> 1000 mm/yr precipitation) miombo woodlands (1.1 - 1.7 tC/ha/yr Chidumayo, 1990). The low woody productivity we observe in miombo woodlands raises questions about the long-term resilience of C stocks to frequent disturbances and widespread woodland degradation.

Our study did not detect any directional changes to AGB, and provides no evidence that miombo woodlands in Kilwa District are undergoing degradation as a result of frequent fires or land use change. Conversely, there was no evidence that trends of woody biomass increases observed elsewhere in Africa's forests (Lewis et al., 2009) and savannahs (Bond and Midgley, 2000) are occurring rapidly in miombo woodlands. The short time-scale of this study and its limited number of PSPs does mean that this study has little power to detect landscape changes to AGB, so we are only able to rule out very large directional changes to AGB in this study. It was noteworthy that few PSPs were gaining AGB at the ∼0.7 tC/ha/yr rate observed in chronosequence studies following land clearance (Williams et al., 2008; McNicol et al., 2015), implying that the low biomass savannah plots sampled in this study are somewhat stable and are not representative of areas undergoing recovery from deforestation or severe fire. The apparent resilience of low AGB plots may relate to the fire feedback, hydrology, or nutrient availability imposing limits to woody productivity.

There are a number of caveats to our estimates of rates of C cycling, which must only be considered as rough estimates. It is common for forest plot studies to utilise more than two plot re-inventories, reducing the probability of gross errors. For example, the misidentification of a single large tree as dead, or an error in diameter increment calculations in a sparsely vegetated plot can have a large impact on estimated rates of woody C cycling. The short time period of our study limits our capacity to draw generalisations based on this data. Severe fires, for example, are rare, but may have a large impact on rates of tree mortality that will only be detected given a long study period. Whilst C flux data from the tropics remains scarce, and extremely sparse in miombo woodlands (Jin et al., 2013), bottom-up calculations based on sample plots remain one of the few options for estimating C fluxes, and provide a useful ballpark for future studies.

3.4.2 RQ2: What are rates of growth, mortality and recruitment in miombo woodlands, and how do they vary?

The mean stem diameter increment of 1.55 ± 0.57 mm/yr we report from Kilwa District very low, amounting to a period of 165 - 357 years for the mean average tree to reach a mature size of 40 cm DBH. Although these diameter increments are slow relative to other ecosystems, they are similar to other studies of miombo woodland species. A dendrochronological study of *Pterocarpus angolensis* by Therrell et al. (2007) found diameter increments to average 3.5 mm/yr, relative to a mean of 2.6 mm/yr for *P. angolensis* trees measured at our plots. Diameter increments of *Brachystegia spiciformis* measured in Zambia by Trouet et al. (2010) found diameter increments averaging 2.1 - 3.8 mm/yr, comparable to the of 3.0 mm/yr measured in our plots. Similarly, a range of species measured by Holdo (2006) show diameter increments that are broadly congruent with the results presented here. Slow growth rates of trees in miombo woodland calls for careful management, particularly with respect to sustainable harvesting rates of timber species, which may be slow to recover.

Rates of stem turnover in miombo woodlands are low, amounting to 3.5 % of stems per year. Unlike growth, stem mortality and recruitment occurs stochastically, and only once in the lifetime of each tree, meaning more reliable estimates of their rates will require long-term studies. Overall mortality rates were notably lower than those observed in miombo by Ryan and Williams (2011) following experimental fires of a range of intensities. Despite most of our plots burning twice over the course of the experiment, mortality rates are consistent with only the lowest recorded fire intensities, suggesting that we did not capture the impacts of any very intense fires.

Qualitative indicators of the type, mode and cause of stem mortality reflect a range of processes leading to tree death. The rarity of stem top-kill observed in this study is an unusual result in a savannah, where top-kill is expected to dominate over stem mortality (Hoffmann et al., 2009). This result may stem from sampling PSPs in the dry season when trees can appear completely dormant. The majority of stems remained standing after death, which has implications for the manner of their decay from decomposition and fire. The causes of stem death were difficult to ascertain, with the cause of mortality for 79 % of deaths not determined. This study suggests that elephants are a leading cause of mortality, though this may relate to the ease of determining elephant-related mortality. Whilst limited by the frequent unavailability of clear evidence, assessments of stem mortality provide a valuable qualitative supplement to quantitative analysis of stem mortality.

Our study found little evidence that demographic rates differ systematically between PSPs, with similar rates of growth, mortality and recruitment of individual stems recorded in savannahs, woodlands and forests. The greatest differences between tree population dynamics relates more straightforwardly to variation in stem density.

3.4.3 RQ3: What biotic and abiotic processes regulate demographic rates in miombo woodlands?

Our models indicate that stem growth and mortality do not occur wholly at random in miombo woodlands, with evidence that stem damage and stem size alter tree population dynamics. The variance explained by all of our models is modest, suggesting that the deterministic component to growth rates and probability of mortality is low. Residual variation in our model will partly result from the short time-period of our study, leading to a low signal-to-noise ratio where growth rates are slow and stem mortality rare. We note, however, that growth models of individual trees commonly represent poor fits to data, even in larger studies (Fox et al., 2001). Residual variation in our models may also relate to unmeasured influences, for example fluctuating precipitation and water availability (Therrell et al., 2006; Rossatto et al., 2012), regrowth from shifting cultivation (McNicol et al., 2015), or complex small-scale vegetation patchiness (Caylor and Shugart, 2004). The relative unpredictability of savannah ecosystems is a further consideration, with non-equilibrium vegetation dynamics and stochastic events likely to have a substantial and complicating influence on tree populations (Higgins et al., 2000).

Stem diameter increments were unrelated to DBH, a property associated with increasing woody productivity as stems get larger. Invariance of DBH increment with size makes it a useful metric for comparing species growth rates (e.g. Table S3.1). Stem mortality followed expected patterns, with juvenile trees much more vulnerable to mortality. We note that although this study measured 216 ha of trees $>$ 40 cm, sample sizes of large trees remained small, with only 72 of 2270 trees in the LSPs recording mortality during the monitoring period. Further study will be necessary to more tightly constrain the mortality rates of large trees.

Stem damage had a large impact on growth rates, accounting for a 27 % reduction to stem DBH increment where evidence of damage was recorded in the first inventory. Similar results were obtained by Holdo (2006), who found that diameter increment was particularly reduced in the largest of trees where damaged. Reduction of growth rates suggests that wounded or senescent trees are unable to commit resources to woody production, which given the large proportion of trees that show some form of damage will have a significant impact on rates of C cycling. The size of the effect on mortality is also large; although only recorded in 15 % of stems, damage was noted in 29 % of all stems that died during the monitoring period. Stem damage may be a direct cause of mortality, such as through a weakened defence against fire ingress, or an indirect predictor of mortality by indicating reduced vigour and an incapacity to perform maintenance. Growth and mortality in damaged stems are likely to interact, with slow growth rates reducing the capacity of a stem to escape from the small size classes where fire results in high rates of top-kill. Whilst our study is not able to fully address the causes of damage, our observations and previous work suggests that physical damage of stems is often the result of fire and elephants (Ribeiro et al., 2008), both which are common in Kilwa District.

Evidence that fire has a large impact on tree communities is less clear, with no differences detected in growth and mortality in PSPs that burned, an outwardly surprising result given the strong evidence of fire's role in top-kill in miombo woodlands (Ryan and Williams, 2011). We consider this the likely outcome of the ubiquity of fire in typical miombo woodlands of Kilwa District, where out of 24 PSPs only 5 were not observed to burn during the study period. Amongst the plots that did not burn, three plots (P06, P22, P25) were closed-canopy forests and resultantly sparingly flammable, one plot (P03) had very shallow soils and little grass growth, and one plot (P09) was isolated from fire spread by surrounding topography. Thus the PSPs not observed to burn are in many ways unusual, where growth and survival may be limited by very different processes.

3.5 Conclusions

This study has provided useful estimates of woody C cycling and tree demographic rates, and their patterns of variation across a heterogeneous miombo woodland landscape. We further identified important differences in stem demographic data relating to damage, competition and fire, with potentially significant impacts on rates of C cycling in miombo woodlands.

3.6 Acknowledgements

Permanent Sample Plots were established in Kilwa District by the Mpingo Conservation & Development Initiative (MCDI), in collaboration with The University of Edinburgh. Re-measurement was coordinated by the staff of the MCDI.

3.7 References

Baddeley, A., Rubak, E., and Turner, R. (2015), *Spatial Point Patterns: Methodology and Applications with R*, London: Chapman and Hall/CRC Press, url: `http://www.crcpress.com/Spatial-Point-Patterns-Methodology-and-Applications-with-R/Baddeley-Rubak-Turner/9781482210200/`.

Bartoń, K. (2015), *MuMIn: Multi-Model Inference*, R package version 1.15.1, url: `http://CRAN.R-project.org/package=MuMIn`.

Bates, D., Maechler, M., Bolker, B., and Walker, S. (2014), *lme4: Linear mixed-effects models using Eigen and S4*, R package version 1.1-6, url: `http://CRAN.R-project.org/package=lme4`.

Bond, W.J. (2008), 'What Limits Trees in C_4 Grasslands and Savannas?', *Annual Review of Ecology, Evolution, and Systematics*, **39**, pp. 641–659.

Bond, W.J. and Midgley, G.F. (2000), 'A proposed CO_2-controlled mechanism of woody plant invasion in grasslands and savannas', *Global Change Biology*, **6**, pp. 865–869.

Burnham, K.P. and Anderson, D.R. (2002), *Model selection and multimodel inference: a practical information-theoretic approach*, Springer-Verlag, New York, USA.

Caylor, K.K. and Shugart, H.H. (2004), 'Simulated productivity of heterogeneous patches in Southern African savanna landscapes using a canopy productivity model', *Landscape Ecology*, **19**, pp. 401–415.

Chidumayo, E.N. (1990), 'Above-ground woody biomass structure and productivity in a Zambezian woodland', *Forest Ecology and Management*, **36**, pp. 33–46.

Chidumayo, E.N. (1991), 'Woody biomass structure and utilisation for charcoal production in a Zambian Miombo woodland', *Bioresource Technology*, **37**, pp. 43–52.

Chidumayo, E.N. (1993), *Responses of miombo to harvesting: ecology and management*, Stockholm Environment Institute.

Dantas, V.d.L., Batalha, M.A., França, H., and Pausas, J.G. (2015), 'Resource availability shapes fire-filtered savannas', *Journal of Vegetation Science*, **26**, pp. 395–403.

Fox, J.C., Ades, P.K., and Bi, H. (2001), 'Stochastic structure and individual-tree growth models', *Forest Ecology and Management*, **154**, pp. 261–276.

Friend, A.D., Lucht, W., Rademacher, T.T., Keribin, R., Betts, R., Cadule, P., Ciais, P., Clark, D.B., Dankers, R., Falloon, P.D., Ito, A., Kahana, R., Kleidon, A., Lomas, M.R., Nishina, K., Ostberg, S., Pavlick, R., Peylin, P., Chaphoff, S., Vuichard, N., Warszawski, L., Wiltshire, A., and Woodward, F.I. (2014), 'Carbon residence time dominates uncertainty in terrestrial vegetation responses to future climate and atmospheric CO_2', *Proceedings of the National Academy of Sciences*, **111**, pp. 3280–3285.

Furley, P.A., Rees, R.M., Ryan, C.M., and Saiz, G. (2008), ‘Savanna burning and the assessment of long-term fire experiments with particular reference to Zimbabwe’, *Progress in Physical Geography*, **32**, pp. 611–634.

Galbraith, D., Malhi, Y., Affum-Baffoe, K., Castanho, A.D., Doughty, C.E., Fisher, R.A., Lewis, S.L., Peh, K.S.-H., Phillips, O.L., Quesada Carlos, A., Sonké, B., and Lloyd, J. (2013), ‘Residence times of woody biomass in tropical forests’, *Plant Ecology & Diversity*, **6**, pp. 139–157.

Garcia, O. (2014), *siplab: Spatial individual-plant modelling*, R package version 1.1, url: `http://CRAN.R-project.org/package=siplab`.

Gelman, A. and Hill, J. (2007), *Data analysis using regression and hierarchical/multilevel models*, Cambridge University Press: Cambridge, UK.

Grace, J., José, J.S., Meir, P., Miranda, H.S., and Montes, R.A. (2006), ‘Productivity and carbon fluxes of tropical savannas’, *Journal of Biogeography*, **33**, pp. 387–400.

Hegyi, F. (1974), ‘A simulation model for managing jack-pine stands’, *Growth models for tree and stand simulation*, pp. 74–90.

Higgins, S.I., Bond, W.J., and Trollope, W.S.W. (2000), ‘Fire, resprouting and variability: a recipe for grass–tree coexistence in savanna’, *Journal of Ecology*, **88**, pp. 213–229.

Hoffmann, W.A., Adasme, R., Haridasan, M., de Carvalho, M.T., Geiger, E.L., Pereira, M.A.B., Gotsch, S.G., and Franco, A.C. (2009), ‘Tree topkill, not mortality, governs the dynamics of savanna-forest boundaries under frequent fire in central Brazil’, *Ecology*, **90**, pp. 1326–1337.

Hoffmann, W.A., Geiger, E.L., Gotsch, S.G., Rossatto, D.R., Silva, L.C.R., Lau, O.L., Haridasan, M., and Franco, A.C. (2012), ‘Ecological thresholds at the savanna-forest boundary: how plant traits, resources and fire govern the distribution of tropical biomes’, *Ecology Letters*, **15**, pp. 759–768.

Holdo, R.M. (2006), ‘Tree growth in an African woodland savanna affected by disturbance’, *Journal of Vegetation Science*, **17**, pp. 369–378.

Holdo, R.M. (2005), ‘Stem mortality following fire in Kalahari sand vegetation: effects of frost, prior damage, and tree neighbourhoods’, *Plant Ecology*, **180**, pp. 77–86.

Hurvich, C.M. and Tsai, C.-L. (1989), ‘Regression and time series model selection in small samples’, *Biometrika*, **76**, pp. 297–307.

Jin, C., Xiao, X., Merbold, L., Arneth, A., Veenendaal, E., and Kutsch, W.L. (2013), ‘Phenology and gross primary production of two dominant savanna woodland ecosystems in Southern Africa’, *Remote Sensing of Environment*, **135**, pp. 189–201.

Lewis, S.L., Lopez-Gonzalez, G., Sonke, B., Affum-Baffoe, K., Baker, T.R., Ojo, L.O., Phillips, O.L., Reitsma, J.M., White, L., Comiskey, J.A., Djuikouo, M.-N., Ewango, C.E.N., Feldpausch, T.R., Hamilton, A.C., Gloor, M., Hart, T., Hladik, A., Lloyd, J., Lovett, J.C., Makana, J.-R., Malhi, Y., Mbago, F.M., Ndangalasi, H.J., Peacock, J., Peh, K.S.H., Sheil, D., Sunderland, T., Swaine, M.D., Taplin, J., Taylor, D., Thomas, S.C., Votere, R., and Woll, H. (2009), 'Increasing carbon storage in intact African tropical forests', *Nature*, **457**, pp. 1003–1006.

Malhi, Y. (2012), 'The productivity, metabolism and carbon cycle of tropical forest vegetation', *Journal of Ecology*, **100**, pp. 65–75.

McNicol, I.M., Ryan, C.M., and Williams, M. (2015), 'How resilient are African woodlands to disturbance from shifting cultivation?', *Ecological Applications*, **25**, pp. 2320–2336.

Midgley, J.J., Lawes, M.J., and Chamaillé-Jammes, S. (2010), 'Savanna woody plant dynamics: the role of fire and herbivory, separately and synergistically', *Australian Journal of Botany*, **58**, pp. 1–11.

Murphy, B.P., Russel-Smith, J., and Prior, L.D. (2010), 'Frequent fires reduce tree growth in northern Australian savannas: implications for tree demography and carbon sequestration', *Global Change Biology*, **16**, pp. 331–343.

Nakagawa, S. and Schielzeth, H. (2013), 'A general and simple method for obtaining R^2 from generalized linear mixed-effects models', *Methods in Ecology and Evolution*, **4**, pp. 133–142.

Phillips, O.L., Aragão, L.E.O.C., Lewis, S.L., Fisher, J.B., Lloyd, J., López-González, G., Malhi, Y., Monteagudo, A., Peacock, J., Quesada, C.A., Heijden, G. van der, Almeida, S., Amaral, I., Arroyo, L., Aymard, G., Baker, T.R., Bánki, O., Blanc, L., Bonal, D., Brando, P., Chave, J., Oliveira, Á.C.A. de, Cardozo, N.D., Czimczik, C.I., Feldpausch, T.R., Freitas, M.A., Gloor, E., Higuchi, N., Jiménez, E., Lloyd, G., Meir, P., Mendoza, C., Morel, A., Neill, D.A., Nepstad, D., Patiño, S., Peñuela, M.C., Prieto, A., Ramírez, F., Schwarz, M., Silva, J., Silveira, M., Thomas, A.S., Steege, H.t., Stropp, J., Vásquez, R., Zelazowski, P., Dávila, E.A., Andelman, S., Andrade, A., Chao, K.-J., Erwin, T., Di Fiore, A., C., E.H., Keeling, H., Killeen, T.J., Laurance, W.F., Cruz, A.P., Pitman, N.C.A., Vargas, P.N., Ramírez-Angulo, H., Rudas, A., Salamão, R., Silva, N., Terborgh, J., and Torres-Lezama, A. (2009), 'Drought sensitivity of the Amazon rainforest', *Science*, **323**, pp. 1344–1347.

Prior, L.D., Eamus, D., and Bowman, D.M.J.S. (2004), 'Tree growth rates in north Australian savanna habitats: seasonal patterns and correlations with leaf attributes', *Australian Journal of Botany*, **52**, pp. 303–314.

Prior, L.D., Murphy, B.P., and Russell-Smith, J. (2009), 'Environmental and demographic correlates of tree recruitment and mortality in north Australian savannas', *Forest Ecology and Management*, **257**, pp. 66–74.

R Core Team (2015), *R: A Language and Environment for Statistical Computing*, R Foundation for Statistical Computing, Vienna, Austria, url: `http://www.R-project.org/`.

Ribeiro, N.S., Shugart, H.H., and Washington-Allen, R. (2008), 'The effects of fire and elephants on species composition and structure of the Niassa Reserve, northern Mozambique', *Forest Ecology and Management*, **255**, pp. 1626–1636.

Rossatto, D.R., Silva, L.d.C.R., Villalobos-Vega, R., Sternberg, L.d.L., and Franco, A.C. (2012), 'Depth of water uptake in woody plants relates to groundwater level and vegetation structure along a topographic gradient in a neotropical savanna', *Environmental and Experimental Botany*, **77**, pp. 259–266.

Ryan, C.M. and Williams, M. (2011), 'How does fire intensity and frequency affect miombo woodland tree populations and biomass?', *Ecological Applications*, **21**, pp. 48–60.

Ryan, C.M., Williams, M., and Grace, J. (2011), 'Above-and Belowground Carbon Stocks in a Miombo Woodland Landscape of Mozambique', *Biotropica*, **43**, pp. 423–432.

Sheil, D. and May, R.M. (1996), 'Mortality and recruitment rate evaluations in heterogeneous tropical forests', *Journal of ecology*, **84**, pp. 91–100.

Therrell, M.D., Stahle, D.W., Mukelabai, M.M., and Shugart, H.H. (2007), 'Age, and radial growth dynamics of Pterocarpus angolensis in southern Africa', *Forest Ecology and Management*, **244**, pp. 24–31.

Therrell, M.D., Stahle, D.W., Ries, L.P., and Shugart, H.H. (2006), 'Tree-ring reconstructed rainfall variability in Zimbabwe', *Climate Dynamics*, **26**, pp. 677–685.

Trouet, V., Esper, J., and Beeckman, H. (2010), 'Climate/growth relationships of Brachystegia spiciformis from the miombo woodland in south central Africa', *Dendrochronologia*, **28**, pp. 161–171.

White, F. (1983), *The vegetation of Africa: a descriptive memoir to accompany the Unesco/AETFAT/UNSO vegetation map of Africa*, UNESCO, Paris, France.

Willcock, S., Phillips, O.L., Platts, P.J., Balmford, A., Burgess, N.D., Lovett, J.C., Ahrends, A., Bayliss, J., Doggart, N., Doody, K., Fanning, E., Green, J.M., Hall, J., Howellll, K.L., Marchant, R., Marshall, A.R., Mbilinyi, B., Munishi, P.K., Owen, N., Swetnam, R.D., Topp-Jorgensen, E.J., and Lewis, S.L. (2014), 'Quantifying and understanding carbon storage and sequestration within the Eastern Arc Mountains of Tanzania, a tropical biodiversity hotspot', *Carbon balance and management*, **9**, p. 2.

Williams, C.A., Hanan, N.P., Neff, J.C., Scholes, R.J., Berry, J.A., Denning, S.A., and Baker, D.F. (2007), 'Africa and the global carbon cycle', *Carbon balance and management*, **2**, pp. 1–13.

Williams, M., Ryan, C.M., Rees, R.M., Sambane, E., Fernando, J., and Grace, J. (2008), 'Carbon sequestration and biodiversity of re-growing miombo woodlands in Mozambique', *Forest Ecology and management*, **254**, pp. 145–155.

Williams, R.J., Cook, G.D., Gill, A.M., and Moore, P.H.R. (1999), 'Fire regime, fire intensity and tree survival in a tropical savanna in northern Australia', *Australian Journal of Ecology*, **24**, pp. 50–59.

Woollen, E., Ryan, C.M., and Williams, M. (2012), 'Carbon stocks in an African woodland landscape: spatial distributions and scales of variation', *Ecosystems*, **15**, pp. 804–818.

3.8 Supplementary materials

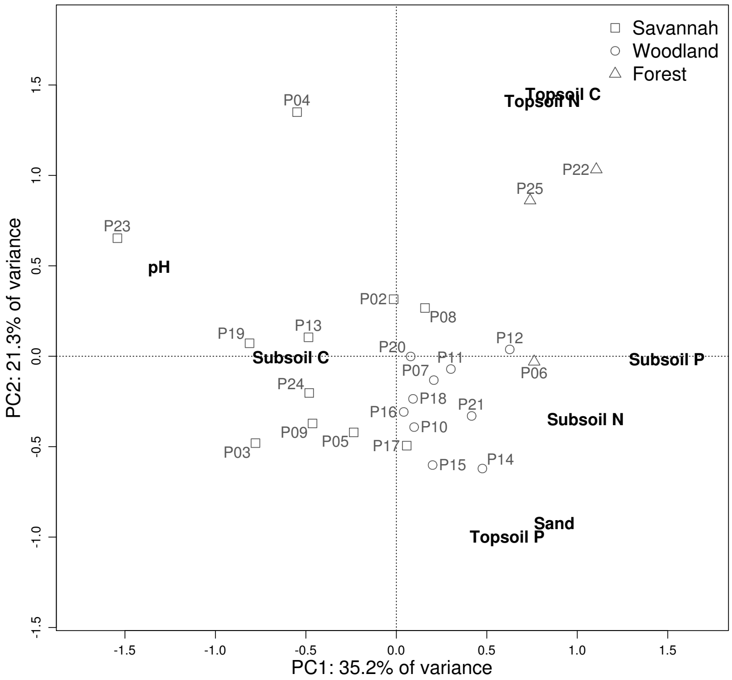

Figure S3.1: Principal component analysis biplot of measured soil properties, where the first principal component is used as a candidate variable in hierarchical modelling.

Table S3.1: Rates of growth (± 1 S.E.M) and mortality of selected species measured in Kilwa District Permanent Sample Plots. Stem growth rates are reported both as a mean, and as the 90^{th} percentile to approximate the potential growth rate of a species in the absence of factors that act to suppress growth (e.g. fire, competition). See Tables 2.2 and 3.2 for full species names.

Species	**Diameter increment, mean (mm/yr)**	**Diameter increment, 90^{th} percentile (mm/yr)**	**Mortality rate (%/yr)**
A. nigrescens	3.3 ± 0.5	3.5	0.7
A. nilotica	2.3 ± 0.2	6.5	5.6
A. quanzensis	2.1 ± 0.4	4.5	2.2
B. petersiana	1.0 ± 0.2	3.0	6.0
B. spiciformis	3.0 ± 0.7	2.5	0.9
B. scleroneura	1.8 ± 0.2	3.0	2.4
B. africana	2.1 ± 0.1	6.8	1.9
C. apiculatum	1.4 ± 0.1	3.8	4.2
C. zeyheri	1.5 ± 0.1	4.5	0.2
D. melanoxylon	1.7 ± 0.1	4.0	1.8
D. mespiliformis	2.1 ± 0.2	2.5	1.6
D. quiloensis	1.3 ± 0.2	5.0	0.6
D. condylocarpon	1.2 ± 0.0	2.5	3.2
F. virosa	-0.4 ± 0.8	4.0	0.0
G. microcarpa	0.7 ± 0.1	4.0	7.6
H. verrucosa	1.6 ± 0.2	4.4	0.5
H. ulmoides	1.7 ± 0.0	6.5	2.7
J. globiflora	3.0 ± 0.4	5.8	4.3
M. discolor	1.8 ± 0.1	4.0	1.4
M. obtusifolia	1.0 ± 0.1	4.5	4.3
M. stuhlmannii	1.9 ± 0.2	2.5	2.4
P. maprouneifolia	1.5 ± 0.1	1.0	1.4
P. myrtifolia	2.0 ± 0.1	3.0	5.2
P. angolensis	2.6 ± 0.4	8.5	1.9
Rytiginia sp.	1.3 ± 0.2	3.5	1.4
S. birrea	3.6 ± 0.6	4.0	0.6
S. cocculoides	1.9 ± 0.2	3.5	2.2
S. spinosa	1.8 ± 0.1	3.5	0.6
S. zanzibariensis	1.2 ± 0.1	6.6	4.2
X. stuhlmannii	2.3 ± 0.4	3.0	1.9

CHAPTER 4

Early burning in miombo woodlands for climate change mitigation

ABSTRACT

Background and aims: Frequent fires in the miombo woodlands of south-central Africa are a poorly understood and potentially large source of greenhouse gas emissions. Recent efforts to mitigate the impacts of climate change have aimed to prevent woodland degradation through fire management, where controlled fires in the early dry season are used to reduce the impacts of hot late dry season fires. Such an intervention may be financed through climate mitigation finance, such as the Reducing Emissions from Deforestation and forest Degradation (REDD+) programme of the United Nations, requiring a robust method to audit results-based payments. In this paper we report on a model-based method for monitoring fire emissions in a pilot REDD+ project aiming to incentivise early burning in miombo woodlands.

Methods: The historical frequency of early and late dry season fires was estimated by measuring burn scars in a 10 year Landsat time-series. We simulate the impacts of this fire on miombo woodland biomass using a process-based model, and project the outcome of early burning on aboveground woody biomass.

Results: Our model predicts that fires are resulting in a gradual degradation of woodlands in Kilwa District. Given substantial reductions to late dry season fire frequency, the model predicts a gradual increase in woody biomass will result from early burning. If late dry season fire frequency is reduced by 50 %, early burning has a climate change mitigation potential of approximately 0.34 tC/ha/yr. Uncertainty in the model is considerable; we discuss methods by which uncertainty can be mitigated in an operational fire management project, and identify key areas for further work.

Conclusions: Fire is an important regulator of vegetation structure in miombo woodlands, with woody biomass vulnerable to degradation as the result intense fires. Early burning has the potential to mitigate this loss, though further monitoring will be required before its long term impacts are made clear.

4.1 Introduction

The miombo woodlands of south-central Africa are under pressure from human expansion linked to agriculture, fuelwood, and timber extraction which all, in turn, influence fire incidence in surrounding woodlands. Recent efforts for the conservation of miombo woodlands have focussed on valuing their resources and paying for the ecosystem services they provide. Monitoring of woodland status, for instance aboveground woody biomass (AGB) stocks, is required for auditing such payments. In miombo woodlands where AGB may be lost as the result of gradual degradation by fire, this monitoring presents a particular challenge.

Fire is an important regulator of carbon (C) storage in miombo woodlands (Trapnell, 1959; Furley et al., 2008; Ryan and Williams, 2011), and as one of the few savannah processes that can be readily manipulated, is a key tool for land management (Chidumayo and Gumbo, 2010). Whilst reducing the frequency of fires as a means to increase woodland AGB may be possible, it is resource intensive, invasive, and often undesirable, therefore management plans commonly aim to moderate fire intensity in degraded savannahs (Hough, 1993; Laris, 2002; Laris and Wardell, 2006; Eriksen, 2007; Russell-Smith et al., 2009). As one of the main drivers of tree top-kill, a reduction in fire intensity can support the maintenance of the productive mature trees comprising the majority of AGB, and aid woodland regeneration by lifting the demographic bottleneck disrupting the growth of saplings (Ryan and Williams, 2011).

Fire intensity in seasonally-dry woodlands is closely related to time of year (Hoffa et al., 1999), a cycle deriving from annual variation in rainfall and grass curing (Smit et al., 2010). Early dry season fires typically are of low intensity, burning slowly and patchily with a low flame height (Fig. 4.1). These fires are unlikely to carry to the tree canopy and often self-extinguish overnight, resulting in limited stem top-kill. Late dry season fires are typified by a high intensity, resulting in larger fires with high rates of

Figure 4.1: Images of eary dry season fires recorded during fire management activities in Nanjirinji VLFR in Southwestern Kilwa District. Early dry season fires usually burn at low intensity, burning on partially-cured fuels with a high moisture content. These fires tend to burn patchily, removing fuel and interrupting the spread of late dry season fires. Low intensity fires result in lower rates of tree top-kill, and encourage recruitment of new tree stems.

stem top-kill (Fig. 4.2). Late dry season fires can be uncontrollable, spread rapidly, and frequently burn through the night. A programme of controlled early dry season burning designed to remove dry grass fuel from the landscape without damaging mature trees can therefore form the basis of a management intervention to support woody C stocks. Such an intervention may be assisted by climate change mitigation finance, such as the incipient Reducing Emissions from Deforestation and Forest Degradation (REDD+) programme of the United Nations.

Moderation of fire intensity has been a goal of management plans across the African continent (Everson et al., 2004), and is a traditional form of land management

Figure 4.2: Images of late dry season fires recorded during fire experiments in Gorongosa District. Late dry season fires are typified by a high intensity as a result of burning on fully-cured fuels in dry conditions. Fires tend to burn continuously over the landscape, and are not usually extinguished overnight. High intensity fires can result in loss of large trees and high rates of juvenile tree top-kill, interrupting woodland regeneration. *Images by Casey Ryan.*

with a long history in the savannahs of Africa and Australia (Laris, 2002; Laris and Wardell, 2006). More recently, fire management protocols aiming to account for the climate change mitigation potential of early burning have been developed in Northern Australia, such as the established West Arnhem Land Fire Abatement Project (WALFA) (Russell-Smith et al., 2009) and the Tiwi Carbon Study (Richards et al., 2012). These projects aim to reduce greenhouse gas emissions from frequent intense late dry season fires being replaced by patchy low intensity early dry season fires. Unlike this study, they do not consider changes to AGB resulting from management activities. Evidence from fire experiments (Trapnell, 1959; Moreira, 2000; Russell-

Smith et al., 2003; Furley et al., 2008), modelling work (Ryan and Williams, 2011; Saito et al., 2014), as well as rough calculations (Stronach, 2009) suggest that the such increases may be substantial. The extent to which woody biomass is being impacted by current fire regimes and the potential outcomes of early burning on AGB not well understood, and robust methods with which to project these impacts are in short supply.

In this paper we report on a pilot REDD+ project aiming to facilitate fire management in miombo woodlands through early burning (VCS, 2015). Our method uses burn scar measurements from a 10-year database of Landsat imagery to determine a baseline frequency of early and late dry season fires. We use a process-based model to predict woodland response to changes in fire regime, with input data from radar-generated maps of AGB and annual field observations of fire activity. We discuss methods of monitoring fire activity, and examine how future woodland state may be predicted under business-as-usual and management scenarios. We also examine the problems presented by data paucity and uncertainty in savannah ecosystems, and present strategies that may be employed to produce reliable estimates of AGB changes resulting from fire management. We aim to address the following two research questions:

1. What is the likely magnitude of emissions reductions achieved from early burning in miombo woodlands?
2. What are the key uncertainties in the method, and how can uncertainty be mitigated in an operational fire-management project?

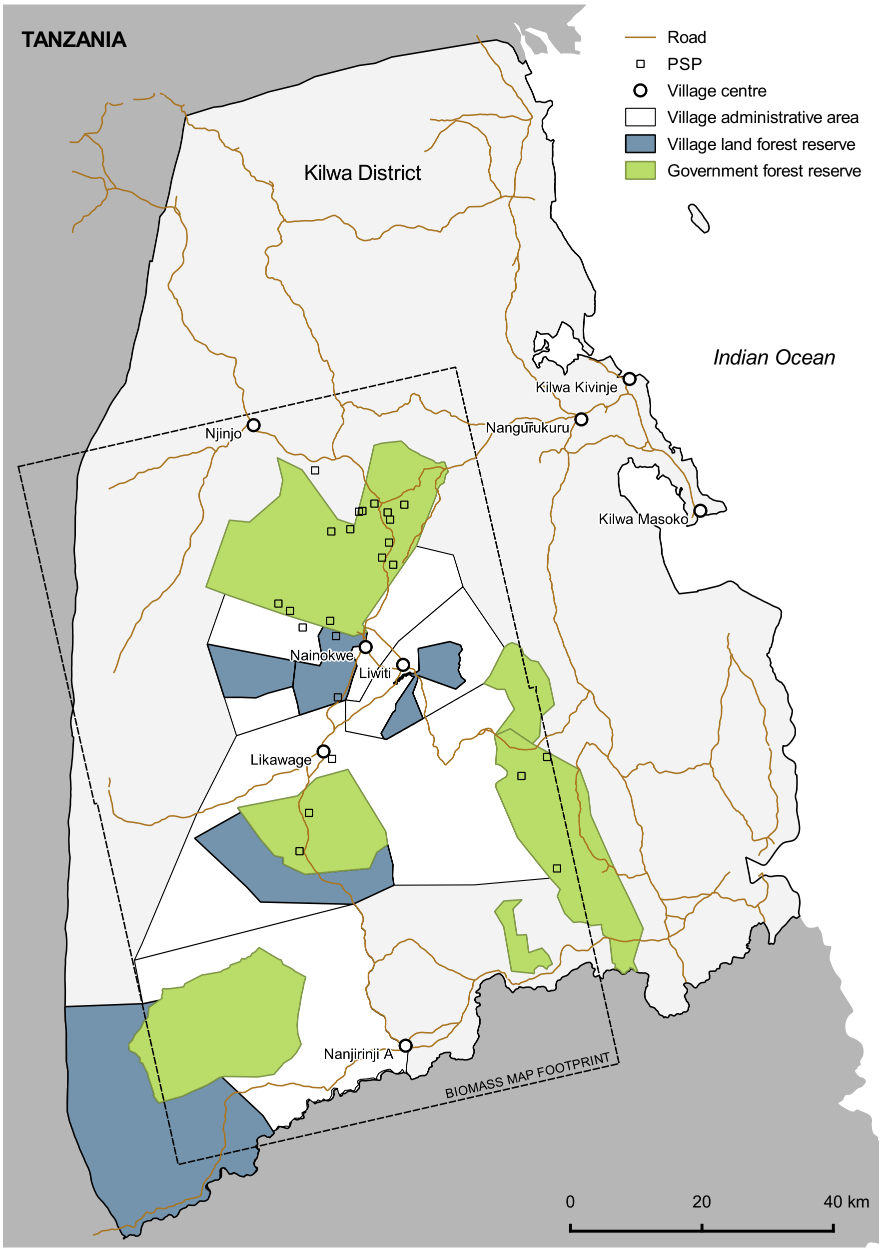

Figure 4.3: Map of Kilwa District, Tanzania. Early burning is proposed for Village Land Forest Reserves, tracts of land managed by local villages for sustainable timber production. Permanent sample plots (PSPs) are semi-randomly located across the District for measurement of woodland biomass. Project proponents the Mpingo Conservation & Development Initiative are based in Kilwa Masoko.

4.2 Methods

4.2.1 Study locations

Kilwa District, Tanzania

Kilwa District in southeastern Tanzania is the location of the Mpingo Conservation and Development Initiative (MCDI), proponents of a pilot REDD+ project funded by the Royal Norwegian Embassy, Tanzania (Fig. 4.3). Land cover in Kilwa District is heterogeneous, encompassing miombo woodlands, grassland savannahs, and patches of threatened East African coastal forest (Prins and Clarke, 2007). Rainfall is highly seasonal, with a pronounced dry season between May and November each year, with total rainfall averaging 900 - 1100 mm/yr across the district. The woodlands and grasslands of Kilwa District have been observed to burn frequently, largely in uncontrolled hot fires in the late dry season. Kilwa District is location of a network of forest inventory Permanent Sample Plot (PSP), as well as a sequence of plots measuring woodland regrowth on abandoned agricultural sites (McNicol et al., 2015).

Gorongosa District, Mozambique

Gorongosa district is located in Sofala Province of central Mozambique. Rainfall has a similar seasonality to Kilwa District, and annual precipitation is similar at 850 mm/yr (Ryan, 2009). Miombo woodlands in this region have hosted a series of experimental fires where fire intensity and tree top-kill rates have been used to parameterise a process-based model of miombo woodland AGB (Ryan and Williams, 2011). Data from this site produced a series of allometric equations used for estimation of AGB (Ryan et al., 2011), and an additional estimate of woodland regrowth rate from a chronosequence study (Williams et al., 2008).

4.2.2 Description of management

Fire management activities are planned in 'village land forest reserves' (VLFRs), woodland reserves established by communities for sustainable forest management. VLFRs are to a large extent protected from agricultural expansion, unsustainable timber harvesting, and charcoal production, leaving uncontrolled fire as the principal potential source of woodland degradation. Fire management is focussed on areas of miombo woodland in the AGB range 5 - 35 tC/ha, excluding savannahs not meeting the requirement for land to be forested (FAO, 2008), and areas where a closed forest canopy typically shades out grass fuel, inhibiting fire spread (see Chapter 2). Eligible woodlands are burnt by local communities as soon as grasses become extensively flammable in the dry season, with burning restricted to backfires to limit fire intensity and to maximise controllability. Early burning ceases when a VLFR is no longer widely flammable, at the end of the early dry season, or when fires begin to burn out of control, defined as the point in the year where fires continue to burn through the night. The requirement for community involvement, capacity limitations, and the small scale of operations in a remote area require management interventions and monitoring methods to be as simple as practicable.

4.2.3 Biomass measurement

PSPs were established in Kilwa District in 2010/11, located over a range of land cover types (n = 25). Each PSP was laid out as a 100 x 100 m square (1 hectare) in which the diameter at breast height (DBH) of all trees > 5 cm DBH was measured, and AGB estimated using a miombo-specific allometric equation (Ryan et al., 2011). AGB estimates were up-scaled across the project area using data from the ALOS PALSAR L-band synthetic aperture radar. Radar backscatter from this instrument is strongly correlated with AGB in moderate biomass savannahs and woodlands, and has been widely applied to the measurement of woody biomass across Africa (e.g. Mitchard et al., 2009; Ryan et al., 2012). All backscatter images (HV cross-polarised) from the 2010 dry season were downsampled to 25 metre resolution, underwent topographic correction, and were averaged. Biomass estimates from PSPs were used to calibrate a linear biomass-backscatter relationship, resulting in an landscape-scale map of AGB. The map was stratified into 5 tC/ha intervals, and pixels with a biomass above or below the target AGB range were excluded from the project.

4.2.4 Fire monitoring

A 10-year record of burn scar maps (2001 - 2010) was generated from medium resolution optical data from Landsat Thematic Mapper (TM) and Enhanced Thematic Mapper (ETM+) to estimate baseline (business-as-usual) fire frequency. All available data acquisitions from this period underwent cloud masking, atmospheric correction and conversion to surface reflectance using the LEDAPS algorithm (Masek et al., 2008). A series of spectral indices were calculated using the multispectral Landsat imagery (Bastarrika et al., 2011), and classified using a regularised logistic regression function which was trained using a series of operator-identified burned and unburned pixels. A burn probability cut-off of 60 % was used to separate burned and unburned pixels into binary classes, a cut-off determined to minimise errors of commission (Giglio et al., 2009).

Burn scars were attributed to early or late dry season fires based on a fixed cut-off date of 1st July, a date established by expert opinion as the average time of year where fires begin to burn out of control in Kilwa District. As cloud cover and infrequent satellite overpasses limit observation opportunity, classified images had to be carefully processed to determine burn season. Some pixels can be unambiguously attributed to early or late dry seasons (e.g. a burn scar detected in the early dry season, a burn scar detected in the late dry season following a previous late dry season unburned detection). Where the burn date of a pixel was ambiguous (e.g. burn scar detected in late dry season following an early dry season unburned observation), fire was assigned probabilistically and uniformly over the period to the last unburned observation. Where no previous observation exists, or was observed more than 90 days prior, burn scars were allocated uniformly over the previous 90 days, a period representing the expected rate of burn scar fading. Pixels were discarded where late dry season observations were insufficient to logically determine its status (e.g. an unburned observation in early dry season followed by no further observations). The probability of early (*p(burn|early)*), late (*p(burn|late)*), and unburned (*p(no burn)*) burn scar observations were averaged for each 5 tC/ha biomass stratum.

Ongoing monitoring of fire activity is planned to be undertaken through direct field observations since availability of remote sensing data is erratic, with a minimum of 100 checkpoints assessed at the end of early and late dry seasons in each VLFR. In order to claim any C emissions reductions a project must succeed in reducing fire impact, either through a shift in burning regime toward the early dry season, or affecting a reduction in fire frequency. As fire management has not been widely applied in Kilwa District at the time of writing, here we generate a range of potential reductions in late dry season fire frequency to assess potential emissions reductions (25 %, 50 %, and 75 %). We assume that there will be no reduction in overall fire frequency or total area burned, consistent with observations from management of savannah fires in South Africa (van Wilgen et al., 2004; van Wilgen et al., 2008).

4.2.5 Prediction of woodland biomass

We use a gap dynamics model named GapFire to simulate the impacts of changes to fire seasonality on woodland AGB in each woodland stratum (Fig. 4.4). GapFire

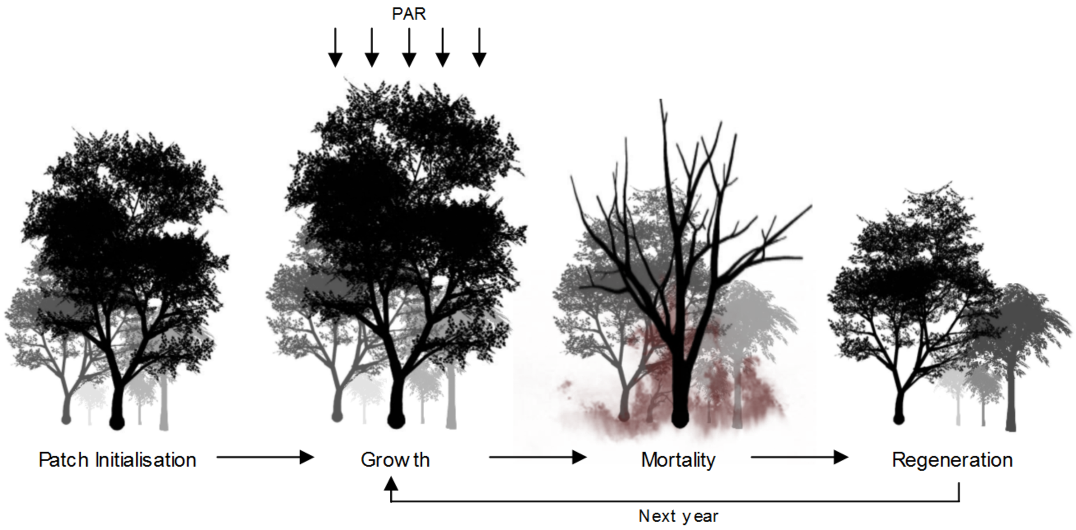

Figure 4.4: Diagrammatic representation of the GapFire model, showing patch initialisation, growth in response to photosynthetically active radiation (PAR), fire-induced mortality and regeneration. The model is described in detail in section 4.9.

is a process-based model of miombo woodland AGB that simulates the growth, top-kill and regeneration of individual tree stems in small woodland ‘patches’, which are initialised to match each AGB stratum. As woodland patches are small, vegetation structure is heterogeneous, and mortality and regeneration processes are stochastic, the AGB change in a single patch will not represent the trends of miombo woodland as a whole. The model is therefore run as an ensemble of many patches (n = 10,000), with the average changes to AGB used to assess the balance between C sequestration through forest regrowth and C emission from woodland disturbance. Gap models are considered an appropriate tool for characterising miombo woodlands where vegetation structure is profoundly modified by frequent stochastic disturbance events and explicit representation of demographic transitions can aid modelling of processes such as fire (Bond, 2008). The model presented here is a modified arrangement of the published model of Ryan and Williams (2011) for the prediction of AGB change, and is described in detail in section 4.9.

The GapFire model has 13 parameters that determine rates of growth, top-kill and

Table 4.1: Model parameters, nominal values (P$_n$), and model sensitivity to parameter changes (S$_{ij}$), which represents the proportional shift in model output following parameter changes, with larger numbers indicating greater sensitivity of model output to that parameter. S$_{ij}$ was assessed for AGB change in the baseline situation, a project scenario (assuming 50% reduction in late dry season fire frequency) and the difference between the two. Uncertainty in model parametrisation is discussed further in section 4.4.2.

			Baseline		**Project**		**Difference**		
Parameter description	**Name**	**P$_n$**	**S$_{ij}$**	**Rank**	**S$_{ij}$**	**Rank**	**S$_{ij}$**	**Rank**	**Source**
Growth parameters									
Fraction of GPP allocated to autotrophic respiration	R_a	0.5 ± 0.1	3.7	2	6.2	1	1.3	2	Waring et al. (1998)
Extinction coefficient for Beer-Lambert law	κ	0.5 ± 0.2	1.1	7	0.9	13	1.1	11	Norman and Campbell (1989)
C allocated to fine roots, as a fraction of leaf allocation	C_{fr}	1.0 ± 0.5	1.2	6	1.3	6	1.1	7	Hendricks et al. (2006) and Castellanos et al. (2001)
Maximum rate of photosynthesis ($\mu molC/m^2/s$)	P_{max}	12 ± 3	4.2	1	6.2	2	1.1	6	Tuohy and Choinski (1990), Tuohy et al. (1991), and Woollen (2013)
PAR intensity at which ½ P_{max} is obtained ($\mu mol/s/m^2$)	K_p	250 ± 75	1.9	4	2.8	3	1.1	8	Tuohy and Choinski (1990), Tuohy et al. (1991), and Woollen (2013)
Leaf carbon per leaf area (gC/m^2)	LCA	50 ± 20	1.6	5	2.3	4	1.2	3	Nottingham (2004) and Chidumayo (1997) and Chapter 2
Mortality parameters									
Intrinsic mortality rate (/yr)	M_i	0.02 ± 0.01	0.8	13	1.1	7	1.1	9	Estimated, similar to Desanker and Prentice (1994)
Early burn fireline intensity (kW/m)	FLI_{early}	1000 ± 500	1.0	8	1.0	11	1.0	12	Estimated, similar to Hoffa et al. (1999), Roberston (1993), and Ryan and Williams (2011)
Late burn fireline intensity (kW/m)	FLI_{late}	3500 ± 1500	2.0	3	1.7	5	1.3	1	Estimated, similar to Shea et al. (1996), Roberston (1993), and Ryan and Williams (2011)
Regeneration parameters									
DBH at which a seedling develops the capacity to resprout (m)	$S_{resprout}$	0.02 ± 0.01	0.9	9	1.0	12	1.2	5	Estimated
Number of seedlings established in a recruitment year (/ha)	S_{new}	5000 ± 2500	0.8	14	1.0	10	0.9	13	Estimated
Probability of a recruitment event occurring (/yr)	$P_{recruit}$	0.03 ± 0.02	0.9	10	1.0	9	1.1	10	Estimated
Probability of a rootstock failing to resprout following fire	S_{mort}	0.04 ± 0.03	0.8	11	1.0	8	1.2	4	Estimated

regeneration in miombo woodlands (Table 4.1). Model parameter values were derived from the literature, field measurements and assessed with reference to local knowledge and professional experience. Although it is usually desirable for a model to generate a best-guess estimate of the value of a management intervention, a C management project is motivated to ensure that predictions are conservative, guaranteeing that all claimed C is representative of genuine AGB changes. In the miombo ecosystem where information is severely limited, working conservative parameter estimates is beneficial to ensure passage of a methodology through verification schemes and to minimise risk of project failure.

We perform multiple simulations using a Monte Carlo approach to characterise model uncertainty, based on assumed uniform probability distribution functions around each parameter and 10,000 randomly generated parameter sets. Model sensitivity to parameter changes was assessed using the Latin-Hypercube One-factor-At-a-Time (LH-OAT) approach of van Griensven et al. (2006), a global sensitivity analysis method using the LH design to sample the full range of parameter space whilst retaining the precision of OAT sampling for attribution of model output changes to a single parameter. Sensitivity of AGB to parameter changes is calculated using an average biomass woodland run for 10 years at baseline fire frequencies, a project scenario assuming a 50 % reduction in late dry season fire frequency, and the difference between the two scenarios. Model predictions of AGB were validated by comparing model predictions of woodland regrowth from clearance to chronosequence data from Kilwa District and Gorongosa District to test model consistency with available data.

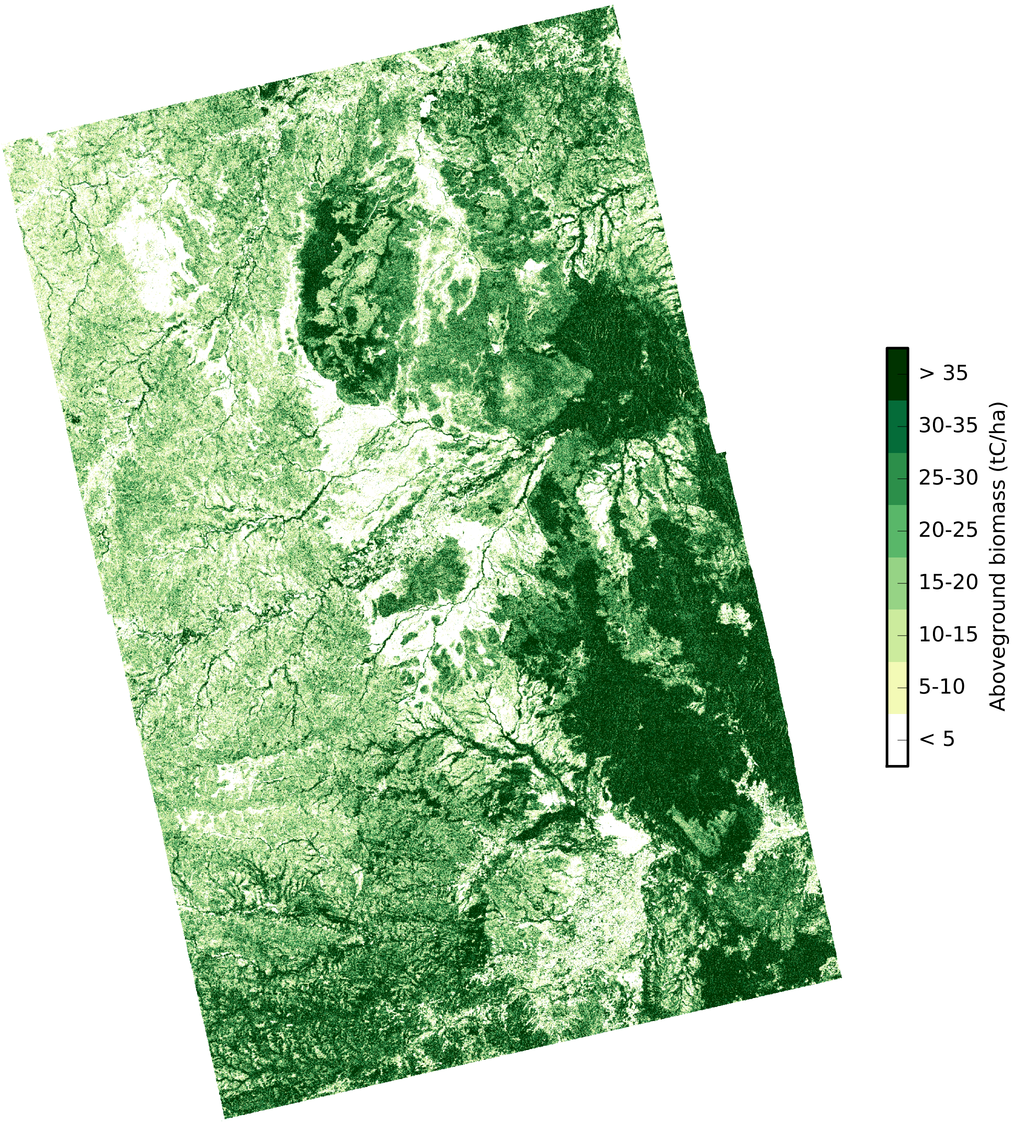

Figure 4.5: Aboveground biomass map of Kilwa district generated using radar backscatter data from ALOS PALSAR, calibrated using AGB estimates from Permanent Sample Plots. The map is stratified into 5 tC/ha bands, where C yield is modelled separately for each stratum, and areas < 5 tC/ha and > 35 tC/ha are excluded from fire management.

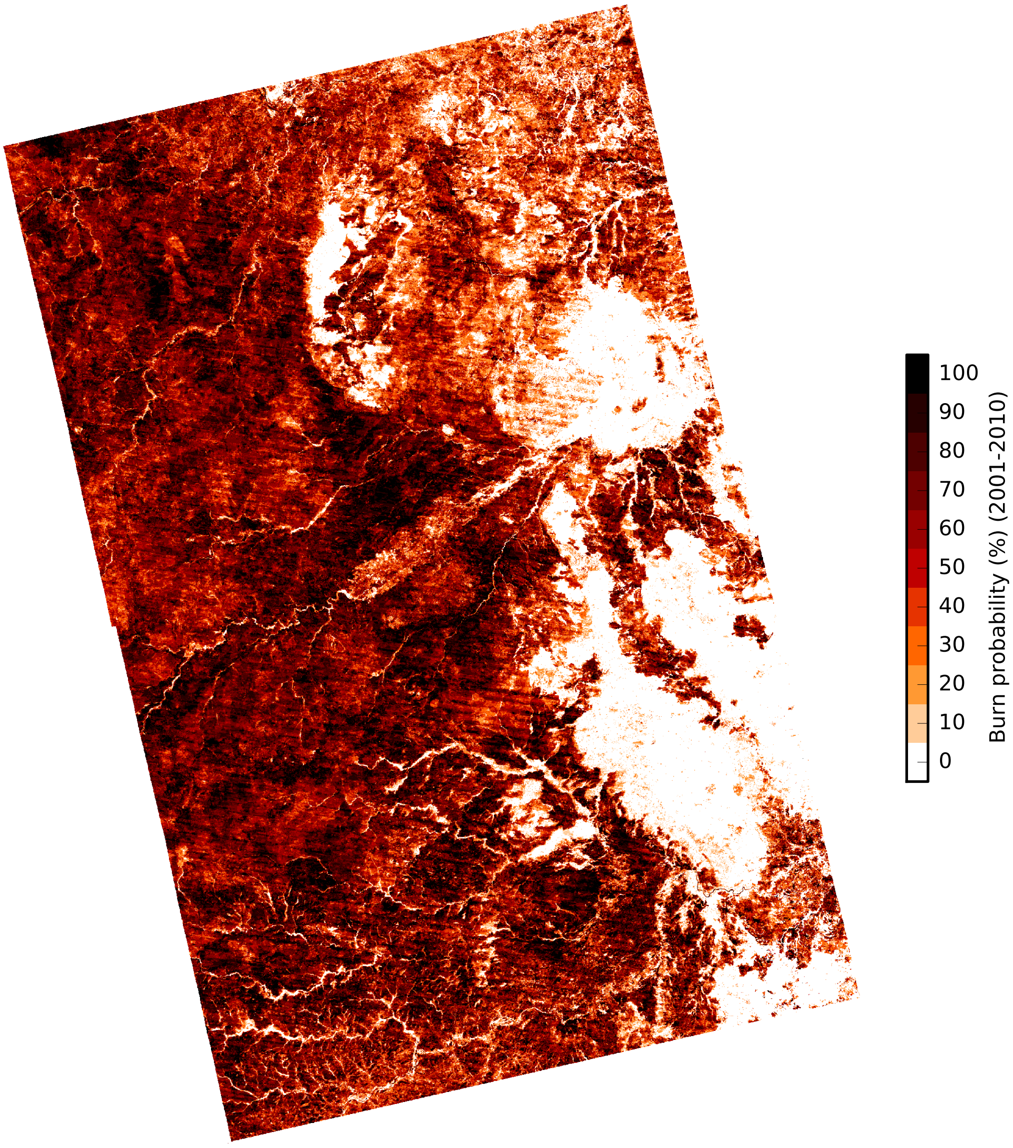

Figure 4.6: Fire frequency estimates from 10 years of burn scars classified in Landsat data. More fires were observed in the sparsely populated drier areas to the west than the wetter and more densely populated east. Fires are near-absent in coastal forest and thicket areas, as well as in riparian forests.

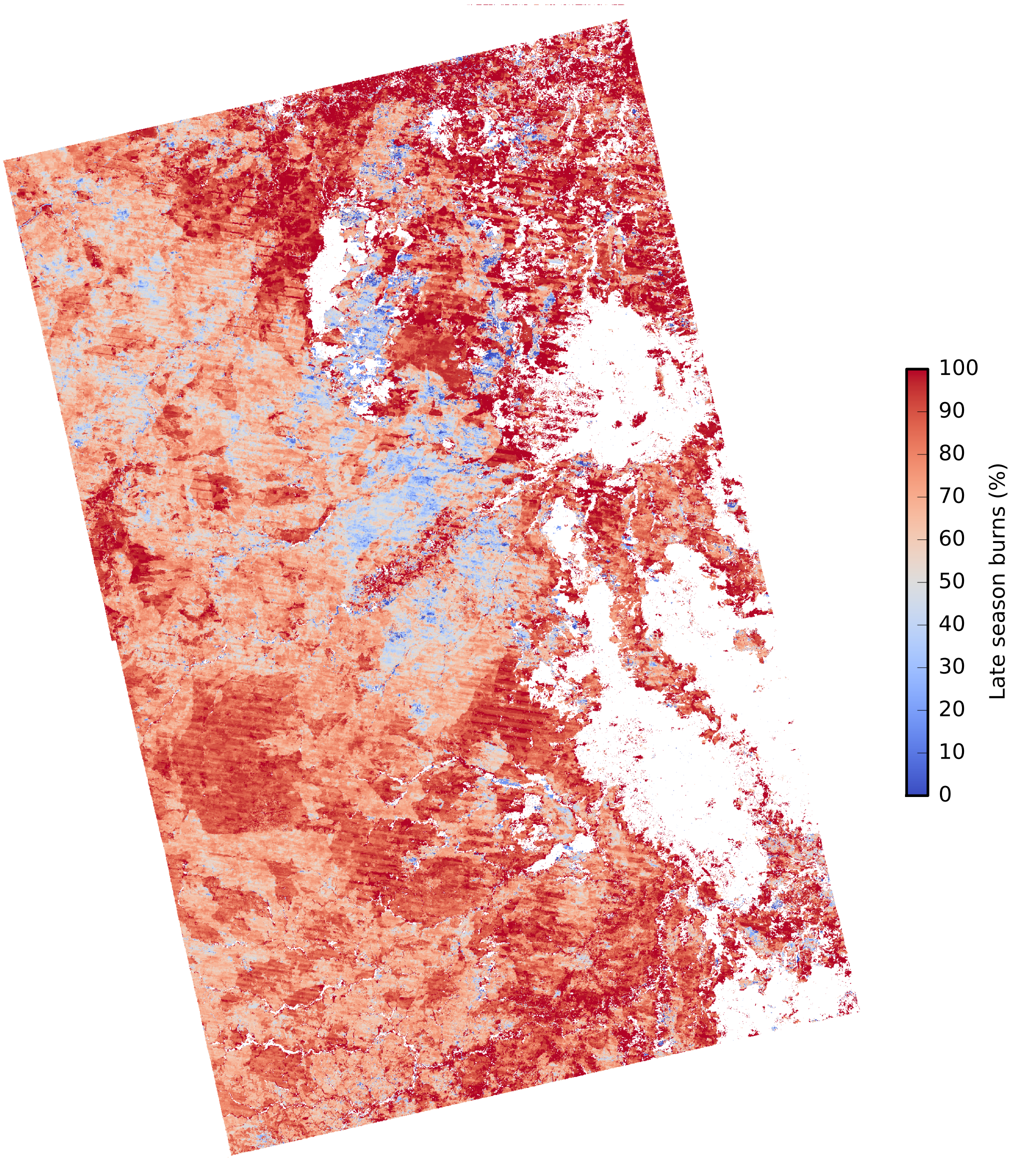

Figure 4.7: Fire seasonality varies across the Kilwa District. The majority of burn scars were assigned to the late dry season, particularly towards the agricultural coastal eastern region where fields are burned at the end of the dry season. There is a preponderance of late dry season fires in most areas. Early dry season fires are most frequently observed in low AGB areas, suggesting their grasses cure earlier in the dry season.

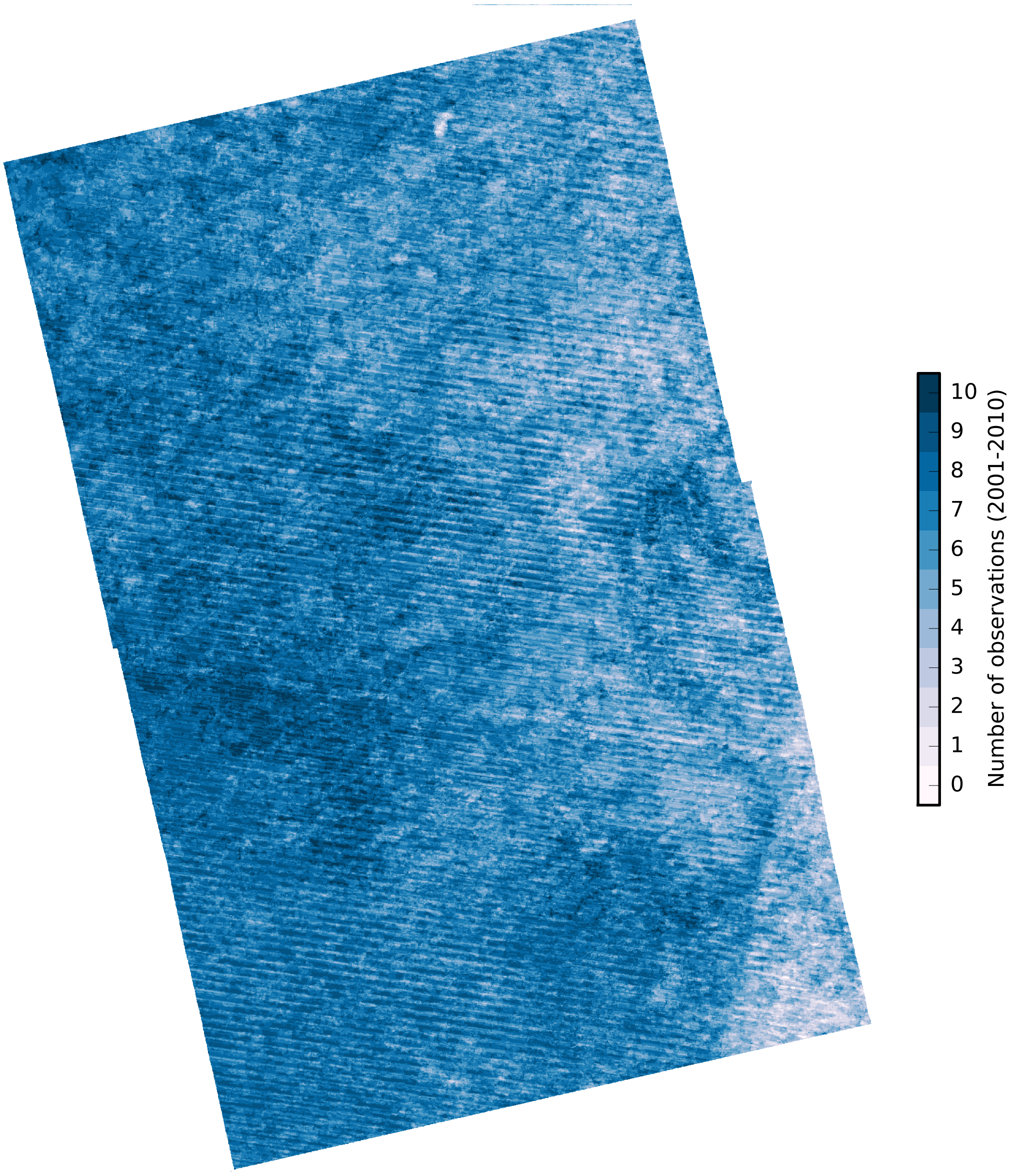

Figure 4.8: Number of years in which burn status was logically determinable for each pixel between 2001 and 2010. Lighter areas show locations where cloud cover, the SLC failure of ETM+ measurements and data availability reduce observation opportunities. Better observational data were available for the south and west of Kilwa District, where cloud cover is lower and data availability is better.

4.3 Results

4.3.1 Biomass assessment

AGB estimates in PSPs ranged between 1.9 - 43.6 tC/ha, averaging 20.2 tC/ha across Kilwa District. The calibration between radar backscatter and AGB yielded a linear model describing a large proportion of variance in backscatter ($p < 0.001$, $R^2 = 0.85$). The calibrated biomass map estimates mean AGB in Kilwa District as 22.5 tC/ha, with 65 % of pixels meeting early burning eligibility requirements of 5 - 35 tC/ha (Fig. 4.5). Of the remaining areas, 12 % of pixels are excluded as low biomass grassland, and 23 % of pixels excluded as high biomass coastal forest or thicket.

4.3.2 Fire history assessment

More than half (56 %) of land area was observed to burn each year, corresponding to a mean fire return interval 1.8 years (Fig. 4.6). Fire frequency varies spatially, with woodlands and grasslands to the west of Kilwa district burning on a near-annual basis, and the coastal and agricultural regions of the east burning infrequently. Few fires were observed in high biomass areas where grass exclusion in dense coastal and riparian forest interrupts the spread of fire. Fire frequency is closely related to AGB, such that low biomass areas are observed to burn much more frequently than high biomass areas. Of all burns observed, 75% were late dry season fires, with early dry season dominated fire regimes mostly confined to areas of very low biomass where grass fuels tend to dry rapidly (Fig. 4.7).

On average, it was possible to logically determine the burn status of 60 % of pixels in the the study region each year, though this varied between 19 % to 85 % depending on availability of satellite data and cloud cover (Fig. 4.8). Although Landsat satellites made an overpass every 8 days, only a small proportion of this data is now accessible,

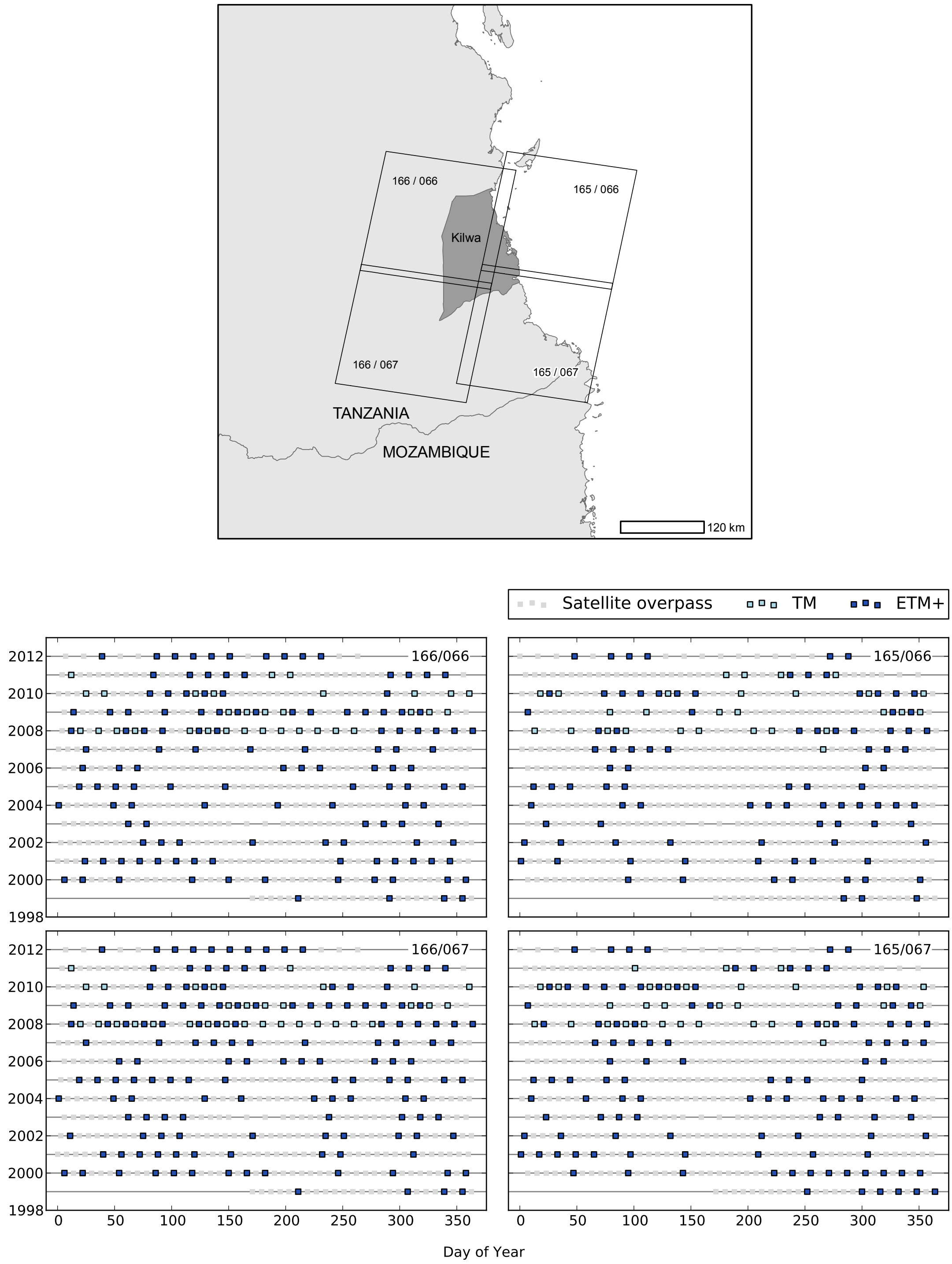

Figure 4.9: Landsat data were assembled for burn scar mapping from the 4 scenes that cover Kilwa District. Of all satellite overpasses, only a small proportion are available (coloured symbols), with most images from the ETM+ sensor of Landsat 7 (dark blue). Images from the older TM sensor of Landsat 5 were only widely available for the years 2008 - 2010 (light blue).

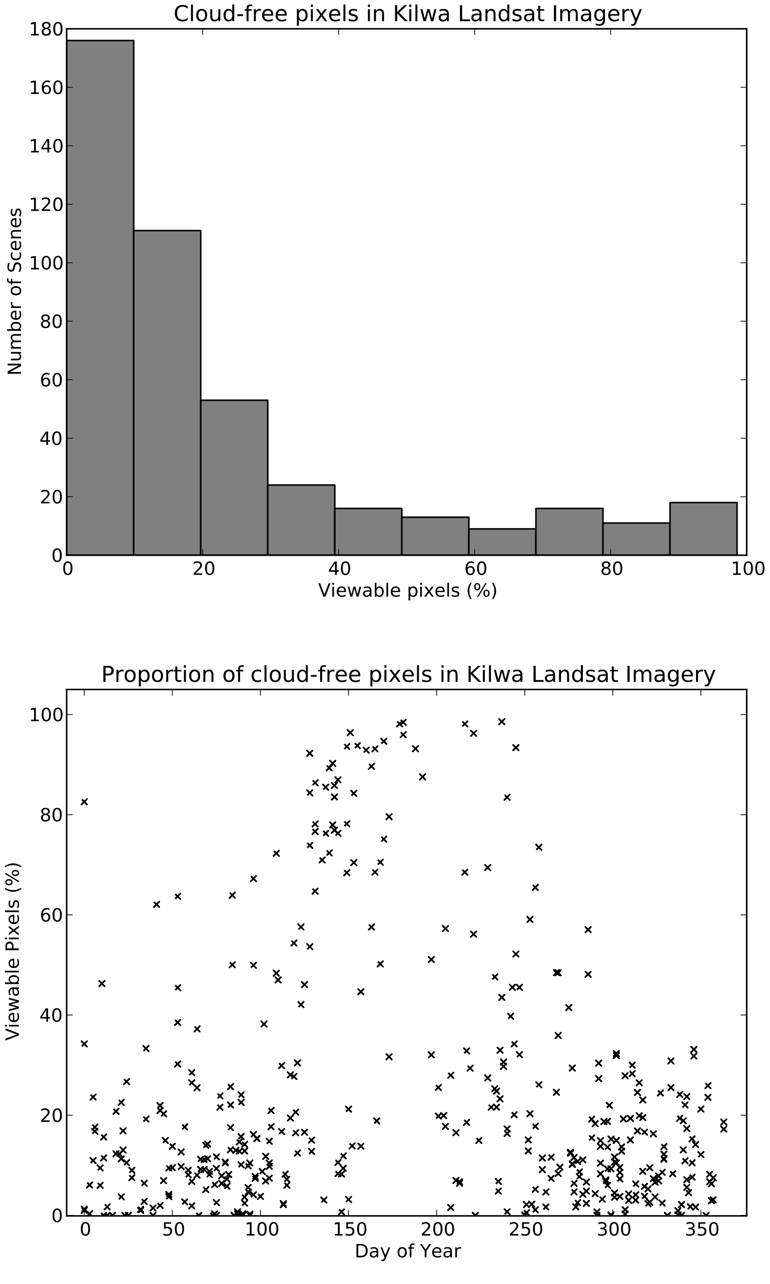

Figure 4.10: Data from Landsat were mostly unusable for burn scar mapping as the result of cloud cover and missing data. The best data were from dry season acquisitions (day of year 150 - 300), coinciding with the fire season.

with some years showing very limited coverage (Fig. 4.9). Of the scenes that were available, a large proportion of pixels are discarded as a result of cloud cover and the scan line corrector failure of Landsat 7 (Markham et al., 2004) (Fig. 4.10). Though burn scar data are limited, the best data is available for the dry season when cloud cover is lower, coinciding with the period of peak fire activity.

4.3.3 Model output

With the present frequency and seasonality of fires, the GapFire model predicts a gradual reduction in woodland AGB across all biomass strata in the baseline scenario (Table 4.2). Assuming that a fire management project is able to halve the incidence of late dry season fires through early burning, the model predicts that management activities will result in a small increase AGB over a 10 year period. The magnitude of expected C return is proportional to initial biomass, with expected AGB change in areas of high biomass significantly greater than low biomass woodlands. Subject to the efficacy of an early burning program, the model predicts a climate change mitigation potential of 0.14 - 0.53 tC/ha/yr (25 % - 75 % reduction in late dry season fire frequency), split roughly evenly between avoided woodland degradation and woody biomass gain.

4.3.4 Model evaluation

Uncertainty

Model uncertainty is considerable for the prediction of AGB change, indicated by wide and overlapping error regions for model projections of AGB under baseline and project fire regime scenarios (Fig. 4.11a). Whilst the magnitude of model uncertainty suggests a difficulty in determining the extent to which woodlands are degrading over landscapes, much of this error is negated by correlation between baseline and project

Table 4.2: Model predictions of AGB change given baseline fire regime, and shifts in fire towards the early dry season of 25%, 50% and 75% of current late dry season fires. The total output reports mean AGB changes in the 5 - 35 tC/ha range over the District, weighted by the land area of each biomass stratum.

	Baseline burn probability (%)				Modelled biomass change (tC/ha/yr)			
Biomass stratum (tC/ha)	**p(burn|early)**	**p(burn|late)**	**p(no burn)**	**Area (%)**	**Baseline change**	**Late fire reduction**	**Project change**	**Carbon yield**
5 - 10	16.3 ± 12.4	50.8 ± 17.9	32.9 ± 16.9	13.8	-0.06	25%	0.03	0.09
						50%	0.13	0.19
						75%	0.25	0.31
10 - 15	15.0 ± 11.6	48.4 ± 16.7	36.5 ± 16.8	13.3	-0.14	25%	-0.04	0.11
						50%	0.13	0.27
						75%	0.29	0.44
15 - 20	13.6 ± 10.4	45.1 ± 15.4	41.3 ± 16.3	11.8	-0.19	25%	-0.04	0.15
						50%	0.16	0.35
						75%	0.37	0.56
20 - 25	12.1 ± 9.1	40.9 ± 14.1	47.0 ± 15.6	10.1	-0.21	25%	-0.08	0.14
						50%	0.18	0.39
						75%	0.41	0.63
25 - 30	10.6 ± 7.9	36.4 ± 12.8	52.9 ± 14.6	8.5	-0.26	25%	-0.07	0.19
						50%	0.22	0.47
						75%	0.44	0.69
30 - 35	9.2 ± 6.8	32.1 ± 11.7	58.7 ± 13.6	7.2	-0.24	25%	-0.01	0.24
						50%	0.24	0.48
						75%	0.52	0.76
Total				64.7	-0.17	25%	-0.03	0.14
						50%	0.17	0.34
						75%	0.36	0.53

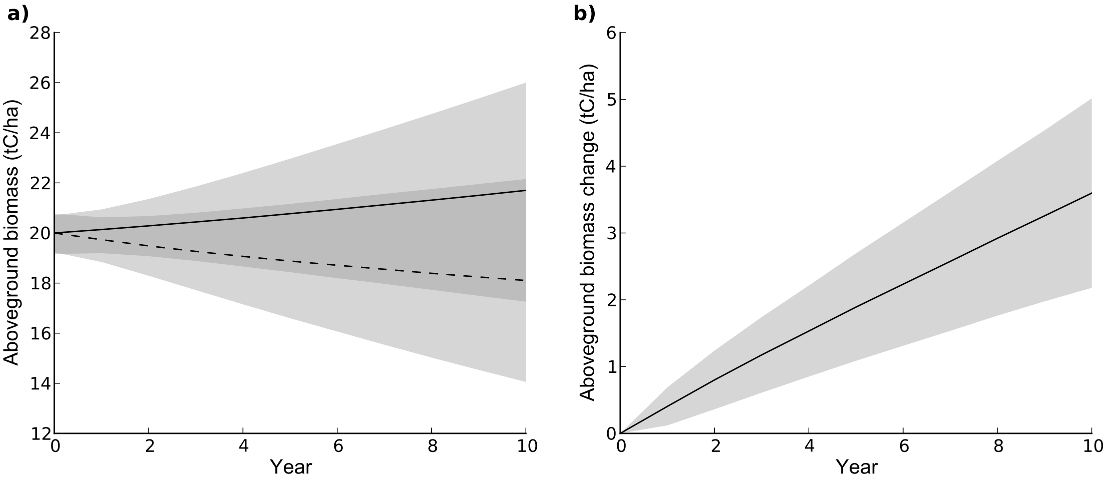

Figure 4.11: **(a)** Mean trends of AGB under project (solid) and baseline (dashed) scenarios are displayed for the initial 10 year management period. The shaded region represents model uncertainty (± 1 standard deviation) as calculated from Monte Carlo analysis with 10,000 random permutations of input parameters. **(b)** As project and baseline trends are autocorrelated under a given parameter set, uncertainty is reduced when considering the net AGB yield of fire management.

fire scenario AGB projections (Fig. 4.11b). This results from model parametrisation leading to a high growth rate in the project scenario being accompanied by a reduced capacity for degradation, and parameters eliciting a low growth capacity in the project scenario being accompanied by rapid degradation in the baseline scenario. This property limits the capacity for changes in model parametrisation to alter net projections of AGB change.

Sensitivity analysis

Model predictions were found to be sensitive to parameters representing respiratory fraction (R_a), maximum photosynthetic rate (P_{max}) and half saturation of photosynthetic rate (K_p), which all relate to the productivity of miombo woodlands by controlling C assimilation and stem growth rates (Table 4.1). R_a is poorly constrained within savannah woodlands as it is very difficult to measure *in situ*. However, it is reasonably well constrained globally at around 50% (Waring et al., 1998), with a significant deviation from this value in miombo woodlands not expected. K_p and P_{max} describe the rate of photosynthesis that is expected under different light conditions, with the model particularly sensitive to P_{max}. In the absence of detailed ecophysiological data from miombo woodlands, parametrisation of the shape of the light response curve introduces a large uncertainty to model predictions.

The model is also sensitive to late dry season fire intensity (FLI_{late}), which is the primary driver of stem top-kill in the model. Model sensitivity to fire-induced mortality is a pre-requisite to the success of an early burning management intervention, though it's capacity to alter model predictions necessitates careful parametrisation of FLI_{late} to avoid the possibility of over-claiming AGB changes. Unlike parameters determining growth and top-kill rates, model projections of AGB are largely insensitive to parameters determining regeneration. This suggests that the AGB changes resulting from early burning are associated with the preservation of large trees rather than the recruitment of new stems. Whilst the near-term changes to AGB resulting from the lifting of the fire trap are likely to be small, these may translate into more significant AGB changes over longer time-scales than are considered here.

Validation

Chronosequence studies from both Kilwa District and Gorongosa District estimate approximately 0.7 tC/ha/yr of AGB accumulation on abandoned land in miombo woodlands, a situation simulated by running the model from a start-point with no large stems and without fire (Fig. 4.12). Mean growth rates amount to a biomass increment of 0.61 tC/ha/yr in the first 25 years, a level slightly lower than observed in the Kilwa District and Gorongosa District chronosequence studies, and 0.88 tC/ha/yr in the first 50 years, a level slightly higher than that observed in Kilwa District. We consider model outputs a conservative prediction for the purposes of a 10 year fire management project, as the model predicts lower growth rates than observed in the first 10 years of

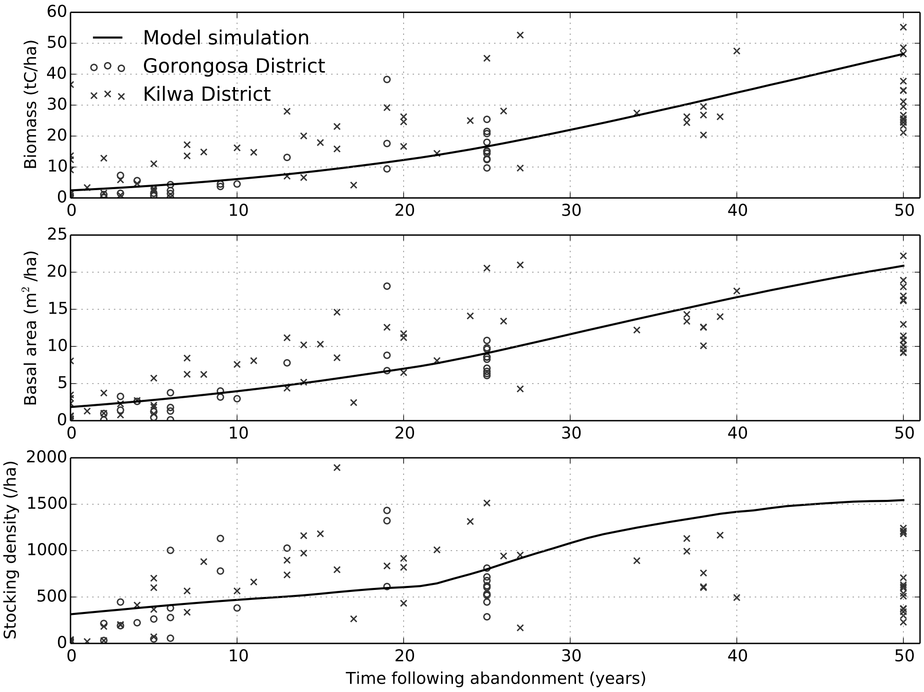

Figure 4.12: Model output comparison to chronosequence data from Gorongosa and Kilwa Districts. AGB increase following abandonment is predicted reasonably (Gorongosa: RMSE = 5.8 tC/ha, R^2 = 0.53, Kilwa: RMSE = 23.8 tC/ha, R^2 = 0.20), as is basal area (Gorongosa: RMSE = 1.7 m^2/ha, R^2 = 0.56, Kilwa: RMSE = 9.0 m^2/ha, R^2 = 0.21), though the model is not able to effectively capture trends in stocking density of trees >5 cm DBH (Gorongosa: RMSE = 236 /ha, R^2 = 0.04, Kilwa: RMSE = 360 /ha, R^2 = -0.74). The model performs better on data from Gorongosa District than Kilwa District, with a notable under-prediction of biomass and basal area in young sites, and an over-prediction at mature sites.

chronosequence data from both sites. The model also performs well in predicting basal area, though is less capable of predicting changes in stocking density, highlighting a weakness in the model's representation of stand structure and regeneration.

4.4 Discussion

4.4.1 RQ1: What is the likely magnitude of emissions reductions achieved by early burning in miombo woodlands?

The miombo woodlands of Kilwa district burn at a high frequency, largely in the late dry season. Many areas experience near annual fires, a rate which has been predicted by models (Ryan and Williams, 2011) and experimentally demonstrated (Trapnell, 1959; Furley et al., 2008) to result in a large reduction of AGB in miombo woodlands. The rates of fire we have measured in Kilwa District are not unusual, and similar fire return intervals and seasonality have been observed in Tanzania (Tarimo et al., 2015), and in other woodland ecosystems across southern Africa (Archibald et al., 2010).

The GapFire model predicts that the current fire regime of Kilwa District is resulting in the gradual reduction in miombo woodland biomass. Given the conservative parametrisation of the model we expect that the degradation predicted by the model is existent, though note that the error bounds of our model are large. Under a managed fire scenario, the model predicts a gradual increase in AGB, provided a project succeeds in substantially reducing the incidence of late dry season fire. Biomass increase resulting from early burning is of a similar magnitude to loss in the baseline scenario, such that C changes resulting from fire management are split between avoided woodland degradation and woodland regrowth. Predicted changes to AGB are greatest in higher biomass areas, where the potential for degradation and capacity for growth is higher.

Even assuming an ambitious 50% reduction in late dry season fire frequency, the predicted climate change mitigation potential of 0.34 tC/ha/yr (1.25 tCO_2e/ha/yr) from fire management is small given the scale of operations. However this compares favourably to fire management protocols that only consider emissions changes, such as the WALFA project (∼0.04 tCO_2e/ha/yr) (Murphy et al., 2009), as well as estimates of AGB changes resulting from the WALFA project by Murphy et al. (2009) (∼0.11 tC/ha/yr) and Cook et al. (2015) (∼0.1 tC/ha/yr). Much of this difference can be attributed to more limited shifts in seasonal fire activity than might be expected in the much smaller and more intensely managed VLFRs of Kilwa District. Our model reports a similar mitigation potential to estimates by Williams et al. (2004) and Liedloff and Cook (2011) (∼0.5 tC/ha/yr), and is somewhat smaller than the C fluxes predicted by Chen et al. (2003) and Beringer et al. (2007). The extent to which fire seasonality can be readily altered in Kilwa District is unclear, so the capacity for an early burning project in miombo woodlands to be financially self-sustaining cannot yet be addressed.

4.4.2 RQ 2: What are the key uncertainties in the method, and how can uncertainty be mitigated in an operational fire-management project?

The uncertainty associated with the method presented in this paper is substantial, with the largest uncertainties stemming from model parametrisation, characterisation of fire regimes, and the dearth of appropriate validation data. Here we discuss the impact of uncertainty on model predictions, the efficacy of efforts to mitigate against uncertainty, and identify areas for future work.

Representation of productivity

Much of the uncertainty in modelled AGB changes relates to the high model sensitivity and poor constraint of respiratory fraction (R_a), and maximum (P_{max}) and half saturation of photosynthetic rate (K_p). Though the individual parameter values determining miombo woodland productivity are uncertain, comparisons of modelled AGB against chronosequence data from Kilwa and Gorongosa Districts demonstrate that selected parameters result in reasonable predictions. Further to this we assume chronosequence plots to have re-grown in the absence of fire, which is unlikely to be the case. The result is that growth in GapFire is likely a conservative representation of miombo woodland productivity. As one of the key uncertainties in projecting AGB change, further data on woodland productivity from flux towers or forest plot re-inventory data (e.g. Chapter 3) will be of considerable value to understanding miombo woodland vegetation dynamics.

Characterisation of fire

Modelled AGB changes are sensitive to top-kill resulting from late dry season fires (FLI_{late}), signalling the importance of fire to miombo woodland C stocks. Whereas fire frequency is reasonably well-measured using remote sensing data, fire intensity is not easily measured either remotely or through field studies. Fireline intensities recorded in miombo woodlands vary from very low (< 300 kW/m) to high intensities (> 6500 kW/m) (Hoffa et al., 1999; Roberston, 1993; Ryan and Williams, 2011). Though our estimates of early and late dry season intensity respectively represent conservatively high and low FLIs, this remains a very simple representation of fire. Fire intensity on a given date is inter-annually variable conditional upon fluctuating weather and fuel conditions. Predictions of fire intensity may be made more realistic by performing experimental fires in a range of fuel conditions (e.g. Sow et al., 2013), allowing for the annual shifting of the early burn cut-off date (Russell-Smith et al., 2009), or by application of widely-used models of fire intensity such as the Rothermel model of fire spread (Rothermel, 1972; VCS, 2015).

A further obstacle to accurate determination of baseline fire regimes was high cloud cover and poor data availability in Kilwa District. Whilst this can to some extent be mitigated by working over large areas, data paucity becomes a significant problem when aiming to enumerate the fire regime of a single VLFR. Future work should benefit from the recent launch of Landsat 8 and Sentinel 2, as well moves towards open data access policies.

Other emissions

As formulated in this paper, no credit or deductions are calculated for other gaseous emissions, or for dead wood. Methane emissions are in particular a large uncertainty, with varied reports of the magnitude and seasonality of emission factors. Previous work in Africa has detected sharp increases in methane emission from early dry season fires (Hoffa et al., 1999; Korontzi et al., 2003; Korontzi, 2005), though recent work in Australia did not detect seasonal differences in methane emission (Meyer et al., 2012). Emissions of NO_x have also been observed to be increased in early dry season fires in African (Mebust and Cohen, 2013) and South American (Castellanos et al., 2014) savannah fires. Such predictions are limited by the small number of studies and the spatio-temporal variability of fire activity, though does have the capacity to counteract the climate mitigation potential of changes to AGB we predict here, and will require the attention of land managers as it has received in Australia.

4.5 Conclusions

In this paper we described a method for accounting for the climate change mitigation potential of early burning in miombo woodlands. Early burning has the potential to reduce woodland degradation from fire and increase AGB, though seasonal shifts in fire frequency will have to be large to have a significant impact on C emissions. Uncertainty in the method is high, though in most cases it is possible to mitigate against this using conservative model parametrisation, and by focusing on quantifying the differences between management scenarios. Future work on this framework can improve AGB projections through improved constraint of stem growth rates and fire-induced top-kill, exploiting future availability of Earth observation data, and with further monitoring of the outcome of early burning in the miombo woodlands in Kilwa District.

4.6 Acknowledgements

This work was supported by the Mpingo Conservation Development Initiative (MCDI), funded by the Royal Norwegian Embassy of Tanzania. Jose Gómez-Dans (University College London) assisted by Samuel Bowers developed the image classification algorithm used for burn scar identification in Landsat data. The GapFire model builds on work in Ryan and Williams (2011). Text written by Samuel Bowers, with input from Steve Ball (MCDI), Jan Fehse (Value for Nature Ltd.) and Mathew Williams.

My thanks are due to the Village Natural Resources Committee of Nanjirinji village who took me along on an early burning expedition. This unsuccessful (but memorable) trip taught me much about the difficulties of fire management.

4.7 Publication

This work forms part of a pilot REDD+ methodology validated by Verified Carbon Standard (VCS). A complete description of the methods described here can be accessed at:

`http://www.v-c-s.org/methodologies/avoiding-degradation-through-fire-management/`

The GapFire model is hosted at:

`http://www.geos.ed.ac.uk/gcel/gapfire.html`

4.8 References

Archibald, S., Scholes, R.J., Roy, D.P., Roberts, G., and Boschetti, L. (2010), ‘Southern African fire regimes as revealed by remote sensing’, *International Journal of Wildland Fire*, **19**, pp. 861–878.

Bastarrika, A., Chuvieco, E., and Martín, M.P. (2011), ‘Mapping burned areas from Landsat TM/ETM+ data with a two-phase algorithm: Balancing omission and commission errors’, *Remote Sensing of Environment*, **115**, pp. 1003–1012.

Beringer, J., Hutley, L.B., Tapper, N.J., and Cernusak, L.A. (2007), ‘Savanna fires and their impact on net ecosystem productivity in North Australia’, *Global Change Biology*, **13**, pp. 990–1004.

Bond, W.J. (2008), ‘What Limits Trees in C_4 Grasslands and Savannas?’, *Annual Review of Ecology, Evolution, and Systematics*, **39**, pp. 641–659.

Castellanos, J., Jaramillo, V.J., Sanford, R.L., and Kauffman, J.B. (2001), ‘Slash-and-burn effects on fine root biomass and productivity in a tropical dry forest ecosystem in Mexico’, *Forest Ecology and Management*, **148**, pp. 41–50.

Castellanos, P., Boersma, K.F., and van der Werf, G.R. (2014), ‘Satellite observations indicate substantial spatiotemporal variability in biomass burning NO_x emission factors for South America’, *Atmospheric Chemistry and Physics*, **14**, pp. 3929–3943.

Chen, X., Hutley, L.B., and Eamus, D. (2003), ‘Carbon balance of a tropical savanna of northern Australia’, *Oecologia*, **137**, pp. 405–416.

Chidumayo, E.N. (1997), *Miombo ecology and management: an introduction*, Intermediate Technology Publications Ltd (ITP).

Chidumayo, E.N. and Gumbo, D.J. (2010), *The Dry Forests and Woodlands of Africa: Managing for Products and Services*, London, UK: Earthscan.

Cook, G.D., Liedloff, A.C., and Murphy, B.P. (2015), ‘Predicting the effects of fire management on carbon stock dynamics using statistical and process-based modelling’, *Carbon Accounting and Savanna Fire Management*, ed. by B.P. Murphy, A.C. Edwards, M. Meyer, and J. Russell-Smith, Victoria, Australia: Csiro Publishing, pp. 321–328.

Desanker, P.V. and Prentice, I.C. (1994), ‘MIOMBO – A vegetation dynamics model for the miombo woodlands on Zambezian Africa’, *Forest Ecology and Management*, **69**, pp. 87–95.

Eriksen, C. (2007), ‘Why do they burn the ‘bush’? Fire, rural livelihoods, and conservation in Zambia’, *The Geographical Journal*, **173**, pp. 242–256.

Everson, T.M., Everson, C.S., de Ronde, C., and Trollope, W.S.W. (2004), ‘Regional fire management: objectives, practices, and prescribed burning application’, *Wildland fire management handbook for Sub-Sahara Africa*, ed. by C. de Ronde and J.G. Goldammer, Compress, pp. 114–143.

FAO (2008), *Global forest resources assessment: terms and definitions*, Forest and Agriculture Organization of the United Nations, Rome, Italy.

Furley, P.A., Rees, R.M., Ryan, C.M., and Saiz, G. (2008), ‘Savanna burning and the assessment of long-term fire experiments with particular reference to Zimbabwe’, *Progress in Physical Geography*, **32**, pp. 611–634.

Giglio, L., Loboda, T., Roy, D.P., Quayle, B., and Justice, C.O. (2009), ‘An active-fire based burned area mapping algorithm for the MODIS sensor’, *Remote Sensing of Environment*, **113**, pp. 408–420.

Hendricks, J.J., Hendrick, R.L., Wilson, C.A., Mitchell, R.J., Pecot, S.D., and Guo, D. (2006), ‘Assessing the patterns and controls of fine root dynamics: an empirical test and methodological review’, *Journal of Ecology*, **94**, pp. 40–57.

Hoffa, E.A., Ward, D., Hao, W.M., Susott, R.A., and Wakimoto, R.H. (1999), ‘Seasonality of carbon emissions from biomass burning in a Zambian savanna’, *Journal of Geophysical Research: Atmospheres*, **104**, pp. 13841–13853.

Hough, J.L. (1993), ‘Why burn the bush? Social approaches to bush-fire management in West African national parks’, *Biological Conservation*, **65**, pp. 23–28.

Korontzi, S., Ward, D.E., Susott, R.A., Yokelson, R.J., Justice, C.O., Hobbs, P.V., Smithwick, E.A.H., and Hao, W.M. (2003), ‘Seasonal variation and ecosystem dependence of emission factors for selected trace gases and $PM_{2.5}$ for southern African savanna fires’, *Journal of Geophysical Research: Atmospheres*, **108**.

Korontzi, S. (2005), ‘Seasonal patterns in biomass burning emissions from southern African vegetation fires for the year 2000’, *Global Change Biology*, **11**, pp. 1680–1700.

Laris, P. (2002), ‘Burning the seasonal mosaic: preventative burning strategies in the wooded savanna of southern Mali’, *Human Ecology*, **30**, pp. 155–186.

Laris, P. and Wardell, D.A. (2006), ‘Good, bad or ‘necessary evil’? Reinterpreting the colonial burning experiments in the savanna landscapes of West Africa’, *The Geographical Journal*, **172**, pp. 271–290.

Liedloff, A. and Cook, G.D. (2011), ‘The interaction of fire and rainfall variability on tree structure and carbon fluxes in savannas: Application of the flames model’, English, *Ecosystem function in savannas: measurement and modeling at landscape to global scales*, ed. by M.J. Hill and N.P. Hanan, CRC Press, pp. 293–308.

Markham, B.L., Storey, J.C., Williams, D.L., and Irons, J.R. (2004), ‘Landsat sensor performance: history and current status’, *IEEE Transactions on Geoscience and Remote Sensing*, **42**, pp. 2691–2694.

Masek, J.G., Huang, C., Wolfe, R., Cohen, W., Hall, F., Kutler, J., and Nelson, P. (2008), ‘North American forest disturbance mapped from a decadal Landsat record’, *Remote Sensing of Environment*, **112**, pp. 2914–2926.

McNicol, I.M., Ryan, C.M., and Williams, M. (2015), ‘How resilient are African woodlands to disturbance from shifting cultivation?’, *Ecological Applications*, **25**, pp. 2320–2336.

Mebust, A.K. and Cohen, R.C. (2013), 'Observations of a seasonal cycle in NO_x emissions from fires in African woody savannas', *Geophysical Research Letters*, **40**, pp. 1451–1455.

Meyer, C.P., Cook, G.D., Reisen, F., Smith, T.E.L., Tattaris, M., Russell-Smith, J., Maier, S., Yates, C.P., and Wooster, M.J. (2012), 'Direct measurements of the seasonality of emission factors from savanna fires in northern Australia', *Journal of Geophysical Research: Atmospheres*, **117**, p. D20305.

Mitchard, E.T.A., Saatchi, S.S., Woodhouse, I.H., Nangendo, G., Ribeiro, N.S., Williams, M., Ryan, C.M., Lewis, S.L., Feldpausch, T.R., and Meir, P. (2009), 'Using satellite radar backscatter to predict above-ground woody biomass: A consistent relationship across four different African landscapes', *Geophysical Research Letters*, **36**, p. L23401.

Moreira, A.G. (2000), 'Effects of fire protection on savanna structure in Central Brazil', *Journal of Biogeography*, **27**, pp. 1021–1029.

Murphy, B.P., Russell-Smith, J., and Watt Felicity A.and Cook, G.D. (2009), 'Fire management and woody biomass carbon stocks in mesic savannas', English, *Culture, ecology and economy of fire management in North Australian savannas: rekindling the Wurrk tradition*, ed. by J. Russell-Smith, P. Whitehead, and P. Cooke, Csiro Publishing, pp. 361–378.

Norman, J.M. and Campbell, G.S. (1989), 'Canopy structure', English, *Plant Physiological Ecology*, ed. by R.W. Pearcy, J.R. Ehleringer, H.A. Mooney, and P.W. Rundel, Springer Netherlands, pp. 301–325.

Nottingham, A. (2004), 'The characterisation of foliar N-concentrations and presence of N-fixers in Miombo woodland, Mozambique', MA thesis, University of Dundee.

Prins, E. and Clarke, G.P. (2007), 'Discovery and enumeration of Swahilian Coastal Forests in Lindi region, Tanzania, using Landsat TM data analysis', *Biodiversity and Conservation*, **16**, pp. 1551–1565.

Richards, A.E., Andersen, A.N., Schatz, J., Eager, R., Dawes, T.Z., Hadden, K., Scheepers, K., and van Der Geest, M. (2012), 'Savanna burning, greenhouse gas emissions and indigenous livelihoods: Introducing the Tiwi Carbon Study', *Austral Ecology*, **37**, pp. 712–723.

Roberston, F. (1993), 'Early-burning in the Brachystegia woodland of the Parks and Wild Life Estate', *Zimbabwe Science News*, **27**, pp. 68–71.

Rothermel, R.C. (1972), *A mathematical model for predicting fire spread in wildland fuels*, United States Forest Service, Utah, USA.

Russell-Smith, J., Murphy, B.P., Meyer, C.P.M., Cook, G.D., Maier, S., Edwards, A.C., Schatz, J., and Brocklehurst, P. (2009), 'Improving estimates of savanna burning emissions for greenhouse accounting in northern Australia: limitations, challenges, applications', *International Journal of Wildland Fire*, **18**, pp. 1–18.

Russell-Smith, J., Whitehead, P.J., Cook, G.D., and Hoare, J.L. (2003), 'Response of Eucalyptus-dominated savanna to frequent fires: lessons from Munmarlary, 1973-1996', *Ecological Monographs*, **73**, pp. 349–375.

Ryan, C.M., Hill, T., Woollen, E., Ghee, C., Mitchard, E., Cassells, G., Grace, J., Woodhouse, I.H., and Williams, M. (2012), 'Quantifying small-scale deforestation and forest degradation in African woodlands using radar imagery', *Global Change Biology*, **18**, pp. 243–257.

Ryan, C.M. and Williams, M. (2011), 'How does fire intensity and frequency affect miombo woodland tree populations and biomass?', *Ecological Applications*, **21**, pp. 48–60.

Ryan, C.M., Williams, M., and Grace, J. (2011), 'Above-and Belowground Carbon Stocks in a Miombo Woodland Landscape of Mozambique', *Biotropica*, **43**, pp. 423–432.

Ryan, C.M. (2009), 'Carbon cycling, fire and phenology in a tropical savanna woodland in Nhambita, Mozambique', PhD thesis, The University of Edinburgh.

Saito, M., Luyssaert, S., Poulter, B., Williams, M., Ciais, P., Bellassen, V., Ryan, C.M., Yue, C., Cadule, P., and Peylin, P. (2014), 'Fire regimes and variability in aboveground woody biomass in miombo woodland', *Biogeosciences*, **119**, pp. 1014–1029.

Shea, R.W., Shea, B.W., Kauffman, J.B., Ward, D.E., Haskins, C.I., and Scholes, M.C. (1996), 'Fuel biomass and combustion factors associated with fires in savanna ecosystems of South Africa and Zambia', *Journal of Geophysical Research: Atmospheres*, **101**, pp. 23551–23568.

Smit, I.P.J., Asner, G.P., Govender, N., Kennedy-Bowdoin, T., Knapp, D.E., and Jacobson, J. (2010), 'Effects of fire on woody vegetation structure in African savanna', *Ecological Applications*, **20**, pp. 1865–1875.

Sow, M., Hély, C., Mbow, C., and Sambou, B. (2013), 'Fuel and fire behavior analysis for early-season prescribed fire planning in Sudanian and Sahelian savannas', *Journal of Arid Environments*, **89**, pp. 84–93.

Stronach, N. (2009), *A review of the impact of fire on the carbon content, dynamics and biodiversity value of miombo woodlands*, Flora and Fauna International, Cambridge, U.K.

Tarimo, B., Dick, Ø.B., Gobakken, T., and Totland, Ø. (2015), 'Spatial distribution of temporal dynamics in anthropogenic fires in miombo savanna woodlands of Tanzania', *Carbon balance and management*, **10**, pp. 1–15.

Trapnell, C. (1959), 'Ecological results of woodland and burning experiments in Northern Rhodesia', *The Journal of Ecology*, **41**, pp. 129–168.

Tuohy, J.M. and Choinski, J.S. (1990), 'Comparative photosynthesis in developing leaves of *Brachystegia spiciformis* Benth', *Journal of Experimental Botany*, **41**, pp. 919–923.

Tuohy, J.M., Prior, J.A.B., and Stewart, G.R. (1991), 'Photosynthesis in relation to leaf nitrogen and phosphorus content in Zimbabwean trees', *Oecologia*, **88**, pp. 378–382.

van Griensven, A., Meixner, T., Grunwald, S., Bishop, T., Diluzio, M., and Srinivasan, R. (2006), ‘A global sensitivity analysis tool for the parameters of multi-variable catchment models’, *Journal of hydrology*, **324**, pp. 10–23.

van Wilgen, B.W., Govender, N., Biggs, H.C., Ntsala, D., and Funda, X.N. (2004), ‘Response of savanna fire regimes to changing fire-management policies in a large African national park’, *Conservation Biology*, **18**, pp. 1533–1540.

van Wilgen, B.W., Govender, N., and MacFadyen, S. (2008), ‘An assessment of the implementation and outcomes of recent changes to fire management in the Kruger National Park’, *Koedoe*, **50**, pp. 22–31.

VCS (2015), *Methodology for Avoided Forest Degradation through Fire Management.* VM0029, Verified Carbon Standard, url: `http://www.v-c-s.org/methodologies/avoiding-degradation-through-fire-management/`.

Waring, R.H., Landsberg, J.J., and Williams, M. (1998), ‘Net primary production of forests: a constant fraction of gross primary production?’, *Tree Physiology*, **18**, pp. 129–134.

Williams, M., Ryan, C.M., Rees, R.M., Sambane, E., Fernando, J., and Grace, J. (2008), ‘Carbon sequestration and biodiversity of re-growing miombo woodlands in Mozambique’, *Forest Ecology and management*, **254**, pp. 145–155.

Williams, R.J., Hutley, L.B., Cook, G.D., Russell-Smith, J., Edwards, A., and Chen, X. (2004), ‘Viewpoint: Assessing the carbon sequestration potential of mesic savannas in the Northern Territory, Australia: approaches, uncertainties and potential impacts of fire’, *Functional Plant Biology*, **31**, pp. 415–422.

Woollen, E.S. (2013), ‘Carbon dynamics of African miombo woodlands: from the leaf to the landscape’, PhD thesis, The University of Edinburgh.

4.9 Supplementary materials

4.9.1 GapFire model overview

GapFire is a process-based model of miombo woodland aboveground biomass (AGB), which simulates the growth, mortality and recruitment of individual tree stems. Woodlands are represented by individual 'patches' with an area roughly equivalent to the canopy of a large tree (0.02 ha). Model patches are treated as independent, with fire occurrence, stem top-kill and recruitment events occurring randomly in each patch. Each patch are initialised using stem densities and size distributions observed at the Kilwa PSPs, and the AGB of each management stratum established by varying mature tree density. Light is intercepted by the leaves of each stem at a rate relating to the height of leaves in the woodland canopy. Leaf area is calculated as a function of stem diameter, and varies through the year with observations of leaf phenology, restricting growth to the wet season when soil moisture is plentiful. Intercepted light is used to assimilate carbon (C) using a miombo-specific light response curve (Tuohy and Choinski, 1990; Tuohy et al., 1991; Woollen, 2013), and C allocated to respiration, leaf and fine-root formation, with remaining C allocated to increasing stem and large root biomass. As stems increase in biomass their morphology (DBH, leaf area, canopy structure) is altered according to a series of allometric models (Ryan, 2009; Ryan et al., 2011). Stems are exposed to a chance of top-kill from intrinsic sources or as a result of fire, where probability of stem top-kill is determined by stem size and fire intensity (Saito et al., 2014). Fire occurs probabilistically for each patch at a rate determined by observations, with intensity expressed as representative values of Byram's fireline intensity (Byram, 1959) for early and late dry season fires. Woodland patches regenerate through resprouting of top-killed rootstocks and the recruitment of new seedlings. As patches are small, and mortality and regeneration processes are

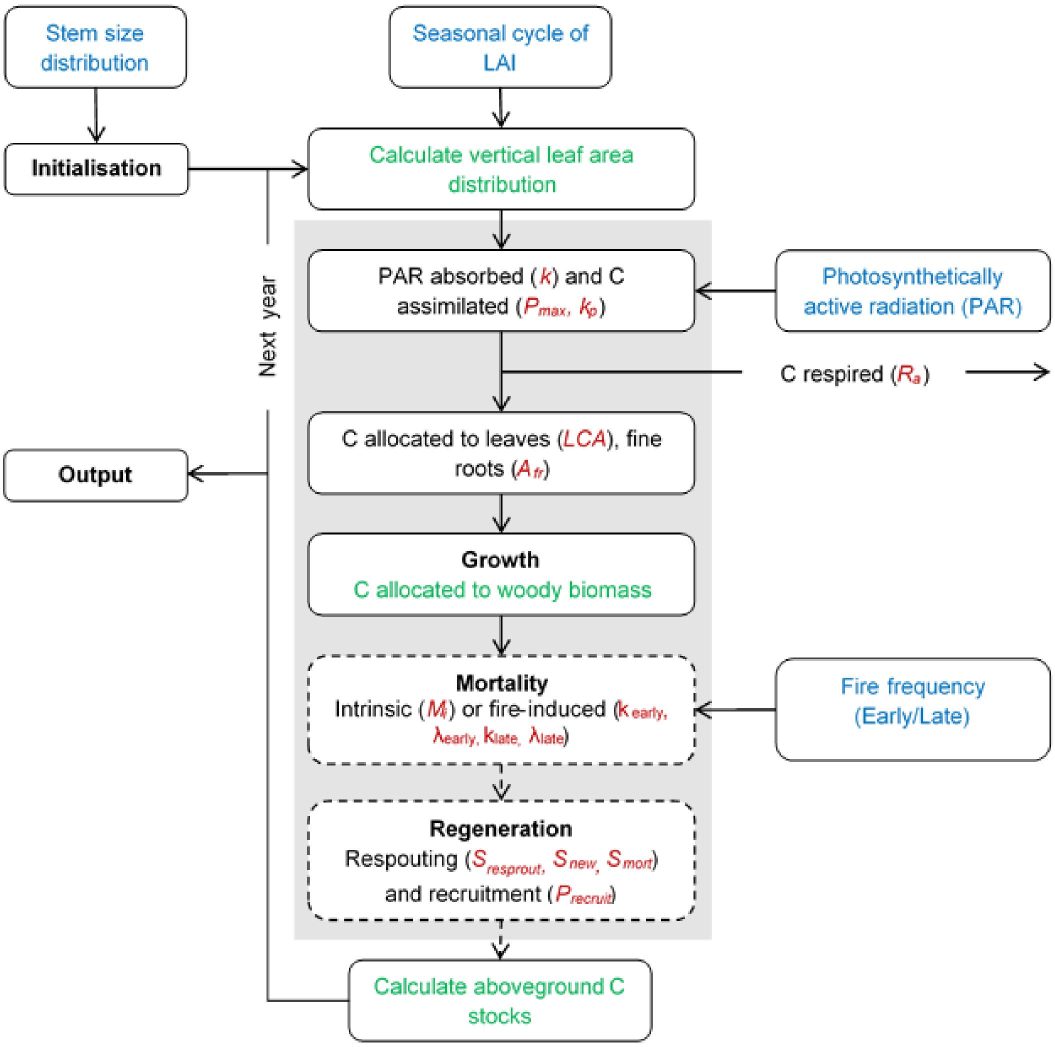

Figure S4.1: GapFire model schematic. Parameters are shown in red, allometric calculations are shown in green, and model driving data is shown in blue. Stochastic processes are indicated with a dashed line. Light and carbon assimilation functions run on hourly time steps, and the model produces annual output. As model patches are very small and mortality and regeneration processes are stochastic, the model runs as an ensemble of many patches.

stochastic, the AGB change in a single patch will not represent the trends of miombo woodland as a whole, therefore the model is therefore run as an ensemble of many patches (n = 10,000). The GapFire model is written in FORTRAN90, and operated with a Python wrapper. The model is summarised in schematic form in Fig. S4.1.

4.9.2 Initialisation

Extensive stem size data gathered from permanent sample plots (PSPs) in Kilwa are used to set up model patches with a representative stem size distribution (SSD). Of the 25 monitored PSPs, a subset of 17 were selected fitting the miombo woodland criteria (5 - 35 tC/ha, no closed canopy). These data comprised of a wide range of biomass measurements (5.2 - 33.9 tC/ha), covering 17 ha of data for stem sizes 5 - 40 cm DBH and 170 ha of stems > 40 cm DBH. The data were fitted with two exponential trend lines, with a break point at 15 cm DBH to optimally fit observations of stem sizes (Fig. S4.2). From these trends, two probability density functions were generated from which stem sizes may be randomly allocated to trees in model patches. A minimum stem size of 1 cm DBH was imposed to match the size that a seedling may reach following one year of growth. An upper limit of 100 cm DBH was set to avoid the generation of implausibly large stems. It is assumed that the relative frequencies of stem size classes are representative of miombo woodlands as a whole and that these do not vary greatly between regions.

AGB is strongly related to large stem density (D_{large}) (linear regression: $R^2 = 0.67$, $p < 0.001$); accordingly the model varies large stem density to attain a range of initial biomass levels. Large stems are comparatively rare and occur infrequently at patch-scale, therefore stems are allocated to patches based on a Poisson distribution. Limited evidence was found that small stem density (D_{small}) at the PSPs varies systematically to a large degree with AGB (linear regression: $R^2 = 0.26$, $p = 0.0564$).

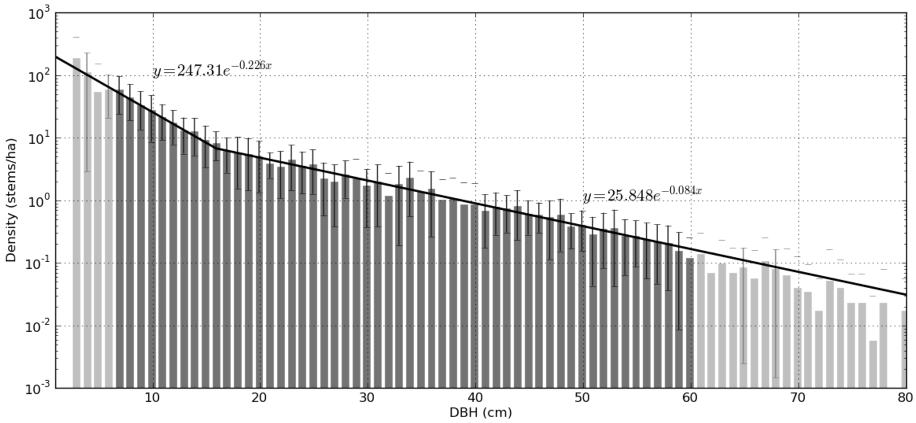

Figure S4.2: The Kilwa PSPs are used to calibrate stem size distribution curves with which the model is initialised. Two models are fitted for small (< 15 cm DBH) and large (> 15 cm DBH) stems, taking account of an apparent break point in the data.

D_{small} was therefore set to the mean density of small stems in the PSPs. This mechanism assumes that in the 5 - 35 tC/ha biomass range that AGB differences are predominantly a function of large stem density in miombo woodlands.

4.9.3 Growth

Growth in GapFire is regulated by the light environment of each stem, which is determined from the canopy structure as determined by allometric equations (Ryan et al., 2011). Stem growth is further moderated by phenology, respiration and maintenance costs of trees in each patch. Stem growth is largely determined by driving data from work on Gorongosa District of Mozambique, and is further constrained by chronosequence data describing biomass accumulation in miombo woodlands.

Canopy structure

At each patch, allometric equations are applied to relate stem DBH to tree-top and canopy base heights. Tree canopy depth (T_{depth}) is calculated as the difference of these two values, giving the vertical space amongst which each tree's leaves are distributed.

A further allometric equation relates basal area of each stem to its leaf area. The canopy of each patch is represented as 25 one metre deep layers, where layers are populated with the leaf area associated with each stem, assuming that leaves are uniformly distributed in the canopy layers over T_{depth}. The total leaf area of each layer (LA_{layer}) is summed to calculate leaf area index (LAI):

$$LAI = \sum_{layer=1}^{25} \frac{LA_{layer}}{gap\_area}$$

where gap_area = 0.02 ha (200 m^2), approximately the area covered by the canopy of a single mature tree.

Light environment

Light availability at each canopy layer is estimated using an application of the Beer-Lambert law (Jones, 2013). The Beer-Lambert law describes the attenuation of light through a tree canopy, where the top canopy layer exposed to all incoming Photosynthetically Active Respiration (PAR) and deeper layers are shaded by those above. PAR is absorbed according to the LA_{layer}, assuming a spherical leaf angle distribution (k = 0.5), that incoming radiation is diffuse, and that leaves have no transmittance or albedo. Hourly estimates of PAR from measurements in Gorongosa District are used to drive photosynthesis in the model (Ryan, 2009). Growth is restricted to the wet season by phenology inputs from monthly measurements of LAI in Gorongosa District, expressed as a fraction of peak LAI (LAI$_{frac}$). PAR absorbed by leaves at the top canopy layer over a year ($PAR_{maxlayer}$) is calculated from the total incoming PAR (PAR_{in}):

$$PAR_{maxlayer} = PAR_{in} \cdot (1 - e^{-\kappa \cdot LA_{layer} \cdot LAI_{frac}})$$

PAR transmitted through to lower layers (PAR_{thru}) is calculated by differencing PAR_{in}

and $PAR_{maxlayer}$:

$$PAR_{thru} = PAR_{in} - PAR_{maxlayer}$$

Light absorption at further layers (PAR_{layer}) is calculated down through the further 24 canopy layers:

$$PAR_{layer} = PAR_{thru} \cdot (1 - e^{-\kappa \cdot LA_{layer} \cdot LAI_{frac}})$$

$$PAR_{thru} = PAR_{layer+1} - PAR_{layer}$$

This produces a vertical profile of light absorption in each patch through each year, which drives the photosynthesis and growth of each stem.

Carbon assimilation

Growth is determined separately for each stem, with absorbed PAR converted to assimilated C using photosynthetic light response curves. Two parameters describe the light response curve: the maximum rate of assimilation (P_{max}) and the amount of light needed to achieve half this rate (k_p). For each stem, mass of photosynthate is summed for each canopy layer for each hour of the 12 diurnal cycles representative of each month, and scaled up to a yearly total. The gross primary production of each stem at each layer for each hour of daylight (GPP_i) is calculated as a proportion of maximum photosynthetic rate (P_{max}) and the total leaf area of each tree (LA_{tree}):

$$GPP_i = \left[P_{max} \cdot \frac{PAR_{layer}}{PAR_{layer} + k_p} \right] \cdot LA_{tree}$$

The sum of GPP_i over all layers over the entire year gives the total C fixation by each stem from photosynthesis (GPP). Net primary production of each stem (NPP) is calculated as GPP minus the fraction of C that is respired by the plant (R_a):

$$NPP = GPP \cdot (1 - R_a)$$

C required for the yearly replacement of leaves (C_{leaf}) is calculated as a function of leaf carbon per unit area (LCA) and the total tree leaf area (LA_{tree}):

$$C_{leaf} = LA_{tree} \cdot LCA$$

C$_{leaf}$ and C in fine roots (C_{fr}) are deducted from NPP, leaving C allocated to woody biomass (C_{wood}):

$$C_{wood} = NPP - C_{leaf} - C_{fr}$$

C allocation for each tree is partitioned to above and below ground pools in proportion shoot_frac, following an allometric relationship. Stem C allocation (C_{stem}) can therefore be calculated as:

$$C_{stem} = shoot\_frac \cdot C_{wood}$$

Stem growth is calculated as the annual increase in C_{stem}, which is related to an equivalent increase in DBH by an allometric model. This series of calculations accounting for growth are repeated for each stem, producing a yearly estimate of growth in each woodland gap.

4.9.4 Mortality

GapFire models stem mortality in response to fire occurrence and intrinsic (non-fire) sources. Because of the importance of resprouting in fire-prone ecosystems (Bond and Midgley, 2001; Chidumayo and Bakker, 2004; Mlambo and Mapaure, 2006), aboveground stem mortality (top-kill) was decoupled from belowground rootstock mortality. The mortality module accounts for stem top-kill, whereas rootstock mortality is calculated with plot regeneration. Fires are stratified into early burns and late burns, which occur with probability p(burn|early) and p(burn|late).

Fire-induced top-kill

Stems are top-killed each year by either intrinsic sources, such as senescence, herbivory, elephant damage and timber extraction, or as a result of fire. In a year that fire does not occur, intrinsic mortality probability (M_i) is set at a constant rate for all size classes. In the case of fire, stem top-kill rates are derived from field experiments in Mozambique, which showed stem top-kill to be a function of stem diameter and thermal anomaly (Ryan and Williams, 2011). As stem diameter increases, thickness of protective bark increases proportionally (Jackson et al., 1999; Miyanishi and Johnson, 2001), offering greater resilience as trees increase in size. In larger stems (>10 cm DBH), this effect saturates, and further increases in DBH provide no additional protection from fire. This relationship was modelled with a sigmoidal function, with saturation for larger stems:

$$\text{log odds of top-kill} = -a_x \cdot DBH + b_x \text{ where } DBH < 10cm$$

$$\text{log odds of top-kill} = b_{x_{sat}} \cdot DBH \text{ where } DBH > 10cm$$

Variables a_x, b_x, and $b_{x_{sat}}$ are determined from fireline intensity (FLI). A continuous relationship between FLI and mortality parameters is determined from measurements from the Nhambita fire experiments (Ryan and Williams, 2011). FLI is defined as the release of heat energy per unit time per unit length of fire front (kW/m) (Byram, 1959). It is widely utilised because it is relatively easy to measure, and it is known to be significantly correlated to biologically important fire impacts including tree top-kill and mortality (Alexander, 1982). Fireline intensity is calculated as:

$$FLI = H \cdot w \cdot R$$

where H = heat yield (kJ/kg), w = mass of available fuel (kg) and R = rate of spread of fire front (m/s). Its relationship to top-kill variables was determined by Saito et al. (2014) to be:

$$a_x = -7.025 \cdot ln(FLI) - 13.112$$

$$b_x = 2.119 \cdot ln(FLI) - 12.451$$

$$b_{x\_sat} = -123.5 \cdot FLI^{-0.498}$$

A minimum mortality rate is set to the value of M_i for all fire intensities. This results in a continuous relationship between fire intensity and top-kill (Fig. S4.3).

4.9.5 Regeneration

Top-killed stems above a minimum size class ($S_{resprout}$) when killed have a probability of resprouting (1 - S_{mort}), where S_{mort} is probability of rootstock mortality based on data from the Nhambita fire experiments. It is assumed that sprouts reach 2 cm DBH in their first year of growth. Additionally there is a chance of a recruitment event occurring ($P_{recruit}$), where a number of new seedlings (S_{new}) are established in a patch, reaching 1 cm DBH in their first year of growth. The initial growth of seedlings is assumed to be smaller than sprouts due to the established sprout rootstocks providing energy for increased growth.

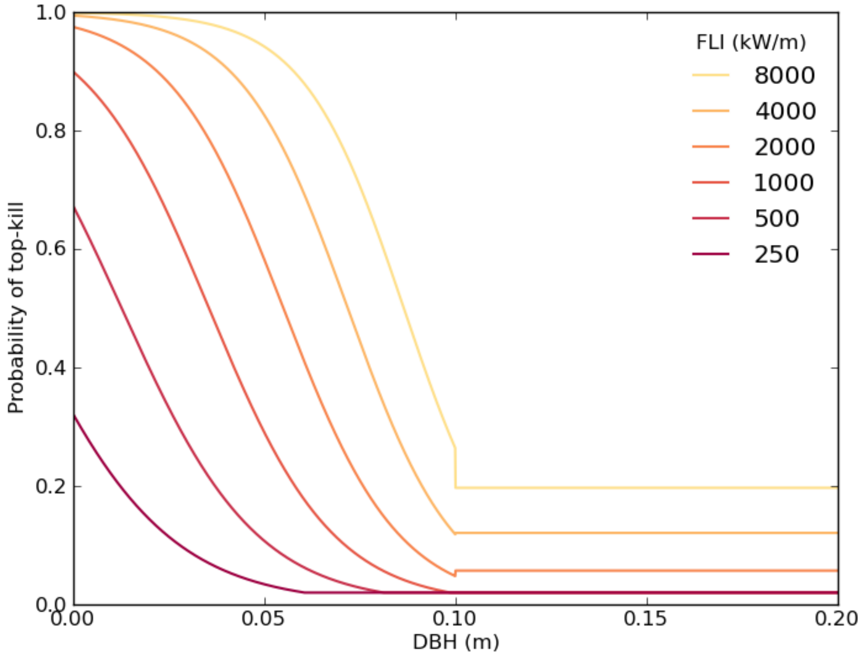

Figure S4.3: Top-kill in GapFire in a function of stem diameter at breast height (DBH) and fireline intensity. Data from Saito et al. (2014).

4.9.6 Output

Following the growth, mortality and regeneration at each patch at each year, C stocks are summed using the allometric relation between stem DBH and AGB. The model only includes stems of > 5 cm DBH when calculating biomass due to uncertainties in the dynamics of small stems and to match measurement protocols at the Kilwa PSPs. As each forest patch is very small and fire and regeneration occur stochastically, the biomass change in a single patch will not represent the trends of miombo woodland as a whole. The model is therefore run as an ensemble, where the biomass trend is taken to be the average biomass trend from a large number of patches (n = 10,000).

4.9.7 References

Alexander, M.E. (1982), ‘Calculating and interpreting forest fire intensities’, *Canadian Journal of Botany*, **60**, pp. 349–357.

Bond, W.J. and Midgley, J.J. (2001), ‘Ecology of sprouting in woody plants: the persistence niche’, *Trends in Ecology & Evolution*, **16**, pp. 45–51.

Byram, G.M. (1959), ‘Combustion of forest fuels’, *Forest fire: Control and use*, **1**, pp. 61–89.

Chidumayo, E.N. and Bakker, J.P. (2004), ‘Development of *Brachystegia-Julbernardia* woodland after clear-felling in central Zambia: Evidence for high resilience’, *Applied Vegetation Science*, **7**, pp. 237–242.

Jackson, J.F., Adams, D.C., and Jackson, U.B. (1999), ‘Allometry of constitutive defense: a model and a comparative test with tree bark and fire regime’, *The American Naturalist*, **153**, pp. 614–632.

Jones, H.G. (2013), *Plants and microclimate: a quantitative approach to environmental plant physiology*, Cambridge University Press.

Miyanishi, K. and Johnson, E.A. (2001), *Forest Fires: Behavior and Ecological Effects*, Academic Press.

Mlambo, D. and Mapaure, I. (2006), ‘Post-fire resprouting of Colophospermum mopane saplings in a southern African savanna’, *Journal of tropical ecology*, **22**, pp. 231–234.

Ryan, C.M. and Williams, M. (2011), ‘How does fire intensity and frequency affect miombo woodland tree populations and biomass?’, *Ecological Applications*, **21**, pp. 48–60.

Ryan, C.M., Williams, M., and Grace, J. (2011), ‘Above-and Belowground Carbon Stocks in a Miombo Woodland Landscape of Mozambique’, *Biotropica*, **43**, pp. 423–432.

Ryan, C.M. (2009), ‘Carbon cycling, fire and phenology in a tropical savanna woodland in Nhambita, Mozambique’, PhD thesis, The University of Edinburgh.

Saito, M., Luyssaert, S., Poulter, B., Williams, M., Ciais, P., Bellassen, V., Ryan, C.M., Yue, C., Cadule, P., and Peylin, P. (2014), ‘Fire regimes and variability in aboveground woody biomass in miombo woodland’, *Biogeosciences*, **119**, pp. 1014–1029.

Tuohy, J.M. and Choinski, J.S. (1990), ‘Comparative photosynthesis in developing leaves of *Brachystegia spiciformis* Benth’, *Journal of Experimental Botany*, **41**, pp. 919–923.

Tuohy, J.M., Prior, J.A.B., and Stewart, G.R. (1991), ‘Photosynthesis in relation to leaf nitrogen and phosphorus content in Zimbabwean trees’, *Oecologia*, **88**, pp. 378–382.

Woollen, E.S. (2013), ‘Carbon dynamics of African miombo woodlands: from the leaf to the landscape’, PhD thesis, The University of Edinburgh.

CHAPTER 5

Retrieval of a data-consistent carbon cycle for southern Africa

ABSTRACT

Background and aims: The terrestrial carbon (C) cycle is the least well understood element of the global C cycle, with poor constraint on the size of C pools, allocation patterns and residence times leading to large uncertainties in the global C budget. Understanding of the African C cycle is limited by perennial data constraints, which are particularly severe in the miombo woodlands of southern Africa. Whilst data from *in situ* ecological monitoring are rare, a long record of remote sensing observations exist over the continent which can be used to retrieve estimates of the miombo woodland C cycle.

Methods: We combine observational data with a diagnostic C cycle model under a model-data fusion framework. The result is a probabilistic assessment of state, flux and allocation variables of the C cycle across southern Africa for the period 2001 - 2010. We compare spatial variation in C cycle properties to observations of vegetation structure, precipitation, soil properties, disturbance, and anthropogenic management to identify the main environmental drivers of ecosystem function.

Results: Retrieved C cycle variables indicate globally important C pools and fluxes in southern Africa, with significant spatial variability. Model parameters imply southern Africa acts as a small source net source of C, though there remains a large uncertainty is associated with this prediction. Three dominant forms of ecosystem functional variation are identified, which relate to variation in woody cover, fire frequency, and rainfall properties.

Conclusions: Model-data fusion is a promising technique for constraint of the African C cycle. We note little correspondence between our estimates of C cycling and established maps of land cover, a concern where these are used for upscaling measurements of the terrestrial C cycle.

5.1 Introduction

The terrestrial biosphere is the most poorly understood component of the global carbon (C) cycle, contributing a large uncertainty to the global C budget and projections of future climate change. Accumulation of CO_2 in the atmosphere implies the presence of a net C sink in terrestrial ecosystems, which over the decade 2002 - 2011 captured 2.6 ± 0.8 PgC/yr from the atmosphere (Le Quéré et al., 2013). Although equivalent to around 30 % of annual global fossil fuel CO_2 emissions, we know little about the nature of the land surface sink, and for how long it might keep pace with anthropogenic CO_2 emissions (Luyssaert et al., 2008; Pan et al., 2011). Terrestrial ecosystems also act as a large source of inter-annual variability in atmospheric CO_2 growth, fluctuating between a large sink of 4.1 PgC/yr and a small source of 0.4 PgC/yr (Le Quéré et al., 2013). This accounts for the majority of the inter-annual variation in atmospheric CO_2 growth, yet we are currently unable to adequately account for this variability in models of the global C cycle.

The need for robust quantification of the terrestrial C cycle is epitomised by the African continent. The African C cycle is unusual in by being dominated by emissions from the terrestrial biosphere, which dwarf the *ca.* 0.3 PgC/yr from fossil fuel emissions (Boden et al., 2011). Africa is thought to be source of around 15 % of net C flux from global land use change (Houghton and Hackler, 2006), and has been reported to contribute up to half of inter-annual variation in the global C balance (Williams et al., 2007). Uncertainties in the African C cycle are particularly large in savannahs, an ecosystem constituting around 50 % of the land surface (Menaut, 1983) and source of 90 % of burned area (Giglio et al., 2013). Despite the importance of Africa's savannahs to the global C budget, we have little knowledge of how patterns of C exchange vary spatially (Williams et al., 2007; Valentini et al., 2014), which are the key environmental controls on vegetation dynamics (e.g. disturbance, precipitation, soil properties), and we do not know whether Africa's savannahs are a net source or sink of C (Bombelli et al., 2009; Ciais et al., 2009; Ciais et al., 2011; Valentini et al., 2014).

Resolving the terrestrial C cycle is difficult; reliable observations are scarce, and our understanding of key processes is limited. Particular uncertainty derives from unknowns in the sizes of ecosystem C pools (Houghton et al., 2009; Todd-Brown et al., 2013) and their turnover rates (Friend et al., 2014), and the nature of spatial and temporal variation in C cycle dynamics (Williams et al., 2007; Ciais et al., 2011). Although field studies in African savannahs are very limited, we have increasingly ready access to long records of satellite observations. One promising approach to utilising this information is in model-data fusion (MDF) techniques, where observational data are combined with vegetation models to constrain the C cycle (e.g. Keenan et al., 2012; Ziehn et al., 2012; Smith et al., 2013; Bloom et al., 2016). The aim of MDF is to generate estimates of C cycle parameters that are consistent with available data constraints, and to generate robust estimates of parametric uncertainty. By using simple models of the C cycle, MDF techniques are well adjusted to handling multiple streams of input data to disaggregate the C cycle into its constituent pools, fluxes, and residence times. Spatially-explicit estimates of C cycle attributes also offer a novel opportunity to explore spatial variation in vegetation traits, where differences in C cycle dynamics can be used to characterise ecosystem functional properties.

In this study we investigate the C cycle of Africa's largest savannah formation; the miombo woodlands of sub-equatorial Africa (White, 1983). We merge data on leaf phenology, woody biomass, soil C, and fire emissions with a mass-balance model of the terrestrial C cycle to retrieve estimates of C cycle state and process variables. We explore variation in ecosystem functional properties across southern Africa, and aim to identify the main environmental drivers of C cycle spatial variability.

We address the following research questions:

1. What is the magnitude of carbon fluxes, pools and residence times in the miombo ecoregion?
2. Is the miombo ecoregion a net source or sink of carbon?
3. How do ecosystem functional properties vary across the miombo woodland ecoregion, and what are its main environmental drivers?

5.2 Methods

5.2.1 Study region

This study is centred on the miombo woodland ecoregion of southern Africa (Olson et al., 2001), bounded by 0°00' - 27°00' S, 11°00' - 41°00' E. As the geographical extent of miombo woodlands is poorly delineated, we define a study region that encompasses an area containing all countries with large-scale miombo woodland cover; namely Angola, Malawi, Mozambique, Tanzania, Zambia, and Zimbabwe, as well as Katanga Province at the southern extent of DR Congo. This region totals 4.57 million km^2 of land area. Though dominated by savannah woodlands, the study region also includes smaller expanses of forest, desert, thicket and grassland (see Fig. 1.5). Diversity of vegetation structure is accompanied by substantial variation in precipitation, soil properties, disturbance frequency, and intensity of human management (Fig. S5.1).

5.2.2 The 'CARbon DAta MOdel fraMework'

We use the CARbon DAta MOdel fraMework (CARDAMOM) to retrieve estimates of C cycle state, flux, and allocation variables for miombo woodlands (Bloom et al., 2016). CARDAMOM is an MDF system that is used to merge observations of leaf area, woody biomass, and soil C with a diagnostic model of the terrestrial C

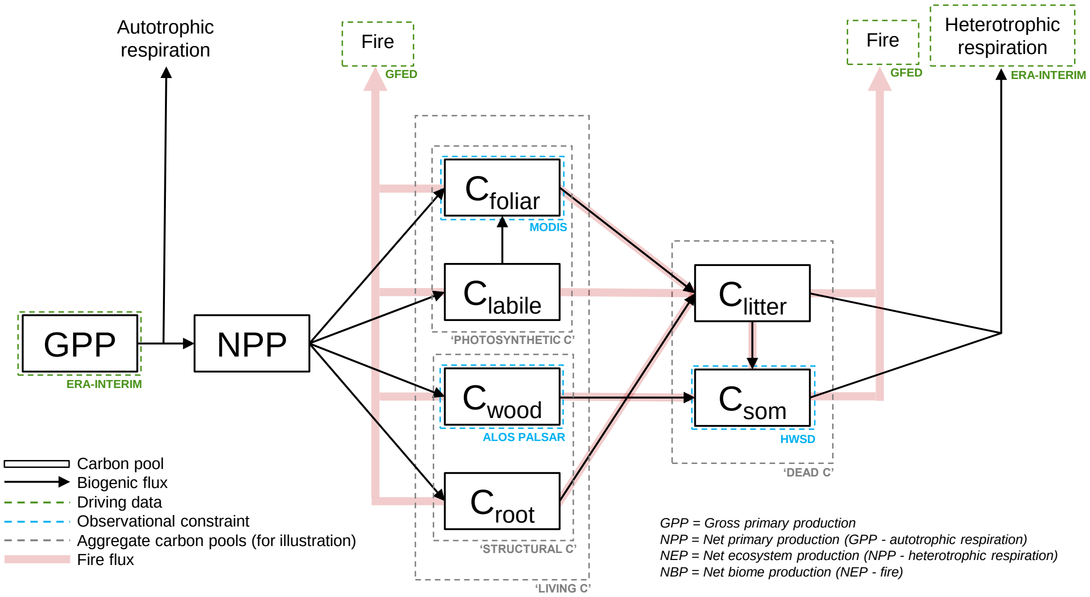

Figure 5.1: DALEC model schematic, showing C pools, fluxes, and the observational constraints on C cycle dynamics. Model parameters are described in Table 5.1.

cycle, the Data Assimilation Linked Ecosystem Carbon model (DALEC) (Bloom and Williams, 2015). CARDAMOM operates using a Metropolis-Hastings Markov chain Monte Carlo (MHMCMC) algorithm, a Bayesian method to generate parameter sets that minimise the mismatch between model predictions and C cycle observations. The output is a probabilistic assessment of each DALEC model parameter with specified uncertainty ranges. The operation of CARDAMOM is described in detail in Bloom et al. (2016).

DALEC (version 2.0) is an ecosystem C balance model that simulates C pools in vegetation and soils, and the fluxes connecting them (Fig. 5.1). DALEC is notable for its simplicity, lending it to studies assimilating large volumes of remote sensing data and producing robust estimates of uncertainty. Unlike conventional models of the terrestrial C cycle, DALEC does not specify plant functional types based on pre-assigned land cover maps, and makes no assumptions of steady state. The DALEC model is described in detail in Bloom and Williams (2015) with sensitivity analysis in

Table 5.1: DALEC model parameter description, and prior ranges based on ecologically viable limits (see Bloom et al. (2016)).

Parameter	Description	Prior range	Units
Allocation of primary production			
R_a	Fraction of GPP to autotrophic respiration	0.3 - 0.7	
A_{fol}	Fraction of NPP allocated to C_{fol}	0.01 - 0.5	
A_{lab}	Fraction of NPP allocated to C_{lab}	0.01 - 0.5	
A_{wood} *	Fraction of NPP allocated to C_{wood}	0.01 - 0.5	
A_{root}	Fraction of NPP allocated to C_{root}	0.01 - 0.5	
Carbon pools†			
C_{fol}	Foliar C pool	0.2 - 20	tC/ha
C_{lab}	Labile C pool	0.2 - 20	tC/ha
C_{wood}	Woody (above and belowground) C pool	1 - 1000	tC/ha
C_{root}	Fine root C pool	0.2 - 20	tC/ha
C_{lit}	Litter C pool	0.2 - 20	tC/ha
C_{som}	Soil organic matter C pool	1 - 2000	tC/ha
Canopy properties			
D_{onset}	Leaf onset day	1 - 365	day
D_{fall}	Leaf fall day	1 - 365	day
c_{ronset}	Labile C release period	10 - 100	days
c_{rfall}	Leaf fall period	20 - 150	days
c_{eff}	Canopy efficiency parameter	1 - 100	
c_{lma}	Leaf mass per unit area	10 - 400	gC/m^2
c_{lf}	Annual leaf loss fraction	0.125 - 1	
Turnover rates‡			
T_{wood}	Turnover of C_{wood}	2.5×10^{-5} - 2.5×10^{-3}	/day
T_{root}	Turnover of C_{root}	10^{-4} - 10^{-2}	/day
T_{lit}	Turnover of C_{lit}	10^{-4} - 10^{-2}	/day
T_{som}	Turnover of C_{som}	10^{-7} - 10^{-3}	/day
T_{min}	C_{lit} mineralisation rate	10^{-5} - 10^{-2}	/day
Θ	Temperature dependence exponent factor	0.018 - 0.08	

* $A_{wood} = 1 - A_{fol} - A_{lab} - A_{root}$

† *at year t*

‡ *Residence time = 1 / turnover rate*

Bloom et al. (2016); what follows is a brief overview of the model.

DALEC simulates six terrestrial C pools (C_{fol}, C_{lab}, C_{wood}, C_{root}, C_{lit}, C_{som}), allocation fractions of gross primary production (R_a, A_{fol}, A_{lab}, A_{wood}, A_{root}), canopy properties (D_{onset}, D_{fall}, c_{ronset}, c_{rfall}, c_{eff}, c_{lma}, c_{lf}), and residence times of C (T_{wood}, T_{root}, T_{lit}, T_{som}, T_{min}, Θ), detailed in Table 5.1. Gross primary production (GPP) is estimated using the Aggregated Canopy Model (ACM), an empirical simplification of the Soil-Plant-Atmosphere (SPA) model (Williams et al., 1997). ACM estimates GPP for each day of each year from inputs of atmospheric CO_2, minimum and maximum temperature, incoming radiation, and DALEC parameter values C_{fol}, c_{lma}, and c_{eff}. GPP is returned to the atmosphere by autotrophic respiration, leaving net primary production (NPP) which is allocated to living C pools in foliar, labile, wood and root biomass. Living biomass pools turnover C to dead biomass pools in litter and soil, which are subject to heterotrophic respiration based on temperature-dependent losses to the atmosphere. Fires are incorporated into the model as monthly removals from live and dead C pools, and fluxes from live to dead biomass. Emissions of C to the atmosphere are based on the proportion of area burned and an emissions factor for each C pool (based on van der Werf et al., 2010), and fluxes from living C pools to litter and soil based on a fixed 50 % resilience factor of non-combusted biomass.

DALEC C pools and fluxes were modelled on a monthly time-step over the decade 2001 - 2010. The study region is represented by 6279 0.25° grid cells, where model parameters in each grid cell are treated as unknown values limited to ecologically viable ranges (Table 5.1). We use CARDAMOM to sample 1500 parameter sets split across 3 converged MHMCMC simulations. The result is a probability density function for each model parameter in each grid cell. Grid cells are treated as independent, a simplification that is necessary for computational tractability.

5.2.3 Model constraints and driving data

Observational constraints are provided by datasets describing canopy phenology, woody biomass and soil C. Canopy phenology was characterised with a monthly time series of leaf area index (LAI) from the Moderate Resolution Imaging Spectrometer (MODIS), data product MOD15A2. Data were aggregated to 0.25° resolution, and a conservative uncertainty factor of 2 assumed. Soil C data were collated from the Harmonized World Soil Database (HWSD) (Fischer et al., 2008), an empirically-derived global dataset that describes soil organic matter content at 0 - 100 cm depth. HWSD data are prescribed an uncertainty factor of 1.5, which is increased in the locations where woody biomass is very low (see Bloom et al., 2016). We also use a novel woody biomass dataset derived from a mosaic l-band radar backscatter data from ALOS PALSAR for each year over the period 2007 - 2010 (McNicol and Ryan, *in prep*). The map was calibrated using estimates of aboveground biomass (AGB) from plot inventory data from across southern Africa. AGB was converted to total woody biomass using a fixed root:shoot ratio (Ryan et al., 2011), and downsampled from 25 m to 0.25° resolution using the mean biomass within each grid cell. In the absence of a fully quantified uncertainty estimate, a confidence interval of ± 50 % was applied to the data.

Given presently available observational data, DALEC represents an underdetermined system where there are more unknowns than there is prior information to constrain the C cycle. Ecosystem C cycling can be further constrained through the use of ecological and dynamical constraints (EDCs); a range of conditions enforcing sensible parameter inter-relations and change trajectories (Bloom and Williams, 2015). Imposition of EDCs aims to limit the generation of nonsensical parameter sets that can match observations whilst violating prior ecological knowledge (Fox et al., 2009). For example, EDCs enforce turnover rates that are consistent with knowledge of relative residence times in each pool, and parameter sets must not result in an exponential accumulation or collapse in C pools on inter-annual timescales. This method reduces uncertainty by limiting the possible configurations DALEC can take, and ensures that generated parameter sets are a realistic representation of reality. Where EDC conditions are not met by a parameter set generated by the MHMCMC algorithm, these parameters are rejected as ecologically inconsistent, and a new parameter set generated. We employ the set of EDCs detailed in Bloom and Williams (2015).

Climate driving data were collated from the European Centre for Medium-Range Weather Forecasts (ECMWF) Reanalysis interim (ERA-interim) dataset (Dee et al., 2011). Estimates of monthly burned area and fire emissions were taken from the Global Fire Emissions Database (GFED, version 4) (van der Werf et al., 2010; Giglio et al., 2013).

5.2.4 Statistical Analysis

C fluxes and residence times are presented as median parameter values weighted by land area, with a 50 % confidence interval representing parameter uncertainty. For illustrative purposes we refer to C allocation to aggregate ‘photosynthetic’ (C_{fol} + C_{lab}) vs. ‘structural’ (C_{wood} + C_{root}) C pools, and ‘living’ (C_{fol} + C_{lab} + C_{wood} + C_{root}) vs. ‘dead’ (C_{lit} + C_{som}) C pools. Ecosystem fluxes are calculated for each year 2001 - 2010, and summed to generate estimates of net ecosystem production (NEP) and net biome production (NBP). Principal component analysis (PCA) is used to identify trade-offs in ecosystem functional properties, and indicate how these vary in space. Ecosystem functional properties are defined as the median DALEC parameters for GPP, allocation patterns, turnover rates, and canopy properties, in each grid cell.

The first three principal components of ecosystem functional variation were

Table 5.2: Candidate environmental drivers of ecosystem function. Maps of spatial variation are displayed in Fig. S5.1.

Driver of variation	Description	Units	Source(s)
Precipitation			
Rainfall total	Mean annual precipitation (2001 - 2010) from the tropical rainfall monitoring mission (TRMM). MAP separates 'climatically determined' from 'disturbance-maintained' savannahs.	mm/year	Sankaran et al. (2005), Huffman et al. (2007), and Staver et al. (2011)
Rainfall seasonality	An index based on monthly precipitation vectors from TRMM, where a value of 0 represents evenly spread rainfall, and a value of 100 that all precipitation falls in a single month.	0 – 100	Markham (1970) and Lehmann et al. (2011)
Rainfall period	Midpoint of rainfall distribution, calculated as the angle of rainfall seasonality vector. This measure estimates of the timing of peak rainfall.	day of year	Markham (1970)
Soil properties			
Soil fertility	Total exchangeable bases estimates from the harmonised world soil database (HWSD) are representative of savannah soil fertility. Measurements are taken to 1 m depth, expressed on an aerial basis using soil bulk density.	mol/m^2	Nix (1983), Fischer et al. (2008), and Lehmann et al. (2011)
Soil pH	From HWSD to 1 m depth. Soil pH is a strong correlate of tree species composition in miombo woodland landscapes.		Fischer et al. (2008) and Chapter 2
Soil texture	From HWSD to 1 m depth, represented as proportion of sand. Soil texture is a predictor of vegetation structure in miombo woodland landscapes.	%	Fischer et al. (2008) and Woollen et al. (2012)
Disturbance			
Burn fraction	Mean annual burn fraction of each pixel from MODIS burned area product. Fires are have a large impact on miombo woodland structure.	%/yr	Ryan and Williams (2011) and Chapter 4
Topographic roughness	Mean of standard deviation of SRTM elevation within 10 x 10 (∼1 km) cells. Topographic roughness is related to the ease of fire spread into an area.	m	Jarvis et al. (2008) and Archibald et al. (2009b)
Vegetation properties			
Tree cover	Mean tree cover in each grid cell (2010). Tree cover is associated with species community make up, flammability, and woody productivity.	%	Staver et al. (2011), DiMiceli et al. (2011), and Chapters 2 and 3
Anthropogenic impacts			
Population density	Population density for the year 2000	people/km^2	CIESIN (2005)
Cropland	Proportion of grid cell subject to cultivation, estimated for 2005.	%	Fritz et al. (2015)

compared to a range of environmental and ecological properties thought to be associated with miombo woodland heterogeneity with the aim of identifying those factors driving vegetation heterogeneity over continental scales. Candidate drivers representing vegetation structure (tree cover), disturbance (fire frequency, topographic roughness), precipitation (rainfall total, rainfall seasonality, rainfall timing), soil properties (soil texture, total exchangeable bases, pH), and anthropogenic impact (population density, cropland area) were assembled and aggregated to 0.25° resolution (Table 5.2 and Fig. S5.1). Candidate variables are based largely on the studies of Archibald et al. (2009b), Lehmann et al. (2011), and Staver et al. (2011), as well as measurements of ecological properties in Kilwa District of Tanzania (see Chapter 2). The relative importance of each predictor of ecosystem function was assessed using random forest regression trees (Breiman, 2001), a supervised learning method that is robust to non-linearity, interactions and outliers. We use 70 % of grid cells to train the Random Forest algorithm to predict each of the first three principal components, retaining 30 % to assess model fit (R^2).

Data analyses were performed in Python, making use of the scikit-learn module (Pedregosa et al., 2011).

5.3 Results

5.3.1 Retrieval of the carbon cycle

CARDAMOM estimates of GPP across southern Africa average 13.5 tC/ha/yr (with a 12.2 - 14.8 tC/ha/yr area-weighted 50 % confidence range) over the period 2001 - 2010. Approximately half of GPP is respired, resulting in an NPP of 6.4 (5.5 - 7.3) tC/ha/yr. Carbon use efficiency (NPP / GPP) averages 47.9 (42.3 - 53.3) % and varies widely across the continent, being notably elevated in regions where C emissions from fire are high (Fig. 5.2a). NPP is allocated in lesser proportion to photosynthetic C pools than to structural C pools, with allocation to photosynthetic C pools averaging 39.2 (29.9 - 50.0) % of total NPP. High C allocations to photosynthetic C are particularly apparent in areas of low woody biomass, and where fires are infrequent (Fig. 5.2b).

Residence times in photosynthetic C are shorter than in structural C, averaging 0.75 (0.58 - 0.94) years in C_{fol}, 0.44 (0.40 - 0.52) years in C_{lab}, 5.40 (4.05 - 7.62) years in C_{wood}, and 2.21 (1.24 - 3.39) years in C_{root}. Like NPP and its allocation, relative C residence times between photosynthetic and structural C are widely variable across study region (Fig. 5.2c). C allocation and residence times result in mean C pool sizes of 2.1 (1.5 - 3.7) tC/ha in C_{fol}, 0.3 (0.2 - 0.5) tC/ha in C_{lab}, 13.7 (9.9 - 17.6) tC/ha in C_{wood}, and 2.6 (1.4 - 4.6) tC/ha in C_{root}. Photosynthetic C pools are much smaller in size than structural C pools, and show similar patterns of spatial variability to C allocation fractions (Fig. 5.2d). The impact of observational constraints on leaf area and woody biomass can be seen in parameter estimates for C_{fol} and C_{wood}, which have lower proportional uncertainty than other C pools.

The total size of the living C pool averages 19.3 (16.1 - 22.6) tC/ha, a value considerably smaller than the dead C pool average of 86.7 (64.6 - 116.8) tC/ha. The dead C pool is dominated by a C_{som}, which averages 84.6 (63.9 - 111.9) tC/ha and dominates terrestrial C stocks in the study region. Storage in live : dead C pools varies widely across southern Africa, with proportionally high storage in living C pools coinciding with areas of high woody biomass and LAI (Fig. 5.2e). Turnover of C_{lit} is rapid, with a mean residence time of 0.75 (0.32 - 1.52) years, and turnover in C_{som} is slower, with a mean residence time of 30.1 (17.1 - 53.2) years. Residence times in living C : dead C show similar spatial patterns to the fraction of total biomass stored in these pools (Fig. 5.2f). Uncertainties in estimates of dead C pool turnover are notably higher than for living C pools, highlighting the lack of observational or mechanistic constraint on heterotrophic respiration. Total ecosystem respiration averages 12.8

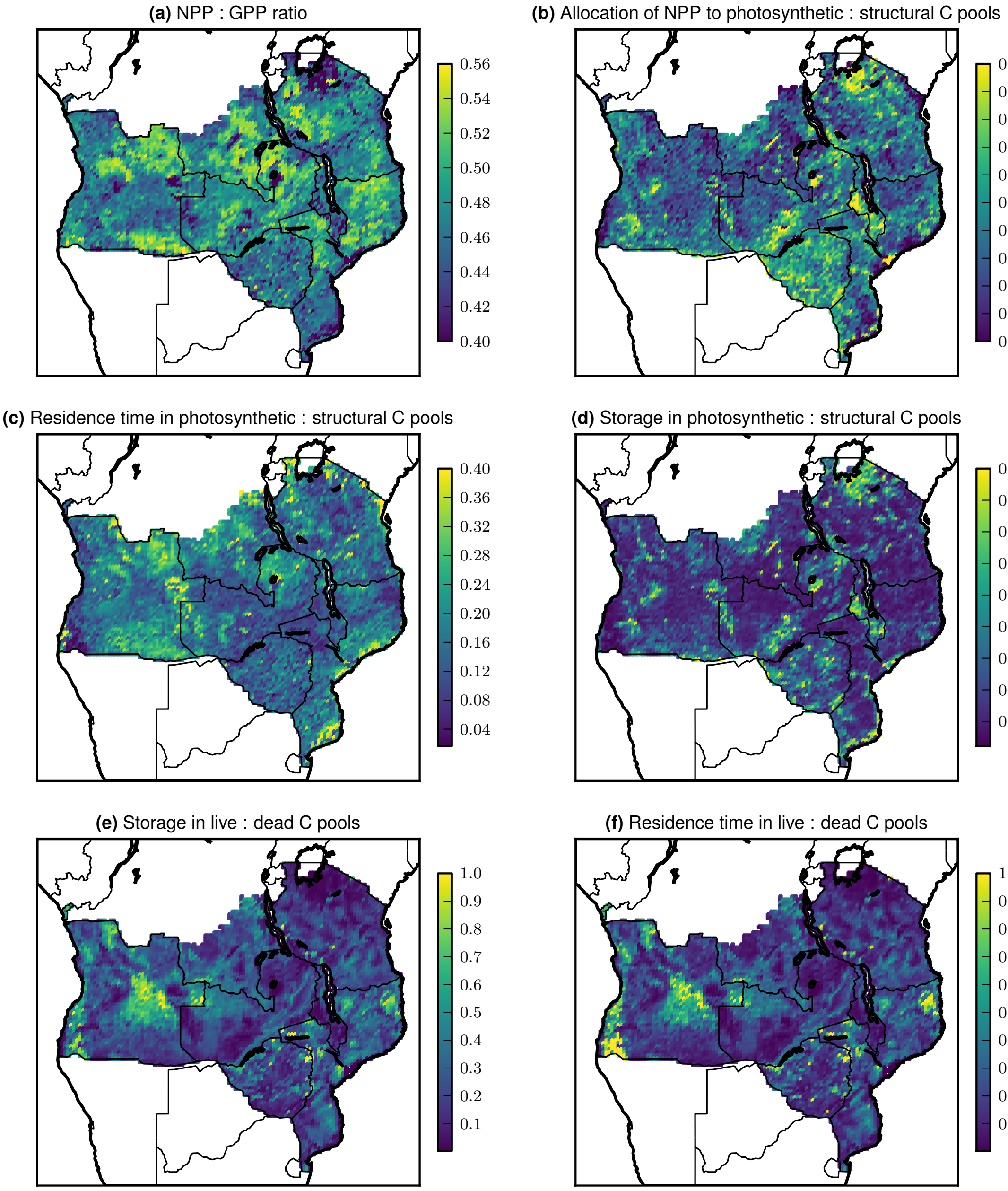

Figure 5.2: Patterns of variation in the southern African C cycle based on median CARDAMOM parameter values. Descriptive outputs show spatial variation in primary production, it's allocation to photosynthetic (foliar & labile) and structural (wood & roots) C pools, C residence times in living and dead C, and the mean size of C pools over the period 2001 - 2010.

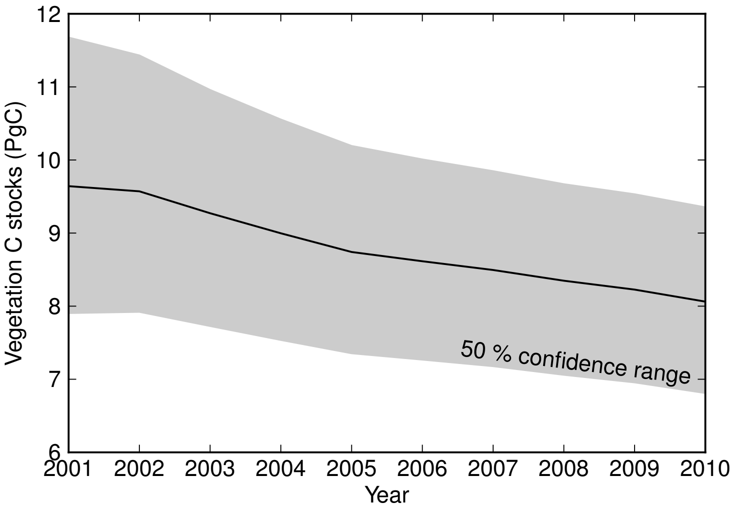

Figure 5.3: Predicted vegetation C change over 2001 - 2010 in southern Africa.

(11.2 - 14.6) tC/ha/yr, and emissions from fire an order of magnitude smaller at 1.1 (0.9 - 1.4) tC/ha/yr.

5.3.2 Net carbon fluxes

CARDAMOM reports total C storage in the study region in 2001 was 50.3 PgC (with a 40.7 - 63.1 PgC 50 % confidence range), which by 2010 was reduced to 48.0 (37.7 - 61.3) PgC. The largest source of C originates from the comparatively small vegetation C pool, which is reported as reducing from 9.6 (7.9 - 11.7) PgC to 8.1 (6.8 - 9.4) PgC (Fig. 5.3). NEP averages 0.36 (-0.17 - 1.18) PgC/yr, with the highest values of NEP aligning with areas where fires are frequent (Fig. 5.4a). Mean NBP is predicted to be -0.17 (-0.68 - 0.62) PgC/yr, implying a slightly greater probability of southern Africa acting as a net C source than a C sink. C flux to the atmosphere varies spatially, with the largest C sources likely located in Angola, DR Congo, Mozambique and Tanzania (Fig. 5.4b). Vegetation in the northern reaches of the miombo ecoregion may be acting as a sink of C (or a relatively small source), with C accumulation apparent in parts of Angola, DR Congo and Tanzania.

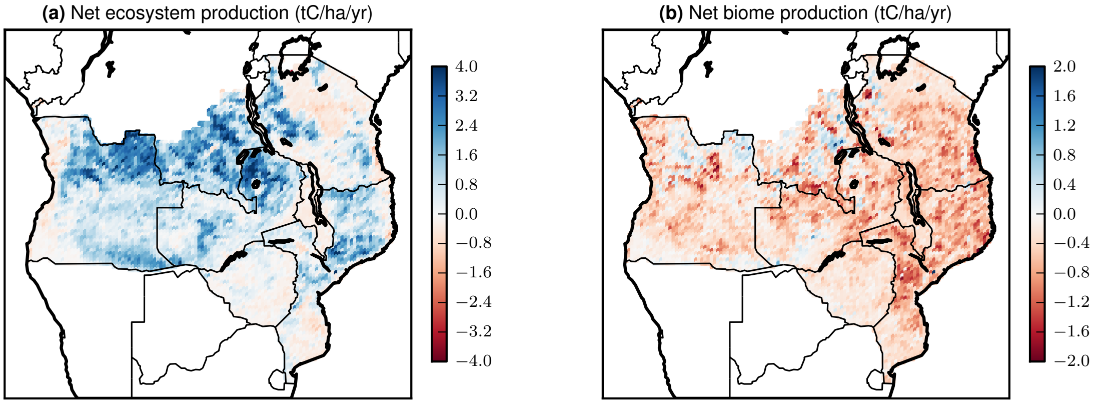

Figure 5.4: Predicted net C fluxes over the period 2001 - 2010 in southern Africa, based on median parameter values from CARDAMOM. **(a)** Net ecosystem production is elevated in regions where fires are frequent. **(b)** Net biome production suggests southern Africa acts as a small net source of C across much of southern Africa, with some parts in the north acting as a net C sink.

5.3.3 Variation in ecosystem properties

PCA of retrieved DALEC process variables finds three dominant axes of variation that account for 56.1 % of variation in ecosystem functional properties (Fig. 5.5). A high score in the first principal component (PC1: 28.6 % of variance) is associated with high productivity (GPP), low respiratory fraction (R_a), large allocations of C to wood (A_{wood}) and small allocations to leaves and roots (A_{fol}, A_{root}), and slow turnover of soil organic matter (T_{som}). Positive scores in PC1 are also associated with high canopy efficiency (c_{eff}), and slow rates of canopy flush (c_{ronset}) and senescence (c_{rfall}). Together these parameters describe the 'woodiness' of an ecosystem, where tree-dominated areas are more productive, allocate more resources to woody C, and have long canopy phenological cycles. High values in PC1 are spread widely across the study region, with low scores in PC1 predominating in northern Tanzania, Malawi, Zimbabwe, southern Mozambique, and parts of central Angola (Fig. 5.6a).

Positive scores in the second principal component (PC2: 17.6 % of variance) indicate tough (c_{lma}), long-lived (c_{lf}) foliar properties, rapid turnover of wood and

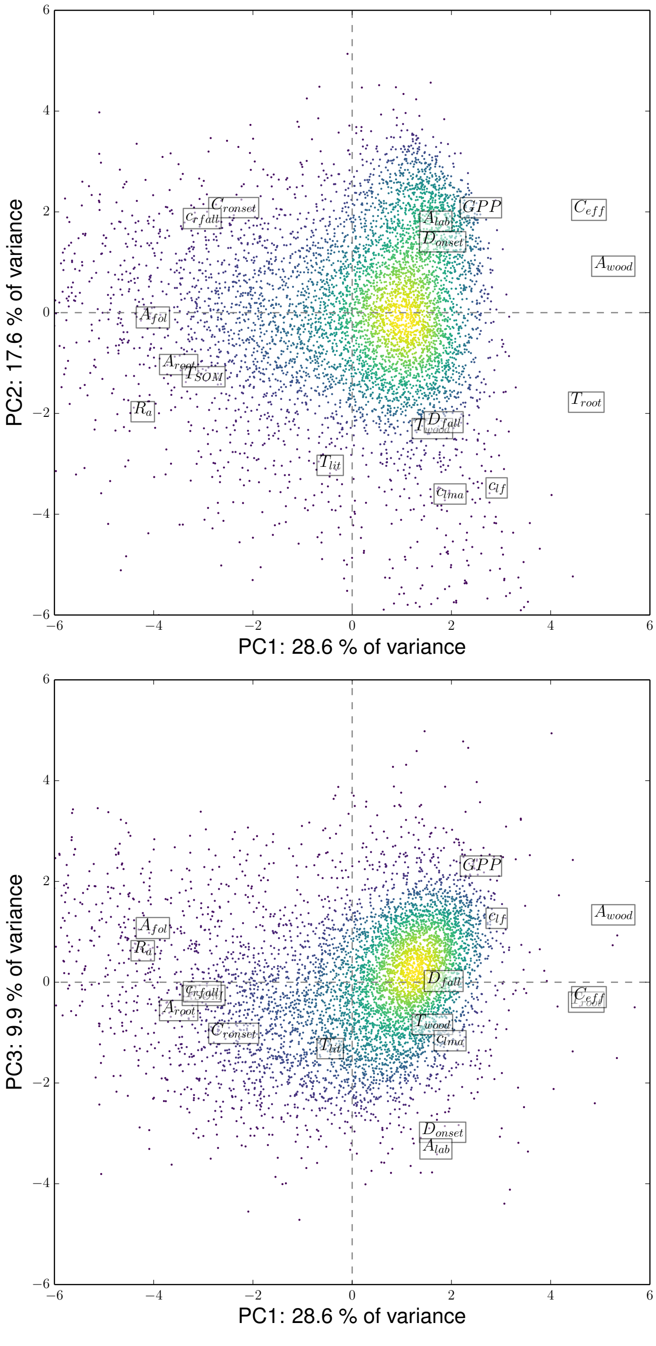

Figure 5.5: Principal component analysis biplots of DALEC process variables, showing median retrieved ecosystem functional properties in the first three principal components (1 point per grid cell, coloured to indicate point density). Colours are assigned as a function of displayed principal components, matching those in Fig. 5.6. Parameter symbol definitions are described in Table 5.1.

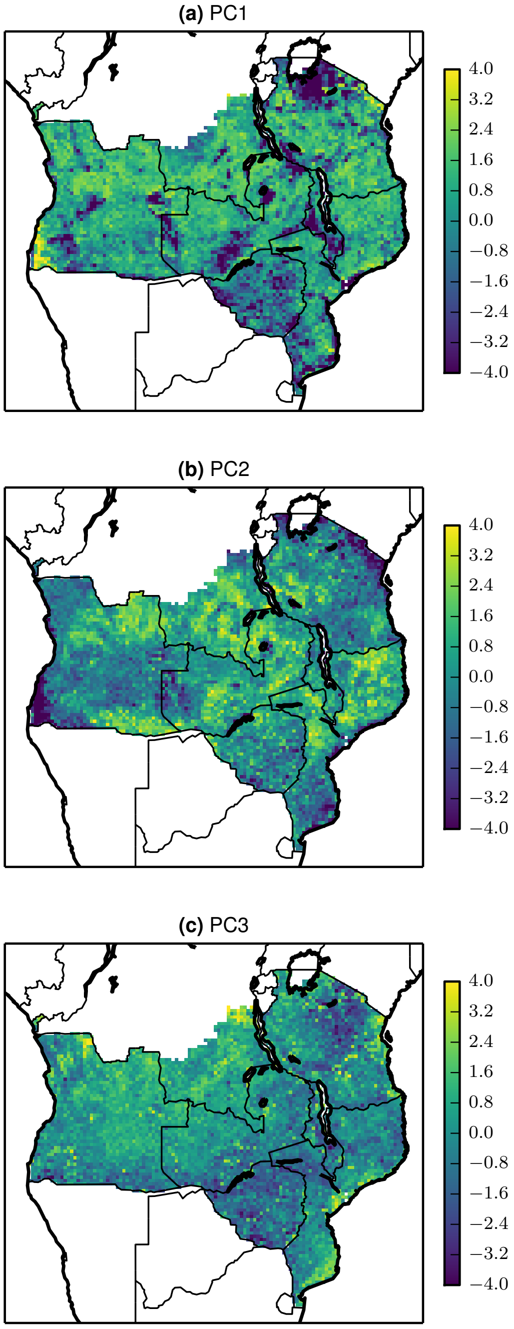

Figure 5.6: Maps of spatial distribution of principal components 1, 2 and 3 of DALEC ecosystem functional properties. See Fig. 5.5 for ecological interpretation. See also individual parameter maps in Fig. S5.2.

litter C pools (T_{wood}, T_{lit}), and late canopy fall (D_{fall}). High values of PC2 are found at the extremities of the study region, and are particularly apparent in southwestern Angola, northern Tanzania, and coastal Mozambique (Fig. 5.6b). Low values of PC2 dominate the northern half of the study area, as well as northern and central Mozambique and southern Angola.

High scores in the third principal component (PC3: 9.9 % of variance) are related to late canopy onset (D_{onset}), a large allocation of C to the labile pool (A_{lab}), and lower productivity (GPP). These together describe canopy phenological properties, ranging from early onset of leaves in a relatively productive environment to late leaf onset with large allocations to labile C. PC3 broadly bisects the study region, showing low values to the north and west and high values to the south and east (Fig. 5.6c). Low scores in PC3 are also apparent in parts of coastal Tanzania and Mozambique.

5.3.4 Environmental drivers of ecosystem function

Correlation between ecosystem functional properties and environmental variation was observed in model outputs (Fig. 5.7). PC1 was associated with tree canopy cover, where productive ecosystems with a large allocation fraction to woody C pools are associated with high tree cover. Population density and rainfall properties also appear related to PC1, though their relative importance is low. PC2, correlated with tough leaves and late leaf fall, was predicted by annual burn fraction, and to a lesser extent rainfall characteristics. Areas of frequent fires were predicted to have low values in PC2, whilst the highest values of PC2 were associated with reduced and more seasonal rainfall. PC3, describing canopy phenological properties, was best predicted by total rainfall, rainfall timing, and tree cover. In particular we note the greater total rainfall and earlier onset of rains where values of PC3 are low. There was little evidence for topographic complexity, cropland distributions, or soil properties being of importance

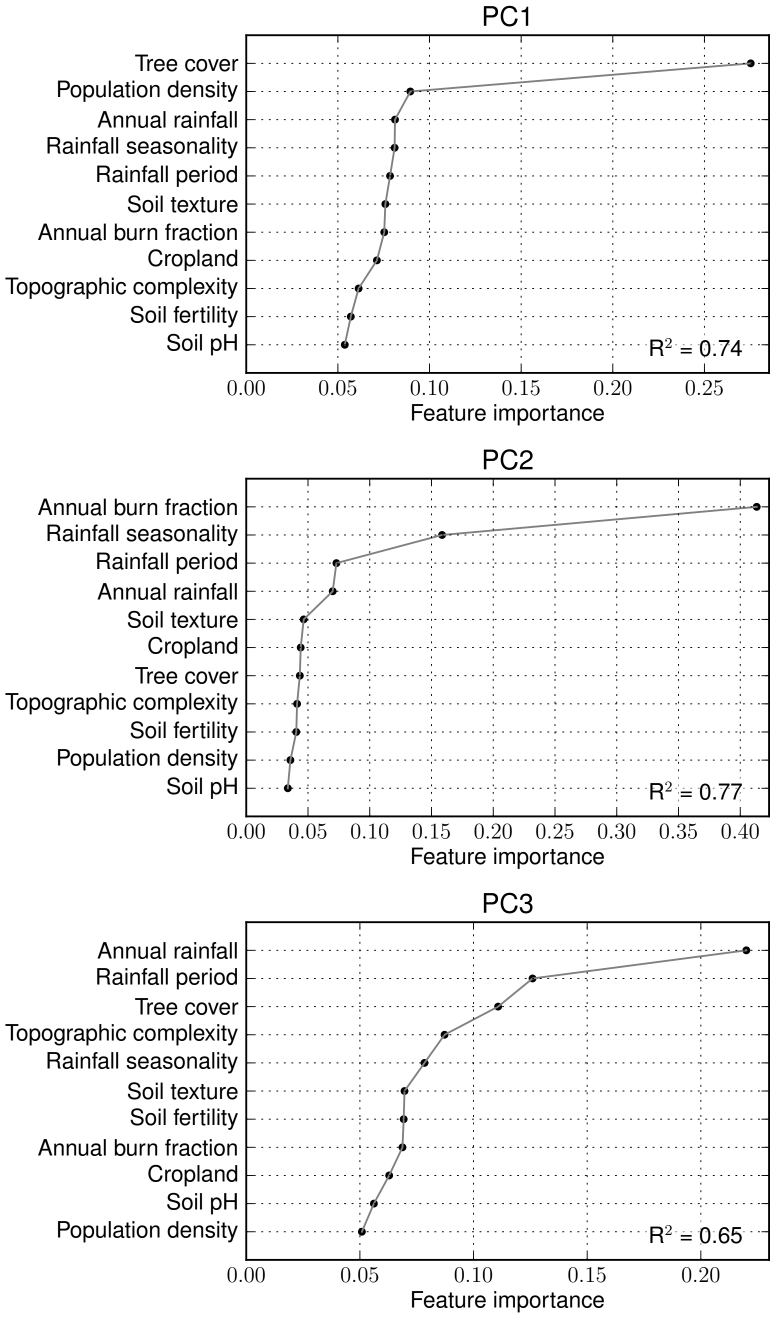

Figure 5.7: Random forest importance values, showing evidence of association between ecosystem functional variation in principal components (PCs) 1, 2 and 3 and a range of environmental properties. Environmental properties are described in Table 5.2.

in determining ecosystem dynamics.

5.4 Discussion

The C cycle of southern Africa's miombo woodlands is poorly constrained, and spatial variation in its dynamics inadequately understood. In this study we used MDF techniques to retrieve spatially-explicit estimates of terrestrial C cycling by merging a diagnostic model of the C cycle with observational data over southern Africa. Results indicate that miombo woodlands play a significant role in the global C cycle, with large C pools and fluxes with the potential to influence the global C balance. The C cycle is spatially variable, with large differences observed in the size of pools and fluxes across southern Africa. Model parameter estimates imply a small and uncertain net C source of 0.17 PgC/yr, largely from the loss of C in living vegetation. CARDAMOM indicates that ecosystem functional properties across southern Africa are heterogeneous, with 56.1 % of variance in modelled process variables described by three principal components of variation. Divergence in ecosystem functional properties is most strongly associated with differences in tree cover, fire activity, and rainfall properties.

5.4.1 RQ1: What is the magnitude of carbon fluxes, pools and residence times in the miombo ecoregion?

Miombo woodlands are very productive. GPP in southern Africa totals 6.14 PgC/yr, equivalent to 5 % of global terrestrial GPP, and *ca.* 20 % of that from savannahs (Beer et al., 2010). With a little over half of assimilated C returned to the atmosphere through respiration, NPP in the study region was estimated as 2.93 PgC/yr, equivalent to around 15 % of global savannah NPP (Grace et al., 2006). On an aerial basis NPP averages

Table 5.3: Net primary production and net ecosystem production estimates from a range of African savannah ecosystems. Table based on Grace et al. (2006) and Ciais et al. (2011).

Source	**Region**	**NPP (tC/ha/yr)**	**NEP (tC/ha/yr)**
This study	southern Africa	6.41 (4.51 - 7.34)	0.36 (-0.17 - 1.18)
Scholes and Walker (1993)	southern Africa	3.81	1.23
Hanan et al. (1998)	West Africa	3.31	0.32
Chidumayo (2002)	southern Africa		0.42
Veenendaal et al. (2004)	southern Africa		0.12
Mordelet and Menaut (1995)	Ivory Coast	6.4	
Mordelet and Menaut (1995)	Ivory Coast	8.1	
Grace et al. (2006)	Africa	5.8	
Kinyamario and Macharia (1992)	Kenya	6.1	
Long et al. (1989)	Kenya	6.2	
Brümmer et al. (2008)	West Africa		4.53
Archibald et al. (2009a)*	southern Africa		-0.25
Lehsten et al. (2009)*	Africa	6.3	
Kutsch and Merbold (*unpublished*)*	southern Africa	8.1	0.05

* NPP obtained by $NPP = 0.5 \times GPP$

6.41 tC/ha/yr, a value which is broadly similar to estimates from a range of savannah ecosystems across Africa (Table 5.3), and roughly half that of tropical rainforests (Grace et al., 2001). Fire emissions of 0.51 PgC/yr are significant, accounting for *ca.* 25 % of global fire emissions (van der Werf et al., 2010).

The C cycle of southern Africa is spatially heterogeneous, with important differences predicted in C allocation, pool sizes and residence times. This result suggests that miombo woodlands cannot be readily be considered as a contiguous region for upscaling of field observations or modelling purposes. For instance, carbon use efficiency (GPP / NPP), which describes the capacity of vegetation to retain atmospheric C in biomass, varied widely across southern Africa. Models of the terrestrial C cycle frequently consider this figure constant at around 50 % (Waring et al., 1998), an approximation that may result in significant uncertainties to projections of global change (DeLucia et al., 2007). In a similar manner, uniform C residence times are often assigned to plant functional types in global C cycle models (Galbraith et al., 2013). CARDAMOM predicts large differences to C residence times across the study region, which implies important biases may exist in many estimates of the

Table 5.4: Comparison between preliminary African carbon balance estimates derived using a range of methods in recent literature and UNFCCC national communication data. Positive values denote a C sink, and negative values a C source. The range of values reported from this study defines the 50 % confidence interval, and the error in valentini2014 defines ±1 standard deviation of a calculation with a range of methods. Table based on Ciais et al. (2011).

Source	NEP (PgC/yr)	NBP (PgC/yr)
This study	0.36 (-0.17 - 1.18)	-0.17 (-0.68 - 0.62)
Valentini et al. (2014)	2.10	0.61 ± 0.58
Bombelli et al. (2009), updated by Ciais et al. (2011)	0.69	0.07
Ciais et al. (2009)	0.28	0.15
Weber et al. (2009)	4.46	3.23
Williams et al. (2007)	0.98	0.4
UNFCCC	0.68	0.16

southern African C cycle (Friend et al., 2014).

5.4.2 RQ2: Is vegetation in south-central Africa a net source or sink of carbon?

NEP in southern Africa averages 0.36 PgC/yr, indicating a large potential C sink in miombo woodlands in the absence of fire. NEP was notably increased in areas subject to a high frequency of fires, which tend to cycle C fixed by vegetation rapidly back to the atmosphere. NBP averaged -0.17 PgC/yr, suggesting that the miombo woodland ecoregion is most likely to be acting as a weak net source of CO_2 to the atmosphere. The largest part of this land-atmosphere flux was the result of loss of living vegetation, consistent with rapid deforestation and forest degradation in miombo woodlands (Ryan et al., 2012). Predictions of of NEP and NBP are are both broadly concordant with pan-African estimates derived from models and measurements (Table 5.4). Though the large uncertainty associated with our NBP predictions mean we cannot confirm southern Africa as a net C source, in explicitly calculating confidence in model outputs C cycle estimates from CARDAMOM are near-unique amongst present estimates of the African C balance.

The median C balance prediction for southern Africa is characterised by large areas acting as a source of C, with C emission greatest in Tanzania and Mozambique where rates of deforestation are high (Hansen et al., 2013). Large parts of southern Africa are characterised by little net change, such as Zimbabwe, Malawi, and northern Tanzania, areas that are distinguished by being densely populated and heavily cultivated. There are also several locations predicted to be acting as a net C sink, centred on areas adjacent to the Congo Basin in northern Angola, southern DRC and western Tanzania. This is an interesting observation that may represent the encroachment of forests into savannahs. Woody encroachment has previously been reported into savannahs in central and southern Africa, an effect that has been attributed to depopulation and management changes (Mitchard et al., 2009; Mitchard et al., 2011), and the effects of CO_2 fertilisation on woody plants (Kgope et al., 2010; Bond and Midgley, 2012). Uncertainties in net C fluxes from CARDAMOM are considerable, with a large minority of retrieved parameter sets predicting a net sink of C in the study region. We cannot therefore with confidence identify whether southern Africa is a net source or sink of C.

The largest uncertainties in CARDAMOM presently stem from the accuracy and availability of C cycle observational data (Bloom et al., 2016). For instance, measurements of woody biomass are only available for the latter part of the decade modelled, offering little constraint on long-term woody C dynamics. It is anticipated that the future availability of from the forthcoming ‘Biomass’ mission (Le Toan et al., 2011) and recently launched ALOS 2 satellite will reduce this uncertainty. There also exists an important obstacle in estimates of ecosystem respiration flux, which in large part results from decomposition of the poorly quantified C_{som} pool. Whilst presently not well constrained by CARDAMOM, this uncertainty may be reduced in future by satellite observations of atmospheric CO_2 concentration (e.g. Crisp et al., 2004; Butz et al., 2011).

5.4.3 RQ3: How do ecosystem functional properties vary across the miombo woodland ecoregion, and what are its main environmental drivers?

The dominant mode of variation in functional properties (PC1: 28.6 % of variation) describes the transition from tree-less grasslands to closed-canopy forests. Regions with grassland vegetation are characterised by comparatively low productivity, large allocation fractions to photosynthetic C, and rapid green-up and senescence of foliar C. Tree-dominated vegetation is more productive, allocates a larger proportion of C to woody biomass, and has slower leaf phenological cycles. This gradient was most closely associated with observations of woody cover, which follows from high allocation and long residence times in woody C.

Distributions of savannah and forest vegetation structures in sub-Saharan Africa are still widely debated, with climate, hydrology, soil, fire, herbivory, and human management all likely to have some impact (Bond, 2008; Lehmann et al., 2011; Staver et al., 2011; Murphy and Bowman, 2012). Our analysis identifies no further strong predictors of vegetation structure in southern Africa, even where woody cover was excluded from the random forest analysis. This may reflect the non-deterministic nature of savannah and forest distributions, where a range of vegetation structures can co-occur under similar climatic and edaphic conditions (see Chapter 2). Alternatively it may relate to the noise and uncertainty introduced to woody cover estimates by the model, diminishing the strength of established correlations with environmental data.

The second mode of functional variation (PC2: 17.6 % of variation) describes differences in foliar properties, and litter and woody turnover rates. Foliar properties c_{lf}, c_{lma}, and D_{fall} together describe the trade-off between canopies with thick, long-lived leaves that fall late in the year to those with thinner, short-lived leaves. The coincidence of high leaf mass per unit area (LMA) and long leaf lifespan represents an emergent parameter relationship in DALEC, and one that is consistent with observations from plant trait databases (Kattge et al., 2011). The main divergences in foliar traits are generally ascribed to a trade-off between stress-tolerant and competitive plant strategies, where high LMA and long leaf lifespan indicate a slow return on investment of C in a marginal environment (Wright et al., 2004). Stress-tolerant foliar traits were particularly apparent in dry climates and where rainfall is highly seasonal. Low LMA and short-lived leaves were predicted in areas where fire is frequent, with flush of C efficient leaves and grasses promoting ecosystem recovery from fire.

The third mode of functional variation (PC3: 9.9 % of variance) is associated with canopy phenology, ranging from early leaf onset (D_{onset}) to a later canopy green-up. Leaf onset begins in the Congo Basin, spreading southwards and eastwards. Predictions of early leaf onset in the northern and western miombo ecoregion are similar to the observations of Ryan (2009), where tree green-up is shown to spread from west to east prior to the onset of of seasonal rains. Areas with early leaf onset were associated with an increased GPP, indicating the importance of effective representation of canopy phenology in C cycle models.

The large differences in ecosystem functional properties predicted by CARDAMOM raises questions about the extent to which miombo woodlands can be considered as a single vegetation class for estimation of C cycling. This is of concern where biome-specific parameters are used for upscaling C cycle estimates over large areas (e.g. Tables 5.3 and 5.4). Ecological patterns modelled by CARDAMOM show little coherence with the large-scale vegetation maps of used in modelling studies (Fig. 5.8). Where land cover maps are a poor representation of the C cycle, using them for upscaling of local-scale ecosystem measurements may result in significant biases to predictions.

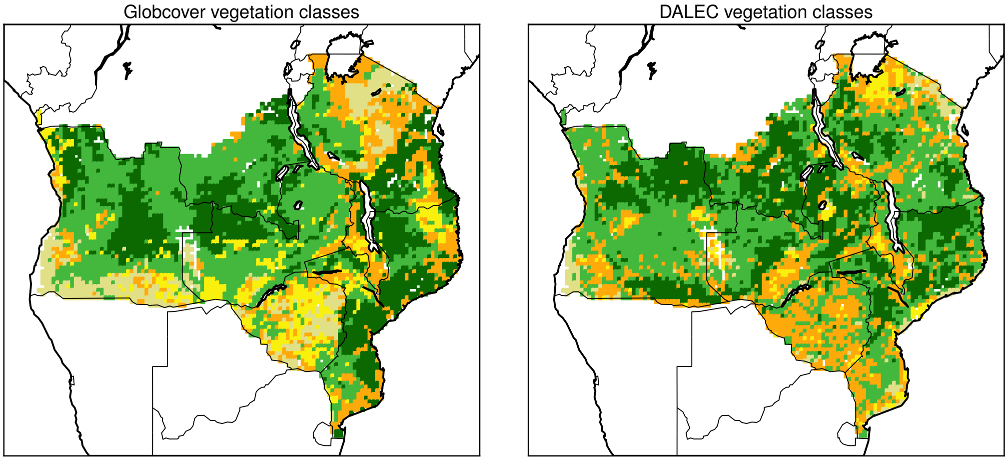

Figure 5.8: Comparison of land cover types in the widely-used ESA GlobCover 2009 land cover map and an analogous k-means classification of DALEC ecosystem functional traits. Colours in GlobCover indicate mosaic cropland (orange), closed forest (dark green), open forest (light green), shrubland (tan), and grassland (yellow). Colours in CARDAMOM outputs are arbitrary, representing the closest spatial match to GlobCover data. The poor correspondence between these maps suggests that the land cover maps that are widely used for upscaling the C cycle may result in unreliable predictions.

5.5 Conclusions

In this study we used MDF to retrieve an estimate of the C cycle of southern Africa with quantified uncertainty ranges. Model outputs indicate the importance of miombo woodlands in the global C balance, and show substantial variation in C cycle properties across southern Africa. Though uncertainties in predictions are presently large, MDF is one of few available techniques available to robustly quantify the C cycle where data are limited. Spatial variation was noted in primary production, C allocation patterns, and foliar and canopy traits, which are associated with differences in woody cover, fire, and precipitation properties. C cycle dynamics correspond poorly to conventional land cover maps, indicating they may be unsuited to upscaling measurements of C cycling in African savannahs.

5.6 Acknowledgements

The CARDAMOM framework was developed by Anthony Bloom, Jean-François Exbrayat, Ivar van der Velde, Liang Feng and Mathew Williams. Jean-François Exbrayat performed CARDAMOM model runs for southern Africa, and contributed to a number of the ideas presented here. Maps of woody biomass were supplied by Iain McNicol and Casey Ryan.

5.7 References

Archibald, S.A., Kirton, A., can der Merwe, M.R., Scholes, R.J., Williams, C.A., and Hanan, N. (2009a), 'Drivers of inter-annual variability in Net Ecosystem Exchange in a semi-arid savanna ecosystem, South Africa', *Journal of Geophysical Research: Biogeosciences*, **6**, pp. 251–266.

Archibald, S., Roy, D.P., Wilgen, V., Brian, W., and Scholes, R.J. (2009b), 'What limits fire? An examination of drivers of burnt area in Southern Africa', *Global Change Biology*, **15**, pp. 613–630.

Beer, C., Reichstein, M., Tomelleri, E., Ciais, P., Jung, M., Carvalhais, N., Rödenbeck, C., Arain, M.A., Baldocchi, D., Bonan, G.B., Bondeau, A., Cescatti, A., Lasslop, G., Lindroth, A., Lomas, M., Luyssaert, S., Margolis, H., Oleson, K.W., Roupsard, O., Veenendaal, E., Viovy, N., Williams, C., Woodward, F.I., and Papale, D. (2010), 'Terrestrial gross carbon dioxide uptake: global distribution and covariation with climate', *Science*, **329**, pp. 834–838.

Bloom, A.A. and Williams, M. (2015), 'Constraining ecosystem carbon dynamics in a data-limited world: integrating ecological" common sense" in a model–data fusion framework', *Biogeosciences*, **12**, pp. 1299–1315.

Bloom, A.A., Exbrayat, J.-F., van der Velde, I.R., Feng, L., and Williams, M. (2016), 'The decadal state of the terrestrial carbon cycle: Global retrievals of terrestrial carbon allocation, pools, and residence times', *Proceedings of the National Academy of Sciences*, **113**, pp. 1285–1290.

Boden, T.A., Marland, G., and Andres, R.J. (2011), *Global, regional, and national fossil fuel* CO_2 *emissions*, Carbon Dioxide Information Analysis Center, Oak Ridge National Laboratory, U.S. Department of Energy, Tennessee, U.S.A.

Bombelli, A., Henry, M., Castaldi, S., Adu-Bredu, S., Arneth, A., de Grandcourt, A., Grieco, E., Kutsch, W.L., Lehsten, V., Rasile, G.A., Reichstein, M., Tansey, K., Weber, U., and Valentini, R. (2009), 'The Sub-Saharan Africa carbon balance, an overview', *Journal of Geophysical Research: Biogeosciences*, **6**, pp. 2085–2123.

Bond, W.J. (2008), 'What Limits Trees in C_4 Grasslands and Savannas?', *Annual Review of Ecology, Evolution, and Systematics*, **39**, pp. 641–659.

Bond, W.J. and Midgley, G.F. (2012), 'Carbon dioxide and the uneasy interactions of trees and savannah grasses', *Philosophical Transactions of the Royal Society B*, **367**, pp. 601–612.

Breiman, L. (2001), 'Random forests', *Machine learning*, **45**, pp. 5–32.

Brümmer, C., Falk, U., Papen, H., Szarzynski, J., Wassmann, R., and Brüggemann, N. (2008), 'Diurnal, seasonal, and interannual variation in carbon dioxide and energy exchange in shrub savanna in Burkina Faso (West Africa)', *Journal of Geophysical Research: Biogeosciences*, **113**, G02030.

Butz, A., Guerlet, S., Hasekamp, O., Schepers, D., Galli, A., Aben, I., Frankenberg, C., Hartmann, J.-M., Tran, H., Kuze A ad Keppel-Aleks, G., Toon, G., Wunch, D., Wennberg, P., Deutscher, N., Griffith, D., Macatangay, R., Messerschmidt, J., Notholt, J., and Warneke, T. (2011), 'Toward accurate CO_2 and CH_4 observations from GOSAT', *Geophysical Research Letters*, **38**, p. L14812.

Chidumayo, E.N. (2002), 'Changes in miombo woodland structure under different land tenure and use systems in central Zambia', *Journal of biogeography*, **29**, pp. 1619–1626.

Ciais, P., Bombelli, A., Williams, M., Piao, S.L., Chave, J., Ryan, C.M., Henry, M., Brender, P., and Valentini, R. (2011), 'The carbon balance of Africa: synthesis of recent research studies', *Philosophical Transactions of the Royal Society of London A: Mathematical, Physical and Engineering Sciences*, **369**, pp. 2038–2057.

Ciais, P., Piao, S.-L., Cadule, P., Friedlingstein, P., and Chédin, A. (2009), 'Variability and recent trends in the African terrestrial carbon balance', *Journal of Geophysical Research: Biogeosciences*, **6**, pp. 1935–1948.

CIESIN (2005), *Gridded Population of the World, Version 3 (GPWv3) Data Collection*, Center for International Earth Science Information Network (CIESIN) and Centro Internacional de Agricultura Tropical (CIAT).

Crisp, D., Atlas, R.M., Breon, F.-M., Brown, L., Burrows, J.P., Ciais, P., Connor, B., Doney, S., Fung, I.Y., Jacob, D., Miller, C., O'Brien, D., Pawson, S., Randerson, J.T., Rayner, P., Salawitch, R.J., Sander, S., Sen, B., Stephens, G., Tans, P.P., Toon, G.C., Wennberg, P., Wofsy, S.C., Yung, Y., Kuang, Z., Chudasama, B., Sprague, G., Weiss, B., Pollock, R., Kenyon, D., and Schroll, S. (2004), 'The orbiting carbon observatory (OCO) mission', *Advances in Space Research*, **34**, pp. 700–709.

Dee, D.P., Uppala, S.M., Simmons, A.J., Berrisford, P., Poli, P., Kobayashi, S., Andrae, U., Balmaseda, M.A., Balsamo, G., Bauer, P., Bechtold, P., Beljaars, A.C.M., Berg, L. van de, Bidlot, J., Bormann, N., Delsol, C., Dragani, R., Fuentes, M., Geer, A.J., Haimberger, L., Healy, S.B., Hersbach, H., Hólm, E.V., Isaksen, L., Kållberg, P., Köhler, M., Matricardi, M., McNally, A.P., Monge-Sanz, B.M., Morcrette, J.-J., Park, B.-K., Peubey, C., Rosnay, P. de, Tavolato, C., Thépaut, J.-N., and Vitart, F. (2011), 'The ERA-Interim reanalysis: Configuration and performance of the data assimilation system', *Quarterly Journal of the Royal Meteorological Society*, **137**, pp. 553–597.

DeLucia, E., Drake, J.E., Thomas, R.B., and Gonzalez-Meler, M. (2007), 'Forest carbon use efficiency: is respiration a constant fraction of gross primary production?', *Global Change Biology*, **13**, pp. 1157–1167.

DiMiceli, C.M., Carroll, M.L., Sohlberg, R.A., Huang, C., Hansen, M.C., and Townshend, J.R.G. (2011), *MODIS vegetation continuous fields (MOD44B)*, University of Maryland, Maryland, USA.

Fischer, G., Nachtergaele, F., Prieler, S., Velthuizen, H.T. van, Verelst, L., and Wiberg, D. (2008), *Global Agro-ecological Zones Assessment for Agriculture (GAEZ 2008)*, IIASA, Laxenburg, Austria and FAO, Rome, Italy.

Fox, A., Williams, M., Richardson, A.D., Cameron, D., Gove, J.H., Quaife, T., Ricciuto, D., Reichstein, M., Tomelleri, E., Trudinger, C.M., and van Wijk, M.T. (2009), 'The REFLEX project: comparing different algorithms and implementations for the inversion of a terrestrial ecosystem model against eddy covariance data', *Agricultural and Forest Meteorology*, **149**, pp. 1597–1615.

Friend, A.D., Lucht, W., Rademacher, T.T., Keribin, R., Betts, R., Cadule, P., Ciais, P., Clark, D.B., Dankers, R., Falloon, P.D., Ito, A., Kahana, R., Kleidon, A., Lomas, M.R., Nishina, K., Ostberg, S., Pavlick, R., Peylin, P., Chaphoff, S., Vuichard, N., Warszawski, L., Wiltshire, A., and Woodward, F.I. (2014), 'Carbon residence time dominates uncertainty in terrestrial vegetation responses to future climate and atmospheric CO_2', *Proceedings of the National Academy of Sciences*, **111**, pp. 3280–3285.

Fritz, S., See, L., McCallum, I., You, L., Bun, A., Moltchanova, E., Duerauer, M., Albrecht, F., Schill, C., Perger, C., Havlik, P., Mosnier, A., Thornton, P., Wood-Sichra, U., Herrero, M., Becker-Reshef, I., Justice, C., Hansen, M., Gong, P., Abdel Aziz, S., Cipriani, A., Cumani, R., Cecchi, G., Conchedda, G., Ferreira, S., Gomez, A., Haffani, M., Kayitakire, F., Malanding, J., Mueller, R., Newby, T., Nonguierma, A., Olusegun, A., Ortner, S., Rajak, D.R., Rocha, J., Schepaschenko, D., Schepaschenko, M., Terekhov, A., Tiangwa, A., Vancutsem, C., Vintrou, E., Wenbin, W., Velde, M. van der, Dunwoody, A., Kraxner, F., and Obersteiner, M. (2015), 'Mapping global cropland and field size', *Global change biology*, **21**, pp. 1980–1992.

Galbraith, D., Malhi, Y., Affum-Baffoe, K., Castanho, A.D., Doughty, C.E., Fisher, R.A., Lewis, S.L., Peh, K.S.-H., Phillips, O.L., Quesada Carlos, A., Sonké, B., and Lloyd, J. (2013), 'Residence times of woody biomass in tropical forests', *Plant Ecology & Diversity*, **6**, pp. 139–157.

Giglio, L., Randerson, J.T., and Werf, G.R. (2013), 'Analysis of daily, monthly, and annual burned area using the fourth-generation global fire emissions database (GFED4)', *Biogeosciences*, **118**, pp. 317–328.

Grace, J., Malhi, Y., Higuchi, N., and Meir, P. (2001), 'Productivity of tropical rain forests', *Terrestrial global productivity: past, present and future*, ed. by H. Mooney, J. Roy, and B. Saugier, Academic Press, San Diego, California, USA, pp. 401–426.

Grace, J., José, J.S., Meir, P., Miranda, H.S., and Montes, R.A. (2006), 'Productivity and carbon fluxes of tropical savannas', *Journal of Biogeography*, **33**, pp. 387–400.

Hanan, N.P., Kabat, P., Dolman, A.J., and Elbers, J.A. (1998), 'Photosynthesis and carbon balance of a Sahelian fallow savanna', *Global change biology*, **4**, pp. 523–538.

Hansen, M.C., Potapov, P.V., Moore, R., Hancher, M., Turubanova, S.A., Tyukavina, A., Thau, D., Stehman, S.V., Goetz, S.J., Loveland, T.R., Kommareddy, A., Egorov, A., Chini, L., O, J.C., and Townshend, J.R.G. (2013), 'High-resolution global maps of 21st-century forest cover change', *Science*, **342**, pp. 850–853.

Houghton, R.A. and Hackler, J.L. (2006), 'Emissions of carbon from land use change in sub-Saharan Africa', *Journal of Geophysical Research: Biogeosciences*, **111**, G02003.

Houghton, R.A., Hall, F., and Goetz, S.J. (2009), 'Importance of biomass in the global carbon cycle', *Journal of Geophysical Research: Biogeosciences*, **114**, G00E03.

Huffman, G.J., Bolvin, D.T., Nelkin, E.J., Wolff, D.B., Adler, R.F., Gu, G., Hong, Y., Bowman, K.P., and Stocker, E.F. (2007), 'The TRMM multisatellite precipitation analysis (TMPA): Quasi-global, multiyear, combined-sensor precipitation estimates at fine scales', *Journal of Hydrometeorology*, **8**, pp. 38–55.

Jarvis, A., Reuter, H.I., Nelson, A., and Guevara, E. (2008), 'Hole-filled SRTM for the globe Version 4', *available from the CGIAR-CSI SRTM 90m Database*, url: `http://srtm.%20csi.%20cgiar.%20org`.

Kattge, J., Diaz, S., Lavorel, S., Prentice, C., Leadley, P., Boenisch, G., Garnier, E., Westoby, M., Reich, P.B., Wright, I.J., Cornelissen, J.H.C., Violle, C., Harrison, S.P., van, B.P.M., Reichstein, M., Enquist, B.J., Soudzilovskaia, N.A., Ackerly, D.D., Anand, M., Atkin, O., Bahn, M., Baker, T.R., Baldocchi, D., Bekker, R., Blanco, C.C., Blonder, B., Bond, W.J., Bradstock, R., Bunker, D.E., Casanoves, F., Cavender-Bares, J., Chambers, J.Q., Chapin, F.S., Chave, J., Coomes, D., Cornwell, W.K., Craine, J.M., Dobrin, B.H., Duarte, L., Durka, W., Elser, J., Esser, G., Estiarte, M., Fagan, W.F., Fang, J., Fernandez-Mendez, F., Fidelis, A., Finegan, B., Flores, O., Ford, H., Frank, D., Freschet, G.T., Fyllas, N.M., Gallagher, R.V., Green, W.A., Gutierrez, A.G., Hickler, T., Higgins, S.I., Hodgson, J.G., Jalili, A., Jansen, S., Joly, C.A., Kerkhoff, A.J., Kirkup, D., Kitajima, K., Kleyer, M., Klotz, S., Knops, J.M.H., Kramer, K., Kühn, I.., Kurokawa, H., Laughlin, D., Lee, T.D., Leishman, M., Lens, F., Lenz, T., Lewis, S.L., Lloyd, J., Llusià, J., Louault, F., Ma, S., Mahecha, M.D., Manning, P., Massad, T., Medlyn, B.E., Messier, J., Moles, A.T., Müller, S.C., Nadrowski, K., Naeem, S., Niinemets, Ü., Nöllert, S., Nüske, A., Ogaya, R., Oleksyn, J., Onipchenko, V.G., Onoda, Y., Ordoñez, J., Overbeck, G., Ozinga, W.A., Patiño, S., Paula, S., Pausas, J.G., Peñuelas, J., Phillips, O.L., Pillar, V., Poorter, H., Poorter, L., Poschlod, P., Prinzing, A., Proulx, R., Rammig, A., Reinsch, S., Reu, B., Sack, L., Salgado-negret, B., Sardans, J., Shiodera, S., Shipley, B., Siefert, A., Sosinski, E., Soussana, J.-f., Swaine, E., Swenson, N., Thompson, K., Thornton, P., Waldram, M., Weiher, E., White, M., White, S., Wright, S.J., Yguel, B., Zaehle, S., Zanne, A.E., and Wirth, C. (2011), 'TRY–a global database of plant traits', *Global Change Biology*, **17**, pp. 2905–2935.

Keenan, T.F., Davidson, E., Moffat, A.M., Munger, W., and Richardson, A.D. (2012), 'Using model-data fusion to interpret past trends, and quantify uncertainties in future projections, of terrestrial ecosystem carbon cycling', *Global Change Biology*, **18**, pp. 2555–2569.

Kgope, B.S., Bond, W.J., and Midgley, G.F. (2010), 'Growth responses of African savanna trees implicate atmospheric [CO_2] as a driver of past and current changes in savanna tree cover', *Austral Ecology*, **35**, pp. 451–463.

Kinyamario, J.I. and Macharia, J.N.M. (1992), 'Aboveground standing crop, protein content and dry matter digestibility of a tropical grassland range in the Nairobi National Park, Kenya', *African Journal of Ecology*, **30**, pp. 33–41.

Le Quéré, C., Andres, R.J., Boden, T., Conway, T., Houghton, R.A., House, J.I., Marland, G., Peters, G.P., van der Werf, G.R., Ahlström, A., Andrew, R.M., Bopp, L., Canadell, J.G., Ciais, P., Doney, S.C., Enright, C., Friedlingstein, P., Huntingford, C., Jain, A.K., Jourdain, C., Kato, E., Keeling, R.F., Klein Goldewijk, K., Levis, S., Levy, P., Lomas, M., Poulter, B., Raupach, M.R., Schwinger, J., Sitch, S., Stocker, B.D., Viovy, N., Zaehle, S., and Zeng, N. (2013), 'The global carbon budget 1959–2011', *Earth System Science Data*, **5**, pp. 165–185.

Le Toan, T., Quegan, S., Davidson, M., Balzter, H., Paillou, P., Papathanassiou, K., Plummer, S., Rocca, F., Saatchi, S., Shugart, H., and Ulander, L. (2011), 'The BIOMASS mission: Mapping global forest biomass to better understand the terrestrial carbon cycle', *Remote sensing of environment*, **115**, pp. 2850–2860.

Lehmann, C.E., Archibald, S.A., Hoffmann, W.A., and Bond, W.J. (2011), 'Deciphering the distribution of the savanna biome', *New Phytologist*, **191**, pp. 197–209.

Lehsten, V., Tansey, K., Balzter, H., Thonicke, K., Spessa, A., Weber, U., Smith, B., and Arneth, A. (2009), 'Estimating carbon emissions from African wildfires', *Journal of Geophysical Research: Biogeosciences*, **6**, pp. 349–360.

Long, S., Moya, E.G., Imbamba, S., Kamnalrut, A., Piedade, M., Scurlock, J., Shen, Y., and Hall, D. (1989), 'Primary productivity of natural grass ecosystems of the tropics: a reappraisal', *Plant and Soil*, **115**, pp. 155–166.

Luyssaert, S., Schulze, E.-D., Börner, A., Knohl, A., Hessenmöller, D., Law, B.E., Ciais, P., and Grace, J. (2008), 'Old-growth forests as global carbon sinks', *Nature*, **455**, pp. 213–215.

Markham, C.G. (1970), 'Seasonality of precipitation in the United States', *Annals of the Association of American Geographers*, **60**, pp. 593–597.

McNicol, I.M. and Ryan, C.M. (*in prep*), 'Aboveground woody biomass dataset for southern Africa's miombo woodlands'.

Menaut, J.C. (1983), 'Vegetation of African savannas', *Ecosystems of the World*, ed. by F. Bourliere, Elsevier, New York, pp. 109–149.

Mitchard, E.T.A., Saatchi, S.S., Lewis, S.L., Feldpausch, T.R., Woodhouse, I.H., Sonké, B., Rowland, C., and Meir, P. (2011), 'Measuring biomass changes due to woody encroachment and deforestation/degradation in a forest–savanna boundary region of central Africa using multi-temporal L-band radar backscatter', *Remote Sensing of Environment*, **115**, pp. 2861–2873.

Mitchard, E.T., Saatchi, S.S., Gerard, F., Lewis, S., and Meir, P. (2009), 'Measuring woody encroachment along a forest-savanna boundary in Central Africa', *Earth Interactions*, **13**, pp. 1–29.

Mordelet, P. and Menaut, J.-C. (1995), 'Influence of trees on above-ground production dynamics of grasses in a humid savanna', *Journal of Vegetation Science*, **6**, pp. 223–228.

Murphy, B.P. and Bowman, D.M.J.S. (2012), 'What controls the distribution of tropical forest and savanna?', *Ecology Letters*, **15**, pp. 748–758.

Nix, H.A. (1983), 'Climate of tropical savannas', *Ecosystems of the World*, ed. by F. Bourliere, Elsevier, New York, pp. 37–62.

Olson, D.M., Dinerstein, E., Wikramanayake, E.D., Burgess, N.D., Powell, G.V.N., Underwood, E.C., D'amico, J.A., Itoua, I., Strand, H.E., Morrison, J.C., Loucks, C.J., Allnutt, T.F., Ricketts, T.H., Kura, Y., Lamoreux, J.F., Wettengel, W.W., Hedao, P., and Kassem, K.R. (2001), 'Terrestrial Ecoregions of the World: A New Map of Life on Earth A new global map of terrestrial ecoregions provides an innovative tool for conserving biodiversity', *BioScience*, **51**, pp. 933–938.

Pan, Y., Birdsey, R.A., Fang, J., Houghton, R., Kauppi, P.E., Kurz, W.A., Phillips, O.L., Shvidenko, A., Lewis, S.L., Canadell, J.G., Ciais, P., Jackson, R.B., Pacala, S.W., McGuire, A.D., Piao, S., Rautiainen, A., Sitch, S., and Hayes, D. (2011), 'A large and persistent carbon sink in the world's forests', *Science*, **333**, pp. 988–993.

Pedregosa, F., Varoquaux, G., Gramfort, A., Michel, V., Thirion, B., Grisel, O., Blondel, M., Prettenhofer, P., Weiss, R., Dubourg, V., Vanderplas, J., Passos, A., Cournapeau, D., Brucher, M., Perrot, M., and Duchesnay, E. (2011), 'Scikit-learn: Machine Learning in Python', *Journal of Machine Learning Research*, **12**, pp. 2825–2830.

Ryan, C.M., Hill, T., Woollen, E., Ghee, C., Mitchard, E., Cassells, G., Grace, J., Woodhouse, I.H., and Williams, M. (2012), 'Quantifying small-scale deforestation and forest degradation in African woodlands using radar imagery', *Global Change Biology*, **18**, pp. 243–257.

Ryan, C.M. and Williams, M. (2011), 'How does fire intensity and frequency affect miombo woodland tree populations and biomass?', *Ecological Applications*, **21**, pp. 48–60.

Ryan, C.M., Williams, M., and Grace, J. (2011), 'Above-and Belowground Carbon Stocks in a Miombo Woodland Landscape of Mozambique', *Biotropica*, **43**, pp. 423–432.

Ryan, C.M. (2009), 'Carbon cycling, fire and phenology in a tropical savanna woodland in Nhambita, Mozambique', PhD thesis, The University of Edinburgh.

Sankaran, M., Hanan, N.P., Scholes, R.J., Ratnam, J., Augustine, D.J., Cade, B.S., Gignoux, J., Higgins, S.I., Le Roux, X., Ludwig, F., Ardo, J., Banyikwa, F., Bronn, A., Bucini, G., Caylor, K.K., Coughenour, M.B., Diouf, A., Ekaya, W., Feral, C.J., February, E.C., Frost, P.G.H., Hiernaux, P., Hrabar, H., Metzger, K.L., Prins, H.H.T., Ringrose, S., Sea, W., Tews, J., Worden, J., and Zambatis, N. (2005), 'Determinants of woody cover in African savannas', *Nature*, **438**, pp. 846–849.

Scholes, R.J. and Walker, B.H. (1993), *Nylsvley: the study of an African savanna*, Cambridge University Press, Cambridge, UK.

Smith, M.J., Purves, D.W., Vanderwel, M.C., Lyutsarev, V., and Emmott, S. (2013), 'The climate dependence of the terrestrial carbon cycle, including parameter and structural uncertainties', *Biogeosciences*, **10**, pp. 583–606.

Staver, A.C., Archibald, S., and Levin, S.A. (2011), 'The global extent and determinants of savanna and forest as alternative biome states', *Science*, **334**, pp. 230–232.

Todd-Brown, K.E., Randerson, J.T., Post, W.M., Hoffman, F.M., Tarnocai, C., Schuur, E.A., and Allison, S.D. (2013), 'Causes of variation in soil carbon simulations from CMIP5 Earth system models and comparison with observations', *Biogeosciences*, **10**, pp. 1717–1736.

Valentini, R., Arneth, A., Bombelli, A., Castaldi, S., Cazzolla Gatti, R., Chevallier, F., Ciais, P., Grieco, E., Hartmann, J., Henry, M., Houghton, R.A., Jung, M., Kutsch, W.L., Malhi, Y., Mayorga, E., Merbold, L., Murray-Totarolo, G., Papale, D., Peylin, P., Poulter, B., Raymond, P.A., Santini, M., Sitch, S., Laurin, G.V., van der Werf, G.R., Williams, C.A., and Scholes, R.J. (2014), 'A full greenhouse gases budget of Africa: synthesis, uncertainties, and vulnerabilities', *Biogeosciences*, **11**, pp. 381–407.

van der Werf, G.R., Randerson, J.T., Giglio, L., Collatz, G.J., Mu, M., Kasibhatla, P.S., Morton, D.C., DeFries, R.S., van Jin, Y., and van Leeuwen, T.T. (2010), 'Global fire emissions and the contribution of deforestation, savanna, forest, agricultural, and peat fires (1997–2009)', *Atmospheric Chemistry and Physics*, **10**, pp. 11707–11735.

Veenendaal, E.M., Kolle, O., and Lloyd, J. (2004), 'Seasonal variation in energy fluxes and carbon dioxide exchange for a broad-leaved semi-arid savanna (Mopane woodland) in Southern Africa', *Global Change Biology*, **10**, pp. 318–328.

Waring, R.H., Landsberg, J.J., and Williams, M. (1998), 'Net primary production of forests: a constant fraction of gross primary production?', *Tree Physiology*, **18**, pp. 129–134.

Weber, U., Jung, M., Reichstein, M., Beer, C., Braakhekke, M.C., Lehsten, V., Ghent, D., Kaduk, J., Viovy, N., Ciais, P., Gobron, N., and Rödenbeck, C. (2009), 'The interannual variability of Africa's ecosystem productivity: a multi-model analysis', *Journal of Geophysical Research: Biogeosciences*, **6**, pp. 285–295.

White, F. (1983), *The vegetation of Africa: a descriptive memoir to accompany the Unesco/AETFAT/UNSO vegetation map of Africa*, UNESCO, Paris, France.

Williams, C.A., Hanan, N.P., Neff, J.C., Scholes, R.J., Berry, J.A., Denning, S.A., and Baker, D.F. (2007), 'Africa and the global carbon cycle', *Carbon balance and management*, **2**, pp. 1–13.

Williams, M., Rastetter, E.B., Fernandes, D.N., Goulden, M.L., Shaver, G.R., and Johnson, L.C. (1997), 'Predicting gross primary productivity in terrestrial ecosystems', *Ecological Applications*, **7**, pp. 882–894.

Woollen, E., Ryan, C.M., and Williams, M. (2012), 'Carbon stocks in an African woodland landscape: spatial distributions and scales of variation', *Ecosystems*, **15**, pp. 804–818.

Wright, I.J., Reich, P.B., Westoby, M., Ackerly, D.D., Baruch, Z., Bongers, F., Cavender-Bares, J., Chapin, T., Cornelissen, J.H., Diemer, M., Flexas, J., Garnier, E., Groom, P., Gulias, J., Hikosaka, K., Lamont, B.B., Lee, T., Lee, W., Lusk, C., Midgley, J.J., Navas, M.L., Niinemets, Ü., Oleksyn, J., Osada, N., Poorter, H., Poot, P., Prior, L., Pyankov, V.I., Roumet, C., Thomas, S.C., Tjoelker, M.G., Veneklaas, E.J., and Villar, R. (2004), 'The worldwide leaf economics spectrum', *Nature*, **428**, pp. 821–827.

Ziehn, T., Scholze, M., and Knorr, W. (2012), ‘On the capability of Monte Carlo and adjoint inversion techniques to derive posterior parameter uncertainties in terrestrial ecosystem models’, *Global Biogeochemical Cycles*, **26**, GB3025.

5.8 Supplementary materials

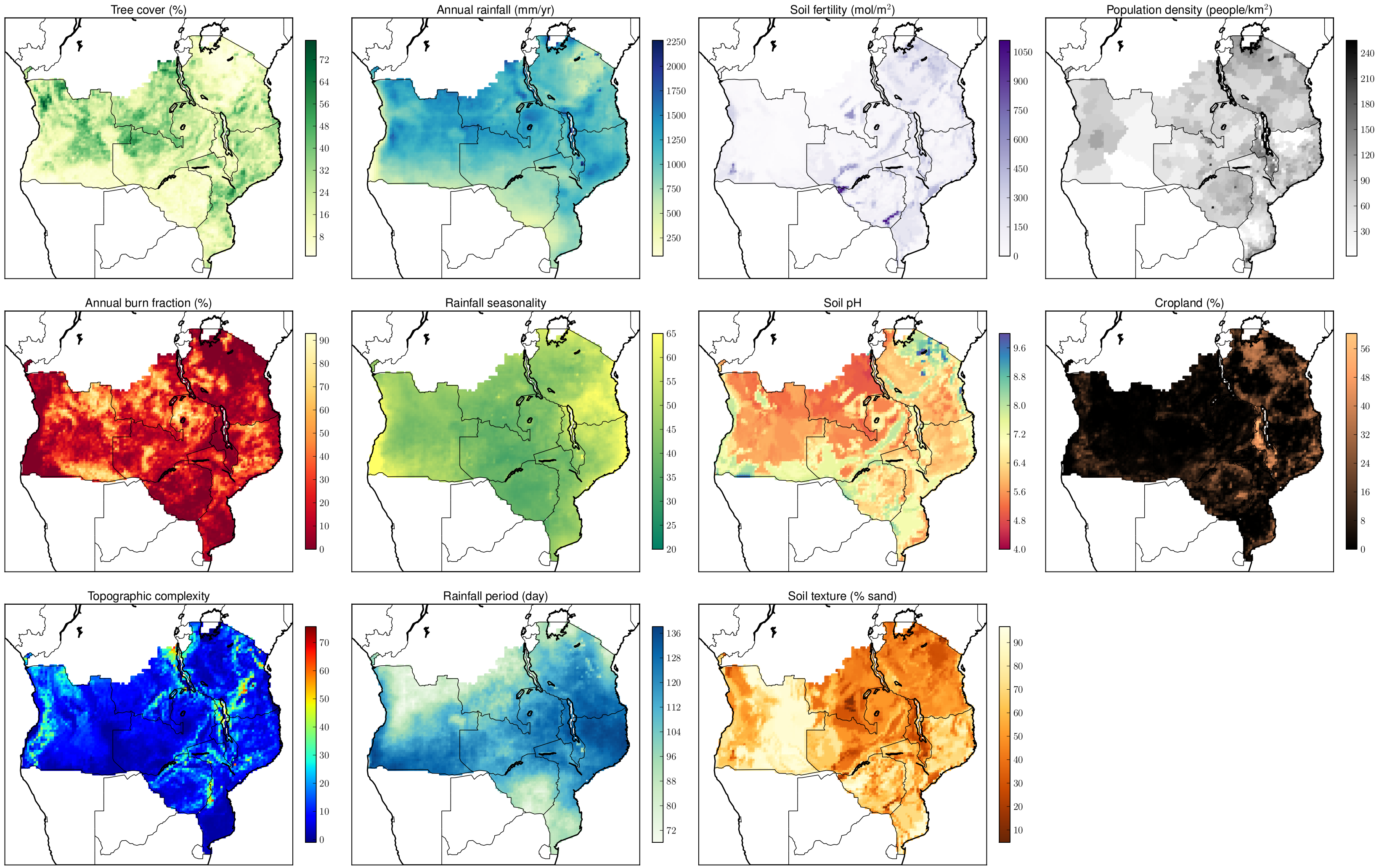

Figure S5.1: Candidate environmental drivers of ecosystem function in southern Africa. Data are from a range of sources, detailed in Table 5.2.

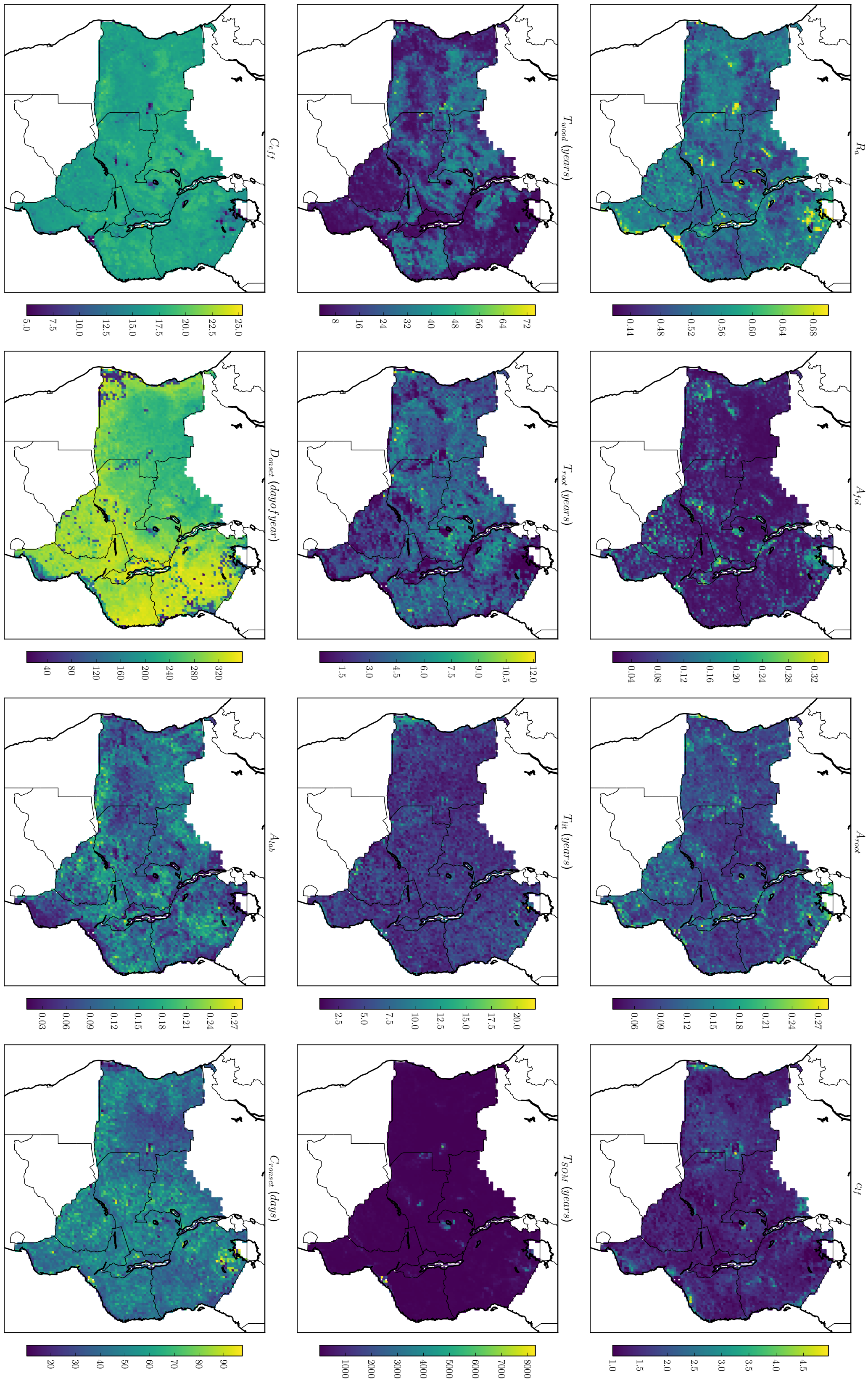
C_{eff}
5.0 7.5 10.0 12.5 15.0 17.5 20.0 22.5 25.0
T_{wood} (years)
8 16 24 32 40 48 56 64 72
R_a
0.44 0.48 0.52 0.56 0.60 0.64 0.68
D_{onset} (dayofyear)
40 80 120 160 200 240 280 320
T_{root} (years)
1.5 3.0 4.5 6.0 7.5 9.0 10.5 12.0
A_{fol}
0.04 0.08 0.12 0.16 0.20 0.24 0.28 0.32
A_{lab}
0.03 0.06 0.09 0.12 0.15 0.18 0.21 0.24 0.27
T_{lit} (years)
2.5 5.0 7.5 10.0 12.5 15.0 17.5 20.0
A_{root}
0.06 0.09 0.12 0.15 0.18 0.21 0.24 0.27
C_{ronset} (days)
20 30 40 50 60 70 80 90
T_{SOM} (years)
1000 2000 3000 4000 5000 6000 7000 8000
c_{lf}
1.0 1.5 2.0 2.5 3.0 3.5 4.0 4.5

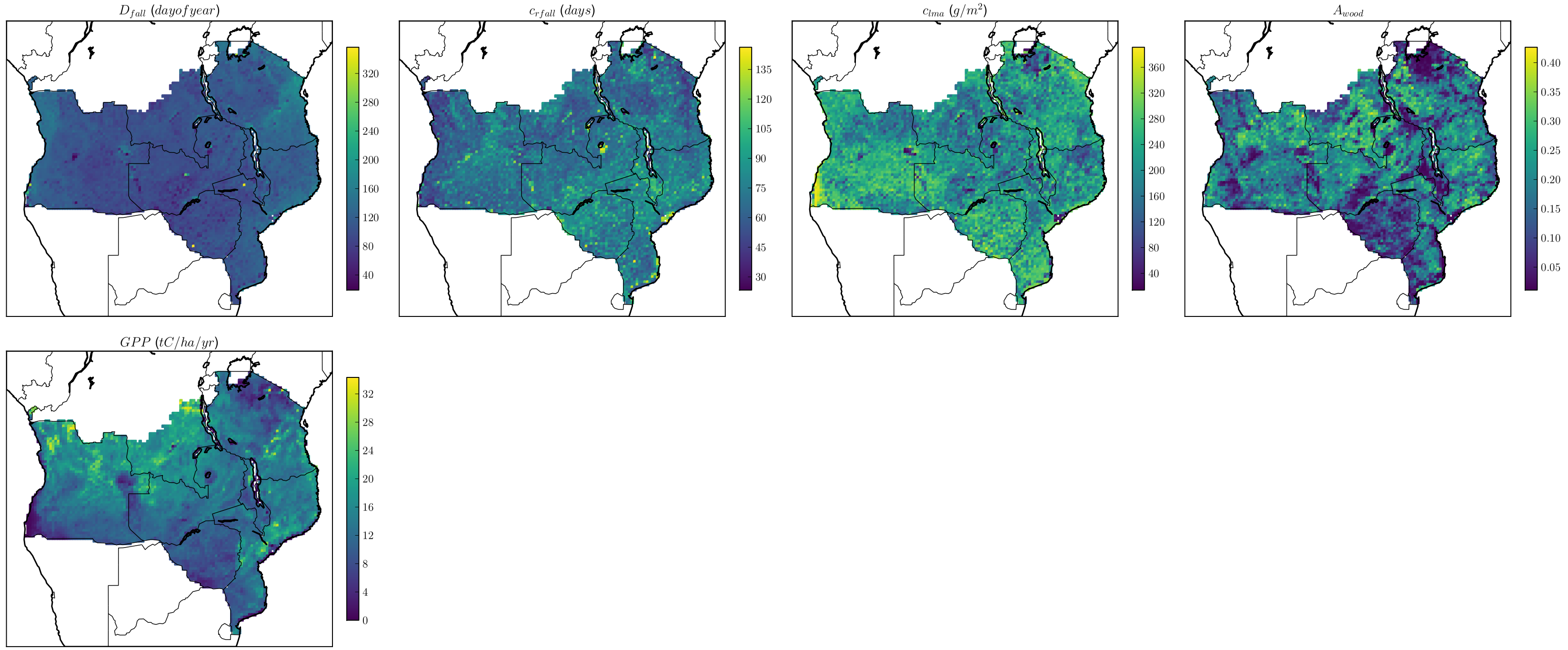

Figure S5.2: DALEC model parameter maps estimated using CARDAMOM, showing median parameter values for each grid cell in southern Africa. Model parameters are defined in Table 5.1.

CHAPTER 6

Discussion and key conclusions

6.1 Thesis overview

The objective of this thesis was to improve our understanding of key uncertainties in the carbon (C) cycle of the miombo woodland ecosystem of southern Africa. I conducted investigations of:

i. The floristic and functional properties associated with diverse miombo woodland vegetation structures.

ii. Woody productivity and turnover, and the regulation of stem growth and mortality in miombo woodlands.

iii. C emissions reductions resulting from introduction of an early burning fire regime in miombo woodlands.

iv. Estimation of the C balance of the miombo woodland ecoregion with a model-data fusion framework.

Through the results of these studies, I aimed to advance understanding of the following broad research questions:

1. What are the causes and consequences of structural heterogeneity in miombo woodlands?
2. What is the role of fire in miombo woodlands?
3. How can we most effectively resolve the C cycle of miombo woodlands?

In this chapter I summarise the main results of each of the 4 research chapters, and review their application to the aims of this thesis. I will also identify key areas for further research arising from the outcomes of this work.

6.2 What are the causes and consequences of structural heterogeneity in miombo woodlands?

6.2.1 At landscape-scales

Vegetation in miombo woodlands is profoundly variable at landscape scales. In Chapter 2 I identified differences in tree community composition across the structurally heterogeneous miombo woodland landscape of Kilwa District, Tanzania. Species composition was correlated with differences in biotic and abiotic environmental properties, and species communities expressed a range of divergent functional traits. Floristic and functional variation was represented by three structurally-defined land cover classes: ‘savannahs’, ‘woodlands’, and ‘forests’ (Fig. 6.1).

Savannahs are areas of very low woody biomass, characterised by trees of the species *Acacia nilotica*, *Dalbergia melanoxylon*, and *Sclerocarya birrea*. Savannahs have sporadic tree cover, high grass biomass, and were subject to very frequent fires. A particularly notable property of savannah areas was their low topographic prominence and their commonly waterlogged soils. Species in open savannahs are geared for persistence in an adverse environment, with thick bark indicating defence against fire, leaf morphology associated with drought resilience, efficient use of nutrients, and specialised nutrient acquisition strategies. Together these suggest that areas of open vegetation in miombo woodlands are marginal environments, most frequently associated with seasonally flooded ‘dambos’ (von der Heyden, 2004; Woollen et al., 2012).

Woodlands have an intermediate woody biomass, and are dominated by the characteristic miombo woodland species *Brachystegia spiciformis*, *Julbernardia globiflora* and *Pterocarpus angolensis* . Relative to savannahs, woodlands have greater tree cover, less grass biomass and a similar frequency of fires, and occur in well-

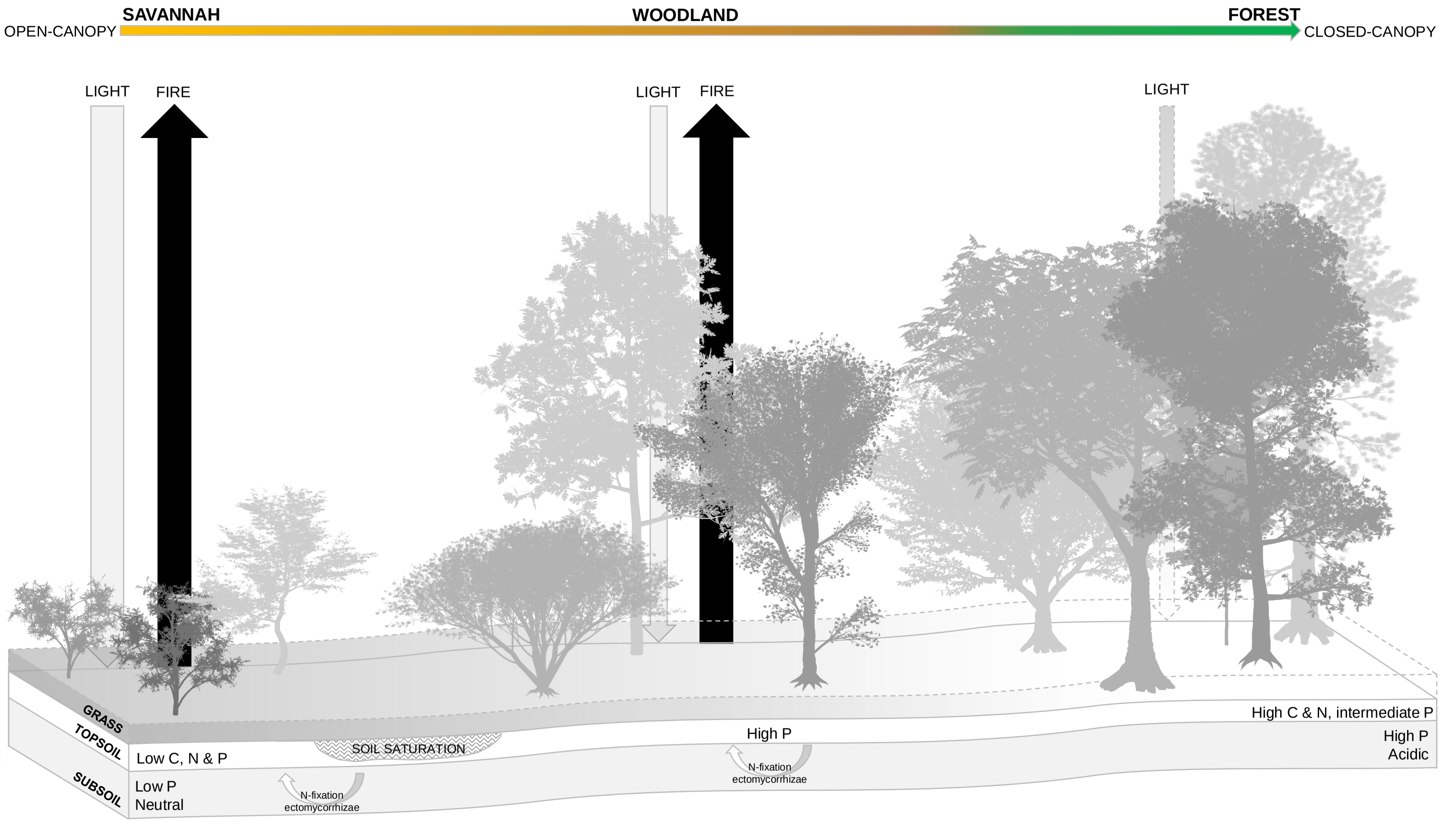

Figure 6.1: Summary of environmental controls on savannah-forest development in miombo woodland landscapes. Savannahs have sparse tree cover and tall grasses, frequent disturbance from fire, and were often associated with areas of seasonal inundation at low elevations. Woodlands exhibited co-dominance of trees and grasses, frequent fires, and were well-drained. Forests were mostly confined to the highest elevations, and had a closed-canopy that excludes a grassy understory and fire. Soil properties did not appear to be a major control on vegetation structure, though topsoil nutrient stocks varied widely and specialised mechanisms for the acquisition nutrients were absent in forests, possibly related to fire exclusion.

drained locations. Soil properties were generally similar between savannahs and woodlands, with the exception of a lower soil pH and greater subsoil extractable P in woodlands. Woodland vegetation was less adapted to nutrient-use efficiency and drought resilience than savannahs, though showed similar adaptations to fire and for nutrient acquisition. Water-use efficiency was significantly increased in woodlands, suggesting less abundant water resources or greater competition in woodland areas. Woodlands likely represent less marginal environments than open savannahs, perhaps as the result of their relative protection from seasonal inundation. Savannahs and woodlands share a number of species and have many similar ecological properties, likely representing a gradient of land cover.

Forests are areas of high woody biomass, identifiable by the species *Hymenaea verrucosa*, *Hymenocardia ulmoides* and *Pteleopsis myrtifolia*, which are very rare in savannah and woodland vegetation types. Forests have a closed-canopy, a very limited grassy understory, do not generally burn, and were dominant on the highest ground. Soil pH is low and topsoil carbon and nitrogen are more abundant than in savannahs and woodlands. Forest vegetation showed low nutrient use efficiency, less investment in fire resilience and nutrient acquisition, and low water use efficiency. Forests represent a more benign environment with trees that are geared towards productivity and competition over persistence. The distribution of forests in Kilwa District may be related to orographic precipitation, remoteness from habitation, or simply occur randomly as an alternate stable-state to fire-prone savannah and woodland vegetation.

There is an urgent requirement for improved monitoring of African savannah ecosystems such as miombo woodlands. Efficient representation of heterogeneous landscapes with forest inventory plots will require effective strategies for landscape stratification. The Kilwa permanent sample plot (PSP) network was established with the aid of optical remote sensing data classified into ‘savannah’, ‘woodland’ and ‘forest’ land cover classes (McNicol et al., 2012), though this initial classification was a poor match to the final vegetation types in Chapter 2. The strong correlation between vegetation composition and aboveground woody biomass (AGB) provides a useful means of landscape stratification in future, as AGB is readily measured by radar backscatter data in miombo woodlands (Ryan et al., 2012).

Results from Chapter 2 suggest it should be a priority to retain a wide range of AGB in miombo woodland landscapes in order to maintain landscape (beta) diversity. Effective management should therefore take into account the diversity of vegetation form and it's associated environmental context. For example, limiting the spread of fire into coastal forest might be beneficial, as tree species are poorly adapted to surviving frequent fires and a closed-canopy is required to exclude flammable C_4 grasses. However, mismanagement of a fire-resilient savannah as a forest through fire suppression could cause harm, with cascading ecosystem changes resulting in a loss of beta diversity (Parr et al., 2012). The results of Chapter 2 also indicate a degree of resilience to the distribution of vegetation types across the landscape. Where vegetation form is determined by topographic position and hydrology, the impact of differences in landscape management such as early burning will be restricted.

There also exist important differences in the C cycle associated with landscape vegetation heterogeneity, which are considered in Section 6.4.1.

6.2.2 At continental-scales

Divergences in miombo woodland functional properties were also identified across the African continent. In Chapter 5 I used the CARbon DAta MOdel fraMework (CARDAMOM) to quantify terrestrial C cycle state and process variables in southern Africa (Bloom et al., 2016). As well as a means to disaggregate the C cycle, parameter sets retrieved by CARDAMOM reflect spatial variation in ecosystem functional traits. CARDAMOM outputs identified three major trade-offs in ecosystem function, which were associated with variation in tree cover, fire frequency, and precipitation patterns.

The largest differences in ecosystem functional properties were in the allocation and residence time of C in the woody pool, describing the spectrum from grass-dominated to tree-dominated ecosystems. This observation is analogous to the differences in vegetation structure observed at landscape-scales, with vegetation forms running from open grasslands to closed-canopy forests. Vegetation structure was not well predicted by environmental data, being only strongly associated with observations of tree canopy cover. This result is not consistent with other studies, where fire and rainfall have been found to be strong determinants of tree cover in Africa (e.g. Staver et al., 2011; Lehmann et al., 2014), though the noise introduced by model-data fusion may act to obscure these signals.

Further differences in ecosystem function were prominent in foliar properties and phenology. Tough and long-lived leaves were associated with drought, thin and short-lived leaves with frequent fires, and the timing of leaf flush with the spread of rains from the Congo Basin across southern Africa. The emergence of foliar trait variation in CARDAMOM is an interesting observation, with outputs showing similar patterns to those in plant trait databases (e.g. Kattge et al., 2011), and in the measurements of Chapter 2.

As presented in Chapter 5, the Data Assimilation Linked Ecosystem Carbon (DALEC) model that underlies CARDAMOM is formulated for flexibility. This is helpful in representation of global ecosystem functional trait patterns, where data inputs and computational power are limited (Bloom et al., 2016). Further evaluation of ecosystem functional traits may be possible with altered model structures that better represent savannah function. For example, the separation of DALEC's foliar C pool into trees and grasses may be used to answer questions about the factors leading to tree-grass co-existence, and incorporation of simple hydrological limitations to growth and allocation patterns used to identify the importance of water supply on vegetation function at continental scales. Changes to the specification of DALEC are considered in section 6.4.2.

6.3 What is the role of fire in miombo woodlands?

6.3.1 Measurement of fire

The effective measurement of fire regimes and their impacts on vegetation remains a limitation to understanding miombo woodland dynamics. In Chapter 4, I used a 10 year time-series of burn scars identified in Landsat data to measure fire frequency in Kilwa District. Resultant maps show fire to be pervasive, with an average return interval of 1.8 years. Compared to commonly used 500 m resolution burned area data from MODIS (used in Chapter 5), Landsat data reveal fires to be more widespread than otherwise predicted (Fig. 6.2). It is likely that coarse-resolution MODIS data misses many small and patchy fires, an important component of fire activity in human-dominated miombo woodland landscapes (Randerson et al., 2012). The improved resolution of Landsat data presently comes at the cost of a sparse time-series, with infrequent satellite overpasses and cloud cover severely limiting observation opportunities. This deficiency in temporal resolution results in lower fire counts in most areas than MODIS data, and uncertainty on determination of fire seasonality. The recent launches of Landsat 8 (Roy et al., 2014) and Sentinel 2 (Drusch et al., 2012) should mitigate this issue in future work.

Efforts to detect the impacts of individual fires on miombo woodland tree populations were largely unsuccessful. In Chapter 3 I investigated the status of 12,201 tree stems in the Kilwa PSP network following 2 years of fire activity monitoring. There was no evidence of an association between stem top-kill and whether a plot burned, a result which stands in stark contrast to observations from controlled fire

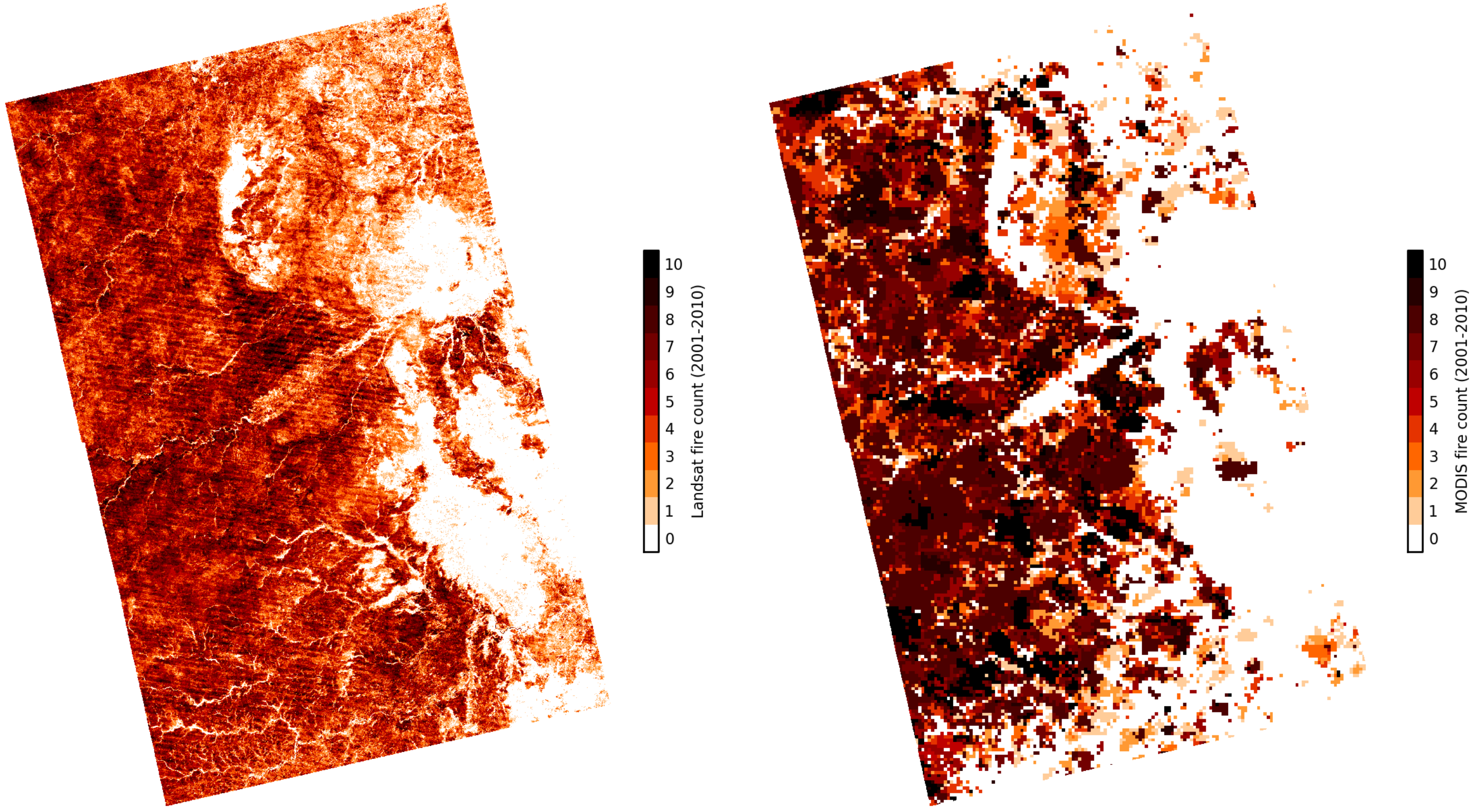

Figure 6.2: Side-by-side comparison of 30 m resolution Landsat burn scar detection results (see Chapter 4) and MODIS 500 m resolution burned area product. There exists a clear trade-off between detail in the Landsat data vs increased observation opportunity in MODIS data.

experiments (e.g. Ryan and Williams, 2011). This is best interpreted a null result, where fires were found to be so frequent in miombo woodlands that very few PSPs did not burn over the monitoring period, and that PSPs that did not burn were unusual in being nonflammable closed-canopy forest, heavily grazed, or topographically isolated. Although there was little direct evidence of the impact of fire, models of mortality show that small stems are particularly vulnerable to top-kill, an observation consistent with the smallest stems rarely surviving fire (Ryan and Williams, 2011). The ubiquity of fire in savannahs presents a challenge to experimental design, where very large networks of plots measured at high frequency will be required to generate the statistical power to reliably quantify the impacts of an existing fire regime on tree populations. It is also likely such plots would have to be monitored over a long time period in order to detect the infrequent extreme fires that may be an important control of vegetation dynamics. As such intensive monitoring is unlikely to be forthcoming in the near future, progress is more likely to be made through controlled fire experiments (e.g. Hoffa et al., 1999; Ryan and Williams, 2011; Sow et al., 2013), and by linking these to landscape measurements of fire.

6.3.2 Modelling of fire

The use of process-based models is a promising approach to understanding of fire dynamics in savannah ecosystems. In Chapter 4 I used the GapFire model to predict the impacts of a range of fire regimes on miombo woodland AGB. The largest uncertainties in GapFire's representation of fire is in the characterisation of fire intensity, a parameter which is both difficult to measure and has a large impact on model predictions. GapFire uses a simple measure of fire season (early/late) that defines fire intensity, though in reality fire characteristics will vary spatially with fuel properties and temporally with grass accumulation, fuel moisture, and time of day. More realistic descriptors

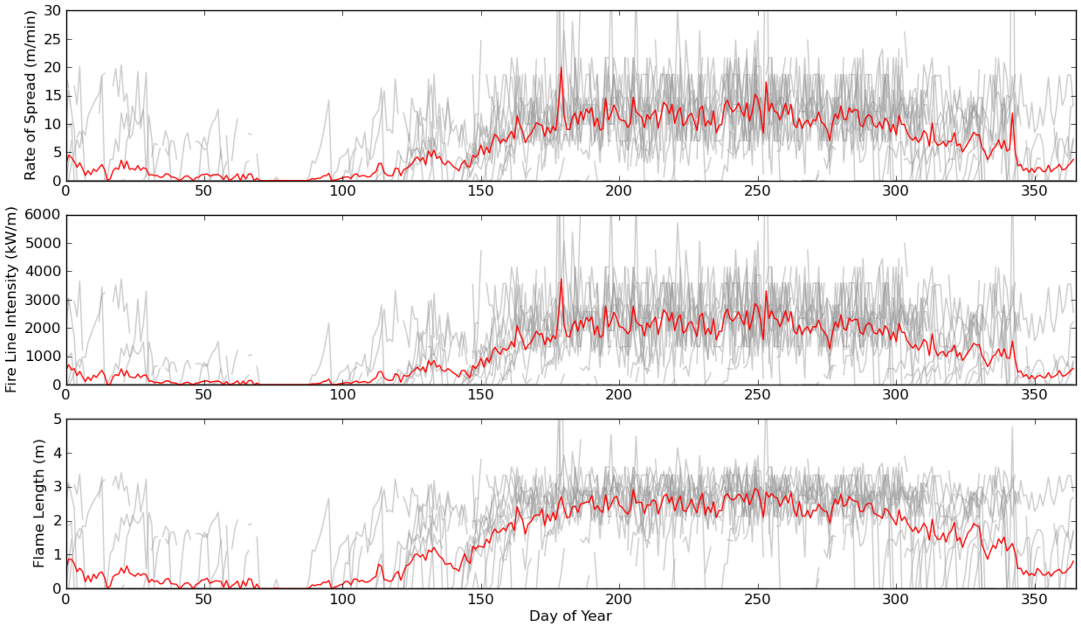

Figure 6.3: Predictions of fire seasonality using an application of the Rothermel model of fire spread (Rothermel, 1972). Outputs are shown for Kilwa District over the period 2001-2010 (grey lines), and mean average (red lines). Whilst such predictions are useful, little data presently exists to parameterise and validate this model. See VCS (2015) for methodological details.

of fire seasonality may be generated with fuel models, such as the Rothermel model of fire spread (Rothermel, 1972) (Fig. 6.3), though without detailed information on fuel structure and extensive validation data such predictions presently add little to the quality of the representation of fire. Remote sensing data may also reduce uncertainty in fire seasonality through direct measurement of active fire hotspots (Roberts et al., 2005; Wooster et al., 2005). As such measurements are presently only available at coarse-scale or from infrequent satellite overpasses, it is not yet a viable solution to the problem of determining fire intensity at landscape scales.

Fire activity is also represented in CARDAMOM (see Chapter 5), where estimates of fire emissions from the Global Fire Emissions Database (GFED) (van der Werf et al., 2010) are removed from living and dead C pools on a monthly basis. By being calculated over very large areas, predictions of fire impacts by CARDAMOM sidestep many of the limitations of GapFire; uncertainties resulting from burned area estimates are reduced, and seasonal estimates of fire intensity from active fire detections are more reliable. However, this is at the cost of a substantial simplification to the mechanistic representation of fire, with combusted biomass removed as fixed-fractions from C pools, and mortality represented by a constant resilience factor of non-combusted biomass. Inclusion of fire in biogeochemical models is still rudimentary, with additional work on emissions data and vegetation impacts required for more robust predictions.

6.3.3 Informing fire management and policy

The sensitivity of woodland ecosystems to fire raises important questions about their management, particularly where fire regimes are now largely anthropogenic in origin. In Chapter 4 I described the development of a project proposing the (re)instatement of a low severity fire regime in the miombo woodlands of Kilwa District (Fig. 6.4). Analysis of burn scar data from Landsat and modelling with GapFire suggest that the present regime of frequent late season fires is resulting in the progressive loss of AGB from Kilwa District. A reduction in fire severity through introduction of an early burning fire regime was predicted to have the capacity to halt or reverse this degradation, given that a substantial shift in fire seasonality is achieved.

The current frequency of fires observed in Kilwa District is not consistent with stability of woodland biomass, with the implication that the miombo woodlands of Kilwa District are remnant from a more moderate fire regime than is currently present, and that further loss of woody biomass is likely before woodlands reach an equilibrium state. This is consistent with fire experiments (e.g. Trapnell, 1959; Furley et al., 2008; Ryan and Williams, 2011), where fire regimes of the type observed in Kilwa

Figure 6.4: Trials of fire management in Kilwa District in Tanzania have aimed to implement early burning as a management strategy to support woody biomass. The utility of this management intervention is as yet unclear.

District result large losses of AGB. The idea that fire severity has increased and is resulting in woodland degradation is further supported by new palaeoclimatology data from Mozambique, where fire regimes of the relatively recent past were much less severe than those now present (McWethy et al., 2016). However, there are other possible interpretations of our inability to reconcile present-day woodlands with their fire-regimes. Trees may be more productive than we currently believe, though this is not supported by chronosequence studies (Williams et al., 2008; McNicol et al., 2015), or by the tree demographic measurements of Chapter 3. The leading alternate hypothesis is therefore that uncertainty and bias in top-kill measurements and estimates of fire intensity might be resulting in exaggerated rates of stem mortality in GapFire. Additional data from fire experiments will be necessary to further validate the predictions of GapFire.

Management of fire in savannahs is a controversial subject, with its ecological value is questioned by a number of authors (Parr and Andersen, 2006; Archibald, 2011; Bradshaw et al., 2013). Savannahs are fire-adapted systems, and in most cases require frequent fires to retain the characteristic co-existence between grasses and trees. We note that many critiques of fire management relate to drier ecosystems, which may be expected to respond very differently to miombo woodlands where tree-grass coexistence is contingent upon disturbance (Sankaran et al., 2005). Other authors have considered the risk of woody thickening, a process whereby woody plants may be encroaching on savannahs as the result of CO_2 fertilisation (Bond and Archibald, 2003; Wigley et al., 2010). Planned hot fires have been proposed as a means to slow or reverse woody thickening (Parr et al., 2012; Smit et al., 2016). Though woody thickening is not yet reported to be a widespread problem in miombo woodlands, it is possible that future management priorities may make early burning an undesirable activity. Both of these eventualities require ongoing monitoring, and the readiness to alter management strategies where conditions necessitate it.

There is no such thing as a savannah which does not burn, and given that fire exclusion is anyway near-impossible, the only management choice for fire in savannahs is between prescribed and non-prescribed fires. Estimates of the climate change mitigation potential of early burning in Chapter 4 are fairly low under realistic early burning management projections, with emissions from land use change probably a much larger and more urgent source of CO_2 emissions (Houghton and Hackler, 2006). Indeed, if agricultural conversion and expansion of livestock grazing leads to the breakup of contiguous miombo woodland landscapes, fire frequency may dramatically reduce in future and give way to problems associated with fire exclusion (Bistinas et al., 2013; Archibald, 2016). Further monitoring of small-scale fire management projects such as that in Kilwa District should help to determine the value of early burning.

6.4 How can we most effectively resolve the carbon cycle of miombo woodlands?

6.4.1 Measuring the carbon cycle

Diverse vegetation structures are associated with significant differences in the miombo woodland C cycle. In Chapter 3 I quantified rates of woody C cycling using repeat-measurements of trees in the Kilwa District PSP network. Woody production was closely associated with woody biomass, with the savannah-forest transition coinciding with increases in AGB increment through growth and loss of AGB through mortality. Landscape heterogeneity is a challenge to bottom-up measurement of the C cycle, leading to difficulty in upscaling and requiring effective monitoring across vegetation types. Whilst local-scale studies such as that in Kilwa District are useful, it is also probable that large-scale differences exist in patterns of C cycling across the miombo ecoregion. Similar studies in the Amazon and Congo Basin rainforests have combined forest plot data over continental scales (Malhi et al., 2002; Lewis et al., 2009; Malhi, 2010), which has proven a powerful means of generating insight into the C cycle.

I also investigated how rates of stem growth and mortality are influenced by environmental variability. Stem damage has a large impact on growth and mortality rates, suggesting that the top-down processes of fire and herbivory are important regulators of the C cycle. No significant differences were observed with vegetation structure, soil fertility, competition, or fire in determination of stem demographic rates (though see section 6.3.1). Stem demographic rates were poorly predicted by statistical models, suggesting a limited deterministic component to stem growth and mortality. Further monitoring of PSPs would be expected to better resolve these models, which are presently limited by a very short re-inventory time. As effective modelling of savannah vegetation is contingent upon knowledge of the processes that control its dynamics, such efforts are of considerable value.

6.4.2 Modelling the carbon cycle

A long-term goal of savannah science is to create robust models of the C cycle in miombo woodland ecosystems. In this thesis I have used two different approaches to this problem: *(i)* GapFire: a dynamic model of miombo woodland biomass (see Chapter 4), and *(ii)* CARDAMOM: a simple box model and data assimilation system that simulates C pools and the fluxes that connect them (see Chapter 5).

A particular strength of demographic models such as GapFire is in the explicit representation of individual stem growth, mortality, and recruitment, which is important where processes affect small trees differently to large trees. For instance, the impact of fires is dependent on both stem size and fire intensity, meaning the simulation of individual stems is valuable for an accurate mechanistic representation of fire. Demographic models such as GapFire show the potential to incorporate other important drivers of miombo woodland dynamics such as stem damage and tree harvesting, though presently available data are not well able to constrain these processes.

Through its simulation of large ensembles of small patches, GapFire is also well-suited to encompassing the heterogeneity of miombo woodland structure. This capacity may be furthered by simulating plant community variation (Bugmann, 2001; Purves et al., 2008), such as through the ‘savannah’, ‘woodland’ and ‘forest’ functional types considered in Chapter 2. Such an effort will require data on the differential rates of top-kill and photosynthetic capacity of these species. GapFire also has the potential to represent community traits, such as simulating the grass-fire-canopy feedback where fire is excluded from woodland patches with insufficient light for C_4 grass growth. Such a modification is currently limited by the identification of the most appropriate scale for the canopy-grass feedback to be applied, and a poor understanding of how fire is likely to spread between woodland ‘patches’.

The main strength of CARDAMOM for C cycle quantification is in its capacity to make efficient use of data from archives of remote sensing data. Where the detailed parameter information and driving data for models such as GapFire are scarce and require intensive monitoring and experimentation to determine, this is a considerable advantage. The use of CARDAMOM comes at the cost of representing important processes such as fire in a very coarse manner. A further concern is whether the parameters that represent 0.25° grid cells account for the the variability we observe at finer scales. As this heterogeneity is significant, its impact on model predictions is worth further exploration.

Uncertainties in CARDAMOM remain very large. For instance, the prediction of southern Africa as a net C source of 0.17 PgC/yr is associated with a 50 % confidence interval of -0.68 to 0.62 PgC/yr. Whilst limited by the availability of C cycle observational data (Bloom et al., 2016), CARDAMOM is unusual in generating reliable estimates of parameter uncertainty, a useful property that aids in the progressive reduction of uncertainty with new data sources and modelling strategies. Over the long-term, reductions to uncertainty in CARDAMOM may come from improved data constraints and new satellite sensors (e.g. Butz et al., 2011; Le Toan et al., 2011), though in the near-term more straightforward alterations can be made to model specification. One development indicated as important by this work is the separation of tree and grass foliar C pools, which have very different patterns of phenology and productivity, and responses to fire. Ecological and dynamic constraints (EDCs), which prevent the generation of ecologically inconsistent parameter sets in CARDAMOM (Bloom and Williams, 2015), can then be used enforce the exclusivity of a flammable grass layer and a closed-canopy. Separation of foliar pools will require an effective method of disaggregating tree and grass phenology in remote sensing observations, which at present remains challenging (see Ryan, 2009).

6.5 Concluding remarks

In this thesis I aimed to improve understanding of important processes determining vegetation dynamics and quantify key aspects of the C cycle in southern Africa's miombo woodlands. This thesis has advanced our knowledge of patterns of vegetation heterogeneity in miombo woodlands at landscape and continental spatial scales, and identified a number of environmental drivers of divergent vegetation structures. It has also generated estimates of the miombo woodland C cycle from plot measurements and models, and presented the C storage implications of changes to fire management. From this work a number of questions were raised about how we can most effectively measure and model miombo woodlands, which will be important for predicting the impacts of future climate change. It also highlighted the need for further observations of C cycling from field experiments and remote sensing observations that effectively take into account variation in vegetation pattern and processes.

6.6 References

Archibald, S. (2011), ‘Book review: Culture, Ecology and Economy of Fire Management in North Australian Savannas: Rekindling the Wurrk Tradition: Edited by Jeremy Russell-Smith, Peter Whitehead and Peter Cooke’, *African Journal of Range & Forage Science*, **28**, pp. 47–49.

Archibald, S. (2016), ‘Managing the human component of fire regimes: lessons from Africa’, *Philosophical Transactions of the Royal Society B*, **371**, p. 20150346.

Bistinas, I., Oom, D., Sá, A.C., Harrison, S.P., Prentice, I.C., and Pereira, J.M. (2013), ‘Relationships between human population density and burned area at continental and global scales’, *PLoS One*, **8**, e81188.

Bloom, A.A. and Williams, M. (2015), ‘Constraining ecosystem carbon dynamics in a data-limited world: integrating ecological" common sense" in a model–data fusion framework’, *Biogeosciences*, **12**, pp. 1299–1315.

Bloom, A.A., Exbrayat, J.-F., van der Velde, I.R., Feng, L., and Williams, M. (2016), ‘The decadal state of the terrestrial carbon cycle: Global retrievals of terrestrial carbon allocation, pools, and residence times’, *Proceedings of the National Academy of Sciences*, **113**, pp. 1285–1290.

Bond, W.J. and Archibald, S. (2003), ‘Confronting complexity: fire policy choices in South African savanna parks’, *International Journal of Wildland Fire*, **12**, pp. 381–389.

Bradshaw, C.J., Bowman, D.M., Bond, N.R., Murphy, B.P., Moore, A.D., Fordham, D.A., Thackway, R., Lawes, M.J., McCallum, H., Gregory, S.D., et al. (2013), ‘Brave new green world–consequences of a carbon economy for the conservation of Australian biodiversity’, *Biological Conservation*, **161**, pp. 71–90.

Bugmann, H. (2001), ‘A review of forest gap models’, *Climatic Change*, **51**, pp. 259–305.

Butz, A., Guerlet, S., Hasekamp, O., Schepers, D., Galli, A., Aben, I., Frankenberg, C., Hartmann, J.-M., Tran, H., Kuze A ad Keppel-Aleks, G., Toon, G., Wunch, D., Wennberg, P., Deutscher, N., Griffith, D., Macatangay, R., Messerschmidt, J., Notholt, J., and Warneke, T. (2011), ‘Toward accurate CO_2 and CH_4 observations from GOSAT’, *Geophysical Research Letters*, **38**, p. L14812.

Drusch, M., Del Bello, U., Carlier, S., Colin, O., Fernandez, V., Gascon, F., Hoersch, B., Isola, C., Laberinti, P., Martimort, P., Meygret, A., Spoto, F., Sy, O., Marchese, F., and Bargellini, P. (2012), ‘Sentinel-2: ESA’s optical high-resolution mission for GMES operational services’, *Remote Sensing of Environment*, **120**, pp. 25–36.

Furley, P.A., Rees, R.M., Ryan, C.M., and Saiz, G. (2008), ‘Savanna burning and the assessment of long-term fire experiments with particular reference to Zimbabwe’, *Progress in Physical Geography*, **32**, pp. 611–634.

Hoffa, E.A., Ward, D., Hao, W.M., Susott, R.A., and Wakimoto, R.H. (1999), ‘Seasonality of carbon emissions from biomass burning in a Zambian savanna’, *Journal of Geophysical Research: Atmospheres*, **104**, pp. 13841–13853.

Houghton, R.A. and Hackler, J.L. (2006), ‘Emissions of carbon from land use change in sub-Saharan Africa’, *Journal of Geophysical Research: Biogeosciences*, **111**, G02003.

Kattge, J., Diaz, S., Lavorel, S., Prentice, C., Leadley, P., Boenisch, G., Garnier, E., Westoby, M., Reich, P.B., Wright, I.J., Cornelissen, J.H.C., Violle, C., Harrison, S.P., van, B.P.M., Reichstein, M., Enquist, B.J., Soudzilovskaia, N.A., Ackerly, D.D., Anand, M., Atkin, O., Bahn, M., Baker, T.R., Baldocchi, D., Bekker, R., Blanco, C.C., Blonder, B., Bond, W.J., Bradstock, R., Bunker, D.E., Casanoves, F., Cavender-Bares, J., Chambers, J.Q., Chapin, F.S., Chave, J., Coomes, D., Cornwell, W.K., Craine, J.M., Dobrin, B.H., Duarte, L., Durka, W., Elser, J., Esser, G., Estiarte, M., Fagan, W.F., Fang, J., Fernandez-Mendez, F., Fidelis, A., Finegan, B., Flores, O., Ford, H., Frank, D., Freschet, G.T., Fyllas, N.M., Gallagher, R.V., Green, W.A., Gutierrez, A.G., Hickler, T., Higgins, S.I., Hodgson, J.G., Jalili, A., Jansen, S., Joly, C.A., Kerkhoff, A.J., Kirkup, D., Kitajima, K., Kleyer, M., Klotz, S., Knops, J.M.H., Kramer, K., Kühn, I.., Kurokawa, H., Laughlin, D., Lee, T.D., Leishman, M., Lens, F., Lenz, T., Lewis, S.L., Lloyd, J., Llusià, J., Louault, F., Ma, S., Mahecha, M.D., Manning, P., Massad, T., Medlyn, B.E., Messier, J., Moles, A.T., Müller, S.C., Nadrowski, K., Naeem, S., Niinemets, Ü., Nöllert, S., Nüske, A., Ogaya, R., Oleksyn, J., Onipchenko, V.G., Onoda, Y., Ordoñez, J., Overbeck, G., Ozinga, W.A., Patiño, S., Paula, S., Pausas, J.G., Peñuelas, J., Phillips, O.L., Pillar, V., Poorter, H., Poorter, L., Poschlod, P., Prinzing, A., Proulx, R., Rammig, A., Reinsch, S., Reu, B., Sack, L., Salgado-negret, B., Sardans, J., Shiodera, S., Shipley, B., Siefert, A., Sosinski, E., Soussana, J.-f., Swaine, E., Swenson, N., Thompson, K., Thornton, P., Waldram, M., Weiher, E., White, M., White, S., Wright, S.J., Yguel, B., Zaehle, S., Zanne, A.E., and Wirth, C. (2011), ‘TRY–a global database of plant traits’, *Global Change Biology*, **17**, pp. 2905–2935.

Le Toan, T., Quegan, S., Davidson, M., Balzter, H., Paillou, P., Papathanassiou, K., Plummer, S., Rocca, F., Saatchi, S., Shugart, H., and Ulander, L. (2011), ‘The BIOMASS mission: Mapping global forest biomass to better understand the terrestrial carbon cycle’, *Remote sensing of environment*, **115**, pp. 2850–2860.

Lehmann, C.E.R., Anderson, T.M., Sankaran, M., Higgins, S.I., Archibald, S., Hoffmann, W.A., Hanan, N.P., Williams, R.J., Fensham, R.J., Felfili, J., Hutley, L.B., Ratnam, J., San Jose, J., Montes, R., Franklin, D., Russell-Smith, J., Ryan, C.M., Durigan, G., Hiernaux, P., Haidar, R., Bowman, D.M.J.S., and Bond, W.J. (2014), ‘Savanna vegetation-fire-climate relationships differ among continents’, *Science*, **343**, pp. 548–552.

Lewis, S.L., Lopez-Gonzalez, G., Sonke, B., Affum-Baffoe, K., Baker, T.R., Ojo, L.O., Phillips, O.L., Reitsma, J.M., White, L., Comiskey, J.A., Djuikouo, M.-N., Ewango, C.E.N., Feldpausch, T.R., Hamilton, A.C., Gloor, M., Hart, T., Hladik, A., Lloyd, J., Lovett, J.C., Makana, J.-R., Malhi, Y., Mbago, F.M., Ndangalasi, H.J., Peacock, J., Peh, K.S.H., Sheil, D., Sunderland, T., Swaine, M.D., Taplin, J., Taylor, D., Thomas, S.C., Votere, R., and Woll, H. (2009), ‘Increasing carbon storage in intact African tropical forests’, *Nature*, **457**, pp. 1003–1006.

Malhi, Y. (2010), ‘The carbon balance of tropical forest regions, 1990–2005’, *Current Opinion in Environmental Sustainability*, **2**, pp. 237–244.

Malhi, Y., Phillips, O., Lloyd, J., Baker, T., Wright, J., Almeida, S., Arroyo, L., Frederiksen, T., Grace, J., Higuchi, N., et al. (2002), 'An international network to monitor the structure, composition and dynamics of Amazonian forests (RAINFOR)', *Journal of Vegetation Science*, **13**, pp. 439–450.

McNicol, I.M., Williams, M., and Ryan, C.M. (2012), 'Accurately assessing biomass carbon in Miombo woodlands', *The Arc Journal*, **22**, pp. 18–21.

McNicol, I.M., Ryan, C.M., and Williams, M. (2015), 'How resilient are African woodlands to disturbance from shifting cultivation?', *Ecological Applications*, **25**, pp. 2320–2336.

McWethy, D.B., Neumann, F.H., Steinbruch, F., Ryan, C.M., and Valsecchi, V. (2016), 'Late Quaternary vegetation development and disturbance dynamics from a peatland on Mount Gorongosa, central Mozambique', *Quaternary Science Reviews*, **137**, pp. 221–233.

Parr, C.L. and Andersen, A.N. (2006), 'Patch mosaic burning for biodiversity conservation: a critique of the pyrodiversity paradigm', *Conservation Biology*, **20**, pp. 1610–1619.

Parr, C.L., Gray, E.F., and Bond, W.J. (2012), 'Cascading biodiversity and functional consequences of a global change–induced biome switch', *Diversity and Distributions*, **18**, pp. 493–503.

Purves, D.W., Lichstein, J.W., Strigul, N., and Pacala, S.W. (2008), 'Predicting and understanding forest dynamics using a simple tractable model', *Proceedings of the National Academy of Sciences*, **105**, pp. 17018–17022.

Randerson, J.T., Chen, Y., van der Werf, G.R., Rogers, B.M., and Morton, D.C. (2012), 'Global burned area and biomass burning emissions from small fires', *Journal of Geophysical Research: Biogeosciences*, **117**, G04012.

Roberts, G., Wooster, M.J., Perry, G.L., Drake, N., Rebelo, L.-M., and Dipotso, F. (2005), 'Retrieval of biomass combustion rates and totals from fire radiative power observations: Application to southern Africa using geostationary SEVIRI imagery', *Journal of Geophysical Research: Atmospheres*, **110**, p. D21111.

Rothermel, R.C. (1972), *A mathematical model for predicting fire spread in wildland fuels*, United States Forest Service, Utah, USA.

Roy, D., Wulder, M., Loveland, T., C.E., W., Allen, R., Anderson, M., Helder, D., Irons, J., Johnson, D., Kennedy, R., Scambos, T., Schaaf, C., Schott, J., Sheng, Y., Vermote, E., Belward, A., Bindschadler, R., Cohen, W., Gao, F., Hipple, J., Hostert, P., Huntington, J., Justice, C., Kilic, A., Kovalskyy, V., Lee, Z., Lymburner, L., Masek, J., McCorkel, J., Shuai, Y., Trezza, R., Vogelmann, J., Wynne, R., and Zhu, Z. (2014), 'Landsat-8: Science and product vision for terrestrial global change research', *Remote Sensing of Environment*, **145**, pp. 154–172.

Ryan, C.M., Hill, T., Woollen, E., Ghee, C., Mitchard, E., Cassells, G., Grace, J., Woodhouse, I.H., and Williams, M. (2012), 'Quantifying small-scale deforestation and forest degradation in African woodlands using radar imagery', *Global Change Biology*, **18**, pp. 243–257.

Ryan, C.M. and Williams, M. (2011), ‘How does fire intensity and frequency affect miombo woodland tree populations and biomass?’, *Ecological Applications*, **21**, pp. 48–60.

Ryan, C.M. (2009), ‘Carbon cycling, fire and phenology in a tropical savanna woodland in Nhambita, Mozambique’, PhD thesis, The University of Edinburgh.

Sankaran, M., Hanan, N.P., Scholes, R.J., Ratnam, J., Augustine, D.J., Cade, B.S., Gignoux, J., Higgins, S.I., Le Roux, X., Ludwig, F., Ardo, J., Banyikwa, F., Bronn, A., Bucini, G., Caylor, K.K., Coughenour, M.B., Diouf, A., Ekaya, W., Feral, C.J., February, E.C., Frost, P.G.H., Hiernaux, P., Hrabar, H., Metzger, K.L., Prins, H.H.T., Ringrose, S., Sea, W., Tews, J., Worden, J., and Zambatis, N. (2005), ‘Determinants of woody cover in African savannas’, *Nature*, **438**, pp. 846–849.

Smit, I.P.J., Asner, G.P., Govender, N., Vaughn, N.R., and Wilgen, B.W. (2016), ‘An examination of the potential efficacy of high-intensity fires for reversing woody encroachment in savannas’, *Journal of Applied Ecology*.

Sow, M., Hély, C., Mbow, C., and Sambou, B. (2013), ‘Fuel and fire behavior analysis for early-season prescribed fire planning in Sudanian and Sahelian savannas’, *Journal of Arid Environments*, **89**, pp. 84–93.

Staver, A.C., Archibald, S., and Levin, S. (2011), ‘Tree cover in sub-Saharan Africa: Rainfall and fire constrain forest and savanna as alternative stable states’, *Ecology*, **92**, pp. 1063–1072.

Trapnell, C. (1959), ‘Ecological results of woodland and burning experiments in Northern Rhodesia’, *The Journal of Ecology*, **41**, pp. 129–168.

van der Werf, G.R., Randerson, J.T., Giglio, L., Collatz, G.J., Mu, M., Kasibhatla, P.S., Morton, D.C., DeFries, R.S., van Jin, Y., and van Leeuwen, T.T. (2010), ‘Global fire emissions and the contribution of deforestation, savanna, forest, agricultural, and peat fires (1997–2009)’, *Atmospheric Chemistry and Physics*, **10**, pp. 11707–11735.

VCS (2015), *Methodology for Avoided Forest Degradation through Fire Management.* VM0029, Verified Carbon Standard, url: `http://www.v-c-s.org/methodologies/avoiding-degradation-through-fire-management/`.

von der Heyden, C.J. (2004), ‘The hydrology and hydrogeology of dambos: a review’, *Progress in Physical Geography*, **28**, pp. 544–564.

Wigley, B.J., Bond, W.J., and Hoffman, M. (2010), ‘Thicket expansion in a South African savanna under divergent land use: local vs. global drivers?’, *Global Change Biology*, **16**, pp. 964–976.

Williams, M., Ryan, C.M., Rees, R.M., Sambane, E., Fernando, J., and Grace, J. (2008), ‘Carbon sequestration and biodiversity of re-growing miombo woodlands in Mozambique’, *Forest Ecology and management*, **254**, pp. 145–155.

Woollen, E., Ryan, C.M., and Williams, M. (2012), ‘Carbon stocks in an African woodland landscape: spatial distributions and scales of variation’, *Ecosystems*, **15**, pp. 804–818.

Wooster, M.J., Roberts, G., Perry, G., and Kaufman, Y. (2005), ‘Retrieval of biomass combustion rates and totals from fire radiative power observations: FRP derivation and calibration relationships between biomass consumption and fire radiative energy release’, *Journal of Geophysical Research: Atmospheres*, **110**, p. D24311.